

The Fire Hazards of Insulation Materials

by
Sean Thomas McKenna

A thesis submitted in partial fulfilment for the requirements for the degree of Doctor
of Philosophy at the University of Central Lancashire

January 2019

Abstract

Insulation materials are widespread in the modern built environment. They have, particularly in recent years, been a major focus of fire safety research. That focus has been enhanced by the tragic Grenfell Tower Fire that resulted in the death of 72 people. This work aims to understand and quantitatively assess the fire hazards presented by modern insulation materials.

14 materials were selected for analysis, including 7 PIR foams, 4 phenolic foams and 3 mineral wool materials. These materials were tested for their elemental composition, fire toxicity, and reaction-to-fire properties. The data generated was then used to calculate the maximum safe loadings of the insulation materials. The methodology had originally only been used with estimated values based on Euroclass data. In order to practically apply the method, the cone calorimeter was used to generate the mass loss per unit area data, rather than SBI test data or estimated values. Fire toxicity data was generated using the ISO/TS 19700 Steady State Tube Furnace. Additional maximum safe loading values were calculated using material-IC₅₀ values, as incapacitation is arguably a more important end point in fire toxicity assessment. The maximum safe loading values calculated were comparable to the estimated values outlined in the original methodology. This methodology could be used to provide quick estimations of the safe loading of insulation materials in construction, allowing for informed decision making in building design without an overwhelming amount of data for non-fire experts to consider.

The results of this work demonstrate significant differences between the 3 types of insulation material. The mineral wool materials (both glass wool and stone wool) were of low toxicity and flammability. The foam insulation materials (PIR and phenolic) produced high yields of toxic gases in under-ventilated conditions, and had relatively high flammability. The PIR foams, in particular, had the highest toxicity due to the high yields of HCN produced during under-ventilated flaming, which has been linked to their nitrogen content and chemical composition. The phenolic foams lacked the high yields of HCN due to their low nitrogen content, but still produced high quantities of asphyxiating CO, like the PIR foams. Both types of foam insulation also produced hydrogen chloride gas during combustion, which would have a strongly irritating effect on exposed persons, potentially hindering their escape. FED analysis has demonstrated that the PIR foams increased toxicity is largely the result of the high toxicity of HCN. 1 kg of any of the 7 PIR samples burning in under-ventilated conditions is capable of producing enough HCN to create a lethal atmosphere in 50 m³. The maximum safe loading values calculated showed that, on average, phenolic foams present ~50 to 100x higher fire hazard than the

mineral wool materials, and the average PIR foam presented a potential fire hazard ~1.5 to 2.5x higher than the average phenolic foam.

Additional work was performed to optimise a method for the quantification of HCN in fires – the chloramine-T/isonicotinic acid method from ISO 19701. HCN is a highly toxic product of the combustion of nitrogen containing materials. As such, it was important to ensure sampling and analysis was both accurate and reliable. Analysis was performed to understand sample and standard stability, optimal time to analysis, analytical variation, and potential interferences as a result of commonly encountered acid gases in fire effluent.

The cone calorimeter and SBI apparatus were also assessed for their viability in fire toxicity assessment, potentially negating the need to use the ISO/TS 19700 Steady State Tube Furnace. However, the resulting data demonstrated that both tests are inadequate due to their inability to recreate the more toxic fire condition – under-ventilated burning. This emphasises the need for dedicated fire toxicity tests, as most fire tests are well-ventilated reaction-to-fire tests, despite the fact that fire toxicity results in at least 50% of UK fire deaths.

Contents

Abstract.....	ii
Contents.....	iv
List of Figures.....	vi
List of Tables.....	vii
List of Schemes.....	viii
List of Equations.....	viii
List of Abbreviations.....	ix
Acknowledgements.....	xi
Chapter 1.....	1
1.0 Introduction to the project.....	1
1.0.1 Aim of the Project.....	1
1.0.2 Objectives.....	1
1.0.3 Layout of the Thesis.....	2
1.1 Introduction to the Subject.....	3
1.2.1 Fire Types and Ventilation Conditions.....	6
1.2.2 Reaction to Fire and Methods of Assessment.....	9
1.2.3 Fire Toxicity.....	13
1.2.4 Insulation Materials.....	34
Chapter 2.....	47
2.0 Experimental.....	47
2.0.1 Materials.....	47
2.0.2 Elemental Analysis.....	48
2.0.3 Steady State Tube Furnace.....	49
2.0.4 Cone Calorimeter.....	50
2.0.5 Single Burning Item Tests.....	51
2.0.6 Quantification of Hydrogen Cyanide by Colourimetric Spectrophotometry.....	54
2.0.7 Quantification of Acid Gases by High Pressure Ion Chromatography.....	56

Chapter 3.....	57
3.0 Results and Discussion	57
3.1 Development and Optimisation of HCN Quantification in Fires	57
3.2 Elemental Analysis and Material Composition	69
3.3 Reaction to Fire Assessment	71
3.4 Fire Toxicity Assessment	81
3.5 Fire Toxicity Measurements from Standard Reaction to Fire Tests.....	100
3.6 Quantitative Assessment of the Fire Hazards of Insulation Materials.....	109
Chapter 4.....	117
4.0 Conclusions and Future Work.....	117
Chapter 5.....	121
5.0 References.....	121
Appendices.....	128
Appendix A – Results of the EN 13823 SBI Testing	128
Appendix B – Results of the ISO/TS 19700 SSTF Testing.....	137
Appendix C – Publications.....	140
The Fire Toxicity of Polyurethane Foams.....	140
Flame Retardants in UK Furniture Increase Smoke Toxicity More than they Reduce Fire Growth Rate	168
Fire Behaviour of Modern Façade Materials – Understanding the Grenfell Tower Fire ..	191

List of Figures

Figure 1 Causes of UK fire deaths from 1955 to 2013 ³	4
Figure 2 Causes of non-fatal UK fire injuries from 1955 to 2013 ³	5
Figure 3 A simplified fire growth curve	6
Figure 4 The ISO 5660 Cone Calorimeter	10
Figure 5 The SBI test apparatus	11
Figure 6 i) Structure of PVC ii) Structure of TCPP	20
Figure 7 Structures of common aldehydes found in fire effluents i) formaldehyde ii) acrolein iii) acetaldehyde iv) butyraldehyde	26
Figure 8 Structure of isocyanates commonly found in fires involving polyurethane materials i) methyl isocyanate ii) 2,4-toluene diisocyanate iii) 4,4'-methylene diphenyl diisocyanate	27
Figure 9 The Controlled Atmosphere Cone Calorimeter	30
Figure 10 The Steady State Tube Furnace	31
Figure 11 The urethane functional group	36
Figure 12 Other polyurethane functional groups i) urea ii) isocyanurate iii) carbodiimides iv) uretdiones	37
Figure 13 Generalised decomposition mechanism for the thermal decomposition of polyurethane foams ⁵⁷	40
Figure 14 Reaction of i) phenol and ii) formaldehyde to produce a iii) phenolic resin	43
Figure 15 The Govmark CC-2 Cone Calorimeter	50
Figure 16 Schematic of the EN 13832 SBI test apparatus	51
Figure 17 Schematic of the portable gas analysis equipment used during the SBI testing	53
Figure 18 Variation in the absorbance of the reaction as a function of time	62
Figure 19 Effect of 1 ppm of potentially interfering ions on cyanide concentration at 5°C and 21°C after up to 7 days (note concentration scale on y-axis)	66
Figure 20 Effect of 10 ppm of potentially interfering ions on cyanide concentration at 5°C and 21°C after up to 7 days (note concentration scale on y-axis)	67
Figure 21 Heat Release Rates of insulation materials measured in the Cone Calorimeter	73
Figure 22 Heat release rates of PIR samples in the cone calorimeter	74
Figure 23 CO Yields against equivalence ratio for burning insulation materials in the SSTF	82
Figure 24 HCN yield against equivalence ratio for burning materials in the SSTF	85
Figure 25 HCl Yield against equivalence ratio for burning insulation materials in the SSTF	89
Figure 26 ISO 13571 FED calculations for incapacitation by toxic effluent	92
Figure 27 ISO 13571 calculations for incapacitation including the FEC values for NO and HCl ..	93

Figure 28 ISO 13344 FED calculated for lethal exposure to toxic effluent	96
--	----

List of Tables

Table 1 Classifications of characteristic fire stages based on ISO 19706 ⁴	7
Table 2 Description of the Euroclass System requirements and example products	12
Table 3 Effects of acute carbon monoxide exposure at various concentrations.....	14
Table 4 Effects of HCl exposure with increasing concentration ⁴³	21
Table 5 Effects of HBr exposure with increasing concentration ⁴³	22
Table 6 Bond decomposition temperatures of the major polyurethane functional groups	38
Table 7 Material ID codes and descriptions.....	47
Table 8 Absorbance of the standard cyanide solutions for the 4 cm and 1 cm cells.....	63
Table 9 Absorbance of a sample solution stored both in and out of a refrigerator	64
Table 10 List of ions, the salt used to generate the ion, and the acid gas that produces those ions in solution.	65
Table 11 Elemental composition of the insulation samples	70
Table 12 Results of the Cone Calorimeter testing	72
Table 13 Results of burning insulation materials in the SBI apparatus	79
Table 14 HCN yields and fuel nitrogen recovery for specific fire conditions in the SSTF	88
Table 15 Material-IC ₅₀ and material-LC ₅₀ for insulation materials burned in the SSTF	98
Table 16 Average material IC ₅₀ and material LC ₅₀ values for insulation burned in the SSTF	99
Table 17 CO ₂ , CO and HCN yields in the cone calorimeter at 50 kW m ⁻²	101
Table 18 Maximum recorded concentrations of CO ₂ and CO in the SBI test.....	104
Table 19 Mass loss and toxic product yields in the SBI test.....	106
Table 20 Comparison of CO:CO ₂ ratio in the SBI, cone calorimeter and SSTF	107
Table 21 Maximum safe loading values for insulation materials based on cone calorimeter and SSTF data.....	111
Table 22 Maximum safe loading values calculated using incapacitation as the endpoint for fire toxicity assessment	113

List of Schemes

Scheme 1 a) Cyanide Ions b) Chloramine-T c) Cyanogen Chloride d) Isonicotinic Acid e) 1-cyano-4-carboxy-pyridinium chloride f) Carboxy-glutaconic aldehyde product g) 1-phenyl-3-methyl-5-pyrazolone h) Polymethine dye product.....	60
--	----

List of Equations

Equation 1 Definition of equivalence ratio	8
Equation 2 ISO 13344 Purser model for estimating lethality from fire effluent.....	32
Equation 3 ISO 13571 model to estimate compromised tenability from asphyxiant gases	33
Equation 4 ISO 13571 FEC model for compromised tenability from irritant gases	33
Equation 5 Equation relating LC_{50} to FED to calculate a material- LC_{50}	33
Equation 6 Lethal volume of effluent from a burning material in a specific fire condition.....	110
Equation 7 Maximum safe loading of a material in a specific fire condition.....	110

List of Abbreviations

Aq	Aqueous
BFR	Brominated Flame Retardant
CACC	Controlled Atmosphere Cone Calorimeter
CHNS	Carbon, Hydrogen, Nitrogen and Sulphur Elemental Analysis
CNS	Central Nervous System
COHb	Carboxyhaemoglobin
DMF	Dimethyl Formamide
EFiC	European Fire and Conductivity Laboratory
FEC	Fractional Effective Concentration
FED	Fractional Effective Dose
FIGRA	Fire Growth Rate
FPA	Fire Propagation Apparatus
FTIR	Fourier Transformed Infrared Spectroscopy
Hb	Haemoglobin
HPIC	High Pressure Ion Chromatography
HRR	Heat Release Rate
HX	Hydrogen Halide
IC ₅₀	Concentration required to incapacitate 50% of the exposed population
ISO	International Organisation for Standardisation
ISO/TS	ISO Technical Specification
KOH	Potassium Hydroxide
LC ₅₀	Concentration required to kill 50% of the exposed population
LDPE	Low Density Polyethylene
MDI	Methylene Diphenyl Diisocyanate
mIC ₅₀	Material IC ₅₀
mLC ₅₀	Material LC ₅₀
MSL	Maximum Safe Loading
MW	Mineral Wool Insulation
NCO	Isocyanate
NDIR	Non-Dispersive Infrared Spectroscopy
NO _x	Oxide of Nitrogen
PAH	Polycyclic Aromatic Hydrocarbon
PF	Phenolic Foam Insulation

PHRR	Peak Heat Release Rate
PIR	Polyisocyanurate Foam Insulation
ppm	Parts Per Million
PTFE	Polytetrafluoroethylene
PVC	Polyvinyl Chloride
RADS	Reactive Airways Dysfunction Syndrome
RMV	Respiratory Minute Volume
RSET	Required Safe Egress Time
SBI	Single Burning Item Test (EN 13823)
SDC	Smoke Density Chamber (ISO 5659-2)
SEM-EDX	Scanning Electron Microscope with Energy Dispersive X-Ray attachment
SMOGRA	Smoke Growth Rate
SO _x	Oxides of Sulphur
SSTF	Steady State Tube Furnace (ISO/TS 19700)
TCP	Tris-(2-Chloroisopropyl) Phosphate
TDI	Toluene Diisocyanate
THR	Total Heat Released
TSP	Total Smoke Produced
USD	United States Dollars
UV-Vis	Ultraviolet – Visible Spectroscopy
XRF	X-Ray Fluorescence Spectroscopy

Acknowledgements

Firstly, I would like to thank my supervisor, Professor Richard Hull. Your support and guidance over the last 3 years has been absolutely crucial to the progress of this work and to my development as a scientist. I'm incredibly grateful for all of the opportunities you have presented me with. I've been very lucky to have an excellent supervisor, and I hope you know that I appreciate it.

I'd like to thank everyone at UCLan that has helped me over the years, including the technical support staff in both chemistry and the analytical suite. In particular, I would like to direct special thanks to Steve Harris for all of his support throughout my PhD and for his friendship. Without your help, I wouldn't have been able to complete this work. I wish you, and your family, all of the best.

My deepest gratitude goes to all of my colleagues in the fire research group for their support and friendship, whether they have moved onto new things, or are still lucky enough to be working in such an excellent group. Kate and Nicola, you have been there since the beginning and I appreciate every second of our time working together. To Linda Bengstrom, I did not expect to make such a close friend during this PhD, but I consider myself very lucky to have met you.

To my closest and oldest friends, Tash, Brendan and Crene, I'd like to thank you for helping me to (somewhat) maintain my sanity over the years. I cherish our friendship and look forward to many more good times in the future.

I would like to express my love and appreciation to my family for all of their support. My parents Andy and Debi, and my brothers Jack and Sam, have always been there for me when I needed help or some time away from work. I hope I've done you all proud.

Lastly, and most importantly, to my loving and supportive partner, Alicia: thank you for being there for me. Your unfailing support has gotten me through many tough times, both in my work and in my health. I hope that you know that you have my love and appreciation. I look forward to our future together.

Chapter 1

1.0 Introduction to the project

Insulation materials are ubiquitous in the modern built environment. The rising demand for, and importance of, energy conservation, combined with increasing energy costs has resulted in a flourishing industry that is expected to continue to grow each year. The global insulation market was estimated to be valued at USD 52.30 billion in 2017¹. A broad range of insulation materials are commonly available ranging from combustible insulation such as polystyrene, polyurethane and phenolic based foams, to non-combustible products such as glass and stone wool. As a result of their widespread usage, insulation materials have become a focus of research and government regulation for their potential fire hazards.

At the time of writing, the fire hazards of insulation materials are very much in the public mind as a result of the Grenfell Tower fire. 72 people were killed and a further 74 were hospitalised, with an on-going inquiry “to establish the facts of what happened at Grenfell Tower in order to take the necessary action to prevent a similar tragedy from happening again”².

1.0.1 Aim of the Project

The ultimate aim of this project is to quantify the fire hazards of insulation materials.

1.0.2 Objectives

In order to achieve the aim of the project, a number of key objectives were outlined:

- Relate the factors leading to the high fire toxicity of polyurethane foams to their chemical composition.
- Determine the acute toxicants evolved from a range of insulation materials under different fire conditions in the steady state tube furnace (SSTF).
- Develop the methodology for estimation of fire hazard from burning insulation materials based on a combination of fire toxicity data and reaction to fire data.
- Develop and improve methods for the quantification of toxic products from burning insulation materials.
- Support the development of the SSTF as a standard method for the assessment of toxic products released by burning insulation.

1.0.3 Layout of the Thesis

This work follows the traditional format of a scientific thesis. Chapter 1 is an introduction to the project followed by an introduction to the subject of fire science. It covers reaction-to-fire and its assessment, followed by fire toxicity and its assessment. Finally, insulation materials are introduced in terms of their usage, chemistry and fire toxicity. Chapter 2 includes a description of the samples selected for this work, followed by descriptions of the experimental methods used during the analysis of the samples.

Chapter 3 contains the results of this work and a discussion of those results. In order to improve the readability of the results, some data has been moved from chapter 3 to the appendix. Appendix A contains the output reports of the SBI testing in accordance with EN 13823. Appendix B contains the outputs of the steady state tube furnace testing, including equivalence ratios and yields for each material tested in 3 different fire conditions.

Chapter 4 contains the conclusions of this work alongside suggestions of future work that could be used to further develop the outcomes of this thesis.

In addition to the work included in the main text of this thesis, appendix C contains the collected publications that were released throughout the duration of the work. This includes directly relevant publications, such as the review of polyurethane fire toxicity, and publications that are not directly relevant to the thesis, including a publication assessing the flammability and fire toxicity of upholstered furniture.

1.1 Introduction to the Subject

Fires are a costly threat to both life and property. For decades, government and building regulators worldwide have attempted to prevent deaths from fire. As a result of the Great Fire of London in 1666, the UK Government brought in the first building regulations relating to fire which have evolved over the last 350 years.

In the late 1950s, the number of fire deaths in the UK showed a sharp rise until the late 1980s. This can be attributed to a number of factors including the shift from natural construction materials (such as wood and stone) to synthetic construction materials, and the widespread use of synthetic polymer products such as upholstered foam furniture. The higher flammability of these materials caught many by surprise and has been blamed for the almost tripling of fire deaths over 20 years (Figure 1)³. A similar trend became visible in the statistics for the injuries of fire victims (Figure 2). In both sets of data, there is a clear shift from burns being the major cause of death or injury to smoke becoming the most significant factor. Even with the reduction in fire deaths after the 1980s, death or injury by smoke toxicity still makes up a significant proportion of reported data, indicating that fire toxicity is a major factor in loss of life from fires. When factoring in unspecified causes of death (usually because the data could not be recorded as it awaited a formal inquest), and death by a combination of burns and smoke, it is reasonable to consider that fire toxicity contributes to over 50% of fire deaths in the UK.

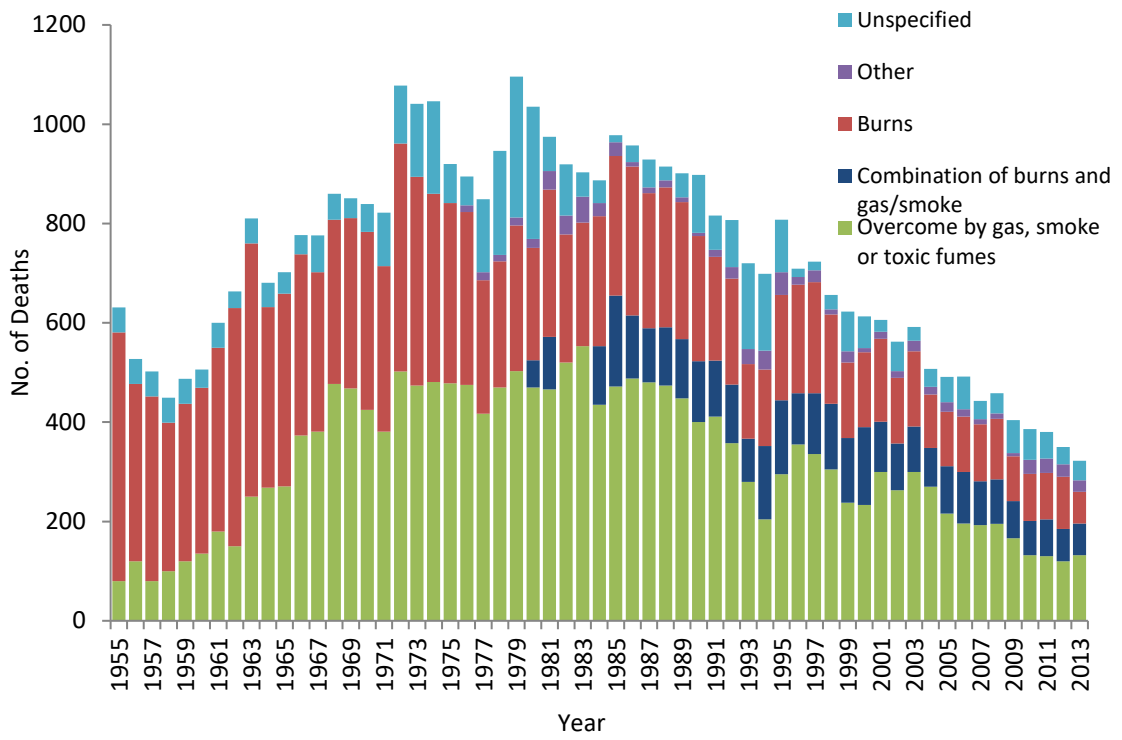


Figure 1 Causes of UK fire deaths from 1955 to 2013³

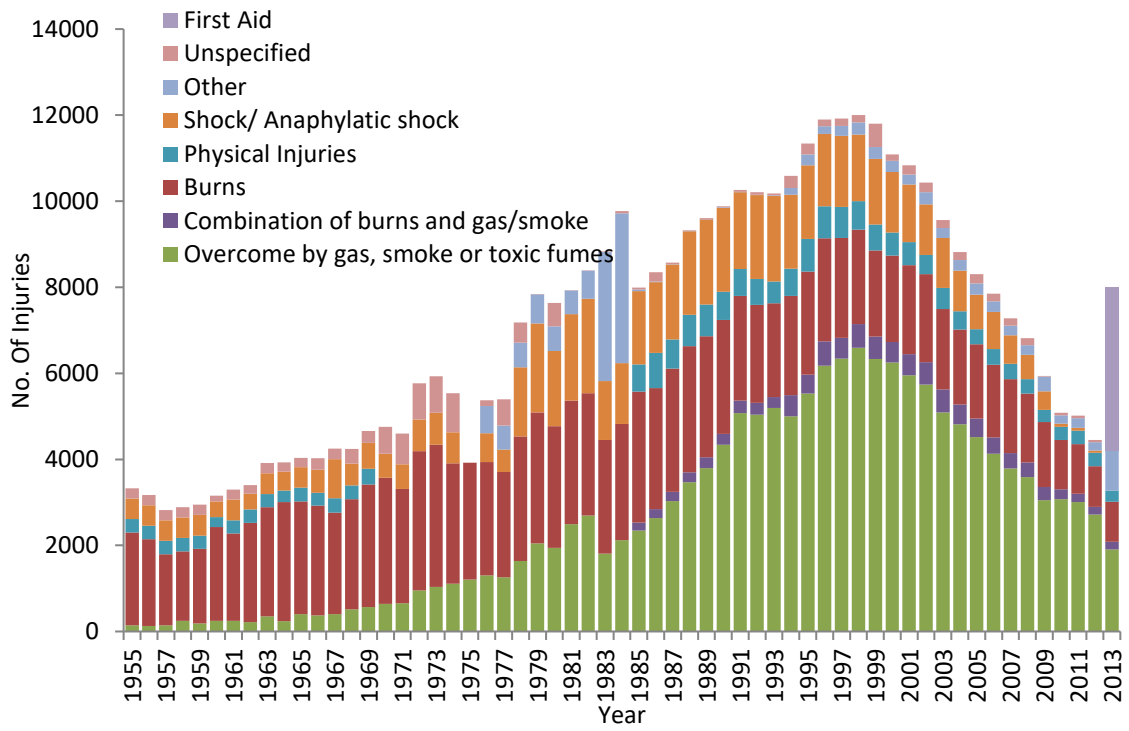


Figure 2 Causes of non-fatal UK fire injuries from 1955 to 2013³

1.2.1 Fire Types and Ventilation Conditions

A large range of factors can be involved when defining a fire. However, the stages of growth of a fire can be simplified into a number of key steps⁴. Figure 3 shows the growth of a hypothetical fire in an enclosure such as a room or building, going through the main stages of fire growth. The fire begins with an early induction period which may include smouldering, followed by ignition with well-ventilated flaming as the fire grows. Once the fire reaches a certain size, the fire growth becomes limited by the oxygen available and the fire becomes under-ventilated. This will continue until fuel and/or oxygen becomes limited enough that the fire begins to decay and possibly smoulder for some time. These characteristic stages of fire growth have been defined in more detail in ISO 19706 (Table 1)⁵. Factors such as heat flux, temperature, oxygen concentrations (to the fire and in the effluent), equivalence ratio, CO:CO₂ ratio, and combustion efficiency all factor into defining the fire stage. Equivalence ratio, in particular, is an effective way of defining the ventilation condition of a flaming fire.

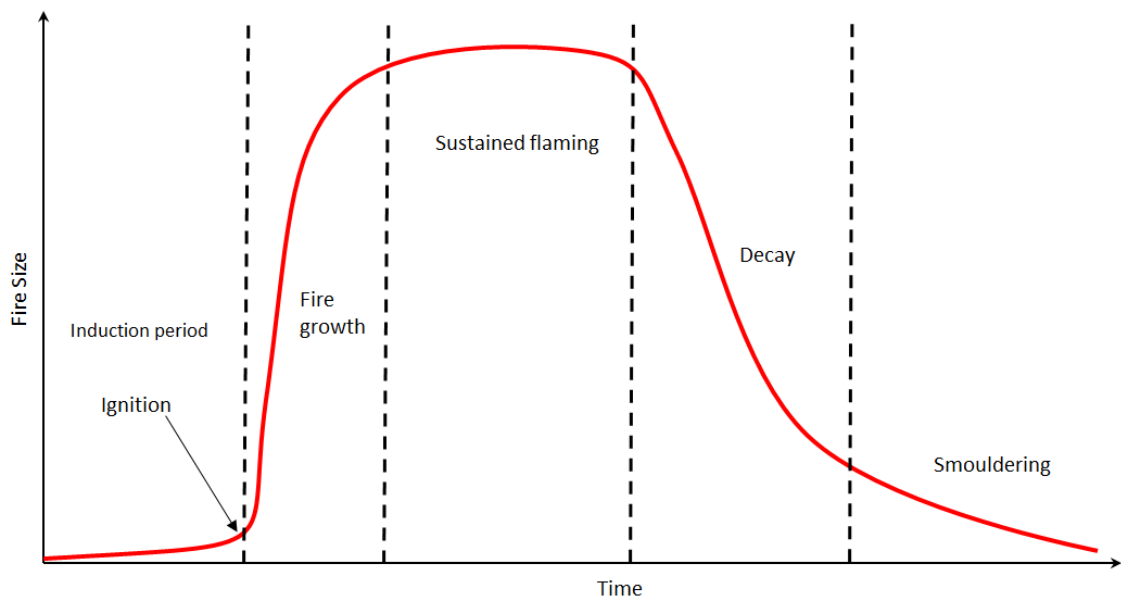


Figure 3 A simplified fire growth curve

Fire Stage	Heat /kW m ⁻²	Max Temperature /°C				Oxygen /%		Equivalence Ratio /φ	V _{co} /V _{co2}	Combustion efficiency /%
		Fuel	Smoke	In	Out	Ratio /φ				
<i>Non-Flaming</i>										
1a. Self sustained <i>Smouldering</i>	N.a.	450-800	25-85	20	0-20	-	0.1-1.0	50-90		
1b. Oxidative, external radiation	-	300-600		20	20	-				
1c. Anaerobic external radiation	-	100-500		0	0	-				
<i>Well-ventilated flaming</i>										
2. Well- ventilated flaming	0-60	350-650	50-500	~20	0-20	<1	<0.05	>95		
<i>Under ventilated Flaming</i>										
3a. Low ventilation room fire	0-30	300-600	50-500	15-20	5-10	>1	0.2-0.4	70-80		
3b. Post Flashover	50-150	350-650	>600	<15	<5	>1	0.1-0.4	70-90		

Table 1 Classifications of characteristic fire stages based on ISO 19706⁴

Equivalence ratio (φ) is defined as the ratio of the actual fuel/air ratio to the stoichiometric fuel/air ratio (Equation 1). ISO 19706 defines the equivalence ratio of well-ventilated flaming as an equivalence ratio of less than 1 and under-ventilated flaming as an equivalence ratio of greater than 1. This is misleading as an equivalence ratio of 0.99 would be well-ventilated and 1.01 would be under-ventilated. In reality, early well-ventilated flaming will generally show an equivalence ratio of 0.5-0.7, which will increase as the fire grows. Once the fire is large enough the equivalence ratio will pass 1 as the amount of oxygen available (more accurately the amount of oxygen actually able to reach the flame) becomes limited. As the fire becomes severely under-ventilated equivalence ratios of 1.5-2.0 and above can be reached before the fire decays.

$$\varphi = \frac{\text{Actual fuel - to - air ratio}}{\text{Stoichiometric fuel - to - air ratio}}$$

Equation 1 Definition of equivalence ratio

In 1995, Pitts demonstrated through a review of available literature that the yield of carbon monoxide from burning simple hydrocarbons is directly related to equivalence ratio⁶. Oxygen-rich conditions result in the near complete combustion of hydrocarbons yielding <0.01 g of CO per gram of fuel (g/g), while ventilation-controlled conditions yield 0.2 to 0.3 g/g. As CO is a product of incomplete combustion, the partial oxidation of fuel carbon due to limited oxygen leads to increased yields. Similarly, an oxidised product such as NO₂ will be in limited yield in oxygen starved conditions, as not enough oxygen is available to achieve complete oxidation and vice versa. As a result of this well-defined relationship, CO yield can act as a useful diagnostic for estimating the ventilation condition of a fire. A CO yield of >0.2 g/g is generally indicative of under-ventilated conditions, although factors such as flaming or non-flaming combustion, temperature and material composition can all affect CO yield. The relationships between toxic products and equivalence ratio have been studied in detail both in the bench^{7,8} and large-scale^{9,10,11}, and the effects of ventilation conditions on specific toxicants are discussed later in this work.

1.2.2 Reaction to Fire and Methods of Assessment

Reaction to fire testing is the assessment of the flammability and ignitability of products, as well as their contribution to fire growth. In order to quantify reaction to fire, countless standard tests have been developed, with varying likeness to real-life fires. While there are countless parameters that contribute to material reaction to fire, there are two major factors that are considered to be most important: heat release (both average heat release rate and peak heat release rate), and ignitability (increasing ignition resistance with higher ignition temperature or longer delays until ignition)¹². However, there is some controversy over which is the most important factor to control to minimise fire hazard.

Heat release rate (HRR) is defined as the mass loss rate of a material multiplied by its heat of combustion, with a plot of heat release rate over time during the combustion of a material providing useful information about its burning behaviour. In particular, peak heat release rate (PHRR) is generally considered to be the most important parameter driving flame spread during polymer combustion. The measurement of heat release rate has been well-established using oxygen depletion calorimetry, although several other methods (of varying reliability) exist including the measurement of temperature rise, mass loss, or CO₂ production¹³. The total heat released (THR) can be calculated by integrating the heat release curve, and is a measure of the total amount of heat released by a burning material in a specific fire condition.

The Cone Calorimeter (ISO 5660), was specifically developed to determine the HRR and effective heat of combustion of burning materials. It has been applied to building materials (ISO 5660-1¹⁴) and to furnishings. In the standard cone calorimeter test, a horizontal 100 mm² sample of thickness up to 50 mm is mounted underneath a cone heater set to produce a uniform 10-100 kW m⁻² (Figure 4). A spark igniter is positioned above the sample to provide an ignition source. The heat release measurements are provided using oxygen depletion calorimetry, with additional measurements of mass loss rate, CO and CO₂ by non-dispersive infrared (NDIR), and smoke measurements.

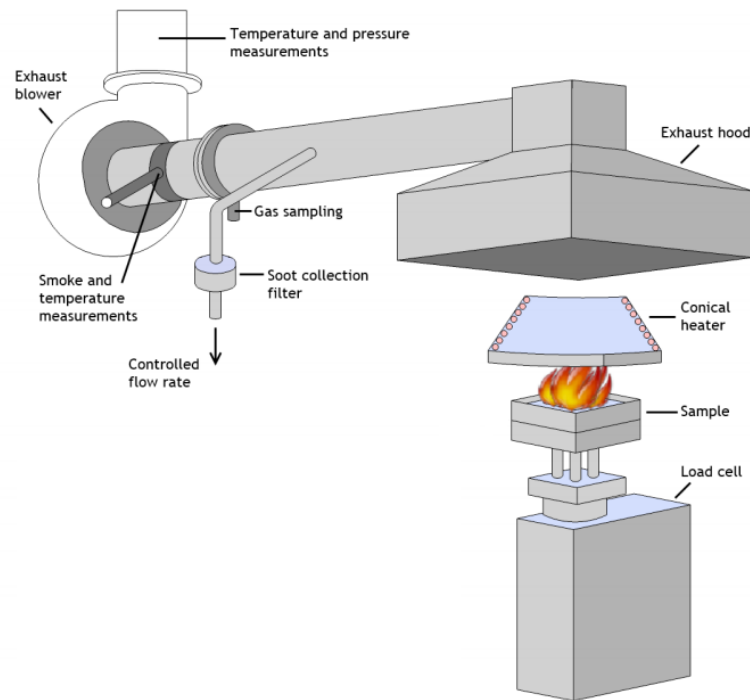


Figure 4 The ISO 5660 Cone Calorimeter¹⁵

As mentioned previously, ignition is another important factor in controlling fire hazard. It can be spontaneous (auto) and piloted (forced). There are a number of factors that influence ignition and ignitability, including the source of ignition (e.g. a flame or radiant heat source), the pyrolysis temperature of the material, and the presence of flame-retardant chemical additives (such as char-formers or gas-phase reaction inhibitors)¹⁶. The ignition temperature of the material is considered by some to be the most common quantitative measure of material flammability; however the time to ignition will depend on the ignition source. Well-defined ignition sources have been used¹⁷. The cone calorimeter provides ignitability data based on time to ignition at a particular heat flux. Other standard ignitability tests exist such as ISO 5657¹⁸ which uses a radiant heat source (also using a cone heater), and ISO 11925-2¹⁹ which uses direct application of a flame.

The argument for the importance of reducing ignitability is obvious in that a fire that does not start cannot pose a threat to life or property, and a fire that is delayed in ignition is more likely to be stopped before the fire can grow to become dangerous. A delayed time to ignition can increase the time it takes for a fire to spread in a compartment – increasing the time available for escape and for fire and rescue teams to respond. In reality it would be difficult to measure how many fires were prevented due to reduced ignitability as they are unlikely to be reported, but this does not detract from the importance of reducing ignitability.

In order to achieve a standard for the assessment of building product reaction-to-fire behaviour (including insulation materials), the European Commission developed the Single Burning Item (SBI) test (EN 13283)²⁰. The SBI test was designed to assess the performance of building products in a real-scale scenario, wherein an L-shaped construction is exposed to a single burning item (a sandbox burner) in a corner configuration where the two panels meet (Figure 5). The SBI test measures a number of reaction to fire properties including the fire growth rate (as a product of heat release rate) (FIGRA), THR, the smoke growth rate (SMOGRA), total smoke produced (TSP), lateral flame spread and several parameters to define flaming droplet and particle production.

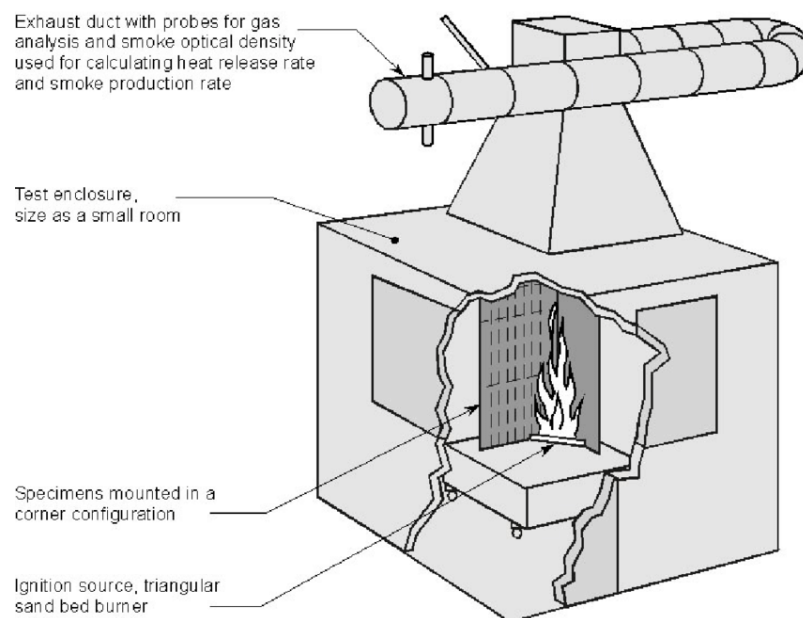


Figure 5 The SBI test apparatus²¹

SBI test data is utilised in the Euroclass system, a harmonised system for reaction to fire performance testing of building materials. Building products are classified based on their reaction to fire properties from a number of tests including ISO 11925-2 (ignitability test), ISO 1182²² (non-combustibility test) and ISO 1716²³ (bomb calorimetry) (Table 2). The system is generally considered to be successful, with coordination from regulators, industry and researchers²⁴. The SBI test can provide classification for approximately 90% of construction materials used in the EU²⁵.

Class	Performance description	Test methods	Fire scenario	Heat attack	Example products
A1	No contribution to fire	ISO 1182 and ISO 1716	Fully developed room fire	At least 60 kW m ⁻²	Products of natural stone, concrete, bricks, ceramics, glass, steel and metallic products
A2	“	ISO 1182 or ISO 1716 and EN 13823	“	“	Products similar to class A1 but with small amounts of organic content
B	Very limited contribution to fire	EN 13823 and ISO 11825-2	Single burning item in a room	40 kW m ⁻² on a limited area	Gypsum boards with thin surface linings and fire retardant wood products
C	Limited contribution to fire	EN 13823 and ISO 11925-2	“	“	Phenolic foam, gypsum boards with different surface linings (thicker than class B)
D	Acceptable contribution to fire	EN 13823 and ISO 11925-2	“	“	Wood products with thickness > 10 mm and density > 400 kg m ⁻³ (depending on end use)
E	“	ISO 11925-2	Small flame attack	Flame height of 20 mm	Low density fibreboard, plastic based insulation products
F	No performance requirements	-	-	-	Products not tested

Table 2 Description of the Euroclass System requirements and example products²⁶

1.2.3 Fire Toxicity

The combustion of polymeric materials is a complicated process which produces a cocktail of chemical products, many of which will vary in yield dependant on the ventilation conditions. The most common of these toxic products can be classified into a number of categories (although many can overlap into different categories).

Asphyxiant Gases

At their simplest definition, asphyxiant gases prevent the proper supply of oxygen to the body and this, in turn, induces generalised hypoxia. The symptoms of acute generalised hypoxia can include tachycardia (abnormally elevated heart rate), arrhythmias (irregular heart rate), increased respiratory rate, dyspnoea (difficult or laboured breathing), impaired judgement, weakness, coma, and eventually death²⁷. Many of these symptoms are likely to impair the ability of a person to escape from a fire, should they not be outright killed by asphyxiation.

Some occupational health sources prefer to break the definition down further into 'simple' and 'chemical' asphyxiants²⁸. Simple asphyxiants act by the displacement of oxygen in the surrounding environment, which will prevent an individual from acquiring sufficient oxygen. Chemical asphyxiants induce asphyxia by interfering with the ability of the body to deliver oxygen to cells (such as carbon monoxide) or for cells to properly utilise oxygen for cellular respiration (such as hydrogen cyanide). For the sake of completion, carbon dioxide and oxygen depletion have been included in this section, although it has been argued that when breathing fire effluent, a person would already have been killed by the combination of CO and HCN (if present) before CO₂ and oxygen depletion become relevant.

Carbon Monoxide:

Carbon monoxide (CO) is a colourless, odourless, non-irritating gas which is commonly formed as the result of incomplete combustion. CO is a toxicant that has affected humans throughout history, with Aristotle noting the toxic fumes produced by the burning of coal in the 3rd century B.C.²⁹. The mechanism by which CO is toxic is related to its affinity to haemoglobin (Hb) in the blood. Its affinity to Hb is 200-250 times greater than the affinity of oxygen to Hb. This results in CO outcompeting oxygen at the binding sites to produce carboxyhaemoglobin (COHb), which is not readily displaced. The formation and persistence of COHb has a cumulative effect that reduces the overall ability of blood to carry oxygen around the body which increases the likelihood of hypoxia³⁰. The effects of increasing levels of CO exposure are well understood (Table 3)³¹.

Concentration /ppm (%)	Symptoms
100 (0.01%)	Dizziness, headaches, weariness, impaired judgement and visual perception in two to three hours.
1000 (0.1%)	Previous effects are enhanced, with potential for convulsions within 45 minutes.
3000 (0.3%)	Intense headache, dizziness and nausea in 10 minutes, death in less than 1 hour.
6000 (0.6%)	Intense headache, dizziness and nausea occur rapidly. Convulsions, respiratory arrest and death within 30 minutes.

Table 3 Effects of acute carbon monoxide exposure at various concentrations³¹

The severity of the symptoms that result from CO inhalation are considered to be directly related to the level of COHb in the blood (usually expressed as a %). This has led to COHb% being frequently quoted to confirm the cause of death by smoke inhalation in a fire. If a person was killed before the fire was started, then they would not have inhaled any CO. A post-mortem COHb level of 70+% following exposure to a fire will suggest a CO poisoning as the cause of death, meanwhile a level between 30-70% will likely be considered a contributing factor to the cause of death. Levels less than 30% are reported to suggest a different cause of death in a fire³². Although blood COHb levels are thought to provide an insight into the cause of death in a fire, the absorption and elimination rate of CO in the blood is complicated by a large number of physiological factors. This fact, in combination with the time between exposure and measurement, means that the amount of CO present in the fire cannot be reliably estimated from blood COHb.

Several authors have noted that the toxicity of CO is not exclusively related to the hypoxia it induces^{33,34}. Many of the 'extra-haemoglobin' effects of CO poisoning are consequence of the fact that CO is a signalling molecule in the body, and can also bind to active sites in enzymes. Such interference of normal bodily function can contribute to the neurological, cardiac, and cardiovascular effects of CO poisoning.

As mentioned previously, CO is commonly a product of the incomplete combustion of organic carbon in fires in both smouldering and flaming combustion. Smouldering conditions can result in relatively high yields of CO; however the actual mass of burning fuel is usually small and thus the total amount of CO a person could be exposed to would therefore be low. The production of CO in flaming combustion is directly related to the ventilation condition, as the fire grows and becomes under-ventilated, the amount of carbon that is not fully oxidised to CO₂ increases, resulting in higher yields of CO. As previously described, this relationship has been firmly established for CO by Pitts in 1995⁵ and many subsequent works.

Hydrogen Cyanide:

Hydrogen Cyanide (HCN) is an organic compound with a faint smell of bitter almonds that boils at 25.6°C and is renowned for its highly toxic nature. Upon exposure by inhalation or absorption through the skin, HCN will dissociate to form cyanide ions in the blood which will be rapidly distributed around the body. The cyanide ion reversibly binds to the metals (commonly iron) in many enzymes, inhibiting their function and in turn inhibiting cellular function. In particular, cytochrome c oxidase is a major target of cyanide exposure, as it is vital to the function of mitochondria in cells. The binding of cyanide will block the transfer of electrons during cellular respiration, inducing cellular hypoxia as cells are unable to properly utilise oxygen. Tissues most vulnerable to this inhibition are those with a high oxygen demand such as the brain, heart and central nervous system (CNS)³⁵.

HCN is a sudden killer, which is ~35 times more toxic than CO. The severity of the exposure is dependant of the concentration of HCN present and the duration of the exposure. A concentration of over 300 ppm will kill extremely rapidly, a dose of 150 ppm is likely to incapacitate in 1-2 minutes and a dose of ~90 ppm is likely to incapacitate after around 30 minutes. Doses lower than 80 ppm will induce toxic symptoms such as headaches, nausea, dizziness, confusion, weakness, loss of coordination, hyperventilation, arrhythmia, bradycardia (abnormally slow heart rate), loss of consciousness and coma³⁶.

In a fire, HCN can be produced to some degree by the combustion of any nitrogen containing organic material³⁷. Materials such as nitrile rubber, wool, nylon, acrylonitrile and polyurethanes can all produce HCN when they burn. This is especially so during under-ventilated burning where the HCN yield increases similarly to CO. Most, if not all, of these materials are found in modern buildings and homes so the likelihood of HCN forming in a fire is high. The toxicity of HCN, combined with its formation from common materials makes it a major factor in fire toxicity. However, the situation in which the yield of HCN is high also correlates with high CO yield. This makes it challenging to fully assess the contribution HCN to incapacitation and death in fires when both CO and HCN are present. Levin and co-workers presented evidence that CO and HCN interacted in an additive manner, reducing the concentration required to produce a fatal dose³⁸. Both CO and HCN place stress on the body through hypoxia (one by denying the delivery of oxygen and the other preventing the utilisation of what little oxygen there is available), and by directly interfering with other biological processes such as cell signalling and enzyme activity.

Carbon Dioxide:

Carbon Dioxide (CO₂) is a colourless, odourless gas present in air at a concentration around 0.04% (400ppm). In addition to being a natural product of the respiration of living organisms, it is also the product of the complete combustion of carbonaceous materials. When a fire is small and well-ventilated, the CO₂ levels will be at their highest, but as the fire grows the production of CO₂ will steadily decrease and shift towards the toxic products of incomplete combustion such as CO. While CO₂ levels will not be a major threat when a fire is at its most 'toxic', exposure to increased CO₂ has several adverse effects that can affect ability to escape a fire.

CO₂ acts as a simple asphyxiant and an increased level of CO₂ in the atmosphere reduces the amount of oxygen available to the body. Since CO₂ effectively replaces oxygen in a fire, oxygen depletion and CO₂ asphyxiation are likely to occur simultaneously. However, in isolation, the CO₂ produced by a fire is not likely to be a significant threat to healthy individuals. Instead, it is the combination of physiological effects of CO₂ inhalation and their subsequent enhancement of the effects of other toxicants that make CO₂ an important factor in fire toxicity. Increased blood CO₂ stimulates both the rate of breathing and the volume inhaled per breath, thus increasing the respiratory minute volume (RMV). RMV can increase by up to 50% in an atmosphere of only 2% CO₂, and 8-10 times in an atmosphere of 10% CO₂³⁹. This results in an increased uptake of other toxic gases in the fire effluent.

Additionally, it has been reported that the interaction of CO and CO₂ can have an additive toxicological effect as a result of severe acidosis³⁹. The effect of metabolic acidosis from CO (a result of reduced oxygen availability causing lactic acid build up in the body) and respiratory acidosis from increased CO₂ (which results in increased blood acidity from carbonic acid build up) caused the death of test animals over the next 24 hours when the levels were expected to be sub-lethal. Severe acidosis can cause a multitude of symptoms that would hinder the ability of a person to escape in a fire such as headache, tiredness, confusion, weakness, seizures, nausea, loss of consciousness, coma and death. Further to this, primary treatment with oxygen for CO exposure may not be enough to offset the symptoms of acidosis which can have a prolonged recovery period (although treatment of acute acidosis can be achieved via alkali therapy once it has been identified).

While, CO₂ is not the biggest factor in fire toxicity (compared to CO or HCN especially) it is important to consider, due to its contribution to the 'asphyxiant load' a person would be exposed to, its additive effects on other toxicants, and the potentially lethal after effects of acidosis.

Low Oxygen Concentration:

While not a direct asphyxiant, the reduction in atmospheric oxygen as a result of its depletion during combustion can result in adverse health effects. As the oxygen concentration decreases from 20.95%, negative effects such as loss of coordination, poor judgement and rapid fatigue can begin to occur. These effects will be compounded with the other asphyxiant effects from exposure to fire effluent, leading to an increased 'asphyxiant load' on the body.

Irritant Gases

Irritant gases and smoke prevent escape from fires by producing sensory and respiratory tract irritation. This can cause effects ranging from discomfort to severe pain depending on concentration. These effects can include pain in the eyes, nose, throat and chest, coughing, bronchoconstriction and laryngeal spasms. If these effects do not incapacitate a person outright, they can potentially have a number of behavioural effects such as causing a person to remain where they are instead of attempting escape. This leaves them effectively 'incapacitated' and susceptible to the lethal effects of CO and HCN⁴⁰.

The most common irritants evolved during combustion include hydrogen halides (HCl, HBr, and HF) and the oxides of nitrogen and sulphur. There are also a large number of organo-irritants whose yields will be more dependent on the chemical composition of the burning material and the ventilation condition (such as aldehydes, isocyanates and organo-phosphorus fragments from the decomposition of chlorinated organo-phosphate flame retardants).

Hydrogen Halides:

Hydrogen halides (HX) are released during the thermal decomposition of halogen containing materials. They form their equivalent halogen acid on contact with liquid water or water vapour (for example in the respiratory tract or eyes). They are highly irritating at relatively low concentrations and directly toxic at higher concentrations. Acid gases such as hydrogen halides present some challenges for sampling due to the water vapour present in fire effluent and potential cold spots in test apparatus allowing for it to condense before it is sampled. This is a common experimental challenge that is relevant to many toxic products in fire analysis, but is particularly prevalent for acid gas products.

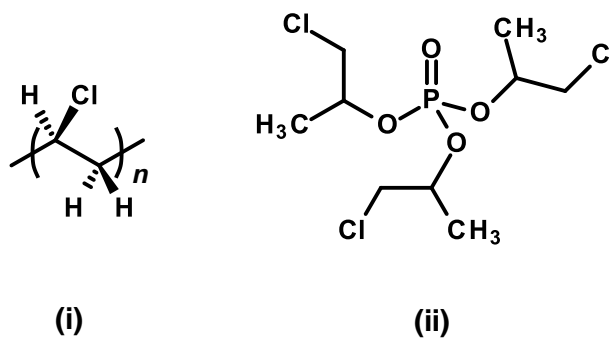


Figure 6 i) Structure of PVC ii) Structure of TCPP

Hydrogen chloride (HCl) is commonly released during the combustion of materials such as polyvinylchloride (PVC) or from the decomposition of chlorinated flame retardants such as the commonly utilised tris-(2-chloroisopropyl) phosphate (TCPP) (Figure 6). Even at low concentrations, the effects of HCl are severe (Table 4)⁴¹. Concentrations higher than 5 ppm cause sensory and respiratory irritation, which will increase in severity with concentration, becoming intolerable above 50-100 ppm. Persistent exposure can lead to damage to the alveoli and pulmonary oedema (fluid accumulation in the lungs)⁴². Levels above of 1000 ppm can be extremely dangerous and could cause death. In situations where pulmonary damage is caused, there is potential for the formation of Reactive Airways Dysfunction Syndrome (RADS) which is an irritant induced asthma.

Concentration (ppm)	Signs and Symptoms
<5	Detection by odour and extremely light irritation
>5	Irritating to nose ,eyes and throat
>10	Increasingly irritating
35	Throat and lung irritation with sneezing and chest pain
50-100	All of the above intensify along with feelings of suffocation
300	Damage to alveoli and pulmonary system, potential RADS after exposure ends
1000+	Extremely dangerous and potentially fatal

Table 4 Effects of HCl exposure with increasing concentration⁴³

Hydrogen bromide (HBr) is another commonly found HX acid gas, and as such can be expected to act similarly to HCl, although there is limited data available on its effects. It is an extremely irritating gas and is a stronger acid than HCl. In fires it is generally formed from the thermal decomposition of brominated flame retardants (BFRs). While there is some argument as to their fire toxicity contribution (due to their comparatively low yields in fires), the severely irritating nature of HBr will contribute to the irritation a person may experience from smoke exposure, hindering escape and decreasing their chance of survival. A summary of the effects of HBr exposure can be found in Table 5⁴³.

HBr Concentration (ppm)	Signs and Symptoms
~5	Nose and Throat Irritation
100	Severe sensory irritation
1000	Incapacitation, pulmonary and alveoli damage
1000+	Potentially fatal

Table 5 Effects of HBr exposure with increasing concentration⁴³

Hydrogen fluoride (HF) is not as commonly found in fires as HCl and HBr, as it is usually only found in small quantities in very specific applications. Sources of HF in fires can include the combustion of fluorinated polymers (such as PTFE) and also from the decomposition of fluorinated 'halon' fire extinguishing systems in high temperature fires (which are mainly used in military applications and rarely in hand-held fire extinguishers⁴⁴). Like other HX compounds, HF is highly irritating at relatively low concentrations. At high concentrations it can penetrate deep into the lungs, causing pulmonary damage and RADS. In addition to being a powerful irritant, HF is also highly toxic due to the effects of the fluoride ion on biologically important ions such as Ca^{2+} and Mg^{2+} , causing nerve damage and potential cardiac arrest. Its effects may not be immediately evident and can result in delays seeking medical treatment⁴⁵.

While HF is unlikely to be present in significant quantities in most fires, chlorinated and brominated polymers are widespread in the modern environment and their decomposition in fires can lead to the production of HCl and HBr. These halogen acids will contribute to the cocktail of irritants produced, increasing the risk of incapacitation and death by prolonging exposure to asphyxiant gases due to inability to escape.

Nitrogen Oxides:

Nitrogen oxides (NO_x) are gaseous products of the combustion of nitrogenous materials. They can also be formed by the reaction of nitrogen and oxygen, but this only occurs at temperatures above 1200°C. The two most commonly described NO_x products in fire effluent are nitrogen oxide (NO) and nitrogen dioxide (NO₂). Both compounds are reported to have toxic effects but there is no clear evidence in the literature of the fire toxicity of each compound; instead their combined toxicity is commonly reported⁴⁶.

NO₂ is a brown, irritating, toxic gas which will hydrolyse into nitrous and nitric acid on contact with water. Exposure to NO₂ results in irritation to the upper respiratory tract and higher dose can lead to pulmonary oedema and death. The most severe symptoms may appear hours or days after the exposure leading to unexpected deaths⁴⁷. There is very little information about the toxicity of NO, and it is expected that acute exposures to NO are not likely to cause a severe reaction, and that chronic exposure is the only concern⁴⁸.

In fires, the toxicity of NO_x compounds are assumed to be equal to treating all NO_x present as NO₂. However, data in the literature suggests that the majority of NO_x present in fire effluent is NO, which is considerably less toxic than NO₂. This indicates that the contribution of NO_x compounds to fire toxicity is overstated by assuming the worst case scenario – that all NO_x is NO₂, when in reality the toxicity would be lower than previously expected⁴⁶.

Sulphur Oxides:

Comparably to fuel nitrogen and NO_x products, the combustion of fuel sulphur can lead to the production of sulphur compounds, such as sulphur oxides (SO_x), in the fire effluent.

Sulphur dioxide (SO₂) is a colourless gas with a distinctively pungent smell. The irritating, rotting smell of SO₂ is detectable by the human nose at concentrations as low as 0.3 ppm. In fires, SO₂ is formed from the combustion of sulphur containing materials such as phenolic resins and foams, and vulcanised rubbers¹⁴.

SO₂ acts as a respiratory irritant and also increases airway resistance, even at concentrations as low as 1 ppm. This effect continues to increase in severity as the concentration increases. This irritation is caused by the formation of sulphurous acid upon its reaction with water. These effects will continue to increase until death occurs as a result of airway blockage and severe irritation⁴⁹. SO₂ presents a particularly high risk to people with pre-existing respiratory conditions, as they will be affected by it much more severely and at lower concentrations than a healthy individual⁵⁰.

Sulphur trioxide (SO₃) is a similarly irritating acid gas that forms sulphuric acid on contact with water. It rapidly takes up water from the atmosphere (and potentially from fire effluent) to produce sulphuric acid which is severely irritating to any tissues exposed. Its action is reportedly similar to that of SO₂ but with a more severe irritant action⁵¹.

Aldehydes:

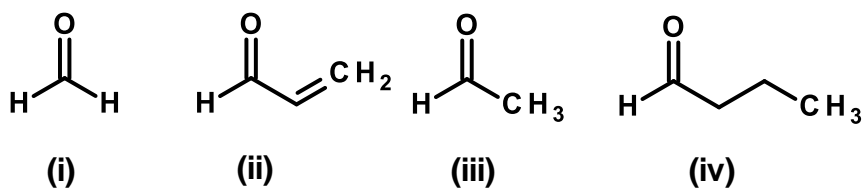


Figure 7 Structures of common aldehydes found in fire effluents i) formaldehyde ii) acrolein iii) acetaldehyde iv) butyraldehyde

The combustion of organic polymers will likely result in the formation of partially oxidised organic fragments such as aldehydes and ketones; the yields of which will increase as the fire becomes under-ventilated. There are several potential aldehydes that could be formed in a fire, but generally formaldehyde and acrolein are most toxicologically significant (with acetaldehyde and butyraldehyde also receiving some attention in the literature) (Figure 7)⁵².

Formaldehyde has been reported from the combustion of wood, but there is limited fire toxicity data available from the combustion of polymers. It is known that it is generated during the incomplete combustion of materials such as polyurethane and phenolic foams. Formaldehyde is strongly irritating to the eyes and upper respiratory tract and can cause mild irritation at concentrations as low as 0.2 ppm. Lower respiratory tract and pulmonary irritation can occur from 5 – 30 ppm, with increasing severity until it reaches a potentially fatal dose at 100 ppm⁵³.

Acrolein is a structurally more complex aldehyde compound that is also formed from the combustion of woods, polyurethane and phenolic materials, albeit in lower concentrations than the simpler molecule formaldehyde. A significant amount of its toxicity data has developed from research into its presence in cigarette smoke⁵⁴. It is a highly potent irritant and can cause negative effects at 0.5 – 5.0 ppm⁵⁵. Exposure to over 10 ppm of acrolein can cause severe respiratory distress and potentially death. However, it is also a highly reactive compound, and as such may not survive for long as it moves away from the source of the fire and is exposed to the cocktail of chemicals found in fire effluent.

Isocyanates:

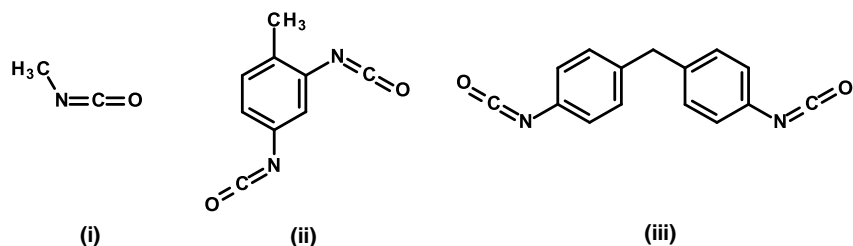


Figure 8 Structure of isocyanates commonly found in fires involving polyurethane materials i) methyl isocyanate ii) 2,4-toluene diisocyanate iii) 4,4'-methylene diphenyl diisocyanate

Isocyanates are commonly used in the production of polyurethane materials. When these polymers thermally decompose, isocyanates are released. While highly reactive and unlikely to persist in fire effluent, isocyanates are highly toxic and irritating so that exposure to even low concentrations can cause harm. Isocyanates can cause severe long term effects even as a result of single exposures, including pulmonary oedema and RADS⁵⁶.

The release of isocyanates from decomposing polyurethane foam generally occurs at lower temperatures and early on in the fire. This is due to their fragile and reactive nature, resulting in their reaction with many components of fire effluent including water, aldehydes, acid gases and more⁵⁷. Both full sized monomers, such as 2,4-toluene diisocyanate (2,4-TDI) and methylene diphenyl diisocyanate (MDI), and also smaller isocyanate fragments such as methyl isocyanate can be formed (Figure 8). Methyl isocyanate is severely irritating as low as 1 ppm and may cause harm to unborn children even from an acute exposure. Any isocyanate fragments are expected to be irritating upon exposure due to the high reactivity of the NCO functional group, so the total isocyanate exposure a person faces may be severe in close proximity to smouldering or flaming polyurethane materials.

Methods of Assessment

Bench-scale methods used for generating toxic effluents from burning materials have been met with controversy. Many are incapable of recreating the most hazardous fire condition from a fire toxicity perspective, under-ventilated burning, which produces the highest yields of CO and HCN.

Under-ventilated conditions are difficult to replicate in the bench-scale. Many methods, such as the smoke density chamber (SDC)⁵⁸ and the NF X 70-100 static tube furnace⁵⁹, have non-constant combustion conditions. The fire is allowed to ignite, grow and decay through the duration of the test, with each stage in this process effectively having a different ventilation condition and yields of toxic products. The ventilation conditions during a fire test are dependent on a combination of material mass loss and available oxygen (which are generally unknown in most bench-scale test methods). Therefore, the ideal scenario requires steady burning in the desired ventilation-condition. The cone calorimeter with controlled atmosphere attachment (CACC) and the fire propagation apparatus (FPA)⁶⁰ are capable of producing a quasi-steady burning period during tests. However, if the ventilation condition is not sustained for a sufficiently long period of time, or the quasi-steady state is unstable as a result of changes in material composition throughout the test (such as surface char formation), then the fire toxicity data generated will have an increased level of uncertainty. The ISO/TS 19700 Steady State Tube Furnace (SSTF)⁶¹ was designed to overcome these problems by feeding a constant mass of material into the hot zone of the furnace to maintain a steady state burn.

As the CACC and SSTF are currently seen as leading contenders for a standardised test method for measuring fire toxicity, both methods are discussed in more detail in the following section.

The Controlled Atmosphere Cone Calorimeter (CACC):

The cone calorimeter is one of the most widely used test apparatus for the assessment of flammability in the world⁶². In order to expand its usefulness, attempts have been made to allow the cone calorimeter to recreate ventilation controlled conditions. The controlled atmosphere cone calorimeter (CACC) operates similarly to the standard cone calorimeter. A sample of up to 100 x 100 x 25 mm is placed horizontally on a load cell below a cone heater, radiating at a known heat flux. This is contained in an enclosure in which a known mixture of nitrogen and air is delivered to control the ventilation conditions within (Figure 9).

The CACC is able, through these modifications, to produce ventilation-controlled conditions. However, when under-ventilated burning is forced, the effluent can continue to burn as it leaves the ventilation controlled enclosure, effectively consuming additional oxygen and affecting the calculated equivalence ratio. This can be overcome by connecting the outlet to an elongated exhaust duct which will allow the effluent to cool before mixing with fresh air.

Another challenge that arises from the CACCs design is the effect on the sample before the test begins. After the sample is inserted into the combustion enclosure, it takes a short amount of time for the desired atmosphere to fill the chamber. During this time, the sample will be pre-heated, which will affect its performance during the test. In under-ventilated conditions, a heat flux of greater than 50 kW m⁻² is required to recreate the conditions of a well-developed under-ventilated fire. This can lead to sample decomposition before beginning of the test. Furthermore, the high heat flux required has the potential to lead to errors in the measurement by the load cell, which is susceptible to the effects of high temperatures. This is due to changes in the physical dimension and structural stability of the load cell resulting in errors in measurement.

The combination of sample decomposition pre-test, and erroneous load cell readings, leads to reduced accuracy of the calculated equivalence ratio, which leads to a poorly defined fire condition. Furthermore, some authors have argued that the CACC is limited in its usefulness as it only gives an 'effective' global equivalence ratio, rather than an averaged local equivalence ratio⁶³. Despite these criticisms, the cone calorimeter is a widely used and well-understood test apparatus, which requires little modification to create a CACC, so research continues in an effort to overcome the challenges presented.

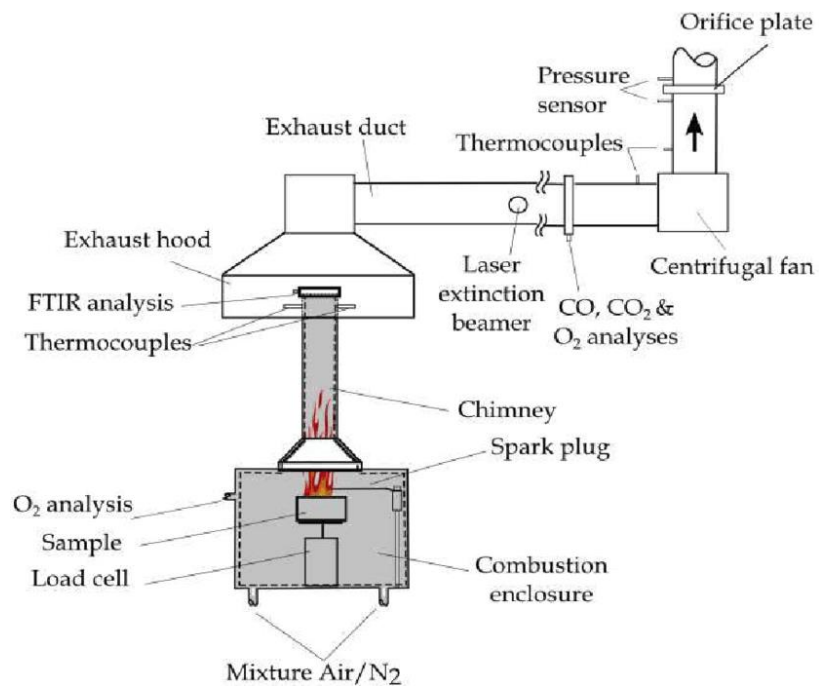


Figure 9 The Controlled Atmosphere Cone Calorimeter⁶⁴

Steady State Tube Furnace (SSTF):

The ISO/TS 19700 Steady State Tube Furnace has been specifically designed for fire toxicity assessment in ventilation controlled conditions⁶¹. An 800 mm sample is fed into the hot zone of a tube furnace at a fixed rate (Figure 10). Air flow into the tube furnace is controlled to achieve the desired ventilation conditions. By adjusting the air flow, temperature and feed rate, the desired fire stage can be recreated in steady burning conditions. These fire stages include oxidative pyrolysis, well-ventilated flaming and under-ventilated flaming. The effluent produced leaves the furnace and enters a mixing chamber where it is diluted by a known amount and sampled for toxic gases. A sample of the effluent may be passed through a secondary furnace to replicate continued burning in the upper layer of a compartment fire. As the SSTF was specifically designed for fire toxicity assessment, it is capable of allowing sampling the toxic gases such as CO, CO₂, HCN, and acid gases. The data generated is readily fed into the methodology outlined in ISO 13344⁶⁵ and ISO 13571⁶⁶ (which are described in the following section) for the purpose of fire toxicity assessment in relation to a specific fire stage.

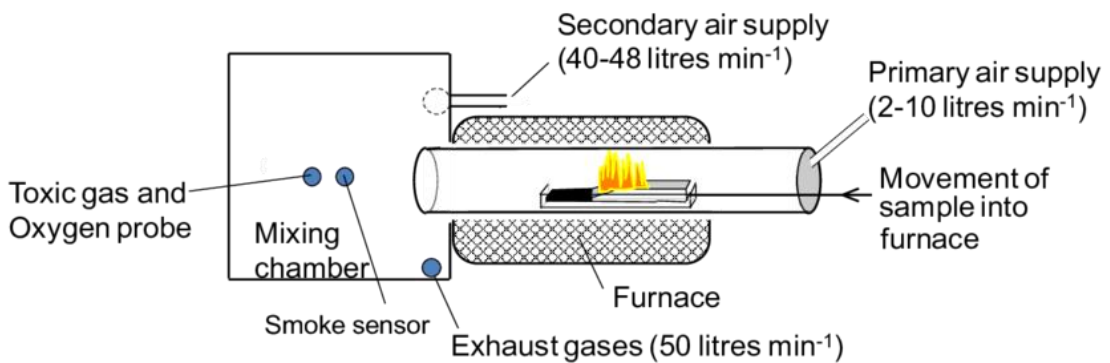


Figure 10 The Steady State Tube Furnace⁶⁷

Quantification of Toxic Hazards from Fires

When the toxicity of fire effluents was first recognised, in the mid-20th century, the toxicity of fire smoke was assessed directly by animal exposure experiments. This provides a measure of the overall toxicity, but does not indicate the specific gases responsible. In recent years, routine use of animal exposure tests is forbidden in most jurisdictions, which has almost completely eliminated their use in fire toxicity assessment. However, modern fire toxicity assessment still relies on some of the data generated during these studies.

In order to quantify the toxic hazard presented by a fire, the general approach adopted is to assume additive behaviour of the individual toxicants, and to present the concentration of each as a fraction of the lethal concentration for 50% of the population. The addition of these fractions gives a fractional effective dose (FED), which when equal to one indicates that the toxic gases will be lethal to 50% of the population. FEDs can be calculated based on rat lethality data for a 30 minute exposure, as described in ISO 13344⁶⁵, or based on estimates of human incapacitation as described in ISO 13571⁶⁶.

The Purser model, outlined in ISO 13344, allows data generated in bench-scale methods (such as the SSTF), to calculate the FED for a 30 minute exposure based on the concentration of toxic gases in the fire (Equation 2). V_{CO_2} is a multiplication factor for CO₂ driven hyperventilation, increasing the contribution of all of the toxic species. The equations also incorporate an acidosis factor to account for CO₂ induced acidosis. The structure of the equation is flexible, allowing for the incorporation of specific toxicants, requiring only their LC₅₀ and the concentration of the gas in the fire effluent.

$$FED = \left\{ \frac{[CO]}{LC_{50,CO}} + \frac{[HCN]}{LC_{50,HCN}} + \frac{[AGI]}{LC_{50,AGI}} + \frac{[OI]}{LC_{50,OI}} \dots \right\} \times V_{CO_2} + A + \frac{21 - [O_2]}{21 - 5.4}$$
$$V_{CO_2} = 1 + \frac{\exp(0.14[CO_2]) - 1}{2}$$

[AGI] is the concentration of acid gas irritants

[OI] is the concentration of organic irritants

A is an acidosis factor equal to $[CO_2] \times 0.05$.

Equation 2 ISO 13344 Purser model for estimating lethality from fire effluent

As the Purser model only accounts for lethality, a different model is required to represent the fact that many people fail to escape from fires due to incapacitation as a result of the compounding effects of asphyxiants, irritant gases, smoke (obscuring visibility), and heat. ISO 13571 considers toxic gases, irritant gases, heat and smoke obscuration individually to present an incapacitation FED/FECs for each. Should any of these factors achieve an FED/FEC over 1 then the persons exposed will be at risk of incapacitation. Equation 3 calculates the FED of the two major asphyxiants, CO and HCN. Unlike the Purser model, the FED is calculated as a function of concentration and time, not just a fixed concentration for a 30 minute exposure. Additionally, HCN has an exponential function to account for the non-linear relationship of its asphyxiating effects. Equation 4 uses a similar principle to calculate the incapacitating effects of irritant gases.

$$FED = \sum_{t_1}^{t_2} \frac{[CO]}{35000} \Delta t + \sum_{t_1}^{t_2} \frac{\exp([HCN]/43)}{220} \Delta t$$

Equation 3 ISO 13571 model to estimate compromised tenability from asphyxiant gases

$$FEC = \frac{[HCl]}{IC_{50,HCl}} + \frac{[HBr]}{IC_{50,HBr}} + \frac{[HF]}{IC_{50,HF}} + \frac{[SO_2]}{IC_{50,SO_2}} + \frac{[NO_2]}{IC_{50,NO_2}} + \frac{[acrolein]}{IC_{50,acrolein}} + \frac{[formaldehyde]}{IC_{50,formaldehyde}} + \sum \frac{[irritant]}{IC_{50,irritant}}$$

Equation 4 ISO 13571 FEC model for compromised tenability from irritant gases

Calculated FED values can be further manipulated to present a 'material-LC₅₀', established in ISO 13344⁶⁵ (Equation 5). This value represents the mass of a burning material in a given fire condition that would produce toxic effluent yielding an FED of one within a volume of 1 m³. The lower the value, the more toxic the material is when burning, for that specific fire condition (and duration of exposure in the case of ISO 13571).

$$\text{material} - LC_{50} = \frac{M}{FED \times V}$$

Equation 5 Equation relating LC₅₀ to FED to calculate a material-LC₅₀

1.2.4 Insulation Materials

Thermal insulation materials have been used throughout human history, but their major development came in the 20th century with demands for increasing energy efficiency alongside the development of new technologies. The widespread use of heating and ventilation in buildings led to architects and engineers developing the first theories of thermal insulation and its related physics. Mineral and glass insulations were used in the early 1900s, with plastic based insulations beginning to appear after the 1950s resulting from the widespread invention of new plastic materials. Polyurethane based materials were developed in 1937 by Otto Bayer and appeared as aircraft coating. The major breakthroughs came in the 1950s with the invention of polyisocyanurate foams. Phenol and formaldehyde foams were developed in the 1970s⁶⁸.

An ideal thermal insulation material would have the desired insulating properties while maintaining desirable physical properties required for the application. The most commonly assessed insulation properties include thermal conductivity, thermal resistance and the U-Value. Thermal conductivity (K or λ) is a constant value for a specific material which describes the ability of heat to travel through a unit area of material. A good insulator will have a low thermal conductivity, minimising the ability of heat to travel through it. Thermal resistance (R-value) is calculated as a function of thermal conductivity and thickness. Materials with a higher thickness will have a higher R-value and a reduced ability for heat to travel through them. U-Value describes heat transfer per unit area through part of a building. Improved insulation is achieved by designing buildings with the aim of reducing U-Values i.e. reducing heat loss through walls, ceilings and floors.

The physical properties of thermal insulation materials that are commonly desired include low density, ease of installation, water resistance, compression resistance and, ideally, reduced cost. Foam insulation materials, such as phenolic and polyurethane foams, are generally cheaper, more lightweight and have good thermal insulation compared to their competitors. However, these foam materials have reduced durability and are flammable. Mineral wool materials, on the other hand, have generally higher density and thickness than foam insulation of the same quality of thermal insulation. This is weighed against benefits of mineral wool materials being non-flammable and having high durability compared to foam insulation in the long-term.

Ultimately, the global market for thermal insulation is expected to grow each year⁶⁹. Governments worldwide are pushing for building construction that utilises energy efficient design, which has led to a widespread demand for insulation materials to meet the goals of these schemes. North America and Europe are the largest and second largest markets for insulation materials respectively. In these regions, domestic construction is the area of highest growth in recent years. However, the thermal insulation market is expected to see significant growth in Asia due to increased construction spending combined with energy efficiency initiatives⁷⁰. Emerging markets, like China and India, will require quality insulation to improve the cost efficiency of their structures and minimise costs.

The main types of insulation assessed as part of this work (PIR, phenolic and mineral wool materials) are discussed in the follow sections.

Chemistry and Fire Toxicity of Polyurethane Foams:

A full and comprehensive review of the chemistry, thermal decomposition and fire toxicity of polyurethane foams was published in the peer-reviewed journal Fire Science Reviews in 2016 as a result of the work carried out as part of this project. The following section contains a condensed version of that review. The full text can be found in appendix C.

(Full citation: McKenna ST, Hull TR (2016) The Fire Toxicity of Polyurethane Foams, Fire Science Reviews, 5(3)).

As mentioned previously, polyurethane materials were discovered in 1937 by Otto Bayer, and since then have developed into a multibillion dollar global industry. Polyurethane insulation materials make up 25% of the polyurethane market, estimated at over \$55 billion in 2016⁷¹. Their other major use is in the furniture and interior industry, with 28% of the polyurethane market.

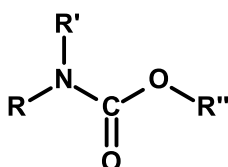


Figure 11 The urethane functional group

Polyurethanes are named for the urethane functional group (Figure 11). Despite their name, the term polyurethane encompasses a broad family of polymers with a large range of functional groups primarily derived from the polyaddition of polyisocyanates and polyalcohol (usually polyether and polyester based polyols). Isocyanates also react with amines, water, ureas, urethanes and even other isocyanates to form a range of functional groups including urethanes, ureas, isocyanurates, carbodiimides and uretdiones that all come under the polyurethane 'family' of structures (Figure 12)⁷². The isocyanurate ring, formed by the self-addition reaction of 3 isocyanate groups, is found in higher concentrations in the polyisocyanurate (PIR) sub-class of polyurethane foams (although many sources class them entirely separately, this is misleading as their fundamental chemistry and much of their fire behaviour is directly related to the more generally termed 'polyurethane' foams).

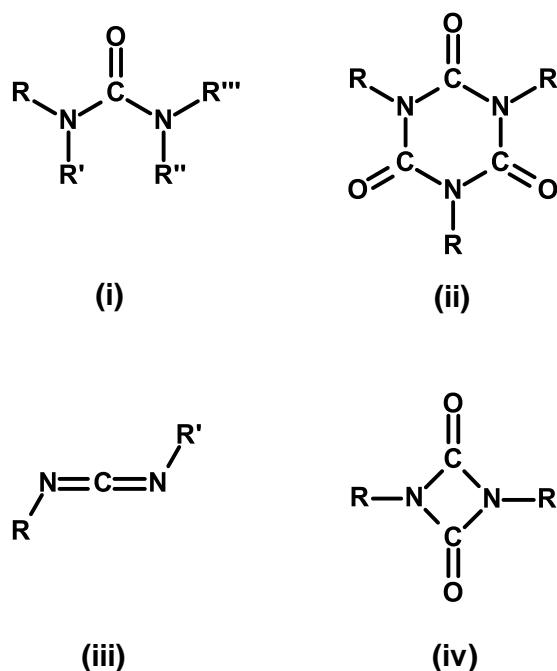


Figure 12 Other polyurethane functional groups i) urea ii) isocyanurate iii) carbodiimides iv) uretdiones

The stability of the bonds in polyurethane foams is well understood from comprehensive thermal decomposition studies in the literature. Upon heating in an inert-atmosphere, polyurethane bonds progressively rupture in relation to their bond stability as the temperature increases. A summary of the bond decomposition temperatures can be found in Table 6⁷³. Isocyanurate bonds are of particular interest due to their increased thermal stability, which contributes to the improved fire performance of PIR foams.

Polyurethane bond	Decomposition temperature range /°C
Urea	160-200
Urethane	180-200
Substituted urea	235-250
Carbodiimide	250-280
Isocyanurate	270-300

Table 6 Bond decomposition temperatures of the major polyurethane functional groups

Once thermal decomposition occurs, the results are usually the reverse of the polymerisation reaction, initially forming the precursor functional compounds – diisocyanates, diamines and dihydroxy- fragments. Diisocyanates (and their equivalent amines) are most commonly 2,4-toluene diisocyanate and methylene diphenyl diisocyanate (MDI) (Over 90% of all industrially produced polyurethanes are based on either TDI or MDI⁷²). Much of this decomposition above 300°C results in browning of the foam, with volatilised isocyanates, amines, and a nitrogen rich ‘yellow smoke’ of partially polymerised isocyanates, with partially polymerised polyols remaining in the condensed phase⁷⁴. Above 600°C, polyols in the condensed phase will fragment and volatilise, leaving behind a char. Above 800°C, the polyol char can decompose to produce simple organic fragments (CO, CO₂, CH₄ aldehydes) and some polycyclic aromatic hydrocarbons (PAHs)⁷⁵.

In the gas phase, isocyanates and ‘yellow smoke’ will begin to decompose above 600°C into low molecular weight nitrogen containing fragments (such as benzonitrile, aniline and HCN). At >800°C, further fragmentation into simple molecules occurs, resulting in compounds such as HCN, CO, CH₄ and formaldehyde. Rearrangement of carbonaceous molecules into PAHs can also occur at high temperatures. HCN yields have been reported to increase significantly at high temperatures, with up to 70% of the foam nitrogen being converted to HCN at 1000°C⁷⁶.

These reactions are accelerated in the presence of oxygen, reducing the overall temperature of the major decomposition steps. Furthermore, polyurethane foams based on polyether polyols will have a lower decomposition temperature in air than polyester polyol based foams⁷⁷. Generally, much of the literature on the thermal decomposition of polyurethane foams does not differentiate between flaming and non-flaming decomposition, with flaming decomposition accelerating the decomposition into simple organic fragments (CO, CO₂, HCN, and NO_x)⁷⁸.

A generalised mechanism for the decomposition of polyurethane based foams can be found in Figure 13, based on a comprehensive literature survey⁵⁷. An understanding of the thermal decomposition of polyurethane foams and the mechanisms by which decomposition occurs is essential in understanding and explaining the fire toxicity of polyurethane foam insulation.

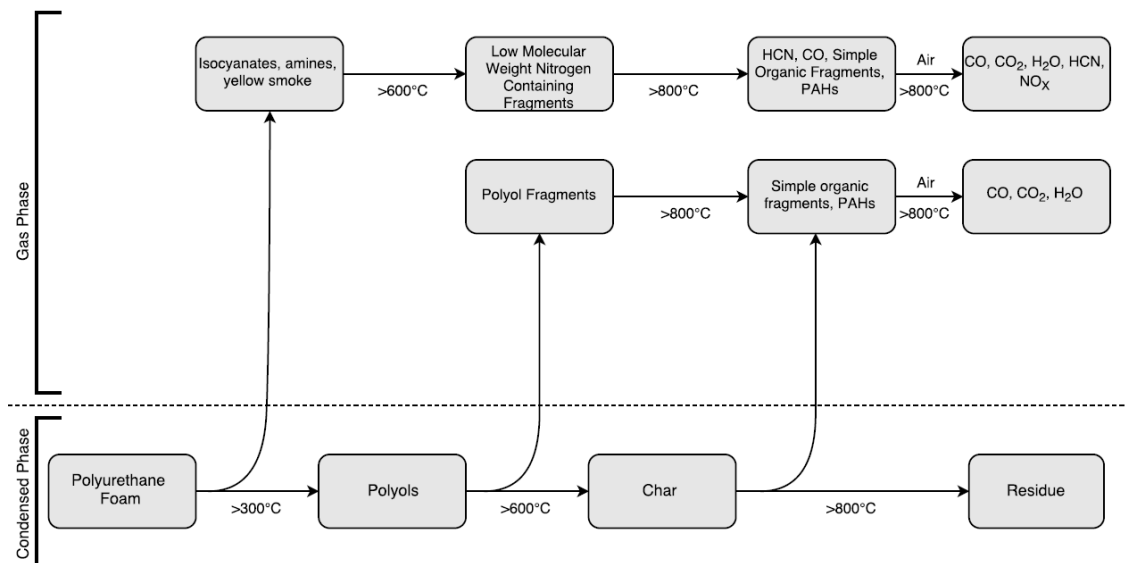


Figure 13 Generalised decomposition mechanism for the thermal decomposition of polyurethane foams⁵⁷

In terms of fire toxicity, polyurethane foams show notable differences dependant on formulation. Stec and Hull assessed the fire toxicity of rigid polyurethane foam and polyisocyanurate foam⁷⁹. In well-ventilated conditions ($\phi < 0.8$), the yields of CO₂ and NO₂ were at their highest as a result of the more complete combustion of nitrogen and carbon in the foam. Meanwhile, the yields of CO and HCN were at their lowest. In ventilation controlled conditions ($\phi > 1.5$), the yields of CO and HCN drastically increased, with the yields of CO₂ and NO₂ decreasing. For both materials there is a clear increase in yield of the major asphyxiant products from well-ventilated to under-ventilated flaming. At $\phi \sim 2.0$, the rigid polyurethane foam produced more CO than the polyisocyanurate (240 mg g⁻¹ vs. 225 mg g⁻¹), but the polyisocyanurate produced more HCN (17 mg g⁻¹ vs. 12 mg g⁻¹). The CO yields measured were within the range expected for carbonaceous polymeric materials burning in under-ventilated conditions (~ 200 mg/g CO); the 33% increase in HCN yield indicates that PIR materials produce higher yields of HCN than PUR materials in comparable ventilation conditions.

FED calculations, using the ISO 13344 Purser model, demonstrated that the CO and HCN are the most toxicologically significant products of the combustion of both rigid PUR and PIR foams. HCN in particular was the biggest contributor to the overall toxicity in all flaming test conditions. The contribution from HCl (generated by the decomposition of chlorinated flame retardants in the insulation) and NO₂ was insignificant compared to the toxic contribution of the asphyxiant gases. However, the presence of HCl will have increased the yield of both CO and HCN in well-ventilated conditions resulting in an indirect contribution to the overall toxicity of the effluent. As a result of its higher HCN yield, the PIR foam was found to present the highest toxic hazard in the under-ventilated conditions.

Additionally, the authors noted increased yields of CO in the well-ventilated conditions, resulting in an increased FED value. This was attributed to the presence of gas-phase radical quenchers which will reduce the conversion of CO to CO₂⁸⁰. The presence of HCl in the fire effluent suggests the presence of chlorinated organophosphates, which are commonly found in polyurethane based foams as a flame retardant additive.

Purser, in 2008, also found similar results when establishing the fate of fuel nitrogen in polymers⁸¹. A PIR foam analysed in the SSTF resulted in HCN yields that increased significantly above $\phi = 1.5$, with an HCN yield of 20 mg g^{-1} at $\phi = 1.75$, which decreased slightly at $\phi = 2.0$ to 18 mg g^{-1} . The conversion of fuel nitrogen at $\phi = 1.75$ was 15% with 6.15% nitrogen in the polymer. The authors noted that the polymers containing fire retardants (including the PIR) had higher recovery fractions of fuel N as HCN. This was attributed to gas-phase radical quenchers, as chlorine was detected at 3.56% by weight, again suggesting the presence of chlorinated organophosphate flame retardants.

The general trend found in the literature followed that flexible PUR foams were the least toxic, with rigid foams showing increased toxicity and PIR foams showing the highest toxicity. In under-ventilated conditions, both rigid PUR foams and PIR foams showed yields of CO ranging from $200\text{-}300 \text{ mg g}^{-1}$ but showed yields of HCN ranging from $10\text{-}15 \text{ mg g}^{-1}$ and $15\text{-}20 \text{ mg g}^{-1}$ respectively. Their high fire toxicity is primarily associated with a combination of CO and HCN, with HCN being the most toxicologically significant factor in under-ventilated conditions.

Chemistry and Fire Toxicity of Phenolic Foams:

Phenolic foam products are formed from the foaming of phenolic resins, which are produced by the reaction of phenols and formaldehydes⁸². Formaldehyde can react with up to 3 sites on a phenol molecule (in the ortho- and para- positions) to produce a cross-linked resin, which can then be foamed with blowing agents (Figure 14). Sulphur is commonly found in phenolic foams as sulphonic acids are often used as catalysts in the foaming and curing stages. This results in phenolic foams that are often acidic in nature and can be potentially corrosive in contact with metals, unless treated. Nitrogen is also found in some phenolic materials (particularly foam insulation) as urea additives improve the thermal conductivity and strength of the foam through increased cross-linking in the polymer. Inorganic fillers and halogenated organics are also added to some phenolic foam as fire retardants to improve the foams reaction-to-fire properties.

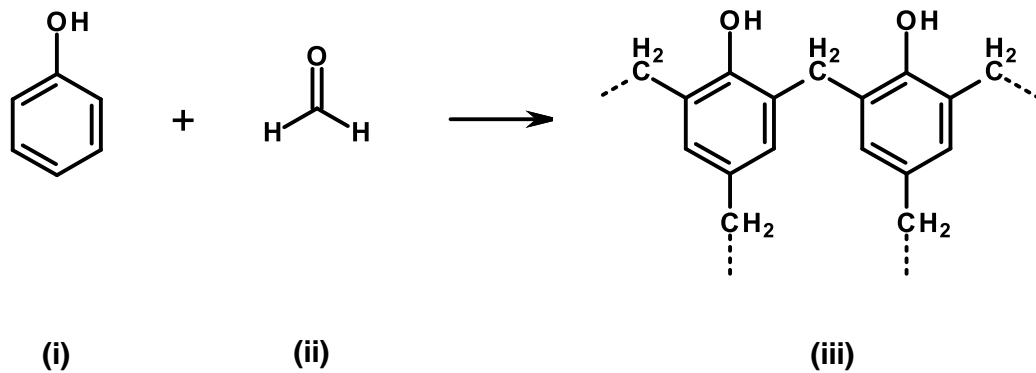


Figure 14 Reaction of i) phenol and ii) formaldehyde to produce a iii) phenolic resin

Phenolic foams generally begin to decompose above 300°C⁸³. The primary decomposition products include CO, CO₂ and organic fragments of varying size as may be expected on heating. Bigger fragments include the aromatic precursors of the polymer including phenols and benzene rings (dependant on bond scission). Simpler fragments are primarily aldehydes (formaldehyde as the main aldehyde, but also including other short chain aldehydes) and simple ketones. Phenolic foams containing sulphur may also produce organo-sulphur and oxidised sulphur products which are both irritating and toxic. At higher temperatures, above 800°C, PAHs can also form. The thermal decomposition of phenolic foams is in many ways comparable to wood, but with lower thermal stability.

In fires, as expected, CO is the major toxic product of phenolic foam combustion. Partially oxidised fragments, such as formaldehyde, will contribute to fire toxicity due to their irritating and sometimes directly toxic effects, but little information quantifying aldehydes in ventilation-controlled conditions is available. As has been mentioned previously, much of the fire toxicity data available for materials are measured using test apparatus that only produce well-ventilated conditions, and are not directly relevant to the most toxic stage of the fire: under-ventilated flaming.

Hull and Stec found that phenolic foam insulation produced increasing yields of CO in the SSTF, comparable to PUR and PIR foams, as the fire condition becomes increasingly under-ventilated (>200 mg g⁻¹)⁷⁹. Interestingly, the phenolic foam also produced similar NO₂ yields ~2 mg g⁻¹. Elemental analysis was not performed, but the presence of NO₂ would prove the presence of nitrogen in the polymer. Despite the comparable yield of NO₂, the yield of HCN reported was low (<1 mg g⁻¹). FED calculations showed that CO was the major contributor to the overall toxicity in under-ventilated conditions, but the presence of chlorine in the polymer resulted in higher than expected toxicity in well-ventilated conditions. Generally, based on the limited literature data available, phenolic foams can be expected to produce CO yields of 200-300 mg g⁻¹ in under-ventilated conditions, with small yields of HCl, HCN and NO_x (if Cl and N are present in the polymer).

Chemistry and Fire Toxicity of Mineral Wool Insulation:

Mineral wool insulation materials have existed since the late 1800s, based on both synthetic and natural products. In modern insulation, they are generally split into two main categories⁸⁴: Glass wool which is primarily composed of recycled glass (~70%), with a phenolic resin binder (0.5-7.0%) and remaining matter composed of materials such as sand, limestone or soda. Stone (or rock) wool is composed of natural stone that is melted and spun into fibres that are then bound with similar amounts of (usually) phenolic binder as glass wool products.

The thermal decomposition of mineral wool products depends on whether they are stone or glass based, and on the binder content. As most binders are phenolic based, their decomposition is largely similar to the decomposition of phenolic resins and foams scaled proportionally to the combustible organic content. Glass wool insulation will melt at much lower temperatures than stone wool (~700°C vs. ~1400°C).

The fire toxicity of mineral wool products is largely insignificant for two related reasons. Firstly, they are mainly composed of non-combustible material, with only a small amount of combustible binder. This results in low yields of toxic gases relative to the total mass of insulation, thus requiring a significantly increased loading of material to produce a toxic atmosphere. Secondly, mineral wool materials do not achieve flaming combustion. Small amounts of binder or paint on the surface may flash on heating, but the vast majority of the material will not ignite. Non-flaming combustion normally leads to higher toxic product yields per mass of burned material than would be obtained during flaming combustion. However, the organic content of mineral wool materials is so low that the amount of toxic gases produced are, ultimately, negligible in terms of fire toxicity.

As these materials do not ignite, it is not correct to assign an equivalence ratio but under non-flaming conditions, toxic gases can still be assigned a yield for a specific temperature that the insulation is exposed to. Hull and Stec burned stone wool (SW) and a glass wool (GW) in the SSTF at 850°C and 825°C respectively, but did not achieve ignition. In both cases the materials produced insignificant yields of toxic gases. This was particularly evident when comparing the FEDs of all of the insulation materials they tested, as the SW and GW sample had FED values lower than even the least toxic combustible insulation materials in well-ventilated conditions⁷⁹.

Subsequent literature available on the fire toxicity of mineral wool materials supports the yields reported by Hull and Stec. A RISE report by Blomqvist and Sandinge, published in 2018, assessed insulation materials in a number of different fire toxicity test methods⁸⁵. The publication does not identify the specific type of insulation tested (e.g. PIR or phenolic foam for the polymeric foam materials), which limits the ability to assess the specific types of material and compare them to other literature. Elemental analysis of the materials by the authors provides clues to the specific type of insulation tested, but it is ultimately speculation as to which specific type of insulation each sample is. Regardless, the four mineral fibre materials analysed did not ignite in any of the tested conditions and were all found to produce insignificant yields of toxic products in the SSTF, CACC and SDC. This suggests that regardless of the specific type of mineral wool material (e.g. glass wool or stone wool), the yields of toxic gases produced relative to the total mass of insulation will be low due to the low organic binder content of the materials.

Based on the literature available and the nature of the materials, mineral wool insulations are likely to produce small yields of CO (< 10 mg g⁻¹) as well as small yields of nitrogenous products such as HCN and NO_x (< 1 mg g⁻¹). The yields will likely scale proportionally to the % binder content, as higher %s will have more organic content to produce toxic gas.

Chapter 2

2.0 Experimental

2.0.1 Materials

14 commercially available insulation materials were selected for analysis (Table 7). A range of combustible and non-combustible insulations were chosen, with 7 PIR foams, 4 phenolic foams, 2 stone wool materials and 1 glass wool. Several of the foam insulation materials contained glass wool additives, either on the surface of the foam, or as an internal layer.

Code	Product Name	Description
PIR1	Celotex CG5000	PIR foam with internal glass fibre layer for cavity walls
PIR2	Recticel Powerdeck B	PIR foam with surface glass fibre layer for roof insulation
PIR3	Kingspan ThermaRoof	PIR foam for roof insulation
PIR4	Kingspan QuadCore	PIR foam for roof, wall and ceiling panels
PIR5	Celotex RS5000	PIR with two internal glass fibre layers for façade applications
PIR6	Celotex FR5000	PIR foam for pitched roofs, walls and floors
PIR7	Kingspan TP10	PIR foam for pitched roof applications
PF1	Kingspan K106	Phenolic foam for cavity walls
PF2	Kingspan K5	Phenolic foam for external use in masonry walls
PF3	Kingspan K15	Phenolic foam for external rainscreen and masonry façade use
PF4	Xtratherm Safe R	Phenolic foam for external wall rainscreens
SW1	Rockwool Spanrock ZL	Stone wool material for cavity walls
SW2	Rockwool Duoslab	Stone wool for external wall rainscreens
GW1	Knauf Ecosé	Glass wool for external wall applications

Table 7 Material ID codes and descriptions

2.0.2 Elemental Analysis

CHNS Analysis: CHNS analysis was performed using a Thermo Scientific Flash 2000 Organic Elemental Analyser. 2-3 mg was analysed from the main foam or mineral component of the sample. The external facing of the phenolic and PIR foam samples was not included in the analysis. The mineral wool samples did not have any outer facing material, and were analysed directly.

X-Ray Fluorescence (XRF) Analysis: Qualitative XRF analysis was performed using a Bruker Trace IV-SD handheld XRF at 25 keV. Samples were prepared by removing any outer facing and cutting off a small amount of foam or mineral wool. This small sample was then inserted into a 32 mm XRF sample cup with a Mylar sheet between the sample and the x-ray window. To increase the contact area and improve the data recorded, the foam samples were pressed down and held in place inside the sample holder. The analysis was then repeated in triplicate, with a new sample each time, in order to account for any potential variation in elemental composition throughout the sample. No such variation was observed for any of the materials tested in the three analyses.

SEM-EDX: Qualitative energy dispersive X-ray spectroscopy (EDX) was performed using a FEI SEM-EDX at 25 keV. Small pieces of foam or mineral wool were attached to an adhesive carbon pad on a standard 12.7 mm pin stub. Similarly to the XRF analysis, EDAX analysis was performed in triplicate in order to ensure a consistent elemental profile on the materials tested.

2.0.3 Steady State Tube Furnace

Fire toxicity was measured in the ISO/TS 19700 Steady State Tube Furnace in accordance with the standard⁶¹. Each material was tested in three fire conditions that are outlined in ISO 19706: fire stage 2 (well-ventilated flaming), fire stage 3a (small under-ventilated flaming) and fire stage 3b (large under-ventilated flaming)⁵. Samples were prepared by cutting an 800 mm strip of foam or mineral wool that weighted ~20 g. Outer facing layers on the foam samples were removed so that only the foam component was included in the test. The sample was then fed into the furnace at 40 mm min⁻¹ which resulted in a mass feed rate of ~ 1 g min⁻¹ of sample. In fire condition 2, the primary air flow was set at 10 L min⁻¹ and the secondary air flow was set to 40 L min⁻¹. In fire condition 3a and 3b, a primary air flow of 2 L min⁻¹ and a secondary air flow of 48 L min⁻¹ was used. This reliably resulted in the desired equivalence ratios in all of the tests. The air flows of both the primary and secondary air were regulated to the set flow rates described by Brooks Instruments 0254 mass flow transmitter with Brooks Instruments GF Series Thermal Mass flow controllers to ensure consistent air flow throughout the tests.

CO₂ concentration throughout the test was measured using non-dispersive infrared (NDIR). CO was measured using an electrochemical cell with a range up to 20,000 ppm. Oxygen concentration was measured using paramagnetic analysers. Each analyser was protected from moisture and soot by a combination of glass wool soot traps, silicone-gel drying agent, and 50 µm microporous (Hepavent) filters. Sampling for HCN was achieved by pumping effluent at 1 L min⁻¹ for the duration of the steady state (a minimum of 5 minutes) into a Drechsel bottle containing 150 mL 0.1 mol L⁻¹ NaOH. A second Drechsel bottle containing the same again was connected in series after the first to ensure no losses of HCN. Sampling for acid gases was achieved using a similar bubbler arrangement and effluent flow rate, this time utilising 100 mL deionised water in the first Drechsel bottle and 50 mL in the second Drechsel bottle for the duration of the steady state.

2.0.4 Cone Calorimeter

The insulation materials were analysed using a Govmark model CC-2 cone calorimeter in accordance with the ISO 5660 standard (Figure 15)¹⁴. The samples were prepared by removing any outer facing material so that only the foam or mineral wool was involved in the test. The foam or mineral wool samples were then cut to 100 x 100 x 25 mm and wrapped in foil around the outer edges leaving only the top face exposed. Each material was tested in triplicate at a heat flux of 50 kW m⁻² without the sample frame or wire grill. Any samples that did not ignite were allowed to pyrolyse under the cone heater for 30 minutes to ensure that they were not able to achieve ignition at that specific heat flux after prolonged exposure.



Figure 15 The Govmark CC-2 Cone Calorimeter

CO₂ and CO were sampled throughout the duration of each test using NDIR for on-line measurement. Additional sampling was performed to measure HCN in the fire effluent. To achieve this, a 4 mm ID stainless steel sample probe was inserted into the exhaust duct of the cone calorimeter next to the position that the standard smoke and gas analysis is performed. The probe measured 1 m in length and was then connected directly to an LDPE line. The effluent was then pumped through the probe and LDPE line at 1 L min⁻¹ into a Drechsel bottle containing 50 mL of 0.1 mol L⁻¹ NaOH (aq). The sampling system was open ended, venting out into the extraction hood above the cone calorimeter. The HCN sampling was performed for the duration of each test. In order to ensure that the sample probe did not become blocked with soot, the probe was removed and cleaned at regular intervals during the testing programme.

2.0.5 Single Burning Item Tests

SBI testing was performed in accordance with EN 13823 at the European Fire and Conductivity (EFiC) laboratory in Denmark (figure)²⁰. Only a limited selection of samples were analysed due to limited access to the test facility and the high relative cost per test. The four samples included PIR1, PIR3, PF1 and SW1. All four of the samples were tested in duplicate with each mounted without modification to recreate their state in real-life applications. This included leaving the external facing on the foam samples. Each sample was mounted on the L-shaped rig with a large wing and small wing at a right angle to create a corner. A gas burner with a heat release rate of 30 kW (the single burning item) was applied to the corner of the sample for the duration of the 21 minute long test. After the test, the remains of the samples were weighed to calculate mass loss.

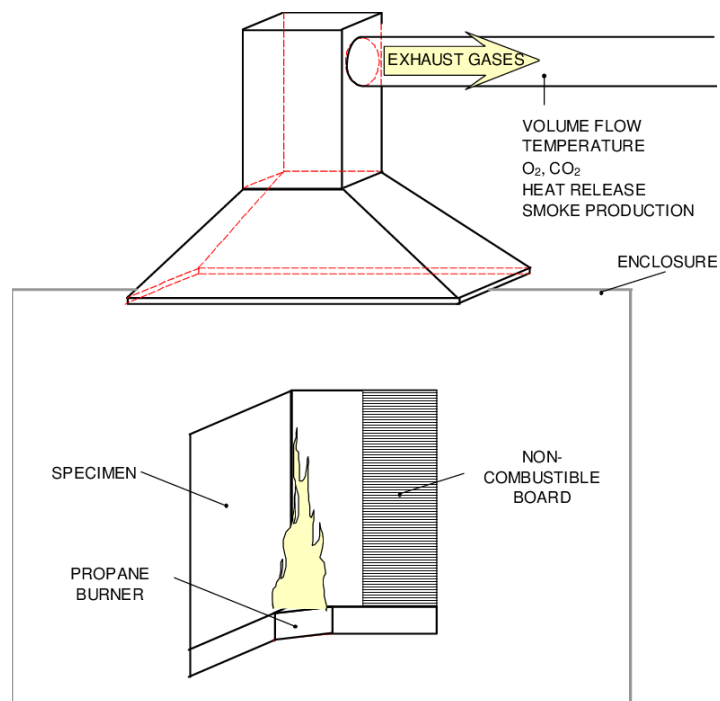


Figure 16 Schematic of the EN 13823 SBI test apparatus⁸⁶

The effluent generated during each SBI test was collected in a large hood and removed by an extraction system. CO₂, CO and O₂ measurements were taken from within the extraction system to provide on-line measurement throughout the duration of the test. In addition to the gases measured as required by the standard, additional sampling was performed for HCN using portable gas analysis equipment (which is described in detail in the following section). A 1m long, 4 mm ID stainless steel probe was inserted into the exhaust duct of the SBI apparatus. This probe was then connected to LDPE line which was inserted into the sampling system. Effluent was pumped at 1 L min⁻¹ into Drechsel bottles containing 150 mL of 0.1 mol dm⁻³ NaOH (aq). The initial Drechsel bottle was used for 6 minutes, before switching to subsequent Drechsel bottles every 5 minutes until the end of the test.

Portable Gas Analysis Equipment

In house portable analysis equipment was constructed to sample fire effluent into Drechsel bottles at a known and controlled flow rate (Figure 17). Drechsel bottles were connected to up to 7 parallel lines using silicone tubing and LDPE line splitters. Each Drechsel bottle was then connected to a solenoid valve which can be independently opened and closed using a switch. Flow through the system is provided by a Charles Austen d5 SE air pump controlled with an adjustable flow valve. By using the switches on the solenoid valves, flow through the desired Drechsel bottle can be achieved, as well as quick switching to the next Drechsel bottle during a test without loss of flow. The effluent itself is pumped is into the system using LDPE tubing, which then comes into contact with silicone tubing, and the LDPE line splitters inside the system. The effluent does not come into contact with any of the metal components in the system. The volumetric flow through the equipment is recorded continuously by an Omega 3100 series 0-5 L min⁻¹ flow meter. Both the pump and filter were protected by 50 μm microporous (Hepavent) filters. The system accumulates soot over time, requiring regular maintenance of the sampling lines and line splitters to prevent blockages during a fire test. In the event of a fire test that is producing particularly high volumes of soot, then additional Dreschsel bubblers filled with water can be connected after the sampling bottles to act as soot trap.

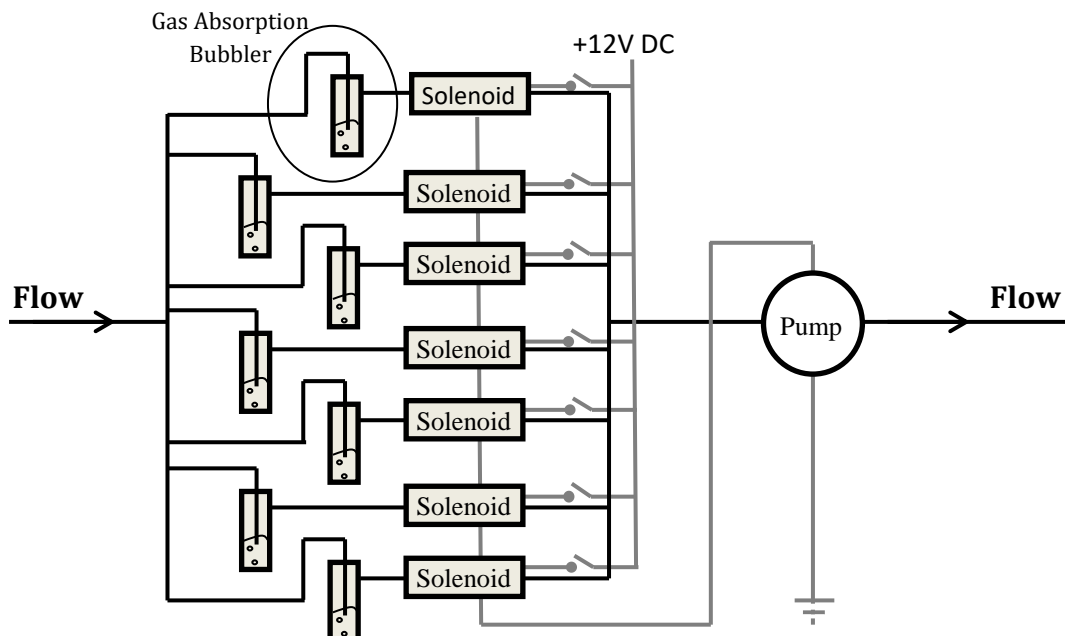


Figure 17 Schematic of the portable gas analysis equipment used during the SBI testing⁸⁷

2.0.6 Quantification of Hydrogen Cyanide by Colourimetric Spectrophotometry

HCN Sampling from Fires:

Fire effluent was bubbled into a Drechsel bottle containing 150 mL of 0.1 mol L⁻¹ aqueous sodium hydroxide (NaOH) at 1 L min⁻¹ for 3 to 5 minutes. A second Drechsel bottle, also containing 150 mL of 0.1 mol L⁻¹ NaOH (aq), was added in sequence to quantify any HCN carry-over. The HCN quantified for each bubbler was summed to give the total HCN sampled. These conditions are generally suitable for a range of common fire tests, but may be modified as needed to ensure optimal HCN trapping, for example in the cone calorimeter where a volume of 50 mL was used.

Reagents:

All reagents were purchased from Sigma-Aldrich. The following solutions were prepared: Reagent A containing 1 mg mL⁻¹ chloramine-T in deionised water; Reagent B containing 7.5 mg mL⁻¹ isonicotinic acid, 1.5 mg mL⁻¹ 1-phenyl-3-methyl-5-pyrazolone and 10% v/v dimethyl formamide (DMF) in deionised water; a buffer solution at pH 7.2, using sodium hydrogen phosphate and potassium dihydrogen phosphate.

Method:

The following steps were repeated for a blank sample, a range of standards (up to 8.0 ppm CN⁻) and the unknown samples. Several analyses were performed sequentially by adding the reagents to unknown samples, with a fixed delay (i.e. adding reagent A to sample 1 at 0 minutes, sample 2 at one minute, etc. and then reagent B to sample 1 at 5 minutes, and to sample 2 at 6 minutes, etc.).

The following reagents were added, in sequence, to a test tube (or other suitable vessel): 1 mL of cyanide containing sample solution; 9 mL of deionised water; 4.5 mL of phosphate buffer; 2 mL of reagent A. 5 minutes after the addition of reagent A, 4.5 mL of reagent B were added.

35 minutes after the addition of reagent A, the sample solution was analysed using an ultraviolet-visible (UV-Vis) spectrophotometer at $\lambda = 638$ nm in both a 4 cm and 1 cm cell. The absorbance was recorded for each standard and unknown sample. The absorbance of the test solutions was then compared with the absorbance of the calibration standards to calculate the concentration of cyanide ions in the original solution. If the absorbance of the unknown samples exceeded the absorbance of the 8.0 ppm standards in the 1 cm cell, or the absorbance of the 2.0 ppm standards in the 4 cm cell, the unknown sample was diluted by 50% and the analysis repeated.

The total HCN sampled (in mg) was calculated using the following equation:

$$HCN_{mass} = [CN^-] \times V_{AS} \times (27/26)$$

Where

HCN_{mass} is the total mass of HCN sampled in mg

$[CN^-]$ is the concentration of cyanide ions in the absorbing solution in mg/L

V_{AS} is the total volume of the absorbing solution in L

(27/26) is the factor that converts cyanide ions to HCN

The concentration of HCN in the fire atmosphere sampled was calculated using the following equation:

$$[HCN] = HCN_{mass} \div V_{Eff}$$

Where

$[HCN]$ is the concentration of HCN in the atmosphere sampled, in mg L⁻¹

V_{Eff} is the total volume of effluent sampled

2.0.7 Quantification of Acid Gases by High Pressure Ion Chromatography

Acid Gas Sampling from Fires:

Acid gases were trapped by bubbling effluent at a known flow rate into a known volume of deionised water. The conditions utilised in the SSTF, as previously described, were bubbling 1 L min⁻¹ of the effluent into 100 mL of deionised water. A second bubbler was connected in series to the first, containing 50 mL of deionised water. The acid gases quantified in each could then be combined to give the total quantified acid gases from that specific test.

Standard preparation:

The following sodium ion salts were purchased from Sigma-Aldrich: sodium chloride, sodium bromide, sodium nitrite, sodium nitrate, sodium nitrate and sodium dihydrogen phosphate.

Standard solutions were prepared by dissolving the appropriate amount of sodium salt precursor into deionised water to achieve the desired ion concentration. Solutions were prepared ranging from 1 to 25 ppm of the target ion. An additional solution containing all 7 target ions was also prepared to assess whether their combined presence affected the quantified concentration of any individual ion. No such affect was observed.

Method:

Acid gas quantification was achieved via High Pressure Ion Chromatography (HPIC) using a Dionex ICS-2000 with an IonPak AS11 column heated to a constant temperature of 30°C. In order to achieve appropriate separation of the target ions a mobile phase containing an increasing gradient of KOH was used at a concentration of 1 nmol mL⁻¹ KOH for the first 14 minutes, increasing linearly to 10 nmol mL⁻¹ at 20 minutes.

Sample solutions were filtered and 0.1 mL of filtrate was injected into the HPIC for analysis. The concentration of ions in solution was then quantified against the standard concentration curves. Any samples that were out of range were diluted by half and re-analysed. From the concentration of ions in solution, the concentration of each acid gas in the sampled effluent was then quantified using the known flow rate of effluent and sampling duration.

Chapter 3

3.0 Results and Discussion

3.1 Development and Optimisation of HCN Quantification in Fires

As discussed in section 1.2.3, HCN is a significant toxic component of the combustion of nitrogen containing materials. As a result, it was considered necessary to compare our current method, the ISO 19701 chloramine-T/isonicotinic acid method, to available alternatives and ensure that it was optimised for accuracy and reliability. The final optimised method can be found in the experimental section - chapter 2.

3.1.1 Comparison with other methods for quantifying HCN:

Methods for the determination of cyanide ions in solutions have generally been designed for use in the analysis of soil, water, food and biological fluids⁸⁸. Historically, spectrophotometric methods have been used to determine the concentration of cyanide ions in solution. Examples of these methods included the use of iron salts (forming iron cyanide complexes), picric acid derivatives and barbituric acid derivatives⁸⁹. However, many of the reagents used are highly toxic or carcinogenic. Alternative, fluorometric, chemiluminescent and potentiometric procedures have been developed, but require the use of specialised equipment.

ISO 19701 describes various methods for the quantification of acute toxicants present in fire effluent, including three methods for the quantification of HCN. Two of the methods utilise colourimetry (one using a chloramine-T/isonicotinic acid based reaction, the other using a picric acid reaction) while the third method utilises High Pressure Ion Chromatography (HPIC) with a specialised detector⁹⁰.

The picric acid method in ISO 19701 is similar to historic methods, but has been developed for fire analysis and involves the reaction of picric acid with cyanide ions in solution to produce a red coloured complex that absorbs at approximately 480 nm⁹¹. The reaction is relatively quick but is dependent on a number of analytical variables, including reaction time and temperature, which increases the potential for experimental variation⁹².

HPIC is also a well-established method for the quantification of HCN. However, much of this analysis has been performed for soil, water and other matrices that contain relatively low concentrations of cyanide and other compounds. ISO 19701 notes that HPIC columns can be sensitive to fire-effluent solutions and they can quickly become blocked. Routine fire sample

analysis can result in the rapid aging of HPIC columns, requiring special care and extra sample preparation to minimise the detrimental effect to the analysis⁹³.

ISO 19702 describes the use of Fourier Transformed Infrared (FTIR) Spectroscopy for the quantification of toxic species in fire effluents, including HCN⁹⁴. While FTIR is a powerful technique for gas analysis, it has a high cost both in terms of equipment and time spent to analyse the spectra generated. This problem is particularly compounded in complex gas mixtures (such as fire effluent) with overlapping peaks which require complex analysis and interpretation. Automated analysis software does not provide a complete solution, as complex mixtures can result in over- or under-estimation of HCN, as a result of spectral interferences.

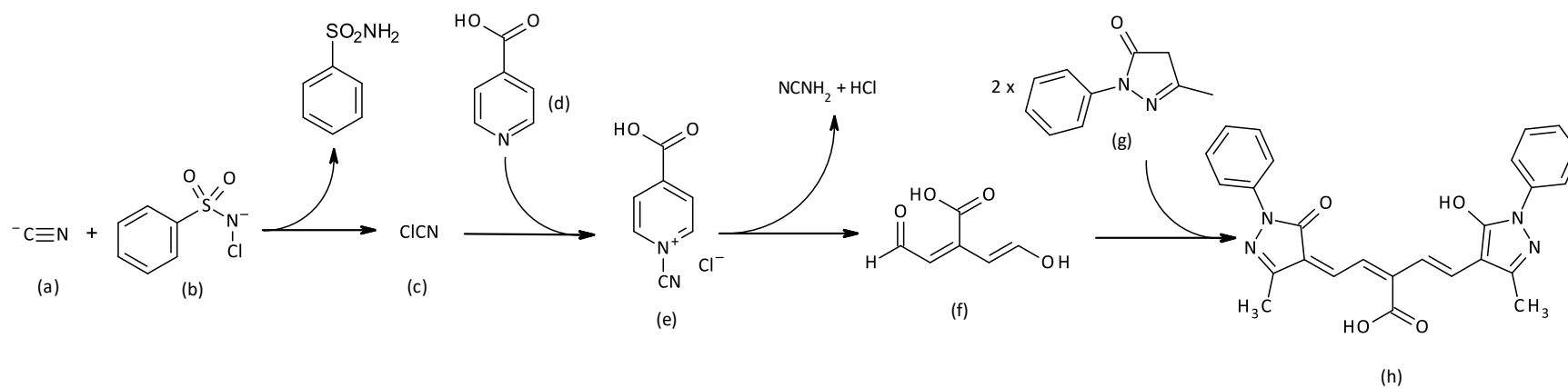
The use of pyridine and pyrazolone reagents for the quantification of cyanide has been well known for almost 100 years⁹⁵. However, the method outlined in ISO 19701 uses isonicotinic acid in place of pyridine, as it is less toxic, while also cheap and readily available. Chloramine-T is reacted with cyanide to produce cyanogen chloride, which is further reacted with a mixture of isonicotinic acid and 1-phenyl-3-methylpyrazol-5-one to produce a blue dye. The presence of a carboxyl group on the dye also improves its water solubility, reducing the need for organic solvents.

3.1.2 Chemistry of the Chloramine-T/Isonicotinic acid method:

Early work synthesising polymethine dye compounds using pyridines and pyrazolone compounds by Gehauf found that the reaction involved the breakage of the pyridine ring by cyanogen chloride, comparable to that reported in the Zincke pyridinium ring opening reaction⁹⁶. However, Gehauf did not confirm the structure of the dye. Other reported structures, such as by Epstein, reported the structure of the dye incorrectly (commonly showing breaks in the alternating double bond chain, and/or incorrectly assigning hydroxyl and carbonyl oxygen atoms to the pyrazolone rings in the structure)⁷. The chloramine-T/isonicotinic acid method is similar to that reported by Gehauf and Epstein, utilising isonicotinic acid as the source of the breakable pyridine ring.

The method utilises a multi-step reaction resulting in a polymethine dye product (Scheme 1). Trapped cyanide ions react with chloramine-T to produce cyanogen chloride. Cyanogen chloride reacts with isonicotinic acid, rupturing the aromatic ring to produce a carboxy-glutaconic aldehyde product and producing cyanamide and hydrochloric acid as a by-product. This step is important, as the cyanide in the reaction mixture is eliminated, preventing it from interfering with the remaining reactants and removing the most toxic component of the reaction mixture. The carboxy-glutaconic aldehyde product then reacts with two 1-phenyl-3-methyl-5-pyrazolone molecules producing the polymethine dye.

The dye acts in agreement with Beer-Lambert law, having an absorbance directly proportional to the initial concentration of cyanide ions in the sodium hydroxide solution at $\lambda = 638$ nm. The concentration of cyanide ions and subsequently the amount of HCN sampled can be calculated.



Scheme 1 a) Cyanide ions b) Chloramine-T c) Cyanogen Chloride d) Isonicotinic Acid e) 1-cyano-4-carboxy-pyridinium chloride f) Carboxy-glutaconic aldehyde product g) 1-phenyl-3-methyl-5-pyrazolone h) Polymethine dye product

3.1.3 Optimisation of Conditions:

ISO 19701 states that 'no data has been collected' for the repeatability and reproducibility of the chloramine-T/isonicotinic acid method for the quantification of HCN – so several steps were taken to optimise the method and assess the potential for interferences from other products in fire effluent.

Optimal Time to Analysis and Variations with Temperature:

ISO 19701 states that the absorbance of the test solution should be measured '30 minutes exactly after the addition of the chloramine-T solution'. However, this does not account for variations in reaction time as a result of temperature. The absorbance of three standard solutions was measured from the time of the addition of the reagents with varying temperatures. 18°C and 25°C were selected to represent normal laboratory temperatures, and 35°C was selected to represent an unusually high temperature (Figure 18).

As expected, there was some variation in the optimal time to analysis, with the 18°C sample taking the longest time to reach peak absorbance (at 35 minutes). As the temperature increased, the time to peak absorbance decreased with temperature, with the solution at 25°C reaching its optimal time to analysis at 32 minutes. The 35°C sample reached peak absorbance quickest at 26 minutes.

When comparing the results between the samples at 30 minutes to their optimal time to analysis, both the 18°C and 25°C sample showed only minor difference in absorbance (~1%). This suggests that the influence of temperature in these ranges is negligible, but to ensure the most accurate result, the ideal time to analysis would be between 35-40 minutes, before the absorbance of the dye solution begins to decrease (it should be noted that this decrease is only minor, with losses of <0.005 up to 60 minutes at 18 and 25°C). Even in cases of increased temperature, the solution remains at its peak absorbance up to 40 minutes before showing losses, as demonstrated by the 35°C sample.

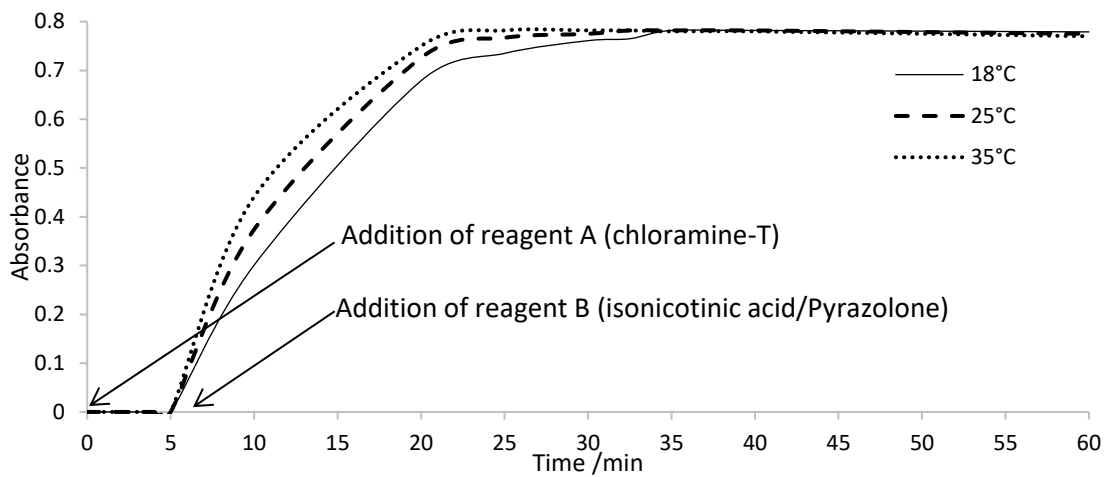


Figure 18 Variation in the absorbance of the reaction as a function of time

Standard Calibration Data:

Replicate testing was performed with calibration standards to ensure their accuracy and consistency (Table 8). Data was taken from 20 analyses of 5 different concentrations of the standard, using both the 4 cm and 1 cm absorbance cell (the 4 cm cell does not give linear absorbance above 2.0 ppm CN⁻, but provides greater sensitivity at CN⁻ concentrations below 2.0 ppm). Variance in the measurements is reported as relative standard deviation (SD). The 1 cm cell showed higher SD at lower concentrations but this decreased with increasing concentration of cyanide ions. In each case the % SD is below 10% and in the conditions used for analysis the value lies between 2 and 4%.

Concentration of Cyanide Ions (ppm CN ⁻)	4 cm Cell Absorbance/ Absorbance ± SD (%)	1 cm Cell Absorbance/ Absorbance ± SD (%)
0.3	0.219 ± 0.008 (3.71%)	0.055 ± 0.005 (8.60%)
0.8	0.545 ± 0.013 (2.38%)	0.143 ± 0.006 (4.34%)
2.0	1.168 ± 0.015 (1.29%)	0.355 ± 0.007 (2.04%)
5.0	-	0.806 ± 0.024 (2.98%)
8.0	-	1.189 ± 0.023 (1.95%)

Table 8 Absorbance of the standard cyanide solutions for the 4 cm and 1 cm cells

Sample Stability Testing:

Sample stability in solution was tested by generating an HCN sample in the ISO/TS 19700 Steady State Tube Furnace (SSTF). The sample was immediately divided equally into separate sample bottles. One half of the resulting sample solution was stored at 5°C and the other half at 21°C for 31 days. Both were stored in airtight polypropylene bottles.

Both samples were tested immediately (Table 9) and showed similar absorption with acceptable random variation (comparable to that observed in Table 8). When compared to their absorption 31 days later, the samples showed small losses from storage, unsurprisingly showing slightly greater loss when stored at 21°C (-1.91% at 5°C, -3.42% at 21°C) (table 2). When calculated as the concentration in ppm of HCN in the SSTF, the difference over 31 days was small (-1.72 ppm at 5°C, -3.01 ppm at 21°C), which is likely to be less than the other limits of experimental error in a fire test.

Sample	1 cm absorption (day 0)	1 cm absorption (day 31)	% Difference (day 31)
5°C	0.418 ± 0.005	0.410 ± 0.001	-1.91
21°C	0.424 ± 0.008	0.409 ± 0.001	-3.42

Table 9 Absorbance of a sample solution stored both in and out of a refrigerator

This result indicates that the samples are fairly stable even when not cooled, reducing concerns of sample losses, for example when transporting samples from external testing locations or when samples cannot be immediately analysed.

Interferences:

Sulphur compounds such as thiocyanates, sulphites and sulphates have been reported to interfere with chloramine-T based methods for quantifying cyanide⁹⁷. Thiocyanate is reported to give a false positive by reacting with chloramine-T to produce chlorothiocyanate in a reaction similar to the reaction of cyanide ions with chloramine-T. Chlorothiocyanate goes on to react stoichiometrically to form the polymethine dye product giving a false positive result. However, the formation of thiocyanate in a fire has not been reported, suggesting this may not be a problem. Materials that may be of concern due to their sulphur content could include rubbers and phenolic foams/resins.

To assess the potential for interference from other common components in fire effluent, a selection of ions (which are the product of the dissolution of acid gases (Table 10)) were added at 1 ppm (Figure 19) and 10 ppm (Figure 20) to a 2 ppm standard solution of cyanide ions. Two sets of each sample were prepared, one stored at 5°C and the other at 21°C. The samples were immediately analysed, then analysed again after 1 and 7 days.

Ion	Salt used	Fire Gas
Carbonate (CO_3^{2-})	Sodium Carbonate (Na_2CO_3)	Carbon Dioxide (CO_2)
Sulphite (SO_3^{2-})	Sodium Sulphite (Na_2SO_3)	Sulphur Dioxide (SO_2)
Sulphate (SO_4^{2-})	Sodium Sulphate (Na_2SO_4)	Sulphur Trioxide (SO_3)
Nitrite (NO_2^-)	Sodium Nitrite (NaNO_2)	Nitrogen Oxide (NO)
Nitrate (NO_3^-)	Sodium Nitrate (NaNO_3)	Nitrogen Dioxide (NO_2)

Table 10 List of ions, the salt used to generate the ion, and the acid gas that produces those ions in solution.

At concentrations of 1 ppm, carbonate and sulphate had little effect beyond their error range (Figure 19). Sulphite, however, resulted in losses of 9.5 to 12.5%. Both nitrite and nitrate resulted in losses ranging from 7 to 8%.

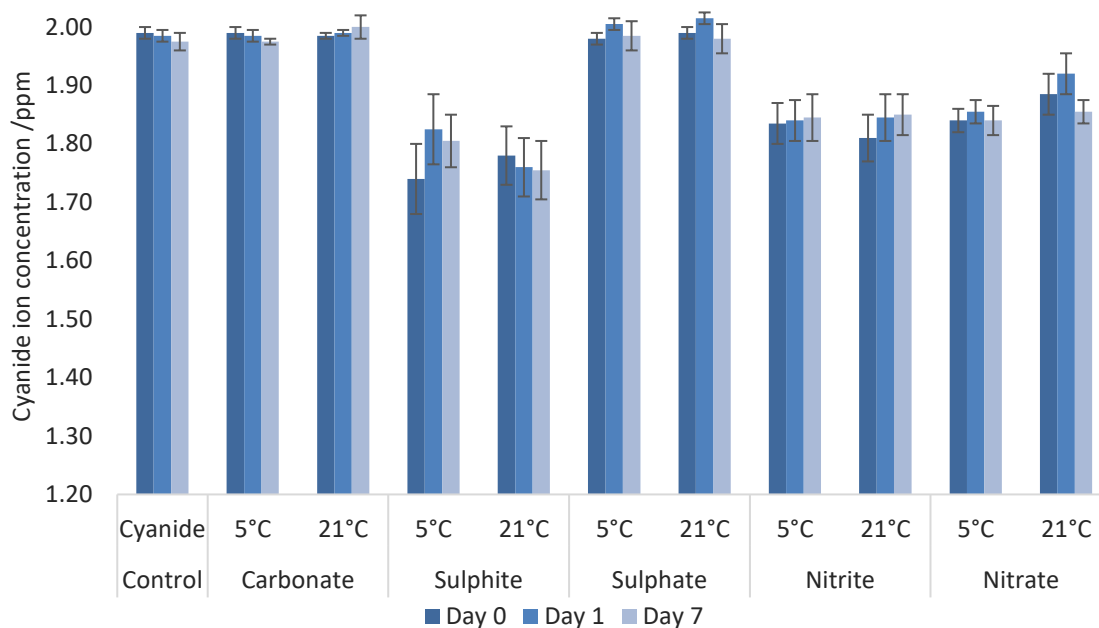


Figure 19 Effect of 1 ppm of potentially interfering ions on cyanide concentration at 5°C and 21°C after up to 7 days (note concentration scale on y-axis).

At 10 ppm, carbonate similarly showed no effect outside the range of error (Figure 20). Sulphite showed increased losses of 26-28% on day 0 which then improved to 13% after 24 hours, possibly due to its oxidation to sulphate. After 7 days there was a small increase which fell within the errors inherent in the analysis.

Sulphate had a larger effect at 10 ppm compared to 1 ppm, showing a difference of 7.5% and 13%, at 5°C and 21°C respectively. Nitrite and nitrate showed increased losses at 10ppm at both 5°C and 21°C.

In all cases, the difference between the 5°C and 21°C samples was small, suggesting that any interference is not significantly affected by temperature, and that it is an inherent interference with the chemistry occurring during analysis, rather than reactions occurring between ions in the sample solution.

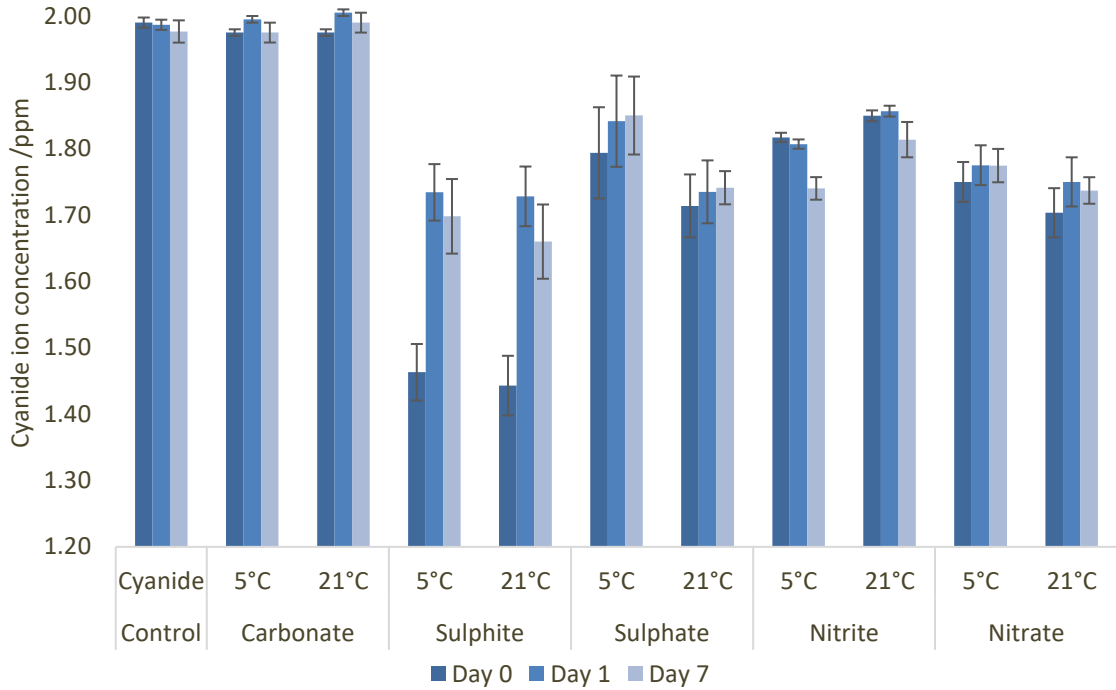


Figure 20 Effect of 10 ppm of potentially interfering ions on cyanide concentration at 5°C and 21°C after up to 7 days (note concentration scale on y-axis).

The notable interference from sulphite can be explained by the reaction of sulphite ions with cyanogen chloride to produce cyanate ions⁹⁸.

Due to the complicated nature of the Zincke-like mechanism, it is no surprise that there is potential for interference from the cocktail of species present in fire effluents. However, in conditions with high levels of NO and NO₂, HCN levels will be low and vice versa⁹⁹. This suggests, fortuitously, that interferences from NO_x products may not be a concern in situations where HCN levels are at their highest (large under-ventilated flaming) and that when the fire conditions produce low levels of HCN, the effect of interference will be negligible in terms of fire toxicity.

Published data on HCN production from burning materials supports this hypothesis. The HCN yields of polyurethane and polyisocyanurate foam were reported from the ISO/TS 19700 Steady State Tube Furnace using the chloramine-T/Isonicotinic acid method of quantifying HCN as outlined in ISO 19701¹⁰⁰. Yields fell well within the expected range for each specified ventilation condition when compared to readily available data in the literature⁵⁷. Furthermore, the contribution of NO₂ to the fire toxicity was negligible compared to the contribution of HCN in all ventilation conditions, indicating that the concentrations of NO₂ generated are not high enough to significantly reduce the HCN below what is normally expected at a specific ventilation condition.

This leaves sulphur products as a major concern; however elemental analysis with methods such as X-Ray Fluorescence (XRF) can provide foreknowledge of the presence of sulphur in the sample. If sulphur is present, sulphur oxides can be quantified from the burning material and used to estimate the level of interference. Regardless, sampling for other acid gas products with methods such as HPIC (as outlined in ISO 19701) will identify the level of potential interferences for hydrogen cyanide measurements which can then be accounted for when HCN is quantified.

Overall, the optimised chloramine-T/isonicotinic acid method for quantifying HCN is robust and reliable, with reagent temperature having little impact on the time to analysis, unlike the picric acid based methods presented in ISO 19701⁹². Further to this, the reagents used and the products of the reaction are less toxic than alternative methods. Interferences commonly expected in fire effluents do not have a significant impact, apart from sulphur oxides. However, this can be accounted for by pre-screening samples for their elemental composition. Analysis can be performed in sequence with little time between each sample, allowing for reliable relatively quick batch analysis, unlike alternative methods such as HPIC or FTIR.

3.2 Elemental Analysis and Material Composition

The 14 insulation materials described in chapter 2 underwent elemental analysis using CHNS, XRF and SEM-EDX, the results of which can be found in Table 11. Knowing the chemical composition of commercial products is valuable in understanding their fire behaviour and, in particular, their fire toxicity.

The PIR samples all show similar compositions with roughly ~65% carbon, ~5-6.5% hydrogen, and ~7-8% nitrogen. The majority of the remaining polymer is likely to be oxygen. The presence of P and Cl are indicative of chlorinated organophosphate flame retardants which are added to the material during production to improve the material's fire behaviour. Based on the % of carbon in the PIR foams, a theoretical upper limit of ~2.6 g/g CO₂ can be calculated. However, this is unlikely to be reached, even in high temperature well-ventilated conditions due to the presence of the P and Cl based flame retardants acting as gas phase radical inhibitors, preventing the oxidation of CO to CO₂ by the •OH radical. The variation in N content from 6.9-7.9% could result in differences in HCN yield of the PIR samples. While some research has gone into the fate of fuel nitrogen in polymeric materials¹¹, no firm relationship has been established between PIR nitrogen content and HCN yield.

The phenolic foam samples show more variation in their composition than the PIR samples but do have a similar carbon content. PF1-3 has 2-2.5% N but PF4 has notably less. The presence of N in the phenolic foam is attributed to the use of urea additives to improve the properties of the foam. Although phenolic foams are not expected to produce high yields of HCN, the presence of nitrogen means that some HCN will be produced during their decomposition. This poses the question whether there is a linear relationship between N content and HCN yield, or whether it is more specific to the chemical structure of PIR foams that results in their high HCN yields when burning.

The sulphur content of the phenolic foams also shows some variation between the four samples. This could affect the fire behaviour of the foam, and could contribute to the fire toxicity of the burning foams through the release of organo-sulphur fragments and sulphur oxides.

Similarly to the PIR foams, the remaining portion of the phenolic foams mass is also likely to be oxygen. The presence of P and Cl, again, indicates the presence of chlorinated organophosphate flame retardants. Unusually, P was not detected in PF1, but Cl was. This suggests the presence of a non-phosphorous-based chlorinated flame retardant, or when taking into consideration the increased N content compared to the other samples, could

indicate a chlorinated nitrogen-based flame retardant such as a chlorinated organo-ammonium compound.

As expected, the mineral wool samples are primarily composed of inorganic material with a small % of organic content. Of the combustible content, there is some difference between the three samples. SW1 contains significantly less nitrogen than the other two mineral wool materials, suggesting a phenol-formaldehyde based binder. The increased presence of nitrogen in the remaining samples could indicate a urea-formaldehyde binder. The remaining elements are comprised of metals and oxygen, which would be expected to be found in stone or glass.

Sample	C %	H %	N %	S %	Remaining %	Elements detected by EDX/XRF
PIR1	64.80	6.40	7.70	0.00	21.1	O, P, Cl
PIR2	64.59	6.01	7.84	0.00	21.6	O, P, Cl
PIR3	65.63	6.66	7.61	0.00	20.1	O, P, Cl
PIR4	66.00	6.23	7.25	0.00	20.5	O, P, Cl
PIR5	65.08	5.74	7.86	0.00	21.3	O, P, Cl
PIR6	65.10	5.82	7.66	0.00	21.4	O, P, Cl
PIR7	64.90	5.20	6.94	0.00	23.0	O, P, Cl
PF1	60.81	6.65	2.46	2.76	27.3	O, S, Cl, K
PF2	61.62	5.55	2.04	6.96	23.8	O, S, P, Cl
PF3	60.84	5.60	2.01	7.10	24.5	O, S, P, Cl
PF4	61.22	6.08	0.10	3.94	28.7	O, S, P, Cl
SW1	3.29	1.29	0.10	0.00	95.3	O, Mg, Al, Si, K, Ca, Fe
SW2	0.30	0.10	2.50	0.00	97.1	O, Mg, Al, Si, Ca
GW1	0.20	0.40	1.80	0.00	97.6	Na, Si, Ca, O

Table 11 Elemental composition of the insulation samples

3.3 Reaction to Fire Assessment

3.3.1 Cone Calorimeter

All of the samples were successfully tested in the cone calorimeter at 50 kW m⁻². Each 100 x 100 x 25 mm was tested in triplicate with their outer facing material removed (i.e. foil on the PIR samples). The main outputs are reported in Table 12. The averaged heat release curve of the three tests for each material is presented in Figure 21. CO₂, CO and HCN data collected is discussed in the fire toxicity section.

Sample	Time to Ignition /s	Peak HRR /kW m ⁻²	Time to PHRR /s	Total Heat Release /MJ m ⁻²	Smoke Production/ m ² m ⁻²	Mass Loss /%	Time to extinction /s
PIR1	2.4 ± 0.4	129.3 ± 2.4	15.5 ± 0.7	10.8 ± 3.4	168.2 ± 37.2	62.9 ± 13.8	214
PIR2	1.8 ± 0.4	207.4 ± 4.0	14.5 ± 0.7	13.6 ± 0.3	347.73 ± 33.9	75.9 ± 2.1	208
PIR3	1.4 ± 0.2	134.7 ± 9.6	15.0 ± 1.4	15.6 ± 5.7	232.2 ± 43.6	74.6 ± 14.5	389
PIR4	1.5 ± 0.2	117.1 ± 3.4	13.3 ± 1.2	12.3 ± 1.6	108.6 ± 20.7	64.7 ± 4.8	341
PIR5	1.5 ± 0.2	104.4 ± 6.2	14.3 ± 1.2	8.0 ± 0.1	136.2 ± 6.4	53.1 ± 1.0	149
PIR6	1.1 ± 0.0	114.0 ± 7.3	14.4 ± 0.6	17.8 ± 1.9	226.9 ± 24.2	65.6 ± 1.6	390
PIR7	1.4 ± 0.2	131.1 ± 17.1	12.0 ± 0.1	10.4 ± 1.0	234.2 ± 53.0	69.1 ± 2.7	211
PF1	2.8 ± 1.0	68.5 ± 4.0	24.5 ± 2.5	18.2 ± 0.2	72.4 ± 2.0	96.0 ± 0.4	596
PF2	8.60 ± 2.7	63.7 ± 5.5	20.0 ± 2.8	18.7 ± 0.7	14.3 ± 4.6	100.0 ± 0.1	686
PF3	7.80 ± 3.7	62.0 ± 3.0	18.0 ± 3.6	17.6 ± 0.7	34.2 ± 9.8	98.4 ± 0.5	737
PF4	8.8 ± 5.2	64.8 ± 3.0	20.7 ± 4.8	19.7 ± 1.0	60.4 ± 5.6	97.1 ± 0.8	985
SW1	-	7.4 ± 1.5	28.3 ± 4.6	0.5 ± 0.1	15.3 ± 1.6	5.2 ± 0.9	N/a
SW2	-	5.6 ± 1.1	25.0 ± 2.2	0.1 ± 0.1	35.2 ± 3.7	4.2 ± 0.8	N/a
GW1	-	8.7 ± 0.8	36.5 ± 3.5	0.7 ± 0.1	9.4 ± 5.9	7.7 ± 2.6	N/a

Table 12 Results of the Cone Calorimeter testing

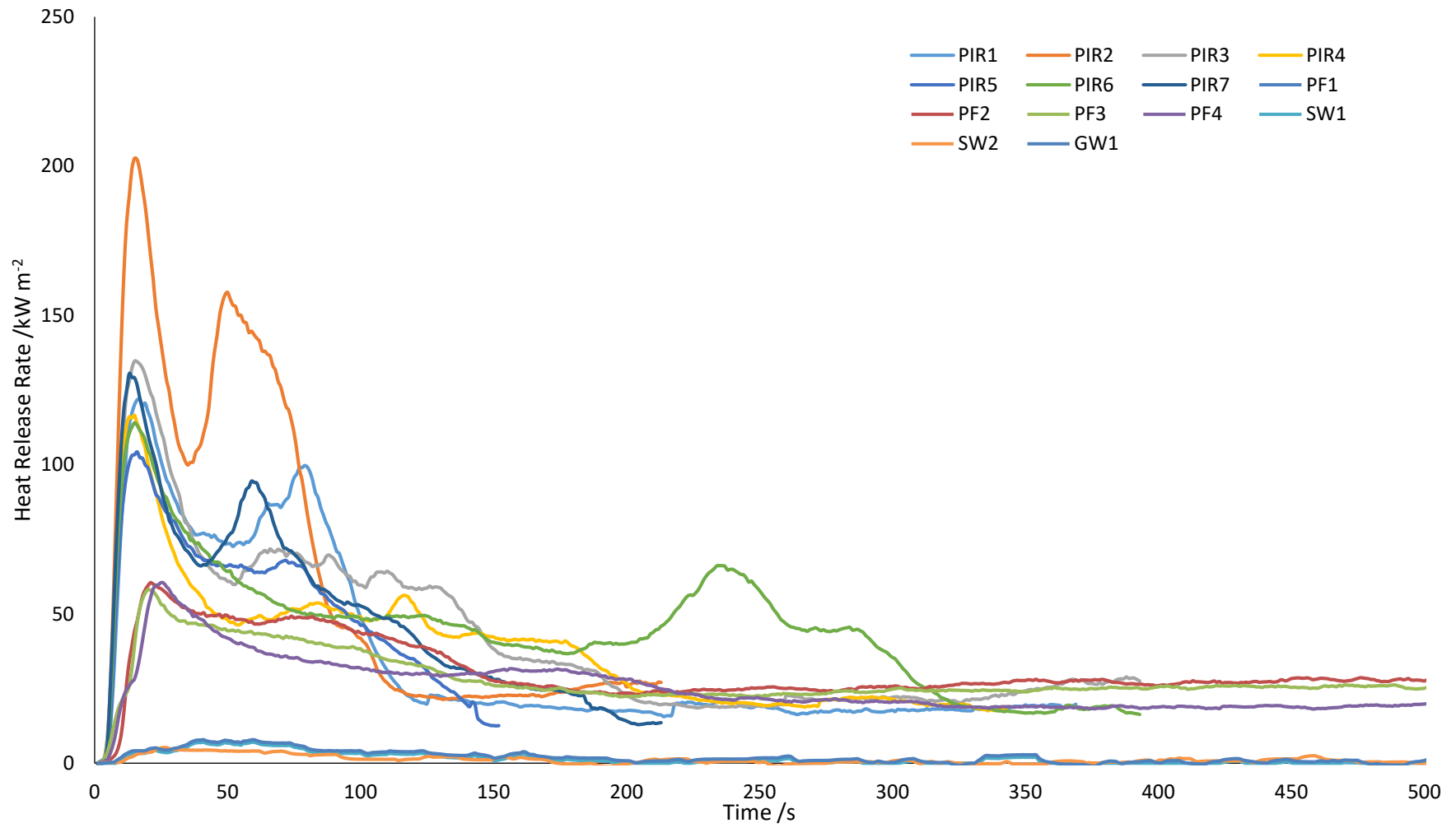


Figure 21 Heat Release Rates of insulation materials measured in the Cone Calorimeter

The PIR samples all showed similar heat release curves, with the exception of PIR2 which had notably increased PHRR while maintaining a middling THR. None of the PIRs tested burned for longer than 400 s, with the majority of the heat released in the first 100 s. Several of the PIR foams also showed a second, lower peak after the first (Figure 22). PIR foams are well-known to form a protective char layer after initially swelling on heating. As the foam swells closer to the cone heater, the protective char layer is diminished, allowing more foam to burn, resulting in a second sharp peak release. Once the protective char layer is stable, the heat release declines rapidly and the material burns out, resulting in ~53 to 76% of its mass lost.

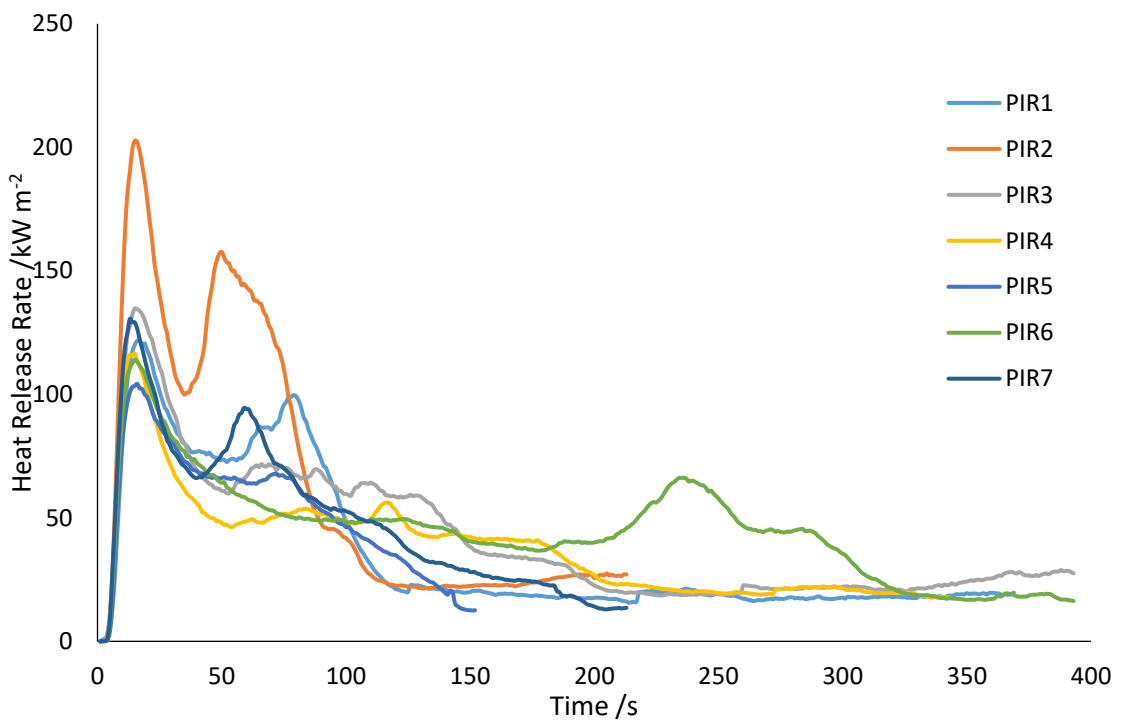


Figure 22 Heat release rates of PIR samples in the cone calorimeter

In terms of other measured characteristics, the PIR foam materials show some variability, which reflects their diverse chemistry. What does remain consistent is their short time to ignition and time to reach PHRR, suggesting a high ignitability when exposed to a radiant heat source at 50 kW m^{-2} . The difference in THR between the highest and lowest of the foams (PIR6 and PIR5) was over double, even when both showed similar PHRR. There was, however, a 12% difference in their mass loss. This demonstrates that differences in chemistry of PIR foams can cause their protective char layer to be more or less effective, resulting in different amounts of fuel burning. PIR foams are also well established to have high smoke production, which as observed in the cone calorimeter, but with high variation between the individual samples. PIR2 had significantly higher smoke than the other materials, with PIR4 producing the least. This high variation in smoke production could be explained by a combination of differences in formulation and differences in fire retardant loading.

The phenolic foam samples showed less variability in many of their measured characteristics when compared to the PIR foams in the cone calorimeter. All four samples had heat release curves that followed a similar trend, and the recorded peak heat release values were relatively similar ($\sim 60\text{-}70 \text{ kW m}^{-2}$). After ignition the heat release curves increased to their peak before declining over a longer duration than the PIR samples. This is due to the lack of a protective char formation, leading to continued burning and THR values similar to that of the highest PIR (PIR6). The lack of a protective char layer also results in the phenolic foams not producing a second sharp heat release peak, instead declining after the initial peak and then achieving a quasi-steady burn. All 4 phenolic foams had significantly longer times to extinction as a result of this, with PF4 burning for over twice as long as the longest PIR foam. This steady burning of the phenolic foams also results in high mass loss values reaching close to 100% for all four samples. The smoke production of the phenolic foams had a fairly diverse range between the four samples, suggesting that the differences in formulation (and possibly flame retardant content) have a notable effect on their smoke production.

The three mineral wool materials did very little in the cone calorimeter due to their high non-combustible content. None of the mineral wool samples achieved ignition, and were allowed to pyrolyse for a full 30 minutes, as per the standard. In Figure 21, the heat release curves have been cut off from the graph at 500s for the sake of presentation. All three materials had low PHRR values and their heat release curves did not show any notable peaks, instead just steadily pyrolysing over the duration of the test. Between the three mineral wool materials, GW1 had the highest PHRR and THR, despite not having the highest binder content. SW2, interestingly, had a significantly higher smoke production than SW1 and GW1, although the smoke production for all three materials was still relatively small. The differences between the mineral wool samples is largely determined by the combination of binder content and formulation, but these differences are insignificant when compared to the results of materials with a high combustible content.

A comparison of the organic content of the mineral wool samples with their observed mass loss observed in the cone calorimeter draws attention to the issues presented by weighing small mass-losses in the cone calorimeter over long test durations. SW1, SW2 and GW1 have 4.7, 2.9 and 2.4% ($\pm 0.1\%$) organic content respectively; however their measured mass loss values are notably higher. This is a result of error in the load cell measurement while the load cell is exposed to high heat flux for 30 minutes. Based on the prolonged exposure to a high heat flux it would be reasonable to assume that the small amount of organic content within the mineral wool samples was completely decomposed.

A comparison of the PIR, phenolic and mineral wool sub-groups of insulation materials highlights distinct differences in their fire properties. Both foam groups (PIR and phenolic) ignited rapidly, with the PIR samples igniting almost instantly. The PIR samples also had much higher PHRR values and reached their PHRR more quickly than the phenolic samples. While their PHRR values were lower, the phenolic foams continued to burn for longer, releasing more heat in total than the PIR foams and losing more mass. Both types of foam also produced varying quantities of smoke within their respective sub-groups, but the PIR foams produced more smoke on average, with values upwards of 10 times the smoke production of the mineral wool samples.

When compared with the foam samples, the mineral wool materials showed significantly reduced ignitability and flammability by not igniting or burning. In terms of fire properties, the mineral wool materials had values lower than the foam samples in every measured characteristic in the cone, apart from higher time to PHRR, from a fire safety point of view, is a desirable result.

The clear differences between the foam and mineral wool samples highlights the potential fire hazards that combustible foam materials present. The rapid fire growth for both the PIR and phenolic foams results in a large amount of heat being rapidly released which could promote further fire growth and flame spread. The PIR is particularly problematic because of its high PHRR values. The phenolic foams also present a fire hazard by burning steadily, potentially sustaining an enclosure fire and supporting flame spread, particularly if installed as a façade on a building. These hazards are compounded by the significant smoke production observed for many of the foams, which can severely hinder the ability of a person to escape by reducing visibility and having potentially irritating effects on the eyes and respiratory tract. Meanwhile, the mineral wool materials are unlikely to contribute to any of these issues in a fire.

3.3.2 Single Burning Item

As described in chapter 2, SBI testing was performed at the Denmark based European Fire and Conductivity (EFiC) laboratory in accordance with the EN 13823 standard. Due to limited access to the equipment, and a relatively high cost per sample tested, only a small selection of samples were taken in order to assess the viability of fire toxicity measurement in a standard SBI apparatus. The full discussion on fire toxicity measurements in the SBI is found in 3.5. The reaction-to-fire data generated is reported here for completeness. The samples were tested in a state reflective of their end-use application, and as such were left with the original out facing material attached, unlike in the cone calorimeter. A summary of the main outputs of the SBI testing can be found in Table 13. The full output reports, including heat release curves, can be found in appendix A.

The four materials showed clear differences in their fire behaviour. The two PIR samples had significantly different FIGRA values. PIR3s fire growth rate was much quicker, reaching a PHRR of almost double that of PIR1. However, the THR_{600s} shows that relatively similar amounts of heat were released by both PIR foams in total. Similarly, PIR3 had a higher SMOGRA, but comparable TSP_{600s} to PIR1. This indicates that PIR3 produced smoke rapidly, while PIR1 released a similar amount of smoke steadily over the duration of the test. PF1 had the highest FIGRA recorded, with a similar THR to the PIR samples, suggesting that the fire grew rapidly, and then burned steadily. SW1 did not ignite in the SBI test and as such produced little heat or smoke.

Sample	Test	Mass Loss /%	FIGRA 0.2 MJ /W s ⁻¹	FIGRA 0.4 MJ /W s ⁻¹	THR 600s /MJ	SMOGRA /m ² s ⁻²	TSP 600s /m ⁻²
PIR1	1	5.7	273	252	4.7	45	96
	2	4.3	332	279	5.2	40	88
PIR3	1	6.5	1241	1232	7.7	93	125
	2	7.0	1072	1054	7.1	67	111
SW1	1	0.9	0	0	1.0	0	15
	2	0.9	3	3	1.0	0	14
PF1	1	19.6	1551	1550	8.2	6	97
	2	33.2	1518	1518	8.0	5	66

Table 13 Results of burning insulation materials in the SBI apparatus

The mass loss data generated from the SBI testing produced some unusual results. Compared to their cone calorimeter results, the foam samples had significantly decreased mass loss. This disparity was most extreme for the PIR samples with 4-7% mass loss in the SBI but 60-75% mass loss in the cone calorimeter. The first reason for this result is that the SBI test is a less severe fire test scenario than the cone calorimeter at 50 kW m⁻². Secondly, PIR foams, in particular, have a number of properties that protect them in this particular scenario. Direct application of flame to PIR foams causes the area in contact with the flame to rapidly char. In accordance with the SBI standard, the PIR foams were tested with their aluminium foil facing. This is able to reflect radiant heat away from the foam, further protecting it from the indirect radiant effects of the flame. This combination of factors allows the PIR materials to minimise mass loss and improve the resulting performance in the SBI test. An example of these properties providing protection against a severe attack by flame can be observed by directly applying a blow torch to a sample of foam. The blow torch rapidly chars the foam in its contact area, and the surrounding foil reflects away the remaining heat; effectively protecting the foam from ignition or any significant mass loss.

In comparison with the rest of their cone calorimeter data, the samples tested in the SBI did not produce coinciding results. PIR1 had a significantly lower PHRR than PIR3 in the SBI, where in the cone their results were similar. All three foam materials also produced similar total quantities of smoke, while in the cone calorimeter; PF1 produced notably less smoke than the PIR samples. These differences could be explained by the low mass loss recorded in the SBI test. Had the PIR foams burned more extensively, their total smoke production may have been much higher and the disparities in heat release rate between PIR1 and PIR3 may have narrowed.

The overall performance of these materials in the SBI test is not entirely unexpected. As it is an essential part of the Euroclass system, manufacturers are able to design their products to perform optimally in that specific test scenario. This is an inevitable result of manufacturers competing to have marketable 'fire safe' construction products and may result in products reaching consumers that perform optimally in specific conditions but are not representative of their real-life fire performance. This is highlighted by the previously mentioned example of applying a blow torch to a foam insulation material for several minutes and it not achieving ignition. This could lead to consumers believing these foam materials are highly fire resistant due to their ability to resist what is perceived to be a severe attack by flame. In reality, foam insulation materials are combustible materials and can be ignited, for example by molten polyethylene drips, which are suspected to have contributed to the rapid flame spread of the Grenfell Tower Fire¹⁰¹.

3.4 Fire Toxicity Assessment

Fire toxicity data was generated in the Steady State Tube Furnace in accordance with ISO/TS 19700. 3 tests were performed on each material to recreate fire conditions 2, 3a and 3b from ISO 19706⁵. These conditions represent well-ventilated flaming, small under-ventilated flaming and large under-ventilated flaming. Each sample was cut into 800 mm strips with the outer facing materials removed. In many cases, the foam samples would begin to swell and bend during the under-ventilated tests (fire stage 3a and 3b). This would negatively affect air flow and commonly resulted in a poor steady state burn. In order to overcome this, the 800 mm samples were cut into thirds and then pinned together. The pinned samples would distort less during the under-ventilated tests resulting in a stable steady state.

Toxic product sampling was achieved by on-line measurement of CO₂ by NDIR, CO by electrochemical cell and O₂ by paramagnetic sensor. HCN and acid gases were sampled by bubbling effluent at 1 L min⁻¹ into bubblers containing 0.1 mol dm⁻³ NaOH and deionised water respectively, followed by post analysis to determine the measured HCN or acid gases. For HCN analysis, two bubblers were chained together containing 150 mL of trapping solution. For acid gas analysis, the first bubbler contained 100 mL and the second contained 50 mL. Sampling was performed for 5 minutes when the test reached a steady state burn – usually during the final 5 minutes of the 20 minute long test.

As expected from their performance in the cone calorimeter, the mineral wool samples did not ignite in the standard temperature range. In accordance with ISO/TS 19700, the mineral wool samples were tested at increasing temperatures up to 900°C and, again, did not ignite. The results of the mineral wool samples are presented in the same three conditions as the foam samples for completeness, but due to their lack of ignition it is not correct to assign an equivalence ratio.

3.4.1 Steady State Tube Furnace Results

The complete results (including equivalence ratios, mass loss and yields with errors ranges) for the SSTF testing of the insulation materials can be found in appendix B.

The mass-charge yields of CO for the foam samples against the equivalence ratio of the test can be found in Figure 23. The yields of CO in well-ventilated conditions were higher than expected for a pure burning polymer in the same condition. This is due to the presence of chlorine in the polymers, which acts as a gas-phase radical inhibitor, preventing the complete oxidation of CO to CO₂ by the hydroxyl radical ($\bullet\text{OH}$). PIR2 and PIR7 had notably higher CO yields in fire stage 2; despite not having a significantly different equivalence ratio or mass loss compared to the other PIR samples.

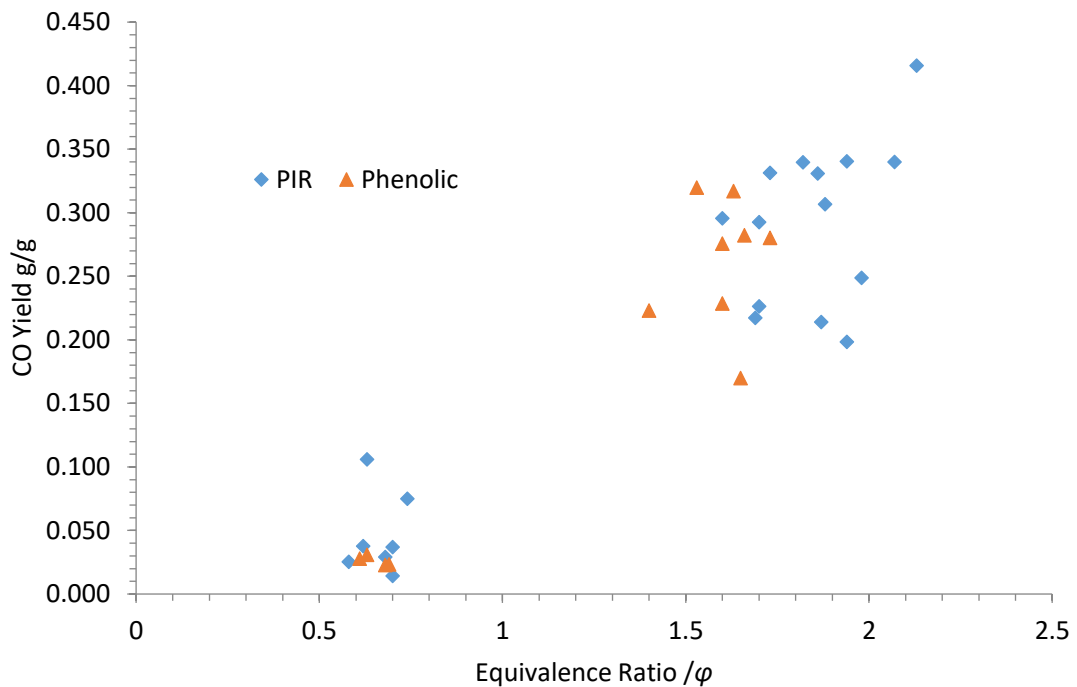


Figure 23 CO Yields against equivalence ratio for burning insulation materials in the SSTF

From well-ventilated to under-ventilated conditions, significant increases in CO yield were recorded for all 7 PIR samples. A relatively wide range of yields from ~0.200 to ~0.400 grams of CO per gram of polymer were quantified. PIR 7 again showed the highest CO yield, with a yield of 0.416 g/g in fire stage 3b. No clear trend can be observed for CO yield between fire condition 3a and 3b, with some samples increasing and while others decrease. This suggests that temperature is not a major factor in determining the yield of CO in under-ventilated conditions, and the variation in CO yield is driven by other factors such as polymer formulation.

The phenolic foam samples followed similar trends to the PIR samples in terms of CO yield. All four samples had slightly elevated CO values in fire stage 2, again probably due to the presence of chlorine in the samples, interrupting the complete oxidation of carbon. In under-ventilated conditions, yields ranging from 0.170 to 0.320 g/g were observed, with PF2 and PF4 reaching similarly high yields of CO (0.320 and 0.317 g/g respectively). In each case, the yield of CO decreased from fire stage 3a to 3b.

The yields of CO quantified for the mineral wool samples were all low. The low carbon content of the samples, and their high non-combustible content, results in CO yields lower than those of the foam samples burning in well-ventilated conditions. Of the three samples, SW1 had the lowest yield, with SW2 having a higher yield, and GW1 having the highest yield of CO. This trend is, unusually, the opposite of the carbon content of the samples. This could be a result of binder formulation or distribution in the sample, but due to the low yields of CO, it is insignificant compared to the yields of CO from carbonaceous materials such as the PIR and phenolic foams.

An interesting trend observed from the mineral wool samples is that the yields of CO decreased from well-ventilated to under-ventilated conditions. This could be due to the reduced air flow allowing the effluent to spend increased time in the hot zone of the furnace. This would increase the amount of CO being oxidised to CO₂ before entering the mixing chamber and cooling. However, the yields of CO₂ from the mineral wool samples do not follow an inverse to this trend. This observation highlights that the SSTF was not designed for the assessment of non-combustible materials with solutions to this challenge are limited due to the nature of the materials being tested. One suggestion could be to adjust the mass feed rate to feed a sufficient amount of binder per minute into the furnace, however this still may not result in combustion. Alternatively, the binder component of the mineral wool could be assessed independently of the non-combustible component and the calculated toxicity scaled proportionally. This, however, may lack relevance because the mineral wool materials are still unlikely to result in flaming combustion in a real-life fire.

A comparison of the CO yields of the three different types of insulation materials tested highlights clear differences between the foams and mineral-wool materials. The mineral wool materials are incapable of producing significant quantities of CO per gram of material because they lack the carbon content necessary. The phenolic and PIR samples, which are carbonaceous, produced relatively similar yields of CO, albeit with some PIR materials reaching higher yields. The yields of CO did exceed expectations in under-ventilated conditions for many of the samples based on knowledge gathered during the literature survey. This could be due to further development in foam manufacturing and changes in their composition, resulting in favoured fragmentation of the polymer to produce CO in under-ventilated conditions. Much of the literature available for PIR and phenolic foams in ventilation-controlled conditions was not performed in the last three years (2015-2018). While the 0.2 g/g CO yield is a useful diagnostic tool for identifying under-ventilated burning of simple polymers (such as polyethylene or polyamides, the data collected as part of this work indicates that complex polymers, like PIR and phenolic foams, can be expected to achieve up to double the yield of CO that simple polymers achieve in under-ventilated conditions.

HCN yields for the foam samples against the equivalence ratio of the test can be found in Figure 24. In well-ventilated conditions, the PIR foam samples produced yields of HCN ranging from 0.001 to 0.006 g/g. PIR7 produced the highest yield of HCN for the PIR foam samples. Like their CO yields, the yields of HCN for the PIR samples increased significantly in under-ventilated conditions ranging from 0.010 to 0.020 g/g HCN. Again, like the CO yields, the yields of HCN did not necessarily increase from fire condition 3a to 3b (i.e. with increased temperature), despite what has generally been accepted in the literature. The original report of this phenomenon was by Saunders in 1959¹⁰² and was based on temperatures upwards of 1000°C. This data suggests that the widely accepted trend of HCN yield increasing with temperature only becomes relevant at temperatures higher than those commonly used in fire testing and that ventilation condition is the primary driving factor in increasing HCN yield.

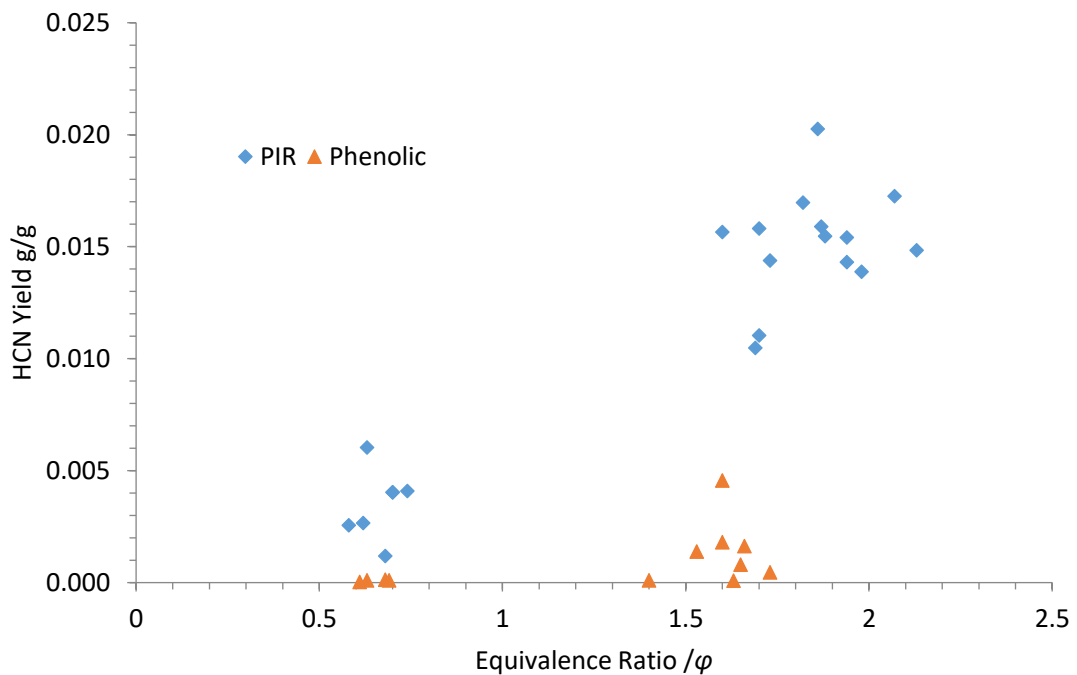


Figure 24 HCN yield against equivalence ratio for burning materials in the SSTF

The remaining two groups of samples produced low yields of HCN in all three of the ventilation conditions compared to the PIR foams. In well-ventilated conditions, PF1 was the only sample of phenolic foam that produced detectable yields of HCN. In under-ventilated conditions the phenolic foams produced varying quantities of HCN. In fire condition 3b, PF3 had a HCN yield comparable to that of PIR foam in well-ventilated conditions. The remaining three samples, however, produced notably less. The mineral wool samples produced detectable but low yields of HCN. Their low organic content and subsequently low nitrogen content, results in very little HCN production as they pyrolyse in the SSTF.

An analysis of the fuel nitrogen content against HCN yield for the foam materials produces mixed results. No trend is immediately visible for the PIR materials, and HCN was either not detected or was below the limit of quantification for the phenolic materials limiting the usefulness of their data. This suggests that there is not a linear relationship between fuel nitrogen and HCN yield. It also suggests that the increased HCN yields of PIR foams is not just a result of their increased nitrogen content, but also a product of the state of the organic nitrogen in the polymer. It is possible that the isocyanurate ring, integral to the structure of PIR foams, favours fragmentation into HCN. This would also explain why flexible and rigid PUR materials do not produce equally high HCN yields to PIR foams, despite in some cases having similar nitrogen content⁵⁷.

Calculating the % of fuel nitrogen recovered as HCN does provide a useful metric for estimating the yield of HCN from PIR foam based on its nitrogen content (Table 14). On average, $10\% \pm 1.5\%$ of fuel nitrogen is recovered as HCN in under-ventilated conditions. This value could act as a useful diagnostic checkpoint for estimating the yield of HCN from burning PIR foam if the nitrogen content is known. This does not, however, translate to well-ventilated conditions as smoothly with $2.5\% \pm 1.0\%$ of fuel nitrogen recovered as HCN. This increased variance in well-ventilated conditions is possible due to the interfering effects of chlorine in radical reactions. Or possible due to the differences in the decomposition of PIR foams in well-ventilated vs. under-ventilated conditions.

Sample	ISO Fire Condition	HCN Yield g/g	Fuel Nitrogen Recovered as HCN %
PIR1	2	0.001	0.79
	3a	0.015	10.41
	3b	0.015	10.37
PIR2	2	0.004	2.70
	3a	0.016	10.51
	3b	0.017	11.41
PIR3	2	0.003	1.81
	3a	0.011	7.52
	3b	0.016	10.77
PIR4	2	0.003	1.83
	3a	0.016	11.20
	3b	0.020	14.49
PIR5	2	0.004	2.66
	3a	0.017	11.19
	3b	0.014	9.43
PIR6	2	0.004	2.72
	3a	0.014	9.73
	3b	0.014	9.39
PIR7	2	0.006	4.50
	3a	0.010	7.83
	3b	0.015	11.09
Average PIR	2	0.004	2.43
	3a	0.014	9.77
	3b	0.016	10.99

Table 14 HCN yields and fuel nitrogen recovery for specific fire conditions in the SSTF

Quantification of the NO_x products from the burning insulation materials resulted in low but detectable yields of NO for many of the samples tested, but no NO_2 was detected for any of the samples. The NO yields were low for all materials tested, with slightly higher yields for the PIR samples compared to the phenolic foams (probably due to their increased nitrogen content) and none detected for the mineral wool samples. The lack of NO_2 detected suggests that either no detectable amount was produced, or that deionised water and HPIC analysis is not a sufficient sampling method for the measurement of NO_x products. It is possible that electrochemical sensors or targeted wet chemical trapping methods could be more effective.

The HCl yields of the foams showed significant variance between samples and could be an indicator of the chlorine content in the samples (Figure 25). In well-ventilated conditions, the PIR foams all produced quantifiable amounts of HCl, which sharply decreased in under-ventilated conditions. This could be explained by the increased smoke generated during incomplete combustion, allowing HCl to adsorb onto the particles and on cold spots in the mixing chamber itself. The yields of HCl from the phenolic foams did not follow the same trend. Their yields were generally lower but did increase in under-ventilated conditions. This indicates a lower fire retardant loading in the phenolic foams, compared with the PIR foams which are generally known to contain increased fire retardant loading.

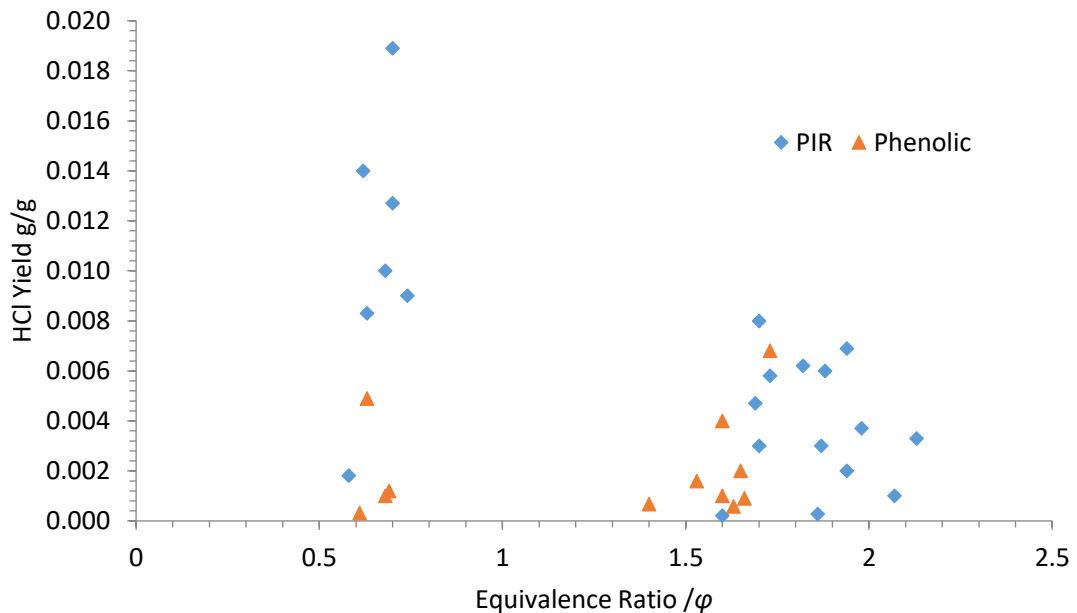


Figure 25 HCl Yield against equivalence ratio for burning insulation materials in the SSTF

Phosphate measured from the effluent has been presented as the yield of H_3PO_4 . Measured phosphate from the burning insulation materials supports earlier assertions of the presence of chlorinated organophosphate flame retardants in the foam samples, excluding PF1 (that did not contain any phosphorous); although no clear correlation between phosphate yield and ventilation condition is evident. In order to assess the toxic contribution of organophosphate flame retardants and organo-phosphorus fragments (which would theoretically increase in yield in under-ventilated conditions due to incomplete combustion), more specific targeted analysis needs to be developed, as it does not currently exist for fire samples.

Overall, the results of the SSTF testing produced useful data for further fire toxicity assessment using FED analysis. The foam samples produced high yields of CO in under-ventilated conditions, with the PIR foams producing high yields of HCN. Additional acid gases were detected from the burning foams, particularly HCl which was highest from the PIR samples. The mineral wool samples did not produce significant quantities of any of the target analytes due to their low combustible content.

3.4.2 FED Analysis

As described earlier in the introduction, a fractional effective dose (FED) calculates the contributions of individual toxicants and their total contribution to an end point (incapacitation or death). In the following sections, the FEDs have been calculated to show the contribution of 1 kg of sample burning in a 50 m³ enclosure. An FED of 1 indicates that there are sufficient toxic gases present, for the given exposure time, to incapacitate or kill (depending on the calculation used) 50% of the exposed population.

The FEDs calculated provide a relative comparison of the toxicity of the burning samples and of the individual contribution of individual toxicants to that toxicity. As the concentrations used are directly from the SSTF, they do not replicate a realistic scenario of exposure, i.e. a person would not be directly inhaling undiluted effluent at a steady concentration, and instead the concentration (and dose) would increase over time. While this is the case, the values have been left unadjusted, and the scenario is assuming that the person has become trapped in a compartment in which 1 kg of sample material has burned in a specific fire condition and the effluent has dispersed evening throughout the space. This serves to provide a simple model scenario for assessing and comparing the fire toxicity of the insulation materials tested.

ISO 13571 – Incapacitation:

ISO 13571 is used to estimate compromised tenability, i.e. incapacitation, by exposure to fire. A situation in which a person is incapacitated will result in their death as they continue to inhale asphyxiant gases such as CO and HCN, unless they are rescued. The model separates the contributions of asphyxiants, irritants, smoke, and heat. The FEDs calculated for the asphyxiant gases are presented in Figure 26. When the fractional effective concentrations (FEC) of the irritant gases are added to the data (Figure 27), their contribution is shown to be clearly negligible compared to that of the asphyxiant gases. At the time of writing, ISO 13571 is currently being updated and is under development as ISO/CD 13571-1¹⁰³.

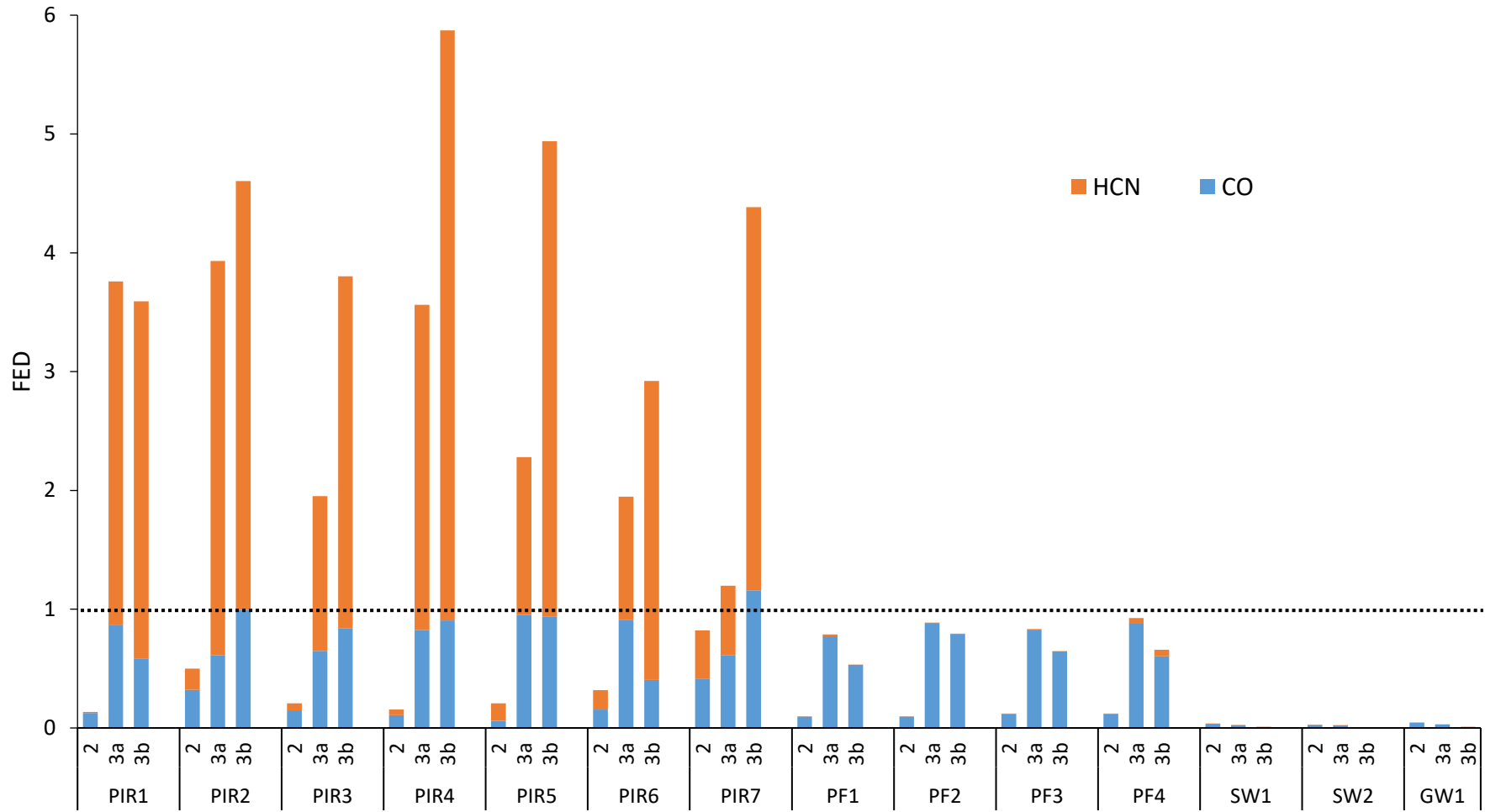


Figure 26 ISO 13571 FED calculations for incapacitation by toxic effluent

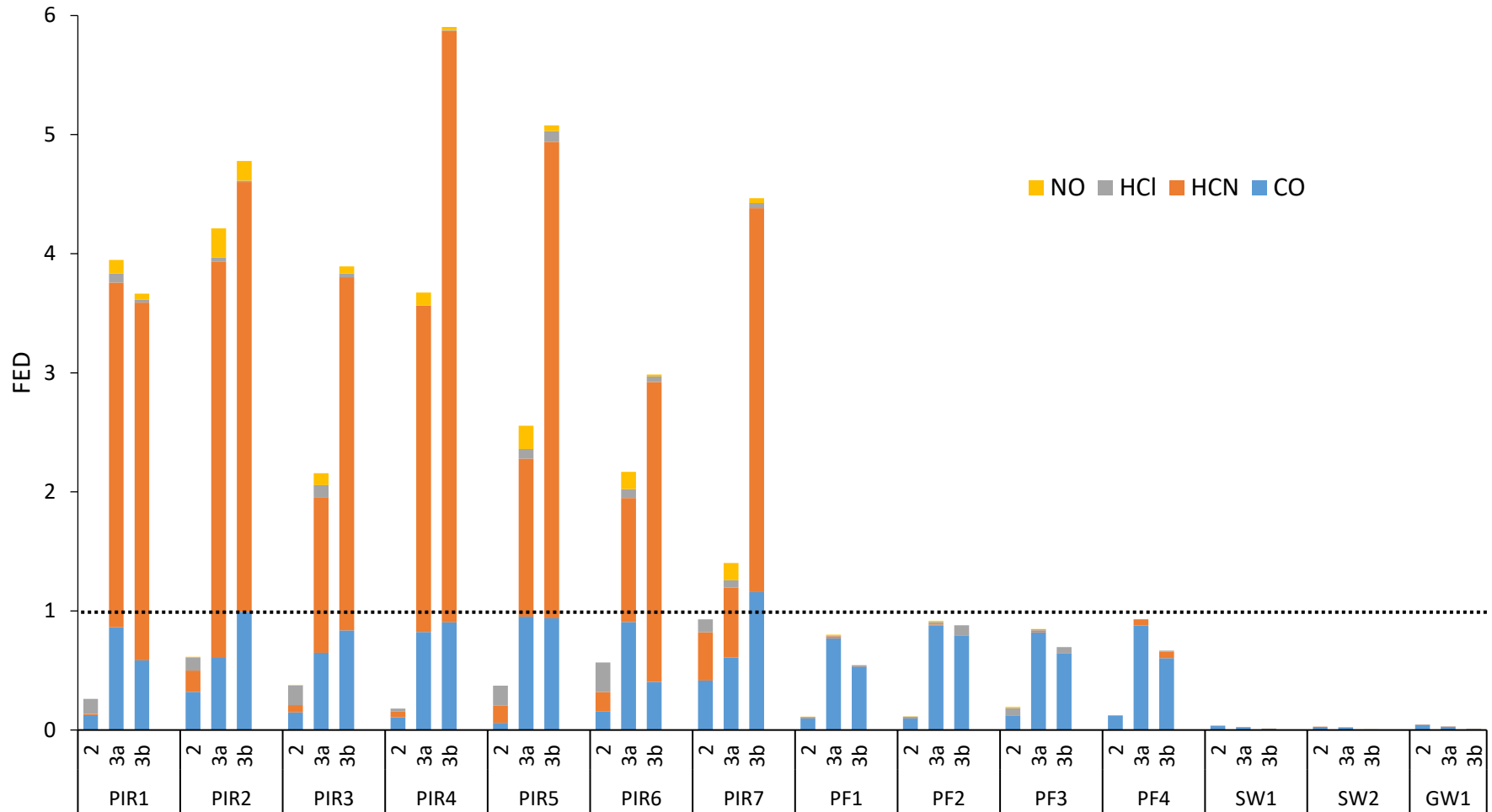


Figure 27 ISO 13571 calculations for incapacitation including the FED values for NO and HCl

The PIR foam samples show high FEDs that increase significantly from well-ventilated to under-ventilated conditions, in correlation with their toxic product yields. The contribution to this high toxicity is primarily the result of HCN, which dominates the FED due to its high toxicity and leads to HCN alone being able to reach an FED greater than 1 in almost every case. The contribution of CO, while lower than that of HCN, is still significant. In several cases, such as PIR4, PIR5 and PIR7, the contribution of CO to FED is almost equal to or higher than 1. In combination, the toxicity of CO and HCN suggest that PIR foams burning in under-ventilated conditions could readily produce an incapacitating atmosphere in a 50 m³ enclosure.

Unlike the PIR foams, the HCN production of the phenolic foams was insignificant in terms of toxicity. Their toxicity is primarily the result of their CO production, with the FED contribution from CO reaching close to FED = 1 for several samples. Unsurprisingly, the mineral wool materials had low FED values in all conditions due to their low non-combustible content and limited production of CO and HCN.

ISO 13344 – Lethality:

The ISO 13344 Purser model calculates the FED based on lethality as its endpoint, instead of incapacitation. The calculation assumes a 30-minute exposure to the effluent with the same mass and volume described previously (1 kg in 50 m⁻³). Unlike ISO 13571, which separates FED and FEC, the ISO 1344 Purser model includes irritants and asphyxiants together when calculating the total contribution to lethality. The ISO 13344 Purser model differs further in that the contribution of CO₂ is accounted for in both CO₂ driven hyperventilation and an acidosis factor. Oxygen depletion is also factored into the calculation. The relative contribution of each toxicant is simplified, not containing an exponent functions, and is calculated using the concentration of the toxicant over its 30 minute LC₅₀ value.

The results are proportional to those of ISO 13571 but the maximum FED values are lower (Figure 28). The contribution of HCN still makes up the majority of the PIR toxicity, but CO has a higher weighting. The contribution of HCN is higher for the phenolic samples compared to ISO 13571, pushing their calculated FED values above 1 in fire condition 3a. The toxicity of the mineral wool samples remains proportionally low due to their low toxic product yields. The contribution of NO is notable for the PIR samples, despite the yields being relatively low. The contribution of NO to fire toxicity is questionable, and likely overestimated, as discussed in section 1.2.3. The contribution of HCl calculated is negligible despite relatively high yields for the PIR samples.

The 13344 Purser model reemphasises the major contribution of HCN to PIR fire toxicity, despite not having an exponential function like in ISO 13571 to drive the FED to high values. It also shows that even without considering HCN, CO continues to be a major factor in the smoke toxicity of burning polymers because of the carbonaceous nature of the foam insulation materials. Meanwhile the mineral wool materials do not produce appreciable quantities of toxic smoke because they simply lack the combustible content to produce toxic gases in lethal quantities.

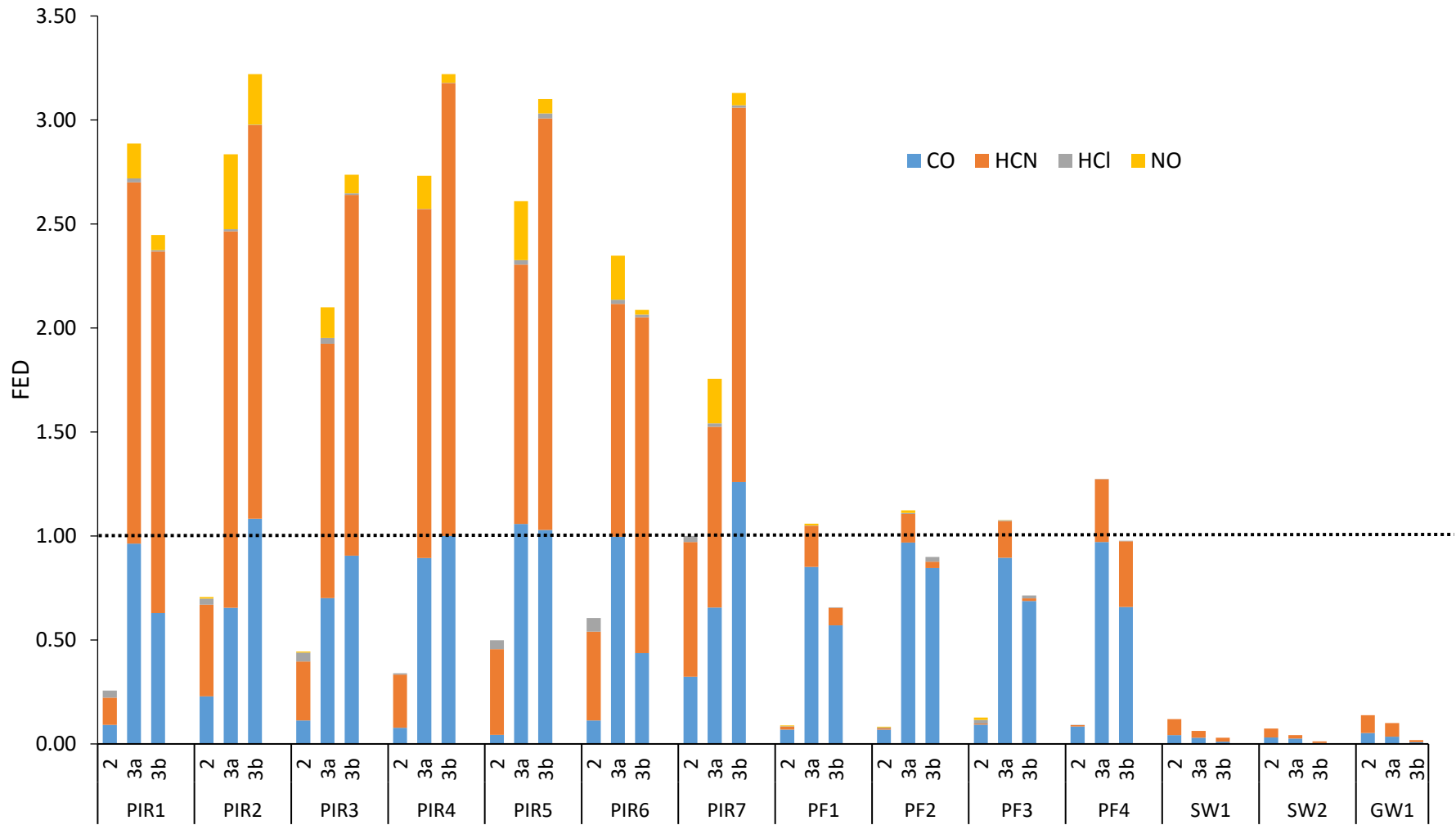


Figure 28 ISO 13344 FED calculated for lethal exposure to toxic effluent

Material LC₅₀ calculations:

The use of material LC₅₀ (m-LC₅₀) and material-IC₅₀ (m-IC₅₀) normalises the toxicity of the burning material for a fixed mass in a given volume for a specific fire condition^{65,66}. It is generally expressed in grams per cubic meter with lower values indicating higher fire toxicity for that specific material in that specific condition. The calculated m-LC₅₀ and m-IC₅₀ are presented in Table 15. Based on the uncertainty estimated in ISO 13344 and ISO 13571, the error associated with the m-LC₅₀ and m-IC₅₀ are ±30% and ±35% respectively.

Ultimately, a comparison of the m-LC₅₀ and m-IC₅₀ values further emphasises the differences between the three types of materials tested in terms of their fire toxicity. On average the PIR foams produced effluent that was 2 to 3 times more toxic than the average phenolic foam, and 20 to 30 times more toxic than the average of the mineral wool materials (Table 16). It also demonstrates that the mass of burning material (in under-ventilated conditions) needed to incapacitate a person after a 5 minute exposure, is not much different from the mass required to potentially kill a person after a 30 minute exposure. If the mass of foam burning is large enough to produce an incapacitating atmosphere then it is reasonable to assume that the person, once incapacitated, will likely die in around 30 minutes unless rescued.

The contribution of acid gases to incapacitation or death appears to be insignificant compared to the high yields and subsequent high toxicity of the asphyxiant gases produced by the burning foams. However, this does not discredit the potential effects of acid gases in irritating smoke to compel people to turn away from their current escape route, or find a place of refuge while they await rescue. A person that is taking refuge during a fire is effectively incapacitated as they are not making their escape. This increases the time they are exposed to the lethal effects of the asphyxiant gases CO and HCN, increasing their risk of death unless rescued.

While the foam samples required relatively low masses to produce a lethal or incapacitating atmosphere, the mineral wool samples would require large masses of sample to produce an incapacitating or lethal atmosphere in a given enclosure due to their high non-combustible content.

Sample	ISO Fire Stage	Material-IC ₅₀ / g m ⁻³ (5 minute exposure)	Material-LC ₅₀ / g m ⁻³ (30 minute exposure)
PIR1	2	46	31
	3a	10	6
	3b	11	7
PIR2	2	26	16
	3a	10	6
	3b	9	5
PIR3	2	35	23
	3a	13	8
	3b	10	6
PIR4	2	43	26
	3a	10	6
	3b	9	5
PIR5	2	32	21
	3a	11	6
	3b	9	5
PIR6	2	27	19
	3a	12	7
	3b	12	8
PIR7	2	21	13
	3a	16	9
	3b	9	5
PF1	2	62	44
	3a	24	15
	3b	33	23
PF2	2	62	46
	3a	22	14
	3b	22	17
PF3	2	57	44
	3a	23	15
	3b	27	21
PF4	2	58	43
	3a	21	12
	3b	28	16
SW1	2	212	129
	3a	384	233
	3b	685	436
SW2	2	371	207
	3a	667	351
	3b	1479	871
GW1	2	188	111
	3a	230	140
	3b	650	423

Table 15 Material-IC₅₀ and material-LC₅₀ for insulation materials burned in the SSTF

Sample	ISO Fire Condition	Average Material- IC ₅₀ /g m ⁻³ (5 minute exposure)	Average Material-LC ₅₀ / g m ⁻³ (30 minute exposure)
PIR	2	33	21
	3a	12	7
	3b	10	6
PF	2	60	44
	3a	23	14
	3b	28	19
MW	2	257	149
	3a	427	242
	3b	938	577

Table 16 Average material IC₅₀ and material LC₅₀ values for insulation burned in the SSTF

3.5 Fire Toxicity Measurements from Standard Reaction to Fire Tests

Despite the fact that fire toxicity kills the majority of people in fires, it is still probably the least researched area of fire science¹⁰⁴. In recent years there has been an increased interest in fire toxicity, in part due to the tragic Grenfell Tower Fire. In 2017 the European Commission published a report evaluating the need to integrate testing for fire toxicity into EU regulations¹⁰⁵. This has led to demand for a widespread fire toxicity test that would ideally be developed from an existing standard in order to minimise costs to integrate the testing. However, it is counter-productive to use a non-ventilation controlled test scenario to measure fire toxicity as it is an essential factor that influences the yields of toxic products.

In order to contribute to this discussion, fire toxicity measurements were taken in the cone calorimeter and SBI test to represent a bench-scale and a large-scale test scenario respectively. The results of these tests were then compared to those of a dedicated fire toxicity test, the steady state tube furnace, to assess the viability of these tests for fire toxicity measurement.

3.5.1 Fire Toxicity in the Cone Calorimeter

As described previously, insulation samples were tested in the cone calorimeter at 50 kW m⁻². The cone calorimeter testing standard requires the measurement of CO and CO₂ already, so additional sampling was performed for HCN. A probe was inserted into the cone calorimeters exhaust duct and the effluent from the exhaust was pumped at 1 L min⁻¹ during the test into a Drechsel bottle containing 50 mL of 0.1 mol dm⁻³ NaOH (aq). The results of the testing are presented in Table 17. The yields presented in Table 17 are calculated over the complete duration of the test and include both flaming and non-flaming combustion.

Sample	CO ₂ Yield g/g	CO Yield g/g	HCN Yield g/g
PIR1	1.971	0.110	0.002
PIR2	2.486	0.113	0.004
PIR3	2.056	0.127	0.004
PIR4	2.075	0.119	0.005
PIR5	1.857	0.060	0.004
PIR6	1.957	0.083	0.003
PIR7	2.151	0.088	0.004
PF1	1.570	0.149	<0.001
PF2	1.913	0.233	<0.001
PF3	1.710	0.204	<0.001
PF4	2.040	0.243	ND
SW1 – NF	0.155	0.003	<0.001
SW2 – NF	0.219	0.006	<0.001
GW1 – NF	0.175	0.005	<0.001

Table 17 CO₂, CO and HCN yields in the cone calorimeter at 50 kW m⁻²

The cone calorimeter has been previously described as a well-ventilated scenario with quantitative data available in the literature to support that conclusion¹⁰⁶. Despite this, the yields recorded in the cone calorimeter for the insulation materials tested give an inconsistent view of the ventilation conditions during the tests. The CO₂ yields for the PIR samples are slightly decreased from what would be expected for well-ventilated burning. Additionally, the CO yields are elevated into the 0.2+ g/g range, which would indicate slight vitiation during the tests. The elevated CO yields could be explained by the presence of chlorinated organophosphates reducing the combustion efficiency of the fire by preventing oxidation of CO to CO₂. However, the values are higher than would be expected from the action of fire retardants alone in a well-ventilated fire, which suggests a combination of slight under-ventilation and the effects of the flame retardant additives. The yields of HCN detected were comparable to that observed for PIR foams burning in well-ventilated conditions.

The yields of toxic products from the phenolic foams in the cone calorimeter are unusual. The yields of CO for the phenolic foams are elevated to 0.150 to 0.250 g/g which would be strongly indicative of under-ventilated burning. However, the CO₂ yields for these three materials are not as low as would be expected for under-ventilated burning, although they are slightly decreased. All four of the phenolic foam samples had near to 100% mass loss, which would suggest well-ventilated burning. Additionally, the HCN yields for the phenolic foams were all below the limit of quantification, and PF4 producing no detectable levels of HCN.

The mineral wool samples produced low yields of all three gases analysed. The yields of CO₂, however, were higher than expected. This is unusual as the mineral wool samples all have low carbon content that would limit the production of CO₂. This could be explained by errors in the measurement of CO₂. The low combustible content of the samples resulted in low concentrations of CO₂ being detected over the duration of each 30 minute test and minor fluctuations in the CO₂ detected could result in 'noisy' data that would affect the recorded yield.

The results of the cone calorimeter testing indicate a scenario with less complete combustion than well-ventilated flaming, but not reaching under-ventilated burning (e.g. $\phi = 1.2+$). While the effect of flame retardants preventing complete combustion could provide a partial answer to explain these results, they do not completely explain why the literature generally reports the cone calorimeter as a well-ventilated scenario ($\phi = 0.7$). The results of sampling for HCN does, however, support a well-ventilated scenario as the yields observed for the PIR foams are concurrent with both literature and data generated as part of this work for HCN yields from burning PIR foams in well-ventilated conditions. These mixed results suggest that the cone calorimeter does not give a clear picture of the ventilation conditions in the test based purely on the yields of toxic products observed.

3.5.2 Fire Toxicity in the SBI Test

Like to the cone calorimeter, the SBI standard requires CO and CO₂ measurements, so additional sampling was performed for HCN. A probe was inserted into the main exhaust at the same point that the CO and CO₂ measurements were taken. The effluent was pumped at 1 L min⁻¹ into a series of Drechsel bottles containing 150 mL of 0.1 mol dm⁻³. Each Drechsel bottle was used for 5 minutes before switching to the next over the duration of the test apart from the first bottle that was pumped for 6 minutes. The SBI standard requires an air flow of 0.50 to 0.65 m³ s⁻¹. For the testing carried out here, the averaged air flow was 0.60 m³ s⁻¹. This is arguably a large air flow which would result in a well-ventilated test scenario compared to the size of the burner and mass of available fuel.

The high air flow required as part of the test standard created challenges for detecting the toxic gases produced. This is evident from the concentrations of gases measured, which were close to the limit of detection of the instruments and had low maximum recorded values (Table 18). This can be seen for all four of the samples tested, with none of the combustible foams reaching concentrations of CO₂ higher than 0.5%. This is also clear from the maximum measured concentration of CO, although this is would be expected to be low in a well-ventilated scenario.

Product	Test	Max CO ₂ Concentration /%	Max CO concentration /ppm
PIR1	1	0.31	100
	2	0.30	74
PIR3	1	0.38	82
	2	0.35	132
SW1	1	0.21	0
	2	0.22	0
PF1	1	0.40	289
	2	0.43	339

Table 18 Maximum recorded concentrations of CO₂ and CO in the SBI test

The yields of toxic gases quantified from the SBI testing provide a mixed impression of the ventilation conditions of the scenario (Table 19). The yields of CO₂ for the combustible foam materials were all low. PIR1 and PF1 produced similar CO₂ yields that would suggest partially under-ventilated combustion. PIR3s CO₂ yield was low enough that it would suggest severely under-ventilated burning comparable to that of a fire burning in ISO fire condition 3a or 3b. This is opposed by the consistently low yields of CO which suggest that the conditions are, in fact, well-ventilated. The yields of CO for the two PIR foams, in particular, are lower than would be expected. The presence of flame retardants in the foam would increase the well-ventilated CO yield higher than is observed here.

The yields of CO₂ and CO for the stone wool sample, SW1, were low as would be expected. CO was not detected during the testing of SW1 and HCN, while detected, was barely above the limit of detection.

The unusual opposition between the CO₂ and CO yields observed for the combustible foams provides a confusing depiction of the ventilation conditions in the SBI test. In reality, the high dilution of the effluent in combination with the low mass of the combustible foam samples (particularly the PIR foams) results in low concentrations of measured gases and subsequently low yields which appear to be inherent to the test scenario.

Sample	Test	Starting Mass	Mass Loss	CO ₂ Yield	CO Yield	HCN
		/kg	/%	g/g	g/g	Yield g/g
PIR1	1	3.84	5.70	1.009	0.016	< 0.001
	2	3.85	4.30	1.003	0.009	< 0.001
PIR3	1	7.97	6.50	0.560	0.007	< 0.001
	2	7.95	7.00	0.572	0.012	< 0.001
SW1	1 – NF	31.51	0.90	0.103	0.000	< 0.001
	2 – NF	31.61	0.90	0.110	0.000	< 0.001
PF1	1	4.51	19.60	1.051	0.025	< 0.001
	2	5.53	33.20	0.857	0.033	< 0.001

Table 19 Mass loss and toxic product yields in the SBI test

3.5.3 Comparison with a Dedicated Fire Toxicity Test – the SSTF

The yields of toxic products quantified in the cone calorimeter and the SBI test do not appear to give a clear picture of the ventilation conditions of the tests. As the SSTF has a clearly defined fire condition in each test, and the cone calorimeter and SBI do not, a quantifiable metric is required to be able to compare the test methods effectiveness for measuring fire toxicity. CO:CO₂ ratio is a useful value for assessing the ventilation condition of a fire as it progresses. The CO:CO₂ ratios of the materials tested are presented in Table 20.

The CO:CO₂ data from the tests gives a clearer view of the ventilation conditions in each scenario. In the SSTF in ISO fire stage 2, the ratio is less than 0.020 for all four of the samples. The PIR samples have a slightly higher value than PF1, but is still of a similar order. These ratios are similar for the PIR samples in the SBI apparatus, but PF1 had a slightly higher value, possibly due to the increased size of the fire. All fires that reach a certain size will begin to become ventilation limited due to the inability of oxygen to reach the flame. Nevertheless the ratio is still low even for PF1. SW1 has a ratio of zero in the SBI because no CO was detected.

In the cone calorimeter, the CO:CO₂ ratios were increased for all of the samples compared to the SBI and SSTF. PIR1 and PIR3 had increased ratios, as did SW1, while PF1 had a similar ratio to its result in the SBI test. The increase of ratio for the PIR samples could be explained by the char formation that is commonly observed for PIR samples. As the sample is exposed to the radiant heat from the cone heater it will rapidly char across its surface. This could reduce the ability of oxygen to reach pyrolysing fuel below the char layer.

Fire Condition	CO/CO ₂ Ratio			
	PIR1	PIR3	SW1 (NF)	PF1
SBI Test 1	0.016	0.012	0.000	0.024
SBI Test 2	0.009	0.020	0.000	0.039
Cone 50 kW m ⁻²	0.056	0.062	0.019	0.094
SSTF 2	0.012	0.017	0.010	0.009
SSTF 3a	0.709	0.400	0.000	0.581
SSTF 3b	0.338	0.523	0.000	0.304

Table 20 Comparison of CO:CO₂ ratio in the SBI, cone calorimeter and SSTF

Despite the slight increases in the cone calorimeter, the comparison of CO:CO₂ ratio between the three test methods demonstrates that the flammability tests are well-ventilated scenarios. As a result of this, the cone calorimeter and SBI test do not come close to being able to replicate the most hazardous fire condition from a fire toxicity perspective – under-ventilated burning. To use such tests for fire toxicity assessment would be unfair as it would misrepresent the toxic hazard that a material presents in a fire. Furthermore, both tests progress through the various stages of a fire, which are their own defined fire stage and as such the yield of toxic products per gram of burning material will vary throughout the test. This makes it difficult to give specific yields, as they are clearly dependant on the fire condition. Therefore, a dedicated fire toxicity test would require a combination of steady state burning and ventilation controlled conditions to be an effective test method for assessing fire toxicity. The SSTF meets all of these criteria and the CACC also produces quasi-steady state conditions, but still has numerous design challenges to overcome as described previously.

Overall, the desire to use a pre-existing test and modify it to measure for fire toxicity is not productive as reaction-to-fire tests, like the cone calorimeter and SBI test, do not produce suitable fire conditions. The reality of fire hazard assessment requires flammability testing to be well-ventilated in order to create the worst conditions for fire growth and flame spread. Fire toxicity assessment, on the other hand, requires clearly defined ventilation controlled conditions to recreate the most hazardous condition from a fire toxicity perspective – under-ventilated flaming. A combination of flammability testing and fire toxicity assessment, with data generated in each areas dedicated testing apparatus will be more representative of material fire hazard than a catch all test derived from an existing test method. The ISO/TS 19700 Steady State Tube Furnace is clearly a strong contender for best available fire toxicity test and should be considered for inclusion in all future fire testing, so as to include fire toxicity in fire hazard assessment.

3.6 Quantitative Assessment of the Fire Hazards of Insulation Materials

In isolation, flammability and fire toxicity measurements do not give a complete assessment of the fire hazards presented by a specific material. Therefore, a methodology to combine these data in a simple way, which could contribute to the safety of people in buildings, is desirable. In 2016, Hull, Brein and Stec presented a methodology for estimating the 'maximum safe loading' of a material in m^2 per 100 m^{-3} . The method utilises estimates of mass loss per unit area based on Euroclass data (or derived from actual test data) combined with fire toxicity data generated in the SSTF to calculate the maximum safe loading for non-layered materials of consistent thickness¹⁰⁷. The fire toxicity data generated in the SSTF was used to calculate a material-LC₅₀ based on ISO 13344. This could then be used in combination with the materials mass loss per unit area to calculate a lethal volume of effluent. The final MSL value was then calculated using the lethal volume of effluent and a precautionary factor. The guidance outlined in ISO 13571 indicates that a factor of 10 would translate to only 1% of the population being estimated to be susceptible to the lethal effects of the effluent. This provides a buffer to minimise the risk to the exposed population, but for vulnerable populations, such as the elderly or movement impaired, larger factors may be necessary.

In order to practically apply the methodology outlined by Hull, Brein and Stec, it was necessary to deviate from the method as described in the paper. The SBI test is a large-scale fire test which requires a high mass of sample and large space for the test itself. Due to the relatively high cost per test and limited access to an SBI apparatus, it was deemed impractical to use the SBI to generate the mass loss data. Taking these factors into consideration, the cone calorimeter was selected to generate the mass loss data. The cone calorimeter is a well-established reaction-to-fire test, with acceptable repeatability and a relatively low cost per sample. Furthermore, the cone calorimeter allows for mass loss per unit area to be consistently measured by the load cell, unlike the SBI test which would require the operator to measure the burn area and depth, potentially increasing error in the measurements. During the cone calorimeter testing programme carried out as part of this work, all 14 of the insulation samples tested were cut to a consistent thickness (25 mm). This would further improve consistency and comparison between the materials tested. Whereas in the SBI, the samples would be tested at the thickness appropriate to their end use, which would differ between the materials selected.

The material-LC₅₀ values used in these calculations can be found in Table 15 and the mass loss per unit area values can be found in Table 12. The area required to produce a lethal volume of toxic effluent per m⁻³ can be calculated using Equation 6. The MSL of a material for a specific fire condition can then be calculated using Equation 7.

$$V_{LC50} = \frac{M_L}{mLC_{50}}$$

Where:

V_{LC50} is the area of material that will produce a lethal atmosphere per cubic meter in m² m⁻³

M_L is mass loss per unit area in g m⁻²

mLC₅₀ is the material-LC₅₀ as described in section 3.4.2

Equation 6 Lethal volume of effluent from a burning material in a specific fire condition

$$MSL = \frac{100}{V_{LC50} \times 10}$$

Where:

MSL is the maximum safe loading of the material for a specific fire condition in m² per 100 m³

Equation 7 Maximum safe loading of a material in a specific fire condition

The MSL values calculated for the samples tested as part of this work are presented in Table 21, with a factor of 10 used to minimise the risk to those exposed. Regardless of the factor chosen (e.g. 3x or 10x or any other value) the relative scale between the results will still be the same.

Sample	Mass Loss /g m ⁻²	ISO Fire Stage 2			ISO Fire Stage 3a			ISO Fire Stage 3b		
		mLC ₅₀ /g m ⁻³	Lethal Volume /m ² m ⁻³	Maximum Safe Loading /m ² per 100 m ³	mLC ₅₀ /g m ⁻³	Lethal Volume / m ² m ⁻³	Maximum Safe Loading /m ² per 100 m ³	mLC ₅₀ /g m ⁻³	Lethal Volume / m ² m ⁻³	Maximum Safe Loading /m ² per 100 m ³
PIR1	520	30.77	16.90	0.59	5.70	91.22	0.11	6.65	78.15	0.13
PIR2	646	16.49	39.18	0.26	5.77	112.05	0.09	5.11	126.39	0.08
PIR3	675	23.31	28.96	0.35	7.73	87.38	0.11	5.98	112.93	0.09
PIR4	603	26.35	22.88	0.44	5.99	100.58	0.10	5.14	117.31	0.09
PIR5	446	21.04	21.20	0.47	6.28	71.04	0.14	5.30	84.19	0.12
PIR6	853	18.52	46.06	0.22	6.95	122.75	0.08	7.75	110.01	0.09
PIR7	520	13.29	39.14	0.26	9.14	56.89	0.18	5.24	99.19	0.10
PF1	535	43.71	12.24	0.82	14.85	36.02	0.28	22.58	23.69	0.42
PF2	786	45.57	17.25	0.58	14.01	56.09	0.18	17.01	46.21	0.22
PF3	867	43.94	19.73	0.51	14.55	59.59	0.17	20.99	41.31	0.24
PF4	950	43.02	22.08	0.45	12.47	76.16	0.13	15.98	59.44	0.17
SW1	286	128.85	2.22	4.51	233.28	1.23	8.16	436.48	0.66	15.26
SW2	320	206.91	1.55	6.47	351.32	0.91	10.98	871.26	0.37	27.23
GW1	100	110.71	0.90	11.07	139.85	0.71	14.00	423.30	0.24	42.33

Table 21 Maximum safe loading values for insulation materials based on cone calorimeter and SSTF data

Both the PIR and phenolic groups of samples showed similarly low MSL values. The PIR samples showed less variation due to their high fire toxicity, even with broader differences in mass loss. The phenolic samples, however, had a much higher variation in MSL, with PF1 having a MSL almost twice as high as PF4. The mineral wool samples showed significantly higher MSL values compared to the foams owing to their combination of low combustibility and low fire toxicity. One observation from the data collected is that the samples with the highest flammability or fire toxicity are not necessarily the most hazardous overall. For example, in fire condition 3a, PIR6 had the third lowest fire toxicity but its notably high mass loss results in it having the lowest MSL (and highest potential fire hazard). This example highlights the need to combine reaction-to-fire data with fire toxicity data.

When compared to the estimated values presented in the original paper outlining the methodology, the calculated values in Table 21 are of a similar order. The estimated mass loss values are also of similar order. However, the mLC_{50} values are somewhat higher. Due to the identities of the insulation in the paper being withheld, it is difficult to more precisely compare these results barring for the mineral-wool samples, which fit well with the estimated results for 'insulation 1' and 'insulation 2'. Nevertheless, one could reasonably predict that insulation 4, 5, 6 and 7 were all combustible foam products due to the comparable MSL values.

The use of material- LC_{50} as the basis for the toxicity contribution to the calculations is arguably not as effective for improving the safety of building occupants. As described previously, incapacitation is a more effective end point for fire toxicity assessment, as a person that is incapacitated is unable to escape from the fire situation and will die due to asphyxiant gases unless rescued. Based on this consideration, the MSL values have been recalculated using material- IC_{50} (Table 22).

Sample	Mass Loss /g m ⁻²	ISO Fire Stage 2			ISO Fire Stage 3a			ISO Fire Stage 3b		
		mIC ₅₀ /g m ⁻³	Lethal Volume / m ² m ⁻³	Maximum Safe Loading /m ² per 100 m ³	mIC ₅₀ /g m ⁻³	Lethal Volume / m ² m ⁻³	Maximum Safe Loading /m ² per 100 m ³	mIC ₅₀ /g m ⁻³	Lethal Volume / m ² m ⁻³	Maximum Safe Loading /m ² per 100 m ³
PIR1	520	46.10	11.28	0.89	9.76	53.27	0.19	10.82	48.08	0.21
PIR2	646	25.62	25.21	0.40	9.84	65.64	0.15	8.94	72.27	0.14
PIR3	675	35.13	19.21	0.52	13.09	51.55	0.19	10.11	66.79	0.15
PIR4	603	42.68	14.13	0.71	10.33	58.40	0.17	8.52	70.81	0.14
PIR5	446	31.90	13.98	0.72	11.30	39.48	0.25	8.85	50.38	0.20
PIR6	853	27.19	31.37	0.32	12.42	68.69	0.15	12.09	70.55	0.14
PIR7	520	20.73	25.08	0.40	16.23	32.03	0.31	9.09	57.19	0.17
PF1	535	61.76	8.66	1.15	24.30	22.01	0.45	33.45	15.99	0.63
PF2	786	62.32	12.61	0.79	21.64	36.33	0.28	22.39	35.11	0.28
PF3	867	56.93	15.23	0.66	23.11	37.51	0.27	27.39	31.65	0.32
PF4	950	57.88	16.41	0.61	21.22	44.76	0.22	27.50	34.54	0.29
SW1	286	211.90	1.35	7.41	383.95	0.74	13.42	684.59	0.42	23.94
SW2	320	371.20	0.86	11.60	666.62	0.48	20.83	1479.08	0.22	46.22
GW1	100	187.74	0.53	18.77	229.50	0.44	22.95	649.93	0.15	64.99

Table 22 Maximum safe loading values calculated using incapacitation as the endpoint for fire toxicity assessment

The results are interesting as although incapacitation occurs at a lower concentration than lethality, the incapacitation based MSL values are ~35% higher on average. This would suggest that a higher loading is safer when in reality that would obviously not be the case. The increase in safe loading is the result of the mIC_{50} values being calculated for a 5 minute exposure to the effluent, rather than a 30 minute exposure for the mLC_{50} values. While this limits the comparison of the two possible options, it still ultimately comes down to the decision of which fire toxicity end point is chosen. A strong argument exists for using incapacitation as the end point and opens up further possibilities for the MSL methodology. By using ISO 13571 to calculate the fire toxicity, it is possible to adjust the amount of time for the exposure to match that of the required safe egress time (RSET). The calculated mIC_{50} for that time window could then be used to calculate a maximum safe loading of a material that, when burning, could not produce an incapacitating atmosphere before occupants are able to escape. This would increase the accuracy of the calculated maximum safe loading value.

While the MSL methodology does present a simple method for estimating material loading, it has some obvious problems that arise from using such a simplified model. Firstly, the assumed burning behaviour is directly linked to the fire test (a cone heater) and as such represents well-ventilated burning. In under-ventilated conditions, the mass loss will be lower. Based on this, the model will be combining well-ventilated mass loss with under-ventilated fire toxicity which represents a worst-case scenario in terms of overall fire hazard. However, it could be argued that because the objective of this method is to calculate the fire hazard and prevent loss of lives, being within safe limits is an appropriate goal. One solution to this concern would be to measure mass loss in a ventilation controlled reaction-to-fire test, such as the CACC. This would generate mass loss data for a specific fire condition, which could be paired with fire toxicity data of the appropriate fire condition. A glaring solution to this problem would be to use the SSTF for mass loss, as the mass loss values measured are specific to a defined ventilation condition. However, the samples in the SSTF are cut into 800mm strips, which will have a higher surface area to volume ratio that would significantly alter their burning behaviour compared to the real-life scenario of large insulation panels exposed to a flame or radiant heat. This renders the SSTF ineffective for providing mass loss data.

In a similar vein to the previous point, the heat flux selected in the cone calorimeter (50 kW m⁻²) is comparable to that of ISO fire stage 2 – well-ventilated flaming. In fully developed fires, the heat flux can exceed that value significantly. This will lead to differences in mass loss, particularly in highly vitiated conditions such as ISO fire stage 3b. The authors of the original methodology noted a similar issue with using data generated in the well-ventilated SBI test and its 30 kW burner. As was noted in section 3.5, the SBI test is not severe enough to produce significant mass loss in materials that are designed to perform well in that specific test scenario. Materials, such as PIR foams, which perform well in the SBI test, thanks to their char forming behaviour and foil outer facing, are still capable of burning and losing significant mass in real-life situations, as evidenced by a number of fires including the Grenfell Tower Fire. This further supports the use of an alternative method to generate mass loss data for burning materials that is to be used for calculating a maximum safe loading value.

Despite these noted weaknesses, this method of calculating a maximum safe loading could allow building designers to quickly take into consideration the materials they are using in construction. An applied maximum safe loading limit of a specific material could potentially reduce the risk to occupants presented by the burning insulation in a fire. Furthermore it directly integrates fire toxicity, which causes the majority of deaths by fire in the UK, into fire risk assessments.

The use of two bench-scale standard tests also supports the use of this methodology in fire hazard assessment as it makes the data straightforward to generate. The cone calorimeter is a widespread test method, and with the recent increased interest in fire toxicity, it seems reasonable to expect more widespread use of the SSTF. However, this does not exclude the need for larger scale fire testing, as it is necessary to understand the burning behaviour of materials that may not be represented in a test like the cone calorimeter (i.e. horizontal vs. vertical sample or radiant heat sources vs. direct flame application). Larger scale testing is also necessary to understand the fire behaviour of materials in the end-use state, such as rainscreen façades, that have more complicated arrangements of materials, joints and fittings.

Ultimately, the ability to condense a large amount of data into a workable and understandable output is essential when making fire safety accessible. Many individuals involved in building design are unlikely to be experts in fire science and would benefit from an accessible method when selecting materials, so that occupant safety is not compromised by a lack of specialised knowledge. The maximum safe loading methodology is not intended to replace rigorous fire safety assessment in construction, but is fully intended to support informed decision making in material selection.

Chapter 4

4.0 Conclusions and Future Work

As part of this work, 14 insulation materials (7 PIR, 4 phenolic, and 3 mineral wool) were analysed for their composition, flammability and fire toxicity. Clear differences were observed between the 3 types of sample. The foam insulation materials (PIR and phenolic) produced high quantities of toxic gases and burned readily in the cone calorimeter. In particular, the PIR samples had the highest fire toxicity due to the generation of HCN from nitrogen in the burning fuel. The primarily non-combustible mineral wool samples produced lower yields of toxic gases and also had very little mass loss, not igniting in any of the fire tests they were exposed to. This demonstrates that there are significant differences between the combustible products and non-combustible products both in terms of flammability and fire toxicity, indicating a disparity in the fire hazards they present.

An assessment of both the cone calorimeter and the SBI apparatus for measuring fire toxicity has been carried out and both methods failed to replicate the high toxicity of under-ventilated flaming. The well-ventilated nature of these tests makes them unsuitable for fire toxicity, as the most dangerous fire condition is under-ventilated burning. This supports the use of the SSTF as a key method for measuring fire toxicity due to its ventilation controlled conditions and steady burning state. This allows for more consistent data to be generated, specific to the fire condition required.

The maximum safe loading methodology has shown promise when practically applied to real data, but required some modification to in order to be used as part of this project. The cone calorimeter was selected to generate the mass loss data, as it is a bench-scale method that is well-established and has a relatively low cost per sample. The mass loss data generated in the cone calorimeter was paired with SSTF data, as it has been established to be a reliable and effective method for generating fire toxicity data in specific ventilation conditions. Further modifications to the original method were made by using material-IC₅₀ values instead of material-LC₅₀ values, as incapacitation is arguably a more important end point in fire toxicity assessment. The methodology requires further development to account for the changes in mass loss in under-ventilated conditions. This would improve the accuracy of the method without overcomplicating what is intended to be a simple way of estimating the maximum safe loading of a material for given enclosure. Furthermore, the use of this methodology serves of a method to integrate fire toxicity into fire risk assessment, as it is lacking in current fire safety assessment.

The maximum safe loading values calculated further demonstrate the significant differences between the materials tested in each specific fire condition. The combination of high mass loss and high fire toxicity results in the foam insulation materials, particularly the PIR foams, having low MSL values indicating a high fire hazard. On the other hand, the mineral wool samples had much higher MSL values, showing their low overall fire hazard. The MSL values calculated for the foam insulation materials are so low that it may be impractical to achieve the desired level of insulation for an enclosure without exceeding a safe loading. The fire hazards presented by foam insulation materials, when their fire toxicity is included in the assessment, suggests that their fire hazard they present is excessively high when safer, non-combustible alternatives exist.

In addition to the analysis of the fire hazards of insulation materials, work has been performed to optimise the quantification of arguably one of the most important toxic products of combustion – HCN. The chloramine-T/isonicotinic acid method for quantifying HCN from ISO 19701 was assessed and then optimised to allow for improved repeatability and reproducibility. As the methods of quantification for the two most important toxicants (CO and HCN) are well established (NDIR) or have been optimised in this work (chloramine-T/isonicotinic acid), the next logical step could be to invest future work into the development of methods for the quantification of other toxicants not covered in this thesis.

Isocyanates are highly toxic and irritating, as well as having several long term consequences to human health, as discussed in section 1.2.3. They are produced during the decomposition of polyurethane based materials (including PIR foams). Isocyanates are highly reactive molecules that will interact with a large number of compounds found in fire effluent, making them difficult to sample and quantify. Several derivatisation compounds found in the literature have been successfully applied to quantify isocyanates⁵⁶. The development of these methods for sampling fire effluent could provide a more detailed analysis of isocyanates in PIR fires, which is currently limited in the literature. In particular, the SSTF could provide useful data for early fire stages, where isocyanates are suspected to be at their highest yield. Furthermore, a ventilation controlled study of isocyanates in PU/PIR fires will contribute to the overall understanding of their fire toxicity.

Similarly to isocyanates, aldehydes (particularly formaldehyde and acrolein) are also highly irritating compounds, with potential long-term health consequences. However, unlike isocyanates, aldehydes are produced in fires from a wide variety of materials and thus are highly likely to be encountered in a fire. Their contribution to the fire toxicity of insulation materials is not well understood, but they are known to be generated from the decomposition of PIR and phenolic foams, as well as from the decomposition of phenolic binders in mineral wool materials. Again, the use of the SSTF would be essential in understanding their relationship with ventilation condition, which has not strongly established in the literature. This work would be beneficial as it would contribute to a more detailed understanding of organic irritants generated by decomposing insulation materials, which can have serious consequences to persons attempting to escape in a fire.

Beyond continuing method development to improve toxicant sampling in fire effluent, this work has raised several interesting questions about the fate of fuel nitrogen in polyurethane fires. How much of the fuel nitrogen remains in the residue? How much was released as other nitrogen containing compounds (HCN, NO, NO₂, isocyanates, amines, etc)? How much is released as N₂? While not directly relevant to fire safety, these questions may be worth answering in order to further the development of new PIR based materials that do not have high yields of HCN in fires. This could be achieved by reducing the amount of fuel nitrogen that is converted to HCN by trapping it in the residue or by increasing the amount of fuel nitrogen released as N₂.

The Grenfell Tower Fire has brought the risks of fires, and particularly the risks presented by insulation materials in fires, into the public eye. This work has demonstrated the significant differences between the different insulation materials commonly found in modern construction. It has also demonstrated that fire toxicity is a major threat to life presented by fire, yet is not required in fire hazard assessment in the UK. When accounting for fire toxicity and flammability, combustible insulation materials such as PIR and phenolic foams have a high fire hazard that needs to be acknowledged in risk assessments when they are incorporated into a structure. The application of a simple maximum safe loading model could support building designers in making informed decisions about material selection and loading, by incorporating material reaction-to-fire and fire toxicity into a single model. An accessible methodology could lead to safer building design and in turn contribute to preventing needless tragedies like the Grenfell Tower Fire from happening again.

Chapter 5

5.0 References

1. Grand View Research (2018) Insulation Market Size & Share Analysis Report By Product (Glass Wool, Mineral Wool, EPS, XPS), By Application (Residential Construction, Non-residential Construction, Industrial, HVAC & OEM), And Segment Forecasts, 2018 – 2025, Report ID: 978-1-68038-196-2
2. Grenfell Tower Fire: Written statement – HCWS18, Parliament.uk retrieved 03/07/18
3. UK Fire Statistics 2013 (and preceding years) – United Kingdom
4. Purser DA, Stec AA, Hull TR (2010) Chapter 2 – Fire Scenarios and Combustion Conditions. In: Fire Toxicity, Woodhead publishing, ISBN: 9781845695026
5. ISO 19706:2011 – Guidelines for assessing the fire threat to people
6. Pitts WM (1995) The global equivalence ratio concept and the formation mechanisms of carbon monoxide in enclosure fires, *Progress in Energy and Combustion Science*, 21(3), p197-237
7. Tewarson A (2002) SFPE Handbook of Fire Protection Engineering, 3rd edition, Edited by P.J. DiNenno et al. National Fire Protection Association, 82, p161
8. ISO TS 19700 (2016) Controlled equivalence ratio method for the determination of hazardous components of fire effluents – the steady state tube furnace
9. Gottuk DT, Lattimer BY (2002) SFPE Handbook of Fire Protection Engineering, 3rd ed. Edited by P.J. DiNenno et al, National Fire Protection Association, Quincy, MA, p54-82
10. Blomqvist P, Lonnermark A (2001) Characterization of the combustion products in large-scale fire tests: comparison of three experimental configurations, *Fire and Materials*, 25, p71-81
11. Purser DA, Purser JA (2008) HCN Yields and fate of fuel nitrogen for materials under different combustion conditions in the ISO 19700 tube furnace, *Fire Safety Science – Proceedings of the Ninth International Symposium*, p1117-1118, International Association for Fire Safety Science
12. Hull TR (2008) 11 – Challenges in fire testing: reaction to fire tests and assessment of fire toxicity, in *Advances in Fire Retardant Materials*, Edited by Horrocks AR and Price D, Woodhead Publishing, p255-290
13. Biteau H et al (2008) Calculation methods for the heat release rate of materials with unknown composition, *Fire Safety Science – Proceedings of the ninth international symposium*, p1165-1178

14. ISO 5660-1:2015 – Reaction-to-fire tests – Heat release, smoke production and mass loss rate – Part 1: Heat release rate (cone calorimeter method) and smoke production (dynamic assessment)
15. Image credit: Efectis – Cone Calorimeter: Predicting fire and smoke behaviour accurately and cost-effectively
16. Wichman IS (2003) Material flammability, combustion, toxicity and fire hazard in transportation, Progress in energy and combustion science, 29, p247-299
17. Quintiere JG (2016) Chapter 4, Principles of fire behaviour: Second Edition, CRC Press, ISBN 1498735703
18. ISO 5657:1997 – Reaction to fire tests – Ignitability of building products using a radiant heat source
19. ISO 11925-2:2010 – Reaction to fire tests – Ignitability of products subjected to direct impingement of flame – Part 2: Single-flame source test
20. EN 13823:2010 + A1:2014 – Reaction to fire tests for building products. Building products excluding floorings exposed to the thermal attack by a single burning item
21. Image Credit: SP Report 2008:29 – “The use of fire classification in the Nordic countries. Proposals for harmonisation”
22. ISO 1182:2010 – Reaction to fire tests for products – Non-combustibility test
23. ISO 1716:2018 – Reaction to fire tests for products – Determination of the gross heat of combustion (calorific value)
24. Sundström, B (2007) Thesis: The development of a European fire classification system for building products – test methods and mathematical modelling, Fire Safety engineering and systems safety, Lund university
25. Messerschmidt B (2008) The capabilities and limitations of the Single Burning Item (SBI) Test, Fire and Building Safety in the Single European Market, One-day symposium, Fire Safety Engineering Applied To (SEAT), Royal Society of Edinburgh
26. INNO firewood – EUROCLASS System – Accessed October 2018 - <http://virtual.vtt.fi/virtual/innofirewood/stateoftheart/database/euroclass/euroclass.html>
27. Martin KT (1985) Hypoxia: Causes and Symptoms, 7th ed, RC Educational Consulting Services, p14-16
28. Greenberg MI (2003) Occupational, Industrial, and Environmental Toxicology, Elsevier Health Sciences p369-370
29. Penney DG (2000) Carbon Monoxide Toxicity, CRC Press, p20-20
30. Wakefield JC (2010) A toxicological review of the products of combustion, HPA Centre for Radiation, Chemical and Environmental Hazards

31. Goldstein M (2008) Carbon Monoxide Poisoning, *Journal of Emergency Nursing*, 34 (6), p538-542
32. Maeda H, et al (1996) Evaluation of Post-Mortem Oxymetry in Fire Victims, *Forensic Sci. Int.*, 81 2-3), p201-209
33. Sykes OT, Walker E (2015) The neurotoxicity of carbon monoxide – historical perspective and review, *Cortex*, ISSN 0010-9452 <http://dx.doi.org/10.1016/j.cortex.2015.07.033>
34. Roderique JD, Josef CS, Feldman MJ, Spiess BD (2015) A modern literature review of carbon monoxide poisoning theories, therapies, and potential targets for therapy advancement, *Toxicology*, 334, p45-58
35. Vale A (2012) Specific Substances: Cyanide Medicine, 40 (3), p121-121
36. Purser DA (2010) 4 – Asphyxiant Components of Fire Effluents, in *Fire toxicity*, Edited by Hull TR and Stec AA, Woodhead Publishing, p163-164
37. Simonson M, Tuovinen H, Emanuelsson V (2000) Formation of Hydrogen Cyanide in Fires – A literature and experimental investigation, SP report 2000:27
38. Levin BC, et al (1987) Effects of exposure to single or multiple combinations of the predominant toxic gases and low oxygen atmospheres produced in fires, *Fundamental and Applied Toxicology*, 9, p236-250
39. Brand G, Jacquot L, Regnier M (2011) Toxicity of Carbon Dioxide: A review, *Chemical Research in Toxicology*, 24, p2061-2070
40. Purser DA (2010) Chapter 3 – Hazards from Smoke and Irritants. In: *Fire Toxicity*, Woodhead publishing, ISBN: 9781845695026
41. Hull TR, Stec AA, Paul KT (2008) Hydrogen Chloride in Fires, *Fire Safety Science*, 9, p 665-676
42. Prien T, Traber DL (1988) Toxic smoke compounds and inhalation injury – a review, *Burns*, 14(6), p451-460
43. Kuligowski ED (2009) Compilation of data on the sublethal effects of fire effluent, NIST Technical Note 1644, NIST
44. Zierold D, Chauviere M (2012) Hydrogen fluoride inhalation injury because of a fire suppression system, *Military Medicine*, 177, p108-112
45. Brock WJ (1999) Hydrogen Fluoride: How toxic is toxic? (A hazard and risk analysis), Halen options technical working conference, 27-29, p559-566
46. Paul KT, Hull TR, Lebek K, Stec AA (2008) Fire Smoke Toxicity: The Effect of Nitrogen Oxides, *Fire Safety Journal*, 43, p243-251

47. Office of Environmental Health Hazard Assessment (1999) Acute Toxicity Summary: Nitrogen Dioxide, Determination of acute reference exposure levels for airborne toxicants, p252-263
48. European Commission (2014) Recommendation from the Scientific Committee on Occupational Exposure Limits for Nitrogen Monoxide, SCOEL/SUM/89
49. US Department Of Health and Human Services (1998) Toxicological profile for sulphur dioxide, US department of health and human services, Public Health Service, Agency for Toxic Substances and Disease Registry
50. Pertruzzi S, Musi B, Bignami G (1994) Acute and chronic sulphur dioxide exposure: an overview of its effects on humans and laboratory animals, *Annali dell'Istituto Superiore di Sanità*, 30(2), p151-156
51. Aleksieva Z (1972) National Research Council Canada: Effects of Sulphur and its Inorganic Derivatives in the Canadian Environment, NRCC No. 15015
52. Einhorn IN (1975) Physiological and toxicological aspects of smoke produced during the combustion of polymeric materials, *Environmental health perspectives*, 11, p163-189
53. Agency for toxic substances and disease registry (ATSDR) (1999) Toxicological profile for formaldehyde, US department of health and human services, Atlanta, US
54. Udeni Alwis K et al(2015) Acrolein Exposure in US Tobacco Smokers and Non-Tobacco Users: NHANES 2005-2006, *Environmental Health Perspective*, 123(12), p1302-1308
55. International Programme on Chemical Safety (IPCS) (1991) Acrolein, *Environmental Health Criteria*, 127, WHO, Geneva
56. Bengstrom L, et al (2016) The role of isocyanates in fire toxicity, *Fire Science Reviews*, 5(4)
57. McKenna ST, Hull TR (2016) Fire Toxicity of Polyurethane Foams, *Fire Science Reviews*, 5(3)
58. ISO 5659-2:2017 – Plastics – Smoke generation – Part 2: Determination of optical density by a single-chamber test
59. NFX 70 100-2:2006 – Fire Tests – Analysis of gaseous effluents – Part 2: Tubular furnace thermal degradation method
60. ISO 12136:2011 – Reaction to fire tests – Measurement of material properties using a fire propagation apparatus
61. ISO/TS 19700:2016 – Controlled equivalence ratio method for the determination of hazardous components of fire effluents – Steady-state tube furnace
62. Schartel B, Hull TR (2007) Development of fire-retarded materials – interpretation of cone calorimeter data, *Fire and Materials*, 31, p327-354
63. Hietaniemi J, Kallonen R, Mikkola E (1999) Burning characteristics of selected substances: production of heat, smoke and chemical species, *Fire and Materials*, 23, p171-185

64. Image credit: Guillaume E, Hermouet F (2014) Presentation of a methodology for predicting the thermal degradation of polymers used in road vehicles under tunnel fire related conditions using the controlled atmosphere cone calorimeter, 2nd Annual Tunnels Fire Safety forum, Amsterdam
65. ISO 13344:2015 – Estimation of the lethal toxic potency of fire effluents
66. ISO 13571:2012 – Life-threatening components of fire – Guidelines for the estimation of time to compromised tenability in fires
67. Image credit: T. Richard Hull (used with permission)
68. Bozsaky D (2011) The historical development of thermal insulation materials, *Architecture*, 41(2), *Periodica Polytechnica*, p49-56
69. Grand View Research (2018) Building Thermal Insulation Market Size, Share & Trends Analysis Report by Product (Glass wool, Mineral wool, EPS, XPS), by application, by end-use, by region and segment forecasts 2018-2025. Report ID: GVR-1-68038-338-6
70. ASD Reports (2017) Building Thermal Insulation Market – Global Forecast to 2022. Report ID: ASDR-418222
71. Markets and Markets Reports (2011) Methylene DiPhenyl Diisocyanate (MDI), Toluene Diisocyanate (TDI) and Polyurethane Market (2011-2016): Markets and Markets CH 1596, July 2011.
72. Avar G et al (2012) *Polymer science: A comprehensive reference*, 10, p411-441
73. Gharehbagh A, Ahmadi Z (2012) Chapter 6: Polyurethane Flexible Foam Fire Behaviour, In: *Polyurethane*, Edited by Fahima Z, Eram S, Intech, p102-120, ISBN 978-953-51-0726-2
74. Wooley WD et al (1975) The thermal decomposition products of rigid polyurethane foams under laboratory conditions, *Fire research note*, No 1039
75. Allan D, Daly J, Liggat JJ (2013) Thermal volatilisation analysis of TDI-based flexible polyurethane foam, *Polymer degradation and stability*, 98, p535-541
76. Saunders JH (1959) The reactions of isocyanates and isocyanate derivatives at elevated temperatures, *Rubber Chemistry and Technology*, 32(2), p337-345
77. Shufen L et al (2006) Studies on the thermal behaviour of polyurethanes, *Polymer-plastics technology and engineering*, 45, p95-108
78. Rogaume T et al (2011) Development of the thermal decomposition mechanism of polyether polyurethane foam using both condensed and gas-phase release data, *Combustion Science and Technology*, 183(7), p627-644
79. Stec AA, Hull TR (2011) Assessment of the fire toxicity of building insulation materials, *Energy and Buildings*, 43, p498-506

80. Schnipper L, Smith-Hansen ES (1995) Reduced combustion efficiency of chlorinated compounds, resulting in higher yields of carbon monoxide, *Fire and Materials*, 19, p61-64
81. Purser DA, Purser JA (2008) HCN yields and fate of fuel nitrogen for materials under different combustion conditions in the ISO 19700 tube furnace, *Fire Safety Science – Proceedings of the ninth international symposium*, p1117-1128, International Association for fire safety science
82. Tingley DD et al (2014) The environmental impact of phenolic foam insulation boards, *Proceedings of the institution of civil engineers*, paper 1400022
83. Johnston PK, Doyle E, Orzel RA (1988) Phenolics: A literature review of thermal decomposition products and toxicity, *Journal of the American college of toxicology*, 7(2), p201-220
84. Gellert R (2010) 8 – Inorganic mineral materials for insulation in buildings, In: *Materials for energy efficiency and thermal comfort in buildings*, Woodhead Publishing Series in Energy, p193-228, ISBN: 978-1-84569-526-2
85. Blomqvist P, Sandinge A (2018) Experimental evaluation of fire toxicity test methods, *RISE Report 2018:40*
86. Image Credit: Tuula Hakkarainen. Image taken from: Hakkarainen T (2002) *Studies of fire safety assessment of construction products*, VTT publications number 459
87. Image Credit: T Richard Hull. Used with permission.
88. Ma J, Purnendu KD (2010) Recent Developments in Cyanide Detection: A Review, *Analytica Chimica Acta*, 673 (2), p117-125
89. Epstein J (1947) Estimation of Microquantities of Cyanide, *Analytical Chemistry*, 19 (4), p272-274
90. ISO 19701:2013 – Methods for Sampling and Analysis of Fire Effluents
91. Fisher FB, Brown JS (1952) Colorimetric Determination of Cyanide in Stack Gas and Waste Water, *Analytical Chemistry*, 24(9), p1440-1444
92. Delgado A, et al (2008) Cyanide Management through Proper Measurement, *Hydrometallurgy, Proceedings of the Sixth International Symposium*, ISBN: 0873352661
93. Hull TR, Stec AA (2015) Generation, Sampling and Quantification of Toxic Combustion Products. In: Purser DA, Maynard RL, Wakefield, JC (eds.) *Toxicology, Survival and Health Hazards of Combustion Products*, RSC, ISBN: 1849735697
94. ISO 19702: 2015 – Guidance for Sampling and Analysis of Toxic Gases and Vapours in Fire Effluents using Fourier Transformed Infrared (FTIR) Spectroscopy
95. Qureshi AM, Patel AN (1978) The Nature of Zolon Red, *Zeitschrift für Naturforschung*, 33b, p450-453

96. König W (1904) Über eine neue, vom Pyridin derivierende Klasse von Farbstoffen, Journal für praktische Chemie, 69(1) p105-137
97. OI Analytical Application Note (2009) An Overview and Comparison of Methods for Cyanide Analysis, #3272
98. Bailey PL, Bishop E (1973) Reaction of Sulphite Ions with Cyanogen Chloride, Journal of the chemical society, Dalton Transactions, p917-921
99. Paul KT, Hull TR, Lebek K, Stec AA (2008) Fire Smoke Toxicity: The Effect of Nitrogen Oxides, Fire Safety Journal, 43(4), p243-251
100. Stec AA, Hull TR (2011) Assessment of the Fire Toxicity of Building Insulation Materials. Energy and Buildings, 43, p498-506
101. BBC News Report 'Grenfell Tower insulation 'never passed fire safety test' – May 2018. Last accessed 19/12/18. <https://www.bbc.co.uk/news/uk-44200041>.
102. Saunders JH (1959) The Reactions of Isocyanates and Isocyanate Derivatives at Elevated Temperatures, Rubber Chemistry, p337-345
103. ISO/CD 13571-1 Life-threatening components in fire – Part 1: Guidelines for the estimation of time to compromised tenability in fires
104. Stec AA (2017) Fire Toxicity – The elephant in the room? Fire Safety Journal, 91, p70-90
105. European Commission Report – Study to evaluate the need to regulate within the Framework of Regulation (EU) 305/2011 on the toxicity of smoke produced by construction products in fires – October 2017
106. Schartel B, Hull TR (2007) Development of fire-retarded materials – Interpretation of Cone Calorimeter Data, Fire and Materials, 31, p327-354
107. Hull TR, Brein D, Stec AA (2016) Quantification of Toxic Hazard from Fires in Buildings, Journal of Building Engineering, 8, p313-318

Appendices

Appendix A – Results of the EN 13823 SBI Testing

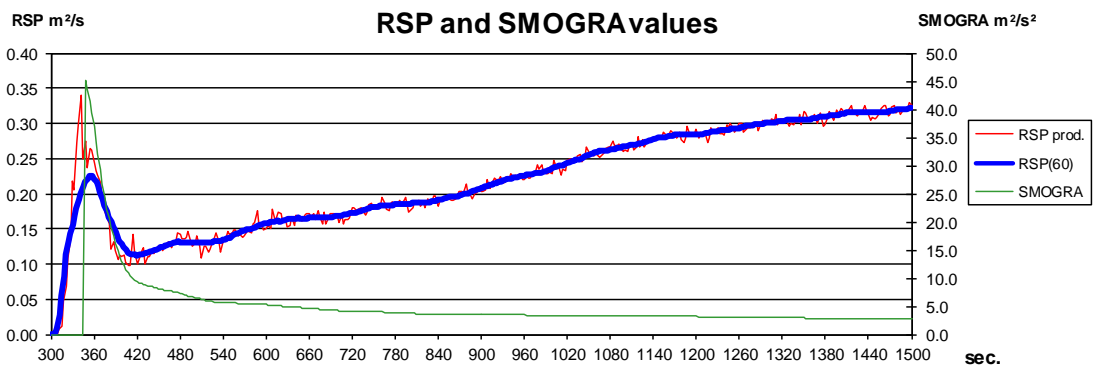
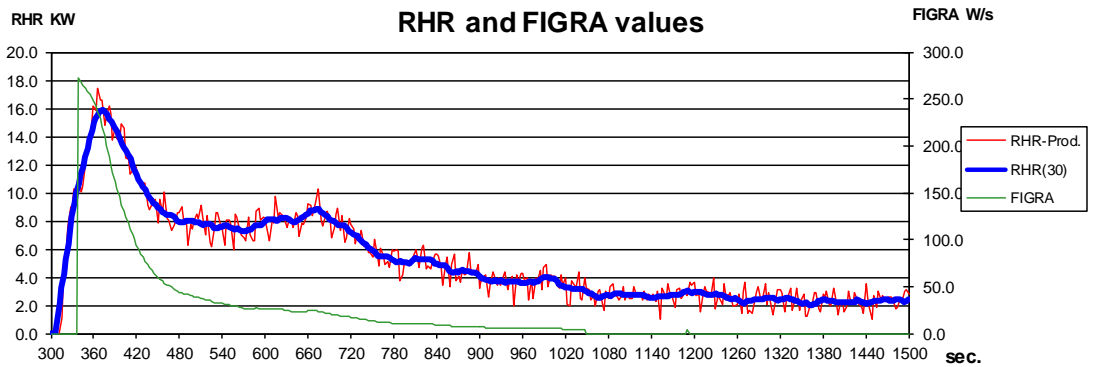
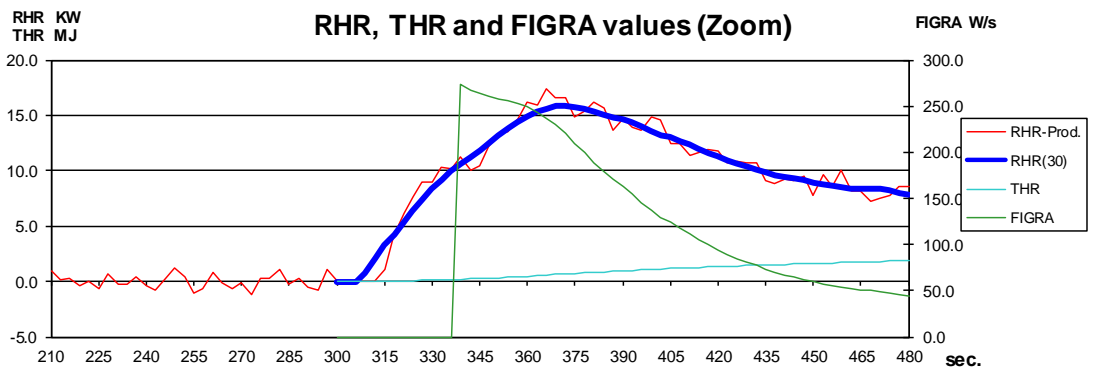
The following test reports were generated as outputs of the EN 13823 SBI testing performed at the European Fire and Conductivity laboratory (EFiC) in Denmark. The experimental methodology used to generate this data can be found in section 2.0.5. Discussion of these results can be found in section 3.3.2 and 3.5.

SBI Test (EN 13823)

EFiC

European Fire & Conductivity lab.

Product:		EFiC No.	Test no.	Operator	Test Date:	Print Date:
PIR1		16-012	1	KuE	29-08-2016	29-08-2016
Test condition		Check points		Results		
Ambient Temp. $(t=30-90)$ [°K]	293.9	RHR _{av, burner} [KW]	32.6	FIGRA [W/s] 0.2 MJ	273	
Ambient pressure. [Pa]	100806	RHR _{std, burner} [KW]	0.617	FIGRA [W/s] 0.4 MJ	252	
Humidity [%]	44.4	CO ₂ /O ₂ Ratio _{burner}	0.575	THR ₆₀₀ [MJ] *	4.7	
K(t)	0.914	RSP _{av, burner} [m³/s]	-0.001	Lateral flame spread (LFS) reach the edge?	No	
K(p)	1.080	RSP _{std, burner} [m³/s]	0.005	SMOGRA [m²/s²]	45	
E [KJ/m²]	17200	Baseline Duct temp. $(t=30-90)$ [°K]	295.0	TSP ₆₀₀ [m²] *	96	
Duct Diameter: [m]	0.306	Min. no. of accep. Thermocouples	3	Flaming droplets/particles (FDP) (flaming <= 10 s)?	No	
Start date for conditioning	22-08-2016	Minimum for flow [m³/s]	0.588	Flaming droplets/particles (FDP) (flaming > 10 s)?	No	
End date for conditioning	29-08-2016	Maximum for flow [m³/s]	0.628			
Total conditioning time [h]	168	Burner response time [s]	9	Time to max Figra [s] *	39	
Baseline O ₂ $(t=30-90)$ [%]	20.713	Weight before conditioning [Kg]	3.840	Tig (2*6KW) [s] *	21	
Baseline O ₂ $(t=30-90)$ [%]	20.956	Weight after conditioning [Kg]	3.840	* After ignition of main burner		
Baseline CO ₂ $(t=30-90)$ [%]	0.037	Weight diff. in percent per day	0.00			
Baseline Light signal $(t=30-90)$	0.994	End data O ₂ $(t=1680-1740)$ [%]	20.957			
		End data CO ₂ $(t=1680-1740)$ [%]	0.044			
		End data Light signal $(t=1680-1740)$	0.976			
				Synchronisation information	Baseline	Last point
				T-Duct (2.5 °K drop from baseline)	320.6	297
				O ₂ (0.05% rise from baseline)	20.670	300
				CO ₂ (0.02% drop from baseline)	0.2015	300

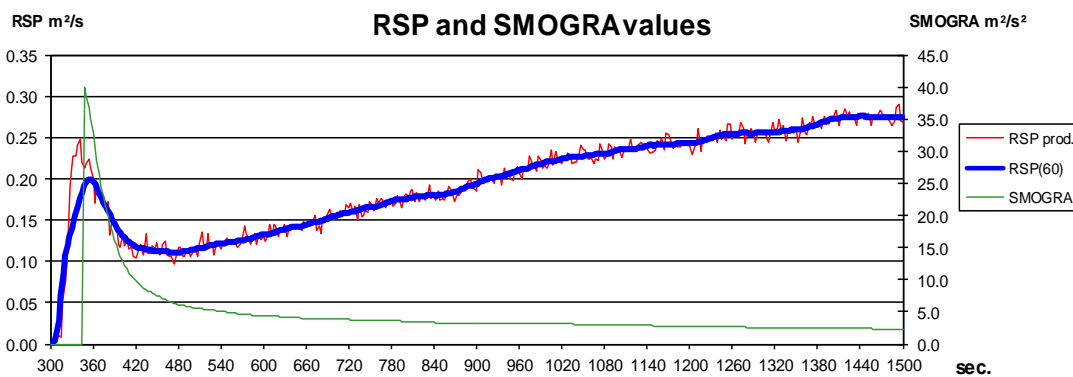
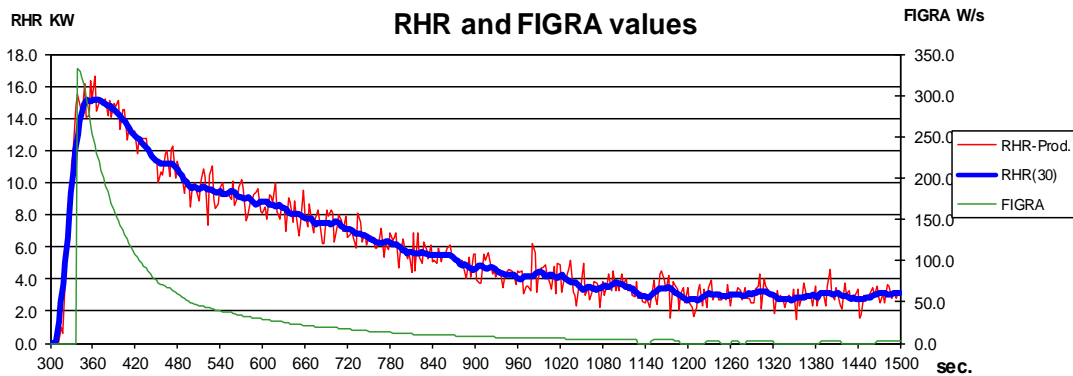
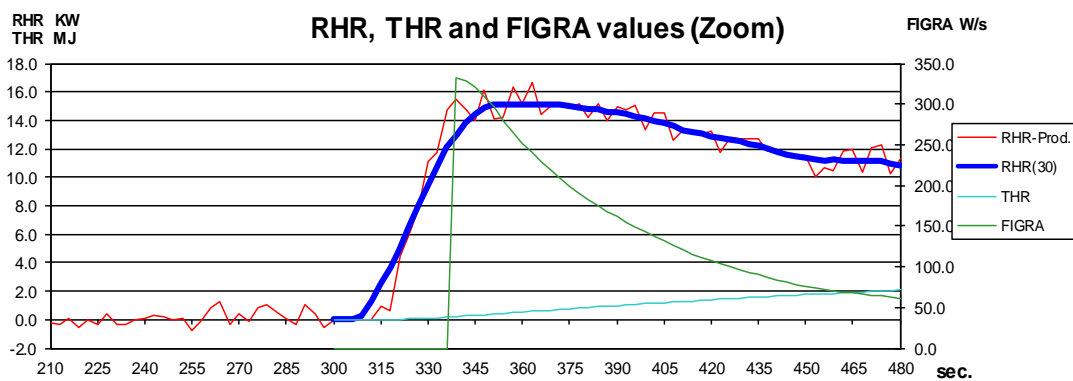


SBI Test (EN 13823)

EFiC

European Fire & Conductivity lab.

Product:		EFiC No.	Test no.	Operator	Test Date:	Print Date:
PIR1		16-012	2	KuE	30-08-2016	30-08-2016
Test condition		Check points		Results		
Ambient Temp. $(t=30-90)$ [°K]	293.3	RHR _{av,bumer} [KW]	32.1	FIGRA [W/s] 0.2 MJ	332	
Ambient pressure. [Pa]	101897	RHR _{std,bumer} [KW]	0.470	FIGRA [W/s] 0.4 MJ	279	
Humidity [%]	41.1	CO ₂ /O ₂ Ratio _{bumer}	0.564	THR ₆₀₀ [MJ] *	5.2	
K(t)	0.914	RSP _{av,bumer} [m ² /s]	0.002	Lateral flame spread (LFS) reach the edge?	No	
K(p)	1.080	RSP _{std,bumer} [m ² /s]	0.004	SMOGRA [m ² /s ²]	40	
E [KJ/m ²]	17200	Baseline Duct temp. $(t=30-90)$ [°K]	294.3	TSP ₆₀₀ [m ²] *	88	
Duct Diameter: [m]	0.306	Min. no. of accep. Thermocouples	3	Flaming droplets/particles (FDP) (flaming <= 10 s)?	No	
		Minimum for flow [m ² /s]	0.583	Flaming droplets/particles (FDP) (flaming > 10 s)?	No	
		Maximum for flow [m ² /s]	0.621			
Start date for conditioning	22-08-2016	Burner response time [s]	9	Time to max Figra [s] *	39	
End date for conditioning	30-08-2016	Weight before conditioning [Kg]	3.845	Tig (2*6KW) [s] *	27	
Total conditioning time [h]	168	Weight after conditioning [Kg]	3.845	* After ignition of main burner		
Baseline O ₂ $(t=30-90)$ [%]	20.740	Weight diff. in percent per day	0.00	Synchronisation information		
Baseline CO ₂ $(t=30-90)$ [%]	0.036	End data O ₂ $(t=1680-1740)$ [%]	20.950	T-Duct (2.5 °K drop from baseline)	Baseline	Last point
Baseline Light signal $(t=30-90)$	0.993	End data CO ₂ $(t=1680-1740)$ [%]	0.040	O ₂ (0.05% rise from baseline)	20.672	300
		End data Light signal $(t=1680-1740)$	0.978	CO ₂ (0.02% drop from baseline)	0.1937	300

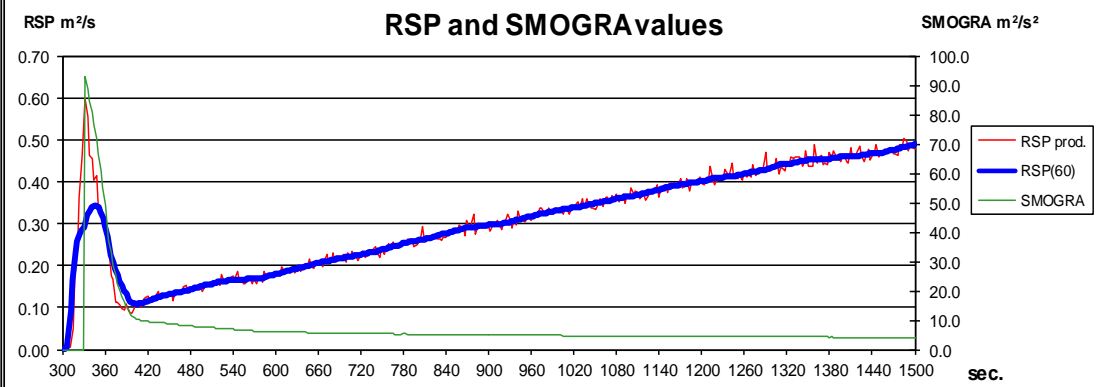
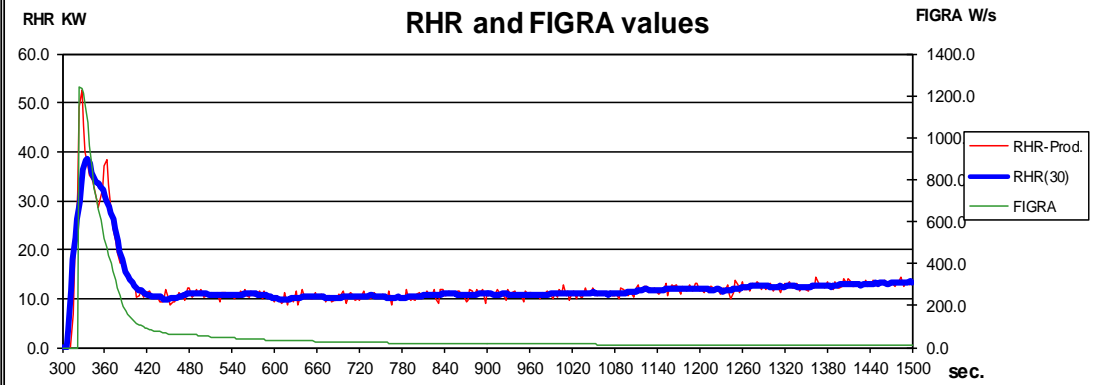
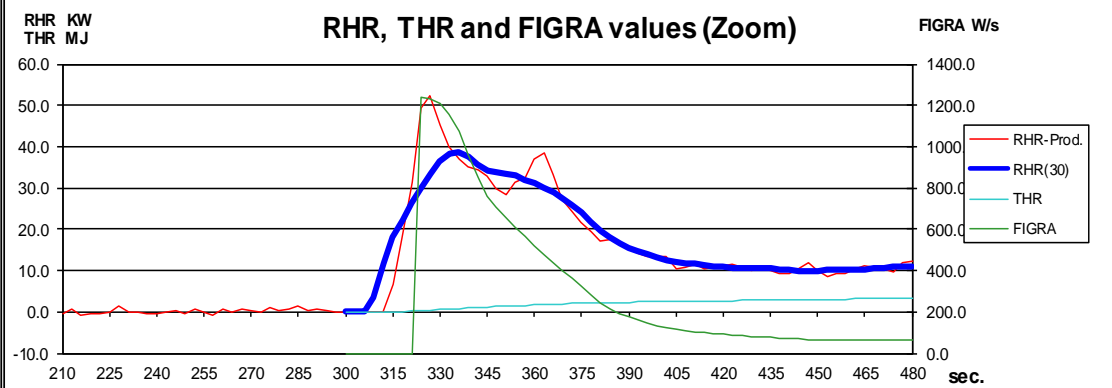


SBI Test (EN 13823)

EFiC

European Fire & Conductivity lab.

Product:		EFiC No.	Test no.	Operator	Test Date:	Print Date:
PIR3		16-012	1	KuE	30-08-2016	30-08-2016
Test condition		Check points		Results		
Ambient Temp. $(t=30-90)$ [°K]	293.9	RHR _{av, burner} [KW]	32.2	FIGRA [W/s] 0.2 MJ	1241	
Ambient pressure. [Pa]	101930	RHR _{std, burner} [KW]	0.566	FIGRA [W/s] 0.4 MJ	1232	
Humidity [%]	41.1	CO ₂ /O ₂ Ratio _{burner}	0.570	THR ₆₀₀ [MJ] *	7.7	
K(t)	0.914	RSP _{av, burner} [m ² /s]	0.006	Lateral flame spread (LFS) reach the edge?	No	
K(p)	1.080	RSP _{std, burner} [m ² /s]	0.004	SMOGRA [m ² /s ²]	93	
E [kJ/m ²]	17200	Baseline Duct temp. $(t=30-90)$ [°K]	295.2	TSP ₆₀₀ [m ²] *	125	
Duct Diameter: [m]	0.306	Min. no. of accep. Thermocouples	3	Flaming droplets/particles (FDP) (flaming <= 10 s)?	No	
		Minimum for flow [m ² /s]	0.556	Flaming droplets/particles (FDP) (flaming > 10 s)?	No	
		Maximum for flow [m ² /s]	0.619			
Start date for conditioning	20-07-2016	Burner response time [s]	9	Time to max Figra [s] *	24	
End date for conditioning	30-08-2016	Weight before conditioning [Kg]	7.970	Tig (2*6KW) [s] *	15	
Total conditioning time [h]	960	Weight after conditioning [Kg]	7.970	* After ignition of main burner		
Baseline O ₂ ^a $(t=30-90)$ [%]	20.719	Weight diff. in percent per day	0.00	Synchronisation information		
Baseline O ₂ $(t=30-90)$ [%]	20.944	End data O ₂ $(t=1680-1740)$ [%]	20.935	T-Duct (2.5 °K drop from baseline)	Baseline	Last point
Baseline CO ₂ $(t=30-90)$ [%]	0.033	End data CO ₂ $(t=1680-1740)$ [%]	0.042	O ₂ (0.05% rise from baseline)	320.4	300
Baseline Light signal $(t=30-90)$	0.991	End data Light signal $(t=1680-1740)$	0.987	CO ₂ (0.02% drop from baseline)	20.656	300

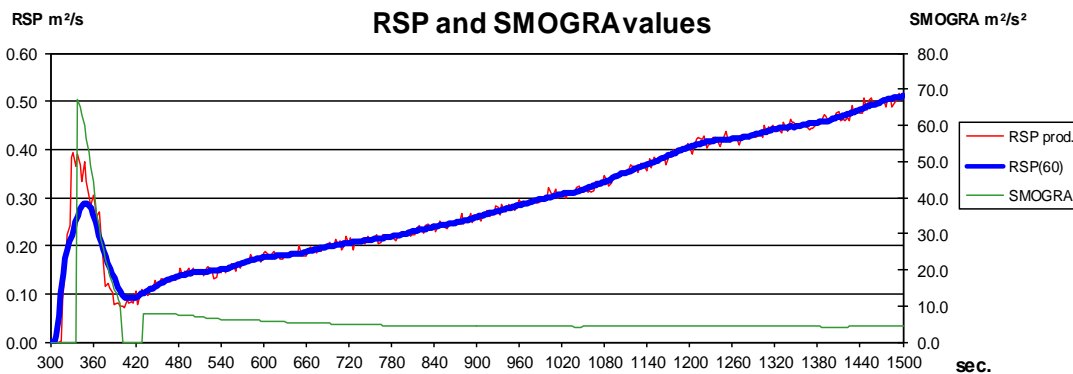
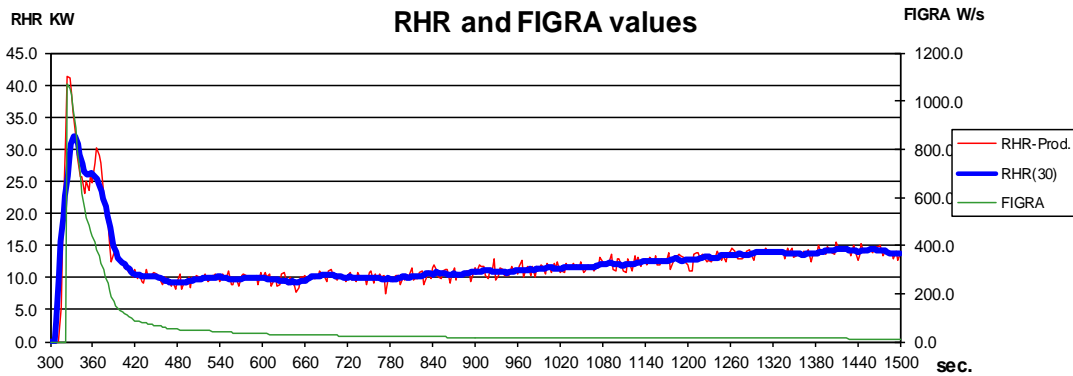
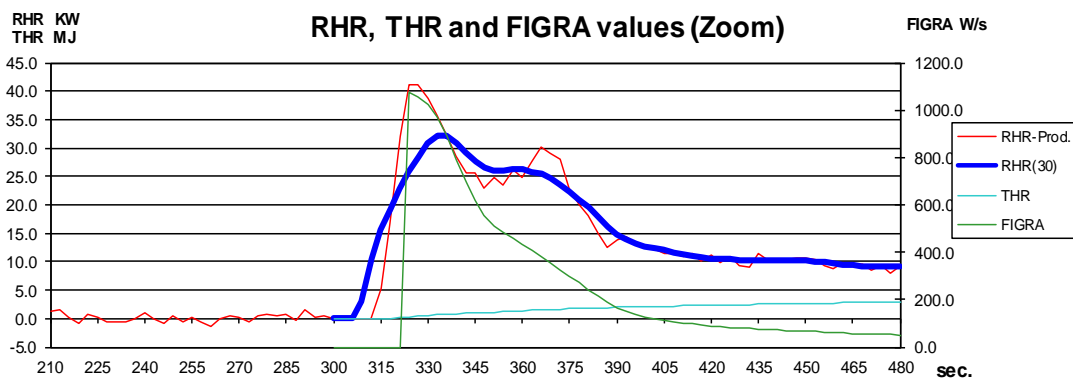


SBI Test (EN 13823)

EFiC

European Fire & Conductivity lab.

Product:		EFiC No.	Test no.	Operator	Test Date:	Print Date:
PIR3		16-012	2	KuE	31-08-2016	31-08-2016
Test condition		Check points		Results		
Ambient Temp. _(t=30-90) [°K]	293.1	RHR _{av, burner} [KW]	32.4	FIGRA [W/s] 0.2 MJ	1072	
Ambient pressure. [Pa]	101882	RHR _{std, burner} [KW]	0.760	FIGRA [W/s] 0.4 MJ	1054	
Humidity [%]	49.3	CO ₂ /O ₂ Ratio _{burner}	0.569	THR ₆₀₀ [MJ] *	7.1	
K(t)	0.914	RSP _{av, burner} [m ² /s]	0.003	Lateral flame spread (LFS) reach the edge?	No	
K(p)	1.080	RSP _{std, burner} [m ² /s]	0.004	SMOGRA [m ² /s ²]	67	
E [KJ/m ²]	17200	Baseline Duct temp. _(t=30-90) [°K]	293.8	TSP ₆₀₀ [m ²] *	111	
Duct Diameter: [m]	0.306	Min. no. of accep. Thermocouples	3	Flaming droplets/particles (FDP) (flaming <= 10 s)?	No	
		Minimum for flow [m ² /s]	0.577	Flaming droplets/particles (FDP) (flaming > 10 s)?	No	
		Maximum for flow [m ² /s]	0.625			
Start date for conditioning	20-07-2016	Burner response time [s]	9	Time to max Figra [s] *	24	
End date for conditioning	31-08-2016	Weight before conditioning [Kg]	7.950	Tig (2*6KW) [s] *	18	
Total conditioning time [h]	984	Weight after conditioning [Kg]	7.950	* After ignition of main burner		
Baseline O ₂ ^a _(t=30-90) [%]	20.699	Weight diff. in percent per day	0.00	Synchronisation information		
Baseline O ₂ _(t=30-90) [%]	20.946	End data O ₂ _(t=1680-1740) [%]	20.938	T-Duct (2.5 °K drop from baseline)	318.9	300
Baseline CO ₂ _(t=30-90) [%]	0.039	End data CO ₂ _(t=1680-1740) [%]	0.042	O ₂ (0.05% rise from baseline)	20.658	300
Baseline Light signal _(t=30-90)	0.991	End data Light signal _(t=1680-1740)	0.982	CO ₂ (0.02% drop from baseline)	0.2031	303

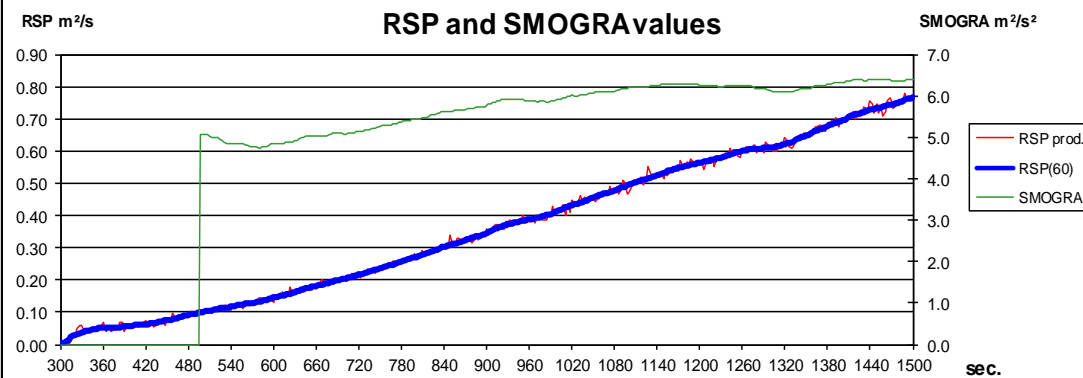
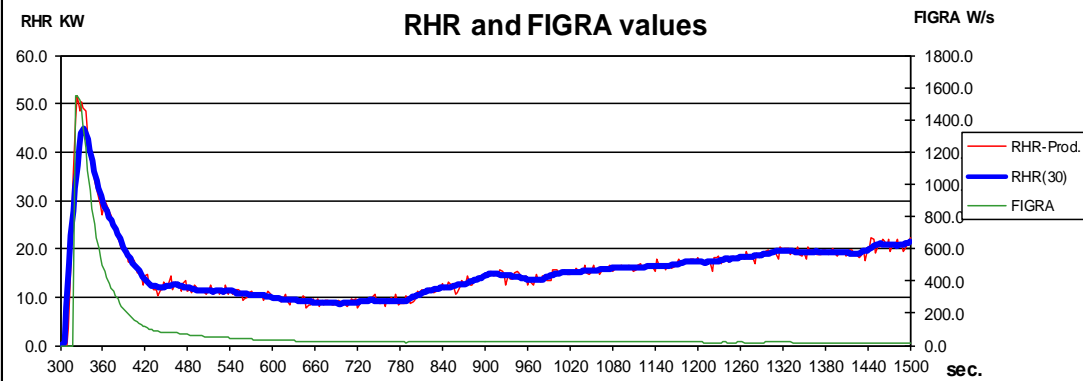
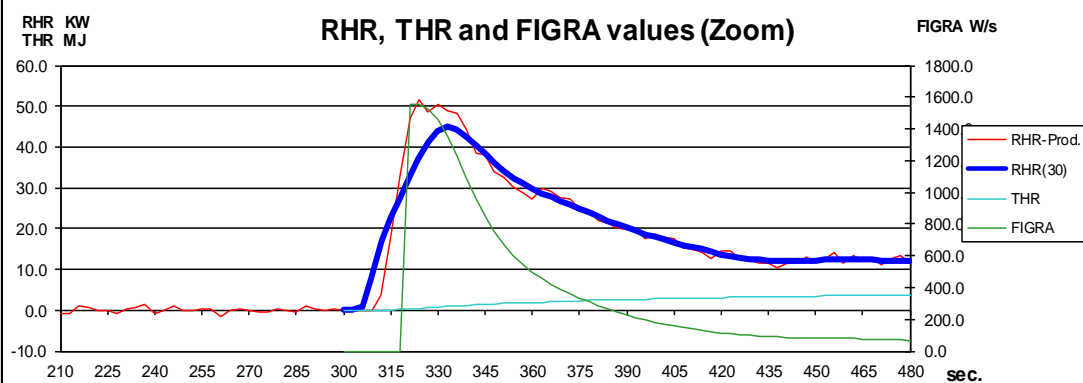


SBI Test (EN 13823)

EFiC

European Fire & Conductivity lab.

Product:		EFiC No.	Test no.	Operator	Test Date:	Print Date:
PF		16-012	1	KuE	29-08-2016	29-08-2016
Test condition		Check points		Results		
Ambient Temp. $(t=30-90)$ [°K]	294.4	RHR _{av,bumer} [KW]	32.3	FIGRA [W/s] 0.2 MJ	1551	
Ambient pressure. [Pa]	100664	RHR _{std,bumer} [KW]	0.714	FIGRA [W/s] 0.4 MJ	1550	
Humidity [%]	44.0	CO ₂ /O ₂ Ratio _{bumer}	0.575	THR ₆₀₀ [MJ] *	8.2	
K(t)	0.914	RSP _{av,bumer} [m ² /s]	0.017	Lateral flame spread (LFS) reach the edge?	No	
K(p)	1.080	RSP _{std,bumer} [m ² /s]	0.004	SMOGRA [m ² /s ²]	6	
E [KJ/m ²]	17200	Baseline Duct temp. $(t=30-90)$ [°K]	294.7	TSP ₆₀₀ [m ²] *	97	
Duct Diameter: [m]	0.306	Min. no. of accep. Thermocouples	3	Flaming droplets/particles (FDP) (flaming <= 10 s)?	No	
		Minimum for flow [m ³ /s]	0.573	Flaming droplets/particles (FDP) (flaming > 10 s)?	No	
		Maximum for flow [m ³ /s]	0.622			
Start date for conditioning	22-08-2016	Burner response time [s]	12	Time to max Figra [s] *	21	
End date for conditioning	29-08-2016	Weight before conditioning [Kg]	4.510	Tig (2*6KW) [s] *	15	
Total conditioning time [h]	168	Weight after conditioning [Kg]	4.510	* After ignition of main burner		
Baseline O ₂ $(t=30-90)$ [%]	20.718	Weight diff. in percent per day	0.00	Synchronisation information		
Baseline O ₂ $(t=30-90)$ [%]	20.955	End data O ₂ $(t=1680-1740)$ [%]	20.955	T-Duct (2.5 °K drop from baseline)	Baseline	Last point
Baseline CO ₂ $(t=30-90)$ [%]	0.031	End data CO ₂ $(t=1680-1740)$ [%]	0.043	O ₂ (0.05% rise from baseline)	20.669	303
Baseline Light signal $(t=30-90)$	0.990	End data Light signal $(t=1680-1740)$	0.943	CO ₂ (0.02% drop from baseline)	0.1953	303

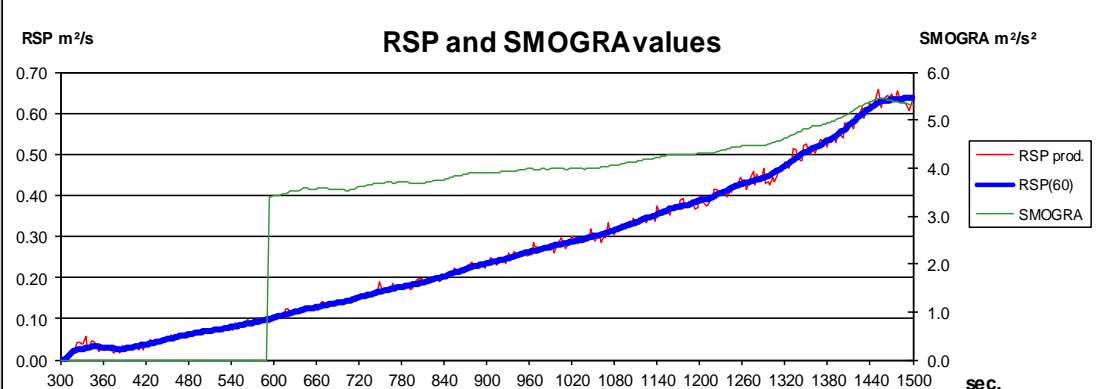
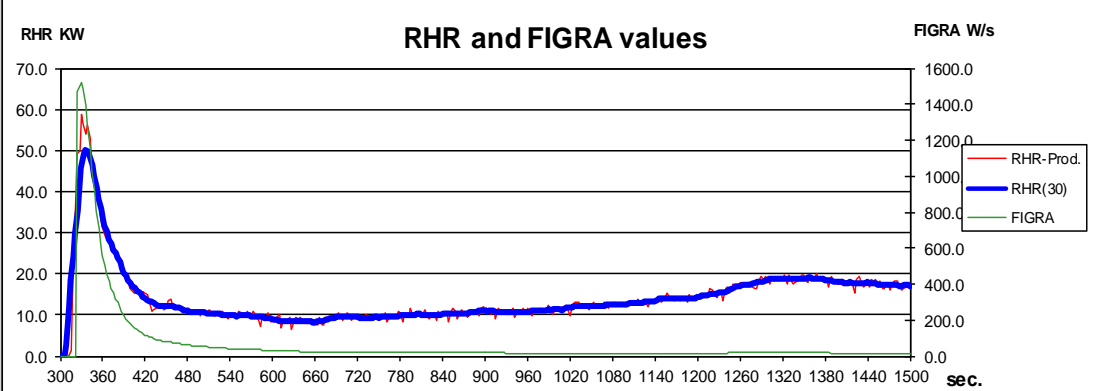
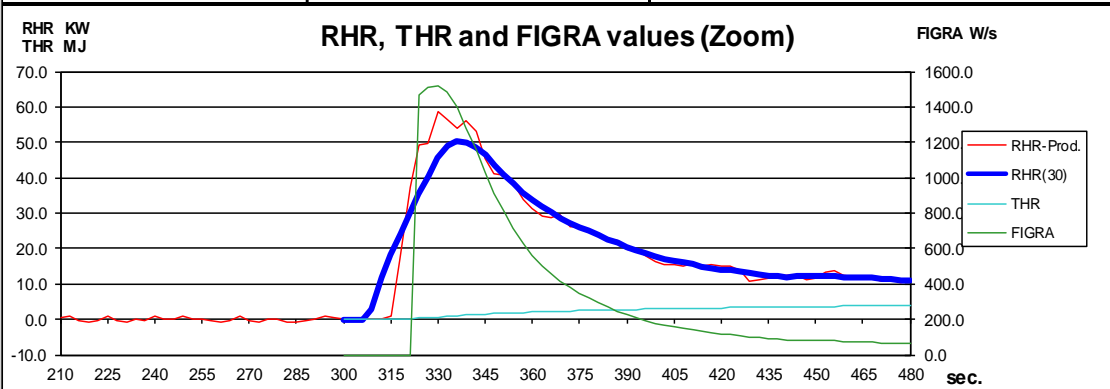


SBI Test (EN 13823)

EFiC

European Fire & Conductivity lab.

Product:		EFiC No.	Test no.	Operator	Test Date:	Print Date:
PF		16-012	2	KuE	30-08-2016	30-08-2016
Test condition		Check points		Results		
Ambient Temp. $(t=30-90)$ [°K]	293.1	RHR _{av, burner} [KW]	32.4	FIGRA [W/s] 0.2 MJ	1518	
Ambient pressure. [Pa]	101821	RHR _{std burner} [KW]	0.613	FIGRA [W/s] 0.4 MJ	1518	
Humidity [%]	43.2	CO ₂ /O ₂ Ratio _{burner}	0.557	THR ₆₀₀ [MJ] *	8.0	
K(t)	0.914	RSP _{av, burner} [m ² /s]	0.006	Lateral flame spread (LFS) reach the edge?	No	
K(p)	1.080	RSP _{std burner} [m ² /s]	0.004	SMOGRA [m ² /s ²]	5	
E [KJ/m ²]	17200	Baseline Duct temp. $(t=30-90)$ [°K]	293.5	TSP ₆₀₀ [m ²] *	66	
Duct Diameter: [m]	0.306	Min. no. of accep. Thermocouples	3	Flaming droplets/particles (FDP) (flaming <= 10 s)?	No	
Start date for conditioning	22-08-2016	Minimum for flow [m ² /s]	0.570	Flaming droplets/particles (FDP) (flaming > 10 s)?	No	
End date for conditioning	30-08-2016	Maximum for flow [m ² /s]	0.632			
Total conditioning time [h]	168	Burner response time [s]	9	Time to max Figra [s] *	30	
Baseline O ₂ $(t=30-90)$ [%]	20.737	Weight before conditioning [Kg]	3.845	Tig (2*6KW) [s] *	18	
Baseline O ₂ $(t=1680-1740)$ [%]	20.950	Weight after conditioning [Kg]	3.845	* After ignition of main burner		
Baseline CO ₂ $(t=30-90)$ [%]	0.039	Weight diff. in percent per day	0.00	Synchronisation information		
Baseline Light signal $(t=30-90)$	0.991	End data O ₂ $(t=1680-1740)$ [%]	20.946	T-Duct (2.5 °K drop from baseline)	318.6	300
		End data CO ₂ $(t=1680-1740)$ [%]	0.046	O ₂ (0.05% rise from baseline)	20.667	300
		End data Light signal $(t=1680-1740)$	0.944	CO ₂ (0.02% drop from baseline)	0.1965	303

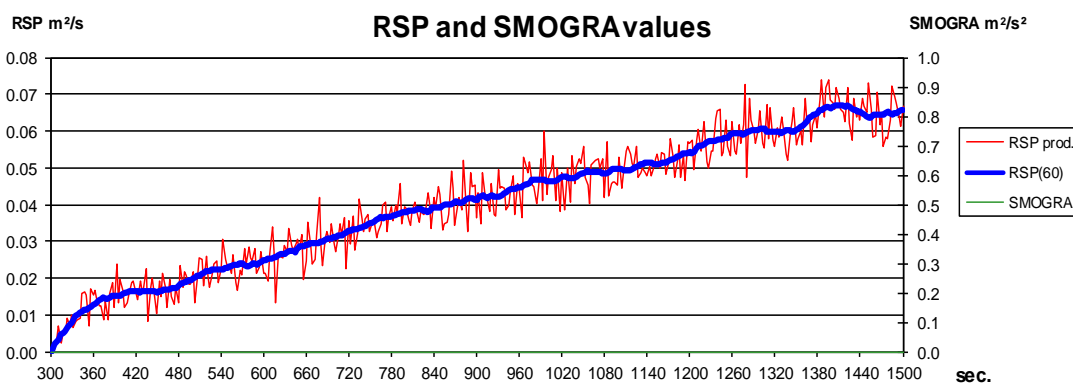
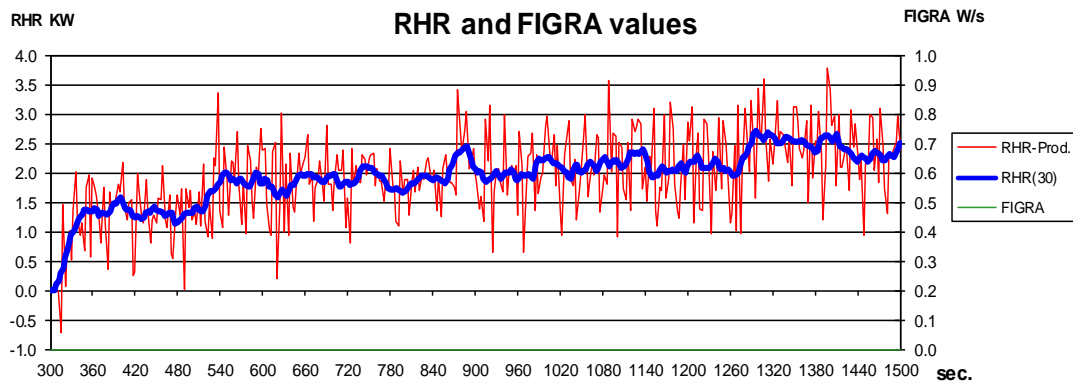
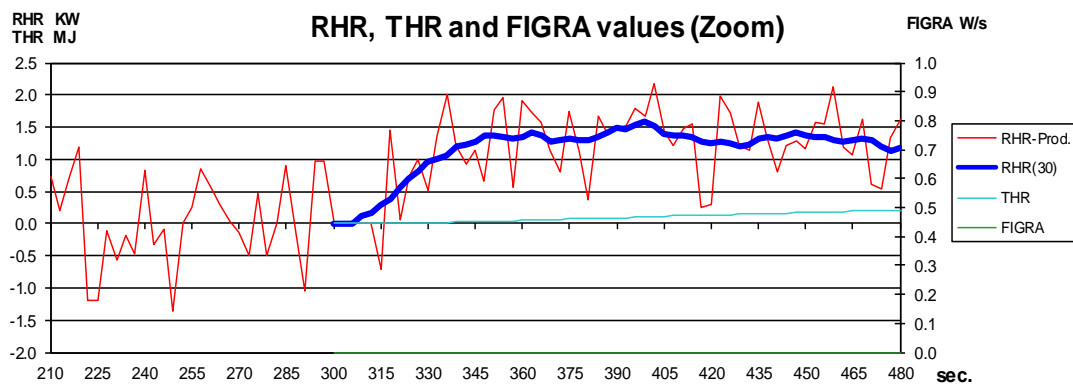


SBI Test (EN 13823)

EFiC

European Fire & Conductivity lab.

Product:		EFiC No.	Test no.	Operator	Test Date:	Print Date:
SW3		16-012	1	KuE	25-08-2016	25-08-2016
Test condition		Check points		Results		
Ambient Temp. $t_{(=30-90)}$ [°K]	298.6	RHR _{av,burner} [KW]	32.0	FIGRA [W/s] 0.2 MJ	0	
Ambient pressure. [Pa]	101739	RHR _{std, burner} [KW]	0.697	FIGRA [W/s] 0.4 MJ	0	
Humidity [%]	48.7	CO ₂ /O ₂ Ratio _{burner}	0.559	THR ₆₀₀ [MJ] *	1.0	
K(t)	0.914	RSP _{av, burner} [m ² /s]	0.025	Lateral flame spread (LFS) reach the edge?	No	
K(p)	1.080	RSP _{std, burner} [m ² /s]	0.003	SMOGRA [m ² /s ²]	0	
E [KJ/m ²]	17200	Baseline Duct temp. $t_{(=30-90)}$ [°K]	299.1	TSP ₆₀₀ [m ²]	15	
Duct Diameter: [m]	0.306	Min. no. of accep. Thermocouples	3	Flaming droplets/particles (FDP) (flaming <= 10 s)?	No	
Start date for conditioning	24-08-2016	Minimum for flow [m ² /s]	0.578	Flaming droplets/particles (FDP) (flaming > 10 s)?	No	
End date for conditioning	25-08-2016	Maximum for flow [m ² /s]	0.620	Time to max Figra [s] *	Not actual	
Total conditioning time [h]	24	Burner response time [s]	12	Tig (2*6KW) [s] *	Not reach	
Baseline O ₂ $t_{(=30-90)}$ [%]	20.610	Weight before conditioning [Kg]	21.010	* After ignition of main burner		
Baseline O ₂ $t_{(=30-90)}$ [%]	20.947	Weight after conditioning [Kg]	21.010	Synchronisation information		
Baseline CO ₂ $t_{(=30-90)}$ [%]	0.029	Weight diff. in percent per day	0.00	Baseline	Last point	
Baseline Light signal $t_{(=30-90)}$	0.991	End data O ₂ $t_{(=1680-1740)}$ [%]	20.939	T-Duct (2.5 °K drop from baseline)	324.1	300
		End data CO ₂ $t_{(=1680-1740)}$ [%]	0.034	O ₂ (0.05% rise from baseline)	20.665	300
		End data Light signal $t_{(=1680-1740)}$	0.975	CO ₂ (0.02% drop from baseline)	0.1864	303

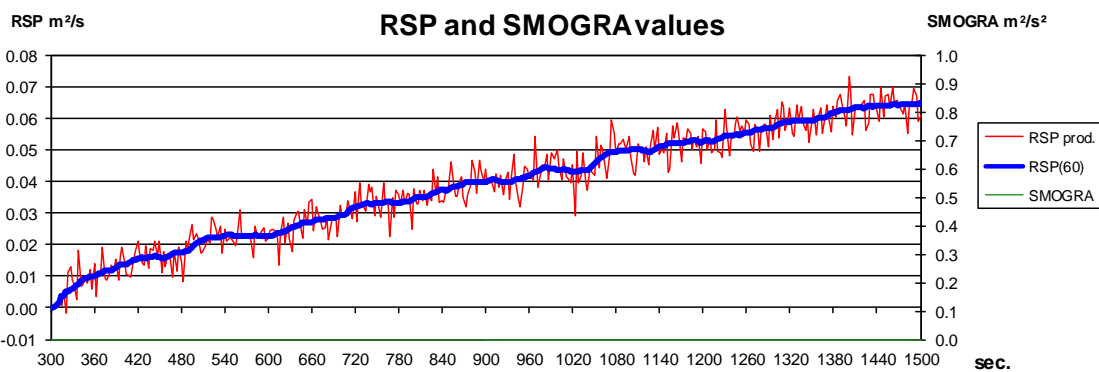
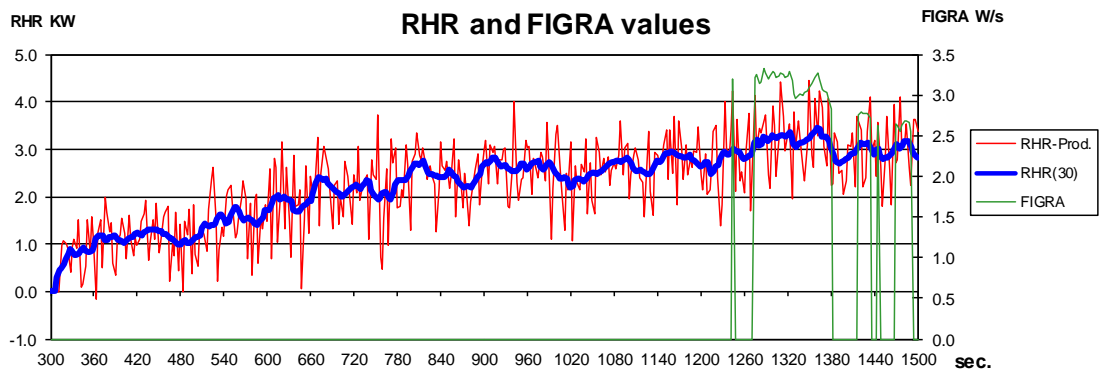
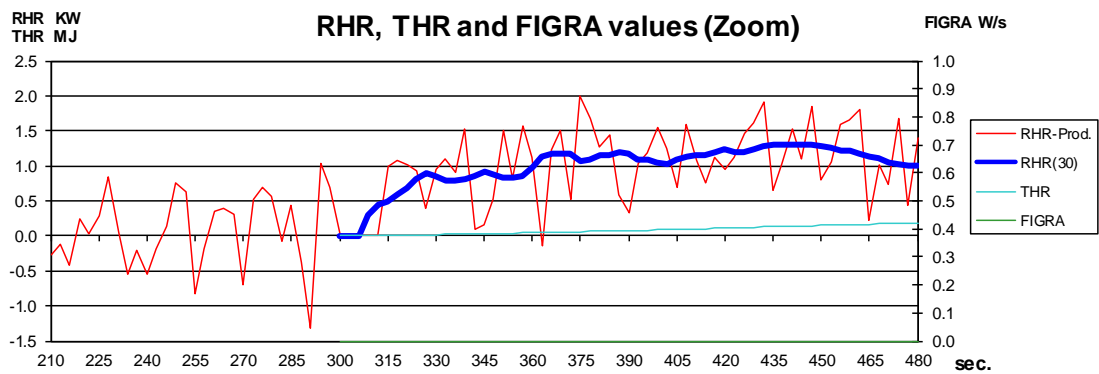


SBI Test (EN 13823)

EFiC

European Fire & Conductivity lab.

Product:		EFiC No.	Test no.	Operator	Test Date:	Print Date:
SW3		16-012	2	KuE	26-08-2016	26-08-2016
Test condition		Check points		Results		
Ambient Temp. (t=30-90) [°K]	297.2	RHR _{av, burner} [KW]	32.1	FIGRA [W/s] 0.2 MJ	3	
Ambient pressure. [Pa]	101020	RHR _{std, burner} [KW]	0.467	FIGRA [W/s] 0.4 MJ	3	
Humidity [%]	50.6	CO ₂ /O ₂ Ratio _{burner}	0.559	THR ₆₀₀ [MJ] *	1.0	
K(t)	0.914	RSP _{av, burner} [m ² /s]	0.034	Lateral flame spread (LFS) reach the edge?	No	
K(p)	1.080	RSP _{std, burner} [m ² /s]	0.002	SMOGRA [m ² /s ²]	0	
E [KJ/m ²]	17200	Baseline Duct temp. (t=30-90) [°K]	297.4	TSP ₆₀₀ [m ²] *	14	
Duct Diameter: [m]	0.306	Min. no. of accep. Thermocouples	3	Flaming droplets/particles (FDP) (flaming <= 10 s)?	No	
Start date for conditioning	24-08-2016	Minimum for flow [m ³ /s]	0.578	Flaming droplets/particles (FDP) (flaming > 10 s)?	No	
End date for conditioning	26-08-2016	Maximum for flow [m ³ /s]	0.618	Time to max Figra [s] *	987	
Total conditioning time [h]	24	Burner response time [s]	9	Tig (2*6KW) [s] *	Not reach	
Baseline O ₂ ^a (t=30-90) [%]	20.633	Weight before conditioning [Kg]	20.965	* After ignition of main burner		
Baseline O ₂ (t=30-90) [%]	20.952	Weight after conditioning [Kg]	20.965	Synchronisation information	Baseline	Last point
Baseline CO ₂ (t=30-90) [%]	0.040	Weight diff. in percent per day	0.00	T-Duct (2.5 °K drop from baseline)	322.6	297
Baseline Light signal (t=30-90)	0.991	End data O ₂ (t=1680-1740) [%]	20.942	O ₂ (0.05% rise from baseline)	20.670	300
		End data CO ₂ (t=1680-1740) [%]	0.050	CO ₂ (0.02% rise from baseline)	0.1973	300
		End data Light signal (t=1680-1740)	0.975			



Appendix B – Results of the ISO/TS 19700 SSTF Testing

The following results were generated in the ISO/TS 19700 Steady State Tube Furnace. The experimental methodology used to generate this data is found in section 2.0.3 and the results are discussed in section 3.4.1.

Sample	Fire Stage	Equivalence ratio / φ	Mass Loss /%	CO ₂ Yield g/g	CO Yield g/g	HCN Yield g/g	HCl Yield g/g	NO Yield g/g	H ₃ PO ₄ Yield g/g
PIR1	2	0.68 ± 0.06	87.41	2.301 ± 0.040	0.029 ± 0.001	0.001 ± 0.0005	0.010 ± 0.0002	ND	0.002 ± 0.0002
	3a	1.88 ± 0.07	66.07	0.433 ± 0.009	0.307 ± 0.006	0.015 ± 0.0010	0.006 ± 0.0008	0.002 ± 0.0002	0.001 ± 0.0004
	3b	1.94 ± 0.10	68.09	0.585 ± 0.014	0.198 ± 0.005	0.015 ± 0.0021	0.002 ± 0.0003	0.001 ± 0.0001	ND
PIR2	2	0.74 ± 0.07	94.69	2.481 ± 0.004	0.075 ± 0.001	0.004 ± 0.0016	0.009 ± 0.0002	<0.001	0.001 ± 0.0001
	3a	1.87 ± 0.13	72.36	0.619 ± 0.013	0.214 ± 0.009	0.016 ± 0.0030	0.003 ± 0.0004	0.003 ± 0.0005	ND
	3b	2.07 ± 0.06	68.37	0.511 ± 0.006	0.340 ± 0.002	0.017 ± 0.0027	0.001 ± 0.0001	0.002 ± 0.0003	ND
PIR3	2	0.62 ± 0.09	88.31	2.252 ± 0.009	0.038 ± 0.001	0.003 ± 0.0005	0.014 ± 0.0018	<0.001	0.001 ± 0.0002
	3a	1.70 ± 0.06	63.73	0.571 ± 0.008	0.226 ± 0.003	0.011 ± 0.0022	0.008 ± 0.0004	0.002 ± 0.0001	0.001 ± 0.0003
	3b	1.70 ± 0.10	69.71	0.560 ± 0.007	0.293 ± 0.004	0.016 ± 0.0027	0.003 ± 0.0003	0.001 ± 0.0001	ND
PIR4	2	0.58 ± 0.12	89.96	2.396 ± 0.136	0.025 ± 0.002	0.003 ± 0.0007	0.002 ± 0.0004	ND	0.001 ± 0.0006
	3a	1.60 ± 0.11	67.02	0.564 ± 0.035	0.296 ± 0.005	0.016 ± 0.0026	<0.001	0.002 ± 0.0002	<0.001
	3b	1.86 ± 0.36	67.55	0.524 ± 0.027	0.331 ± 0.031	0.020 ± 0.0040	<0.001	<0.001	<0.001
PIR5	2	0.70 ± 0.02	92.02	2.376 ± 0.080	0.014 ± 0.007	0.004 ± 0.0001	0.013 ± 0.0004	ND	<0.001
	3a	1.82 ± 0.11	75.86	0.447 ± 0.013	0.340 ± 0.031	0.017 ± 0.0018	0.006 ± 0.0003	0.003 ± 0.0002	<0.001
	3b	1.94 ± 0.44	74.42	0.520 ± 0.061	0.341 ± 0.085	0.014 ± 0.0033	0.007 ± 0.0016	0.001 ± 0.0002	<0.001
PIR6	2	0.70 ± 0.04	94.35	2.375 ± 0.024	0.037 ± 0.014	0.004 ± 0.0002	0.019 ± 0.0011	ND	0.002 ± 0.0001
	3a	1.73 ± 0.08	77.35	0.511 ± 0.056	0.331 ± 0.049	0.014 ± 0.0006	0.006 ± 0.0003	0.002 ± 0.0001	0.001 ± 0.0001
	3b	1.98 ± 0.06	78.89	0.652 ± 0.007	0.249 ± 0.025	0.014 ± 0.0004	0.004 ± 0.0001	<0.001	<0.001
PIR7	2	0.63 ± 0.03	95.32	2.077 ± 0.045	0.106 ± 0.028	0.006 ± 0.0003	0.008 ± 0.0004	ND	<0.001
	3a	1.69 ± 0.14	76.57	0.610 ± 0.04	0.217 ± 0.007	0.010 ± 0.0009	0.005 ± 0.0004	0.001 ± 0.0001	<0.001
	3b	2.13 ± 0.12	78.91	0.554 ± 0.025	0.416 ± 0.048	0.015 ± 0.0008	0.003 ± 0.0002	0.002 ± 0.0001	<0.001

PF1	2	0.68 ± 0.03	94.74	2.569 ± 0.014	0.023 ± 0.001	<0.001	0.001 ± 0.0002	<0.001	ND
	3a	1.60 ± 0.09	59.01	0.475 ± 0.006	0.276 ± 0.003	0.002 ± 0.0003	0.001 ± 0.0001	<0.001	ND
	3b	1.65 ± 0.10	58.74	0.560 ± 0.026	0.170 ± 0.008	0.001 ± 0.0002	0.002 ± 0.0003	ND	ND
PF2	2	0.69 ± 0.02	97.46	2.509 ± 0.049	0.023 ± 0.007	ND	0.001 ± 0.0001	ND	ND
	3a	1.53 ± 0.03	72.68	0.495 ± 0.016	0.320 ± 0.003	0.001 ± 0.0001	0.002 ± 0.0001	<0.001	<0.001
	3b	1.73 ± 0.01	72.34	0.630 ± 0.029	0.280 ± 0.033	<0.001	0.007 ± 0.0006	ND	0.003 ± 0.0002
PF3	2	0.63 ± 0.09	98.1	2.094 ± 0.035	0.031 ± 0.007	<0.001	0.005 ± 0.0007	<0.001	<0.001
	3a	1.66 ± 0.06	75.73	0.511 ± 0.019	0.282 ± 0.011	0.002 ± 0.0001	0.001 ± 0.0001	<0.001	<0.001
	3b	1.60 ± 0.24	73.73	0.638 ± 0.058	0.229 ± 0.028	0.005 ± 0.0008	0.004 ± 0.0006	ND	0.002 ± 0.0008
PF4	2	0.61 ± 0.09	95.68	2.529 ± 0.099	0.028 ± 0.022	ND	<0.001	ND	<0.001
	3a	1.63 ± 0.10	66.14	0.473 ± 0.072	0.317 ± 0.006	<0.001	0.001	ND	0.001 ± 0.0003
	3b	1.60 ± 0.14	63.59	0.562 ± 0.018	0.223 ± 0.014	<0.001	0.001 ± 0.0001	ND	0.003 ± 0.0001
SW1	2 – NF	N/a	4.98	0.100 ± 0.003	0.001 ± 0.001	<0.001	ND	ND	ND
	3a – NF	N/a	4.72	0.093 ± 0.007	<0.001	<0.001	ND	ND	ND
	3b – NF	N/a	4.99	0.086 ± 0.005	<0.001	<0.001	ND	ND	ND
SW2	2 – NF	N/a	1.77	0.027 ± 0.007	0.010 ± 0.002	<0.001	ND	ND	ND
	3a – NF	N/a	1.67	0.020 ± 0.006	0.009 ± 0.001	<0.001	ND	ND	ND
	3b – NF	N/a	1.64	0.051 ± 0.011	<0.001	ND	ND	ND	ND
GW1	2 – NF	N/a	6.21	0.093 ± 0.018	0.018 ± 0.003	<0.001	ND	ND	ND
	3a – NF	N/a	8.63	0.144 ± 0.015	0.011 ± 0.001	<0.001	ND	ND	ND
	3b – NF	N/a	12.69	0.189 ± 0.024	<0.001	<0.001	ND	ND	ND

Appendix C – Publications

The Fire Toxicity of Polyurethane Foams

Published in Fire Science Reviews in 2016. Full citation: McKenna ST, Hull TR (2016) The Fire Toxicity of Polyurethane foams, Fire Science Reviews, 5(3).

REVIEW

Open Access



The fire toxicity of polyurethane foams

Sean Thomas McKenna and Terence Richard Hull*

Abstract

Polyurethane is widely used, with its two major applications, soft furnishings and insulation, having low thermal inertia, and hence enhanced flammability. In addition to their flammability, polyurethanes form carbon monoxide, hydrogen cyanide and other toxic products on decomposition and combustion.

The chemistry of polyurethane foams and their thermal decomposition are discussed in order to assess the relationship between the chemical and physical composition of the foam and the toxic products generated during their decomposition. The toxic product generation during flaming combustion of polyurethane foams is reviewed, in order to relate the yields of toxic products and the overall fire toxicity to the fire conditions. The methods of assessment of fire toxicity are outlined in order to understand how the fire toxicity of polyurethane foams may be quantified. In particular, the ventilation condition has a critical effect on the yield of the two major asphyxiants, carbon monoxide and hydrogen cyanide.

Keywords: Fire, Combustion, Toxic, Toxicity, Polyurethane, Foam, Decomposition, Asphyxiant, Cyanide, HCN

Introduction

Polyurethanes are a diverse family of synthetic polymers that were first synthesised in 1937 by Otto Bayer. Their development continued commercially in Germany, eventually leading to a global multibillion dollar industry (Vilar 2002). The polyurethane market was estimated to be worth \$33 billion in 2010 and is expected to continue to grow to over \$55 billion by 2016. Global usage is expected to expand from 13.65 Mt in 2010 to 17.95 Mt by 2016. 95 % of the demand for polyurethanes is situated in North America, Asian-pacific, and European markets; with demand expected to increase in Eastern Europe and South America in the next 10–15 years. The two main market uses for polyurethane are in the furniture and interior industry and the construction industry with 28 % and 25 % of the market, respectively (Markets & Markets report 2011).

Polyurethane chemistry

Functional groups

Polyurethanes are named from the presence of the urethane (also known as carbamate) functional group (Fig. 1). Despite their name, the term polyurethane is used to describe a family of polymers whose monomers

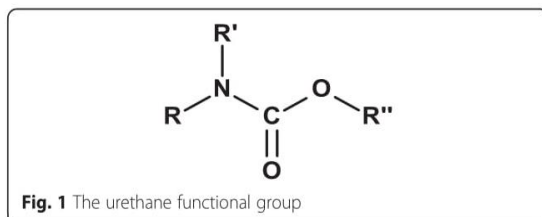
are joined by a range of functional groups primarily derived from the polyaddition of polyisocyanates and polyalcohols. Further reactions occur with amines, water, ureas, urethanes and even other isocyanates to produce a diverse range of functional groups including urethanes, ureas, isocyanurates, carbodiimides and uretdiones. A summary of these structures is shown in Fig. 2 (Avar et al. 2012). This range of functional groups and their ratios in the polymer are a large contributing factor to the wide range of properties that polyurethane materials can possess.

Cross-linking functional groups

Synthetic polymeric materials may be divided into thermoplastics and thermosets. Thermoplastics are composed of linear polymer molecules, whose shape can be changed repeatedly on heating and which may be melted and solidified without chemical change. Thermosets are cross-linked polymer molecules which, on heating, do not melt but will eventually decompose. Most polyurethanes are cross-linked to some degree and decompose without melting. In addition to the more common process of adding cross-linking reagents during the production process, cross-linkages in polyurethanes can be the result of the high reactivity of the isocyanate precursors. These isocyanate derived cross-links can include biurets and

* Correspondence: TRHull@uclan.ac.uk
Centre for Fire and Hazard Science, University of Central Lancashire, Preston
PR1 2HE, UK

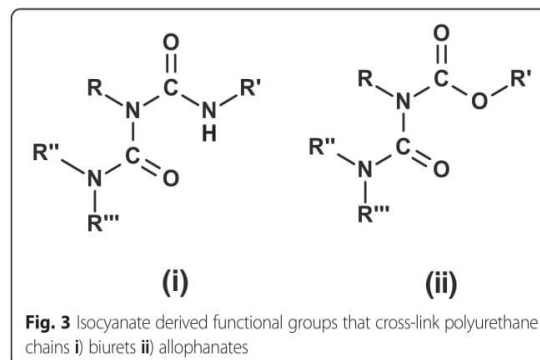
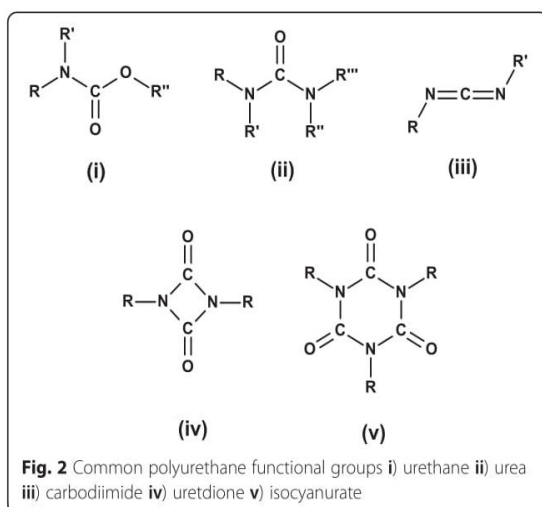




allophanates (Fig. 3) (Aneja 2002). Biurets are the result of the reaction of isocyanates with substituted-urea functional groups and allophanates are formed in small amounts (unless catalysed) by the reaction of isocyanates with urethanes. Additionally, the self-addition of isocyanates to produce isocyanurates (v in Fig. 2), also results in cross-linking in the polymer. Appropriate formulation affords a degree of control over the cross-linking in the polymer without the need for additional cross-linking agents.

Polymerisation reaction

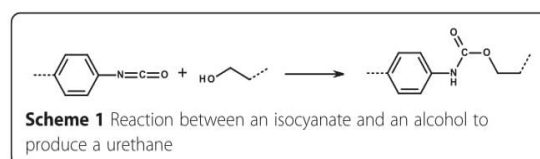
Isocyanates are a highly reactive family of compounds that are characterised by the $R-N=C=O$ functional group (where R can be any aliphatic or aromatic functionality). The strain of two electronegative atoms (N and O) results in electron density being pulled away from the carbon atom, giving it a strong partial positive charge. This makes the isocyanate functional group highly reactive towards nucleophiles with an available hydrogen. These nucleophiles include amines, alcohols, carboxylic acids, thiols, water, ureas and urethanes (Aneja 2002).

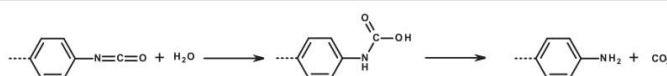


During polymerisation, isocyanates undergo a number of distinct reactions. Primarily, isocyanates react with alcohols to produce urethane linkages in the polymer (Scheme 1). The reaction of an isocyanate functional group with water (Scheme 2) results in the formation of an unstable carbamic acid group, which in turn decomposes to release an amine and carbon dioxide. This amine may then undergo further reaction with other isocyanates present to produce a urea (Scheme 3). The carbon dioxide release by the reaction in Scheme 2 can act as a blowing agent in polyurethane foam production and up to a point the amount of water added will be inversely proportional to the density of the foam. The resulting substituted urea can then react with another isocyanate to produce a biuret linkage (Scheme 4). The reaction of a urethane with another isocyanate will produce an allophanate (Scheme 5).

Isocyanates also react with themselves in various ways to produce dimers, trimers and completely new functional groups. The dimerisation of two isocyanates is a reversible reaction that produces uretidione ring (Scheme 6). The trimerisation results in a highly stable isocyanurate ring which confer additional thermal stability to polyisocyanurates (Scheme 7). Carbodiimides are produced by the reaction of isocyanates in the presence of a catalyst (such as phospholine oxides) (Scheme 8) (Avar et al. 2012).

These reactions make up the basis of polyurethane chemistry and can be used to tailor polyurethanes with a range of properties by varying the structure and ratios of the individual components.





Scheme 2 Reaction of an isocyanate with water to produce a carbamic acid which decomposes to produce an amine and carbon dioxide

Isocyanate reactivity

The reactivity of isocyanates with the various functional groups commonly present in the production of polyurethanes is dependent on both the steric and electronic factors of the R-group, and also the specific functional group the isocyanate is reacting with. Table 1 shows the relative reactivity of isocyanates with nucleophiles at 25 °C without the presence of a catalyst. This shows that the reactions of isocyanates are much faster with amines and slower with carboxylic acids, urethanes and amides than for the alcohols used in polyurethane production. An understanding of the relative reaction rates is vital in controlling the production of the polymer and producing the desired physical properties (Herrington & Hock 1998). In this case, the main reason for including isocyanate reactivity data is to explain the reactivity of isocyanates that are released into fire effluent during combustion. Their apparently transient nature results from their very high reactivity with amines and their fairly high reactivity with water (which is almost always present in fire effluent). The presence of both amines and water in the decomposition products of polyurethane foams are discussed in later sections.

Isocyanate structure also affects the reactivity of the isocyanate group. Bulky substituents that impinge on the isocyanate group can reduce its reactivity. Aromatic isocyanates are more reactive than aliphatic isocyanates due to the electronic effects of the aromatic ring. Substituted aromatics containing electron withdrawing groups further increase the reactivity of isocyanates by increasing the partial positive charge on the isocyanate carbon via a resonance withdrawing effect.

Aromatic diisocyanates, which are commonly used in the production of polyurethanes, have a slightly more complicated chemistry compared to monoisocyanates due to the electronic effects of two isocyanate groups. Aromatic diisocyanates *ortho*- or *para*- to one another will have an activating effect on each other, thus increasing their reactivity. However, once one of the groups forms a urethane or urea, the activating effect on the other isocyanate is reduced, as ureas and urethanes are weaker activating groups than

isocyanates. Additionally, aromatic isocyanates with more steric hindrance are likely to be less reactive (such as the 2 position in 2,4-TDI (Fig. 4)). This steric hindrance can be offset by increasing the temperature of the reaction or by performing the reaction in the presence of a catalyst (Vilar 2002).

Isocyanate precursors

The isocyanate precursors used in the production of polyurethane foams usually consist of aromatic diisocyanates such as toluene diisocyanate (TDI) and methylene diphenyl diisocyanate (MDI). Over 90 % of all industrial polyurethanes are based on either TDI or MDI (Avar et al. 2012).

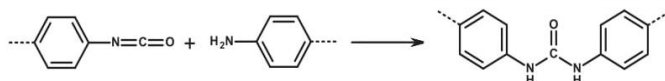
TDI is produced as the 2,4- and the 2,6- isomer which have a boiling point of 121 °C and 120 °C respectively. It is usually used in isomeric mixtures of varying ratios, with 80:20 2,4 to 2,6 being the most commonly used (Fig. 4). TDI is primarily used in the production of flexible foams, which are used in the furniture and interior industries.

MDI is a diaromatic diisocyanate compound that boils at 208 °C and is primarily used in the production of rigid foams. Most rigid foams and speciality polyurethanes use polymeric MDI derivatives which are mixtures components such as dimers and trimers (Fig. 5). Rigid MDI based foams are primarily used for insulation in the construction industry and can also be found in the transport industry.

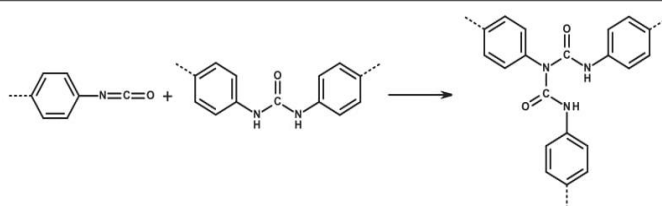
Other common diisocyanates include hexamethylene diisocyanate (HDI), 1,5-naphthalene diisocyanate (NDI) and isophorone diisocyanate (IPDI) (Fig. 6).

Polyol precursors

As the main reactive group that isocyanates react with, polyols are a major component of the resulting polyurethane product. The two main families of polyols used are polyether polyols and polyester polyols (Fig. 7) (Avar et al. 2012). Polyether polyols are more resistant to hydrolysis, but less stable to oxidation, while for polyester polyols it is the opposite. As polyols are prepolymers, their molecular mass is relevant to their application, with flexible foams being derived from 1000 to 6000 daltons and few hydroxyl groups, while those used in rigid foams have short chains from 250 to 1000 daltons with high functionality (3–12 hydroxyl groups per chain).



Scheme 3 Reaction of an isocyanate with an amine to produce a urea



Scheme 4 Reaction of an isocyanate with a urea to produce a biuret linkage

Short chains with high functionality results in highly cross-linked polyurethane polymers which is characteristic of rigid foams.

Thermal decomposition

Inert-atmosphere

It is generally accepted that the thermal decomposition occurring during flaming combustion is best represented by the thermal decomposition of a material in an inert atmosphere. This is due to the concentration of oxygen directly under a flame being close or equal to 0 % (Schartel & Hull 2007). A large number of studies have been performed over the last 50 years to understand the thermal decomposition of polyurethane materials, and as a result of this the mechanism of their decomposition in inert-atmospheres is fairly well understood.

Bond stability

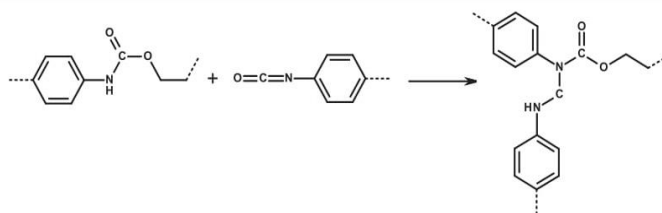
The heating of polyurethanes in an inert-atmosphere results in the progressive rupturing of bonds as a function of temperature. Biuret and allophanate bonds will decompose first between 100 and 125 °C. Ureas and urethanes decompose between 160 and 200 °C. Substituted ureas decompose between 235 and 250 °C and carbodiimides decompose between 250 and 280 °C. Isocyanurate rings are the most thermally stable in an inert atmosphere and decompose between 270 and 300 °C. A summary of the bond decomposition temperatures in polyurethanes is shown in Table 2 (Gharehbagh & Ahmadi 2012). Although these temperatures can provide a good general idea of which bonds will be likely to break down with heating, the steric and electronic effects of the attached groups can affect the strength of the bonds and thus the temperature at which the bond will decompose.

Regeneration of Precursors

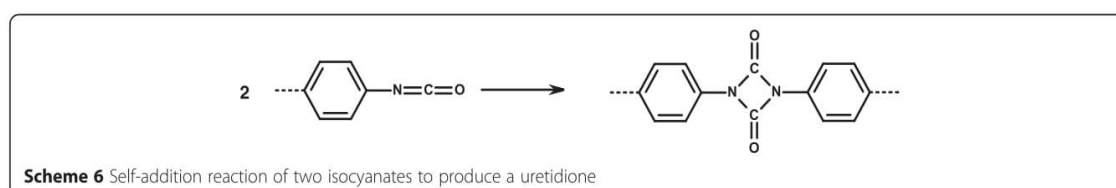
Thermal decomposition of polyurethanes is usually the reverse of polymerisation, resulting in the formation their precursor functional compounds—diisocyanates, diamines and dihydroxy compounds. Therefore, the products of decomposition can be predicted from the composition of the polymer. These processes occur at around 300 °C with the precursor chemicals including TDI, MDI, HDI, polyols (both polyether and polyester-polyols) and aromatic amines.

Early work by Woolley et al (1975) indicated that the decomposition of polyurethanes up to around 600 °C resulted in the volatilisation of fragmented polyurethane and subsequent release into a nitrogen rich 'yellow smoke', containing partially polymerised isocyanates and droplets of isocyanate from the foam. Higher temperatures resulted in the volatilisation of most of the polyurethane precursors via the formation of lower molecular weight compounds.

Chambers et al. (1981) reported similar data by analysing the inert-atmosphere pyrolysis of a series of biscarbamates to act as model compounds representing polyurethane foams. At 300 °C, free isocyanates and alcohols were produced from the decomposition of these biscarbamates. At this temperature around one third of the compounds mass was lost as volatile products, and the regenerated alcohol products were mainly present in the residue of the sample. Again, above 600 °C the compound and any "yellow smoke" present was decomposed into smaller volatile fragments. The study also suggested that any remaining isocyanates residue would react with themselves to produce polycarbodiimides, thus anchoring the isocyanate precursors in the condensed phase until around 600 °C, where they would fragment. While this may occur to some degree, it is



Scheme 5 Reaction of a urethane with an isocyanate to produce an allophanate linkage



generally accepted that the majority of the diisocyanates produced in the decomposition of polyurethanes are either volatilised or converted into their amine derivative and then volatilised.

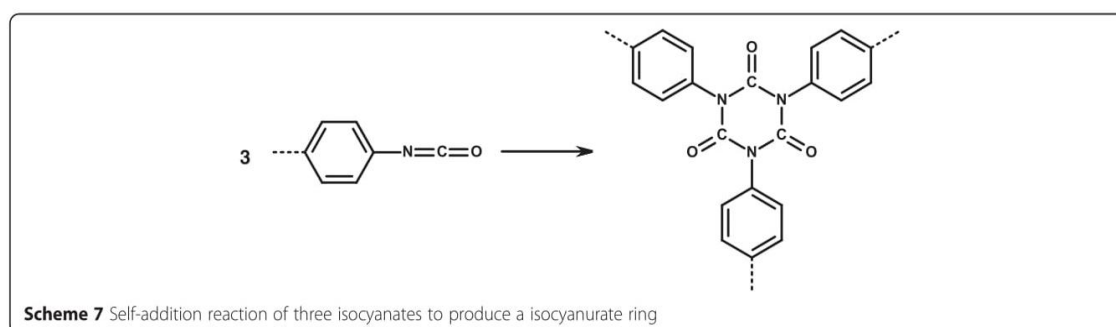
Work by Ravey and Pearce (1997) on the decomposition of a polyether based flexible polyurethane foam suggested that up to 360 °C the decomposition of the foam was achieved by two main mechanisms. The first being a depolymerisation which would dissociate the polymer to isocyanates and alcohols, the second being dissociation to a primary amine, an olefin and carbon dioxide. The results indicated that the formation of the precursor, TDI, was much faster and preferable to depolymerisation when the volatile compounds could escape. However, when the TDI was unable to enter the pyrolysis zone, the slower, irreversible decomposition to diaminotoluene (DAT) would occur. The authors proposed that once formed, these compounds could partially polymerise with volatilised TDI in the vapour phase to produce Woolley's "yellow smoke". Preliminary calculations suggested that 27 % of the TDI should be recovered as DAT. Experimental data reported a 28 % recovery of DAT which supports the proposed decomposition mechanism.

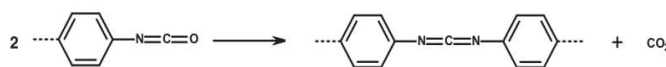
Recent work by Allan et al. (2013) further supported the presence of two separate decomposition mechanisms for flexible foams. The authors noted a primary depolymerisation of the foam which would release volatile TDI and leave the polyol precursors in the condensed phase. Alongside this, the decomposition of the foam into an amine, alkene and carbon dioxide was also proposed. However, no amines were detected in the vapour phase. Instead polyureas were detected in the vapour phase and

also in the condensed phase as a waxy, insoluble white substance. This suggests that any amines formed would have reacted with isocyanates in the vapour phase to form ureas, some of which would have condensed to produce the observed waxy white substance. Sub-ambient differential distillation of the remaining residue yielded a range of short-chain aldehydes (such as formaldehyde and acetaldehyde), ketones, alkenes and high molar mass polyol fragments. The highest concentration these compounds were formed at occurred at a decomposition temperature of 350–400 °C which indicated no new degradation steps had occurred beyond 350 °C. Additionally, the authors suggested the positions on the polyol chain where bond scission could occur, explaining the presence of the short-chain alkenes, aldehydes and ketones (Scheme 9).

More recent studies have supported and expanded upon the aforementioned thermal decomposition mechanisms of polyurethane foams. Garrido and Font (2015) reported two main steps in the inert-atmosphere decomposition of flexible polyurethane foams. The first step is the decomposition of the urethane bonds to release and volatilise isocyanates up to 300 °C, with long chain alcohols being left behind in the condensed phase, followed by the alcohols degrading at around 400 °C. Isocyanates were primarily produced during the first stage, and in the second stage primarily carbonyls ($R_2C=O$) and hydrocarbons were detected using infrared analysis.

The difference in the decomposition of rigid and flexible polyurethane foams was investigated by Chun et al. (2007). They attributed the different decomposition mechanisms to the physical form of the polyurethane





Scheme 8 Reaction of two isocyanates to produce a carbodiimide

foam, rather than to any chemical differences. Rigid foam decomposed between 200 and 410 °C, while flexible foam decomposed between 150 to 500 °C. The authors reported GC/MS analysis of the condensed phase products obtained. In both rigid and flexible foams, aniline and *p*-aminotoluene were reported, which correlates with the work of Ravey and Pearce (1997) who reported that isocyanates that did not volatilise were converted into amines in the condensed phase. Rigid polyurethanes primarily produced aromatic compounds in the condensed phase products of decomposition, whereas flexible polyurethanes produced aromatics, alcohols, aldehydes and heterocycles.

High temperature decomposition

After the initial stages of inert-atmosphere thermal decomposition where the polymer precursors are reformed and volatilised, the decomposition products tend to fragment into smaller molecules. Woolley et al. (1972) noted that the yellow smoke was produced up to around 600 °C, where it would then decompose to give a family of low molecular weight, nitrogen containing products including hydrogen cyanide, acetonitrile, acrylonitrile, pyridine, and benzonitrile. The most notable and abundant of these was hydrogen cyanide which increased in yield from 700 to 1000 °C. At 1000 °C the hydrogen cyanide produced accounted for a range of between 3.8 and 7.3 % by weight. The authors studied decomposition at 900 °C of foams, partly decomposed foams, smokes, and pure MDI to assess the hydrogen cyanide (HCN)

content and noted that the yields of HCN were directly related to the nitrogen content. Work published as early as 1959 supported this mechanism of decomposition at higher temperatures and noted that up to 70 % of the nitrogen in the foam could be converted to HCN at 1000 °C (Saunders 1959).

The use of ¹³C labelling by Chambers et al. (1981) on polycarbodiimides and polyureas enabled the determination of the source of the organonitriles and HCN during thermal decomposition. Their analysis indicated that, above 600 °C, the high temperature decomposition of MDI generated a large number of volatile fragments, including benzene, toluene, benzonitrile and toluonitrile. Further fragmentation of these molecules led to the production of HCN, acetonitrile, acrylonitrile and a range of olefinic fragments. The use of ¹³C labelling in this case allowed the authors to confirm that the nitrogenous compounds, HCN and organonitriles, originated from the thermal fission of the aromatic rings with the nitrile carbon being the 2-,4- or 6- carbon of the MDI ring.

The production of HCN and other low molecular weight nitrogenous compounds from the high temperature decomposition of polyurethanes has been reported in the literature in recent years. Work by Guo et al. (2014) on the catalytic decomposition of rigid polyurethane foam waste showed that ammonia, hydrogen cyanide and both nitrogen oxide and nitrogen dioxide were produced at temperatures up to 1100 °C. Additionally, assorted nitrogenous organics were detected in the tar including aniline, quinoline, pyridine, benzonitrile, indole and acridine derivatives with more than 50 % of the tar nitrogen being bound as 4-[(4-aminophenyl)methyl]aniline (the amino analogue of MDI). The detection of the amino MDI derivative in the tar further supports the literature reports of a

Table 1 Relative reactivity of isocyanates with nucleophiles (Herrington & Hock 1998)

Nucleophile with active hydrogen	Structure	Relative reaction rate (uncatalysed, 25 °C)
Primary aliphatic amine	R-NH ₂	100,000
Secondary aliphatic amine	R-NH-R'	20,000–50,000
Primary aromatic amine	Ar-NH ₂	200–300
Primary hydroxyl	R-CH ₂ -OH	100
Water	H ₂ O	100
Carboxylic acid	R-COOH	40
Secondary hydroxyl	R-CH(OH)-R'	30
Di-urea	R-NH-CO-NH-R'	15
Tertiary hydroxyl	(R) ₃ -C-OH	0.5
Urethane	R-NH-COOR	0.3
Amide	R-CONH ₂	0.1

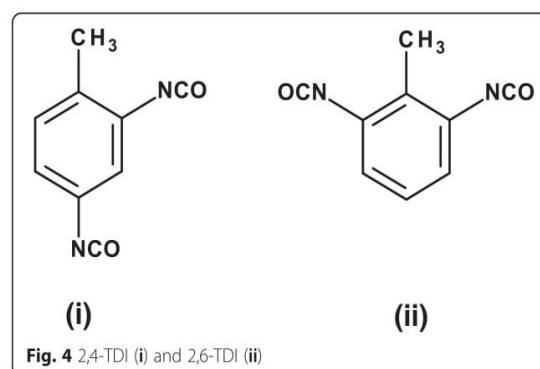
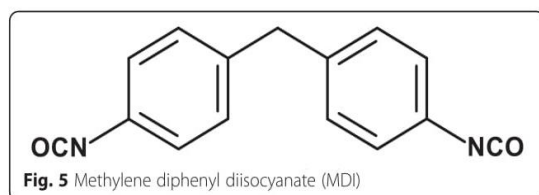


Fig. 4 2,4-TDI (i) and 2,6-TDI (ii)



secondary decomposition mechanism where isocyanates trapped in the condensed phase are converted irreversibly into their amine derivatives.

A review by Paabo and Levin (1987) found that there is no difference in the decomposition products of rigid and flexible polyurethane foams at high temperatures regardless of their differing degradation mechanisms at lower temperatures. Both types of foam yielded very similar products at temperatures above 600 °C.

Oxidative atmosphere

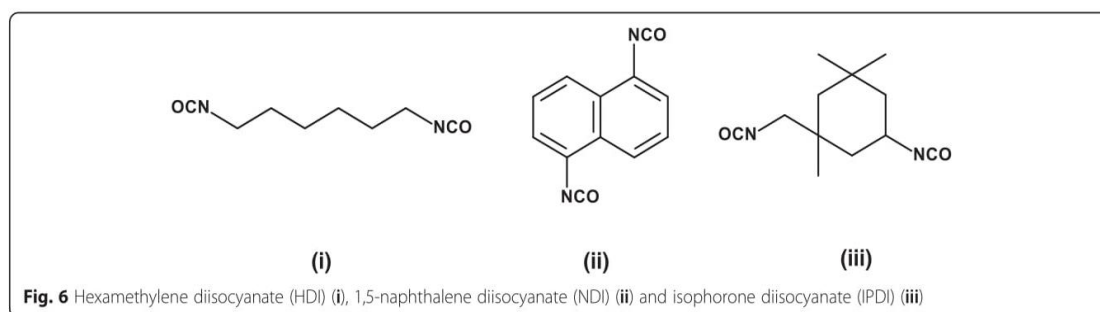
The non-flaming decomposition of non-fire retarded polyurethane foams in air is generally quite well understood and comparable to the inert atmosphere decomposition, in terms of both products and mechanisms. Investigations by Woolley et al. (1972) suggested that the decomposition was initiated by the release of a nitrogen-rich material at 200–300 °C which in turn decomposes into low molecular weight nitrogenous fragments above 500 °C. Additionally, a polyol-rich residue is left behind that begins to fragment and volatilise between 300 and 600 °C. The authors noted that the polyester polyols were more stable than the polyether polyols, with the latter fragmenting at a lower temperature (300–400 °C). Further decomposition occurred about 600 °C with the fragmentation of the “yellow smoke”, primarily into hydrogen cyanide and small quantities of acetonitrile, acrylonitrile and benzonitrile. At higher temperatures the decomposition of the foams produced increasing amounts of HCN from 600 to 900 °C, followed by a sharp rise between 900–1000 °C. The polyester based foam produced nearly double the amount of HCN between 900 and 1000 °C than the polyether foam

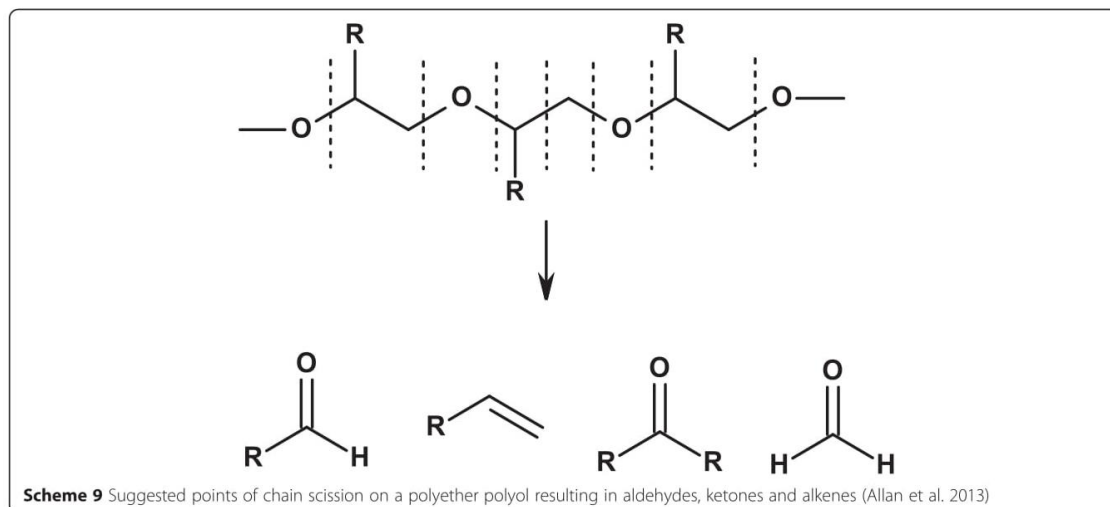
with an increase from 20.8 mg g⁻¹ to 38.0 mg g⁻¹. Similarly, the polyether based foam produced 15.1 mg g⁻¹ to 28.1 mg g⁻¹.

More recent work by Shufen et al. (2006) has supported the claim that polyether based polyurethanes are less stable than their polyester based counterparts when decomposed in air. The polyurethanes used were elastomers based on TDI, which could potentially have differing decomposition mechanisms to their foam counterparts. Thermogravimetric analysis and differential scanning calorimetry (TGA/DSC) showed that the polyether based polyurethane began to decompose at 258 °C, with a second decomposition stage at 350 °C (which could be attributed to the fragmentation of the polyether polyol). The polyester based polyurethane began to decompose at 284 °C with a secondary decomposition step at 359 °C. Overall, the results suggested that the polyether based polyurethane was less thermally stable in the presence of oxygen than the polyester, and both were generally less stable in air than in a nitrogen atmosphere.

While several authors work has focused primarily on the nitrogenous products of decomposition, other publications have focused on the production of other compounds such as carbon monoxide. Bott et al. (1969) reported the decomposition of rigid polyurethane foams in both nitrogen and air to assess the production of CO, HCN and NH₃. When a one gram sample of foam was decomposed in air, CO was formed at a lower temperature than in nitrogen (300 °C vs 400 °C), with a relative concentration of 5000 ppm at 500 °C. The formation of HCN was at a higher temperature in both air and nitrogen (400 °C and 550 °C respectively) with an average concentration of 200 ppm at 500 °C. The authors suggested that the presence of oxygen does not affect the mechanisms by which CO and HCN are produced.

In an attempt to improve the understanding of the thermal decomposition of polyurethanes, Rogaume et al. (2011) developed a mechanism based on both condensed and gas-phase decomposition in air. The authors





affecting occupants over a much wider part of any building. While well-ventilated fire scenarios are routinely used for assessment of flammability, because the object is to stop the fire growing to the out of control stage, where fire toxicity is concerned, the important fire stages are under-ventilated. There are two reasons for this:

1. The volume of effluent is much greater.
2. The yields of the major toxic products (carbon monoxide (CO) and hydrogen cyanide (HCN) from N containing materials) will be much greater.

Almost all unwanted fires are diffusion flames, with inefficient mixing of fuel and oxygen (as opposed to the "premixed" flames found in burner/combustion systems). The interior of large flames are always under-ventilated, because oxygen cannot penetrate the flame. For any larger fire there will always be a significant yield of CO, HCN (from nitrogen containing materials), hydrocarbons and smoke.

Data from large scale fires in enclosures, such as a room, shows much higher levels of the two of the major toxicants, carbon monoxide (CO) and hydrogen cyanide (HCN) under conditions of developed flaming (Andersson et al. 2005; Blomqvist & Lonnermark 2001). It is therefore essential to the assessment of toxic hazard from fire that

each fire stage can be adequately replicated, and preferably the individual fire stages treated separately.

Heat, smoke, asphyxiants and irritants

The toxic hazards associated with fire and the inability of victims to escape from fire atmospheres may be considered in terms of major hazard factors: heat, smoke and toxic combustion products (Hartzell 1993). The time available for escape is the interval between the time of ignition and the time after which conditions become untenable, such that occupants can no longer take effective action to accomplish their own escape. This can result from exposure to radiant and convected heat; visual obscuration due to smoke; inhalation of asphyxiant gases; and exposure to sensory/upper-respiratory irritants. Fire gases contain a mixture of fully oxidised products, such as carbon dioxide (CO₂), partially oxidised products, such as carbon monoxide (CO) and aldehydes, fuel and fuel degradation products, such as aliphatic or aromatic hydrocarbons, and other stable gas molecules, such as hydrogen halides (HCl, HBr) and hydrogen cyanide (HCN) (Kaplan et al. 1984a). Heat, smoke and irritant gases may impair escape, increasing the risk of a lethal exposure to asphyxiant gases, and can sometimes lung damage causes death in those managing to escape.

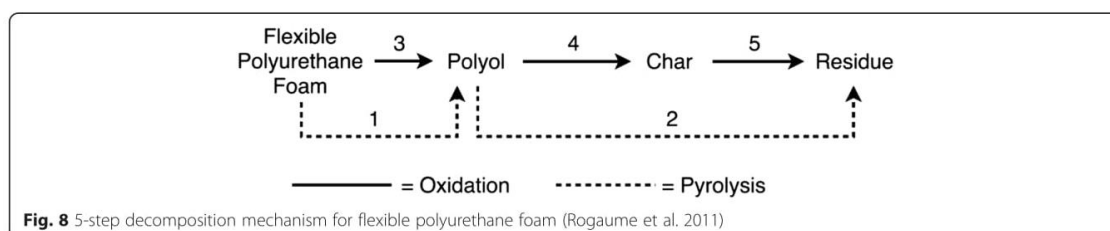


Table 3 Products of decomposition of a flexible polyurethane foam based on decomposition steps from Fig. 8 (Rogaume et al. 2011)

Decomposition step	Gas phase products	Condensed phase products
1	Isocyanates	Polyols
2	Polyol, CH ₂ O, H ₂ O, HCN and CH ₄	Solid residue
3	Isocyanates, polyols, H ₂ O and CO ₂	Mixed polyol and polyol fragments
4	CO ₂ , CO, H ₂ O, Polyol, CH ₂ O, HCN and CH ₄	Char
5	CO, CO ₂ , H ₂ O, CH ₂ O, CH ₄ , HCN and small amounts of polyol.	Residue

The main toxic combustion products can be divided into two classes: asphyxiant gases, which prevent oxygen uptake by cells, with loss of consciousness and ultimately death; and irritant gases which cause immediate incapacitation, mainly by effects on the eyes and upper respiratory tract, and longer term damage deeper in the lung. The effect of asphyxiants and deep lung irritants depend on the accumulated doses, i.e. the sum of each of the concentrations multiplied by the exposure time, for each product; upper respiratory tract irritants are believed to depend on the concentration alone (Purser 2007).

The dangerous concentrations of some important toxic fire gases are shown in Table 4 alongside the influence of ventilation condition on their yields. The yields of acid gases and nitrogen-containing products depend

upon the proportion of the appropriate elements in the materials burned and the efficiency of conversion. In general conversion efficiencies are high for halogen acid gases. Most fuel nitrogen is released as N₂, but in well-ventilated combustion conditions a proportion is released as oxides of nitrogen (mainly NO) and in under-ventilated combustion conditions a proportion is released as HCN (Purser & Purser 2008a). CO yields are generally very low for well-ventilated conditions (in the absence of halogens) but increase considerably under-ventilated combustion conditions. Acrolein and formaldehyde are formed especially from cellulosic materials under non-flaming decomposition conditions, but products of vitiated combustion contain other organic irritants.

Asphyxiant gases

Asphyxiant or narcotic gases cause a decrease in oxygen supplied to body tissue, resulting in central nervous system depression, with loss of consciousness and ultimately death. The severity of the effects increases with dose (Hartzell 1993). The main asphyxiants, carbon monoxide and hydrogen cyanide have been widely studied and are the best understood (ISO 13571 2007). In addition, asphyxiation can also occur as a result of lowered oxygen concentration, and is affected by the carbon dioxide concentration.

Oxygen depletion can be lethal if the oxygen concentration falls below tenable levels (~6%). However, from a fire toxicity perspective it is generally assumed that heat and other gases will have already prevented

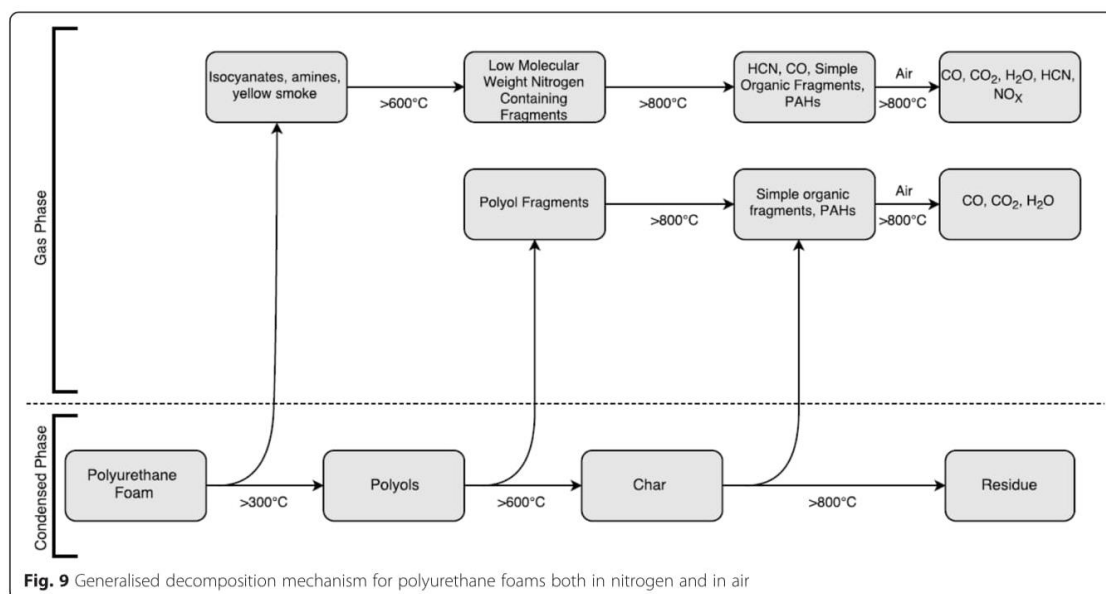


Table 4 The main irritant and asphyxiant components in fire gases and their toxic potencies (in terms of incapacitating; and lethal concentrations) for a 30-min exposure period (ISO 13344 1996; ISO 13571 2012)

Yield largely independent of fire condition	Yield decreases as ventilation decreases	Yield increases as ventilation decreases
HF (500; 2900 ppm)	CO ₂ (~7 %; ~10 %) also replaces O ₂ and increases respiration rate).	CO (1170 ppm; 5700 ppm)
HCl (1000; 3800 ppm)	NO ₂ (170; 250 ppm)	HCN (82 ppm; 165 ppm)
HBr (1000; 3800 ppm)	SO ₂ (150; 1400 ppm)	Acrolein (30 ppm; 150 ppm) Formaldehyde (250 ppm; 750 ppm) Aromatics, aldehydes, ketones etc.

survival, while other toxicants such as CO or HCN, will be present in lethal quantities further from the fire where the oxygen depletion would not be considered harmful.

Carbon monoxide

The toxic effect of carbon monoxide is characterised by a lowered oxygen-delivery capacity of the blood, even when the partial pressure of oxygen and the rate of blood flow are normal. Carbon monoxide binds to the haemoglobin in red blood cells resulting in the formation of carboxyhaemoglobin (COHb), with stability 200 times greater than that of oxyhaemoglobin, impeding the transport of oxygen from the lungs to the cells in the body. This causes deterioration in mental and muscular performance. CO also combines with myoglobin in the muscle cells, impairing diffusion of oxygen to cardiac and skeletal muscles (Purser 2008b). Over short periods, inhaled CO impairs an individual's ability to escape, causing different effects at different concentrations. At a CO concentration of 10 ppm, impairment of judgement and visual perception occur; exposure to 100 ppm causes dizziness, headache, and weariness; loss of consciousness occurs at 250 ppm; and 1000 ppm results in rapid death.

Hydrogen cyanide

Hydrogen cyanide is approximately 25 times more toxic than carbon monoxide through the formation of the cyanide ion, which is formed by hydrolysis in the blood (Hartzell 1993). Unlike carbon monoxide which remains primarily in the blood (as COHb), the cyanide ion is distributed throughout the extra-cellular fluid of tissues and organs (ISO 13571 2007). Two mechanisms have been identified for the toxic effects of cyanide. The first is by combination with the ferric ion in mitochondrial cytochrome oxidase, preventing electron transport in the cytochrome system and inhibiting the use of oxygen by the cells. The second results in a brief stimulation, followed by severe depression, of respiratory frequency, also starving the body of oxygen, and causing convulsions, respiratory arrest and death (Alarie 2002). Whether one or other of these mechanisms

predominates, or their interrelationship, remains unclear. HCN also causes rapid incapacitation, preventing escape, and then, with CO, contributes to death from asphyxiation. One analysis of fire victims' blood showed a trend of declining COHb and a rise in cyanide concentrations (Anderson et al. 1981), probably because of increased use of nitrogen-containing synthetic polymers. The uptake, distribution, metabolism and excretion of cyanide is much more complex than for CO and quantifying CN⁻ in fire victims is more expensive and not routinely undertaken. Therefore the contribution of HCN to fire deaths is difficult to assess, and analysis for CN⁻ is limited to cases where lethal concentrations of CO are absent.

Irritant gases

In contrast to the relatively well-defined effects of asphyxiants, the effects of exposure to irritants are more complex. Irritant gases cause pain and breathing difficulties, leading to incapacitation, such that the victim can no longer effect their own escape (ISO 13571 2012). Sensory and upper respiratory tract irritation stimulates the trigeminal and vagus nerve receptors in the eyes, nose, throat and upper respiratory tract causing discomfort, then severe pain. The effects range from tears and reflex blinking of the eyes, pain in the nose, throat and chest, breath-holding, coughing, excessive secretion of mucus, to bronchoconstriction and laryngeal spasms (Purser 2008b). At sufficiently high concentrations, or when attached to submicron particles, such as soot, most irritants can penetrate deeper into the lungs, causing pulmonary irritation effects which may cause post-exposure respiratory distress and death, generally occurring from a few hours to several days after exposure, due to pulmonary oedema (flooding of the lungs) (ISO 13571 2007).

Hydrogen halides

Hydrogen chloride (HCl) and hydrogen bromide (HBr) are strong acids which dissociate entirely in water. Both may be present in fire effluent, for example from PVC or halogenated flame retardants, and since the damage caused by the acidity (the concentration of H⁺ ions) is independent of the specific anion (Cl⁻ or Br⁻), the discussion on HCl is also applicable to HBr.

Nitrogen oxides

Nitric oxide (NO) and nitrogen dioxide (NO₂) are non-flammable gases present in fire effluents. At high concentrations nitric oxide is rapidly oxidised in air to form nitrogen dioxide, however, at the concentrations found in fire gases, most of the nitric oxide remains unoxidised. Nitrogen dioxide dissolves rapidly in water to form nitric and nitrous acid. At high concentrations these acids can cause pulmonary oedema and death (Paul et al. 2008; Kaplan 1987b). Conversely, nitric oxide gas at low concentrations (~20 ppm) has been used to aid breathing in the treatment of respiratory disorders (Kavanagh & Pearl 1995).

Isocyanates

In general, isocyanate (R-NCO) exposure causes irritation to the skin, mucous membranes, eyes and respiratory tract (NIOSH 1989). The most commonly reported adverse health effects after airborne isocyanate exposure is asthma due to sensitisation (Piiirilä et al. 2008), where inhaled isocyanates rapidly form conjugates with epithelial lung cell proteins (Wisniewski et al. 1999). Once sensitisation has occurred, even extremely low concentrations of airborne isocyanates can trigger fatal asthma attacks (Henneken et al. 2007).

Quantification of toxic hazards from fire

The general approach in generating toxic potency data from chemical analysis is to assume additive behaviour of individual toxicants, and to express the concentration of each as its fraction of the lethal concentration for 50 % of the population for a 30 min exposure (gas-LC₅₀). Summing these contributions generates a fractional effective dose (FED). An FED equal to one indicates that the sum of concentrations of individual species will be lethal to 50 % of the population over a 30 min exposure. These types of approaches have used existing rat lethality data, as described in ISO 13344 (1996) or more recently, based on the best available estimates of human toxicity thresholds as described in ISO 13571 (2007). An equation has been developed for the estimation of the FED for lethality from the chemical composition of the environment in the physical fire (such as the bench-scale methods described in the following section) model taken from ISO 13344 (1996) and uses gas-LC₅₀ values for lethality to provide reference toxicity data for the individual gases to calculate toxic potency, based on rats exposed for 30 min. The Purser model, presented in equation 1, uses V_{CO₂} a multiplication factor for CO₂ driven by hyperventilation, therefore increasing the FED contribution from all the toxic species, and incorporates an acidosis factor A to account for toxicity of CO₂ in its own right (ISO 13344 1996).

Equation 1 Purser model

$$\text{FED} = \left\{ \frac{[\text{CO}]}{\text{LC}_{50,\text{CO}}} + \frac{[\text{HCN}]}{\text{LC}_{50,\text{HCN}}} + \frac{[\text{AGI}]}{\text{LC}_{50,\text{AGI}}} + \frac{[\text{OI}]}{\text{LC}_{50,\text{OI}}} \dots \right\} \\ \times V_{\text{CO}_2} + A + \frac{21 - [\text{O}_2]}{21 - 5.4} \\ V_{\text{CO}_2} = 1 + \frac{\exp(0.14[\text{CO}_2]) - 1}{2} \quad (1)$$

[AGI] is the concentration of inorganic acid gas irritants
[OI] is the concentration of organic irritants
A is an acidosis factor equal to [CO₂] × 0.05

This equation only relates to lethality, or *cause of death*. However, many people fail to escape from fires because of the incapacitating effect of smoke (obscuring visibility) and its irritant components which cause pain, preventing breathing and escape or *reason death occurred*. ISO 13571 (2007) considers the four major hazards from fire which may prevent escape (toxic gases, irritant gases, heat and smoke obscuration). Equations 2 and 3 have been taken from ISO 13571 (2007). Equation 2 calculates the FED of the major asphyxiants, CO and HCN, but without taking oxygen depletion or CO₂ driven hyperventilation into account. Equation 3 calculates the Fractional Effective Concentration (FEC) of sensory irritants in the fire effluent which limit escape. Equation 2 represents the generally accepted case that there are only two significant asphyxiant fire gases, CO and HCN. The FED value is calculated using the exposed dose relationship (concentration-time product, C-t) for CO. The incapacitating C-t product corresponds to CO at a dose of 35 000 μL L⁻¹min (approximately equal to ppm min), predicting incapacitation at around 1200 ppm for 30 min exposure, and an exponential relationship for HCN (because asphyxiation by HCN exposure does not fit a linear relationship), predicting incapacitation at around 82 ppm for 30 min exposure. However, as fires tend to grow exponentially, they do not produce constant concentrations of asphyxiant gases.

Equation 2 FED model from ISO 13571

$$\text{FED} = \sum_{t_1}^{t_2} \frac{[\text{CO}]}{35\,000} \Delta t + \sum_{t_1}^{t_2} \frac{\exp([\text{HCN}]/43)}{220} \Delta t \quad (2)$$

Equation 3 FEC model from ISO 13571

$$\text{FEC} = \frac{[\text{HCl}]}{\text{IC}_{50,\text{HCl}}} + \frac{[\text{HBr}]}{\text{IC}_{50,\text{HBr}}} + \frac{[\text{HF}]}{\text{IC}_{50,\text{HF}}} + \frac{[\text{SO}_2]}{\text{IC}_{50,\text{SO}_2}} \\ + \frac{[\text{NO}_2]}{\text{IC}_{50,\text{NO}_2}} + \frac{[\text{acrolein}]}{\text{IC}_{50,\text{acrolein}}} + \frac{[\text{fomaldehyde}]}{\text{IC}_{50,\text{fomaldehyde}}} \\ + \sum \frac{[\text{irritant}]}{\text{IC}_{50,\text{irritant}}} \quad (3)$$

Equation 3 uses a similar principle to equation 1 to estimate the combined effect of all irritant gases.

In order to relate the fire effluent toxicity to a "maximum permissible loading", the FED can be related to the mass of material in a unit volume which would cause 50 % lethality for a given fire condition. The fire toxicity of a material can also be expressed as a material-LC₅₀, which in this case is the specimen mass M of a burning polymeric material which would yield an FED equal to one within a volume of 1 m³. The relation of the FED to the material-LC₅₀ is given in equation 4.

Equation 4 Relation of LC₅₀ to FED

$$\text{material-LC}_{50} = \frac{M}{\text{FED} \times V} \tag{4}$$

Comparing the toxic potencies of different materials, the lower the material-LC₅₀ (the smaller the amount of materials necessary to reach the toxic potency) the more toxic the material is. LC₅₀ values should be referenced to the fire condition under which they were measured.

The equivalence ratio ϕ

The relatively high yields of CO from under-ventilated fires are held responsible for most deaths through inhalation of smoke and toxic gases. However, in the field of combustion toxicity testing, this under-ventilated burning is the most difficult to create using bench-scale apparatus. Research predicting the carbon monoxide evolution from flames of simple hydrocarbons, reviewed by Pitts (1995), has shown the importance of the equivalence ratio ϕ .

$\phi = \frac{\text{actual fuel to air ratio}}{\text{stoichiometric fuel to air ratio}}$	$\phi < 1$	fuel lean flames	Typical CO yield (g per g of polymer) 0.01
	$\phi = 1$	stoichiometric flames	0.05
	$\phi > 1$	fuel rich flames	0.2

An equivalence ratio of 0.5 represents a well-ventilated scenario, typical of an early growing fire, while a ratio of 2 corresponds to the under-ventilated stage responsible for high yields of toxic effluents. When $\phi = 1$ the theoretical amount of air is available for complete combustion to carbon dioxide (CO₂) and water.

The relationship between equivalence ratio and yields of CO and other products has been studied in detail for a wide range of materials during flaming combustion using two small-scale apparatus designed specifically for this purpose—the ASTM E2058 fire propagation apparatus (Tewarson 2002) and the ISO/TS 19700 tube furnace apparatus (ISO/TS 19700 2013), in conjunction with a series of large-scale experiments used for validation

(Gottuk & Lattimer 2002; Blomqvist & Lonnermark 2001; Purser & Purser 2008a). The findings from these studies demonstrated that yields of different toxic products are highly dependent on equivalence ratio (either positively or negatively correlated), and elemental and molecular composition of the material. To a lesser extent, parameters such as temperature and oxygen concentration also affect the yields of toxic products.

Most fire deaths and injuries actually occur in residential fires, although assessment of fire toxicity is currently focused on areas where escape is restricted, such as aeroplanes, railway carriages, and passenger ships, which include requirements to quantify the fire toxicity of internal components. In most countries, there are no regulations covering the fire toxicity of building components, or for most road vehicles, including goods vehicles in tunnels. In China and Japan, there are specific restrictions on the use of materials with high fire toxicity in high risk applications such as tall buildings, while an increasing number of jurisdictions permit the alternative performance based design approaches to fire safety. Reliable rate of heat release, fire effluent toxicity and smoke generation data are all essential components of such an assessment. The general approach, described in ISO 13571 (2012), is to ensure that the available safe escape time (ASET) before escape routes become obscured by smoke and/or filled with toxic gases, exceeds the required safe escape time (RSET). Various apparatus and protocols for quantifying fire effluent toxicity in different jurisdictions and industries have been critically reviewed (Hull & Paul 2007).

Bench-scale methods for generating toxic effluents

Bench-scale methods used for generating toxic effluents from polyurethane foams have met with controversy. Some methods have proved incapable of properly replicating the most toxic under-ventilated fire condition, where the yields of carbon monoxide and hydrogen cyanide are greatest, while other methods have shown good correlation with large scale test data. Bench-scale methods used for generation of toxic fire effluents ideally should be capable of reproducing individual fire stages or combustion conditions, for input into models of combustion toxicity. Full-scale fires simultaneously involve different fire stages in different places, which are changing with time. However, bench-scale methods which allow the combustion conditions to change during the test are much more difficult to relate to full-scale fires, because the duration of each condition is unknown, and the behaviour of fires changes on scale-up. Most bench-scale methods have non-constant combustion conditions, such as those in closed chambers exposed to a constant source of heat, including the smoke density chamber (SDC) (ISO 5659-2 2012), and static tube furnace tests, such as the NF X 70-100 (2006). Those

with constant combustion conditions are more suited to producing data suitable for comparison and modelling: the steady state tube furnace (SSTF) (ISO/TS 19700 2013) has been specifically designed to achieve this. Intermediate between these two approaches are those that can produce quasi-steady combustion conditions, such as the cone calorimeter (ISO 5660–1 2002) with non-standardised controlled atmosphere attachment (CACC), and the fire propagation apparatus (FPA) (ISO 12136 2011). The difficulty of replicating the conditions of fully developed under-ventilated flaming on a bench-scale is caused by several practical problems. ϕ depends on the mass loss rate of the specimen and the available air; for most methods one or both are unknown; ϕ will be increased by an unknown factor if products are recirculated into the flame zone. Apparatus where ϕ changes rapidly allow little time for sampling and measurement of mass loss and effluent composition at a specific value of ϕ , with resultant errors and uncertainties. Progressive changes in the composition of a static specimen (for example due to char formation) provide additional complexity. In a compartment fire, the reactions of under-ventilated flaming occur in both the flame zone and in the hot upper layer. Only the SSTF has a heated reaction zone which replicates the hot layer. The applied heat flux must be large enough for burning to continue at oxygen concentrations as low as 5 %. In some bench-scale apparatus the heat flux is constant, and often insufficient to sustain flaming at such low oxygen concentrations; further, an unknown quantity of fresh air bypasses the fire plume, so the ventilation condition, and hence ϕ , remains undefined. Some fire models, such as the cone calorimeter, fire propagation apparatus and smoke density chamber use the temperature of the radiant heater to preselect the radiant heat flux, and then check this using a radiant heat flux meter. Others, such as the NF X 70–100, and the ISO/TS 19700 SSTF use the furnace temperature setting to ensure a consistent radiant heat flux. The radiant heat flux in the ISO/TS 19700 apparatus has been measured (Stec et al. 2008) and is 40 kW m^{-2} in the centre of the furnace at $650 \text{ }^\circ\text{C}$ and 78 kW m^{-2} at $825 \text{ }^\circ\text{C}$. Each method is described briefly in the following section.

The smoke density chamber

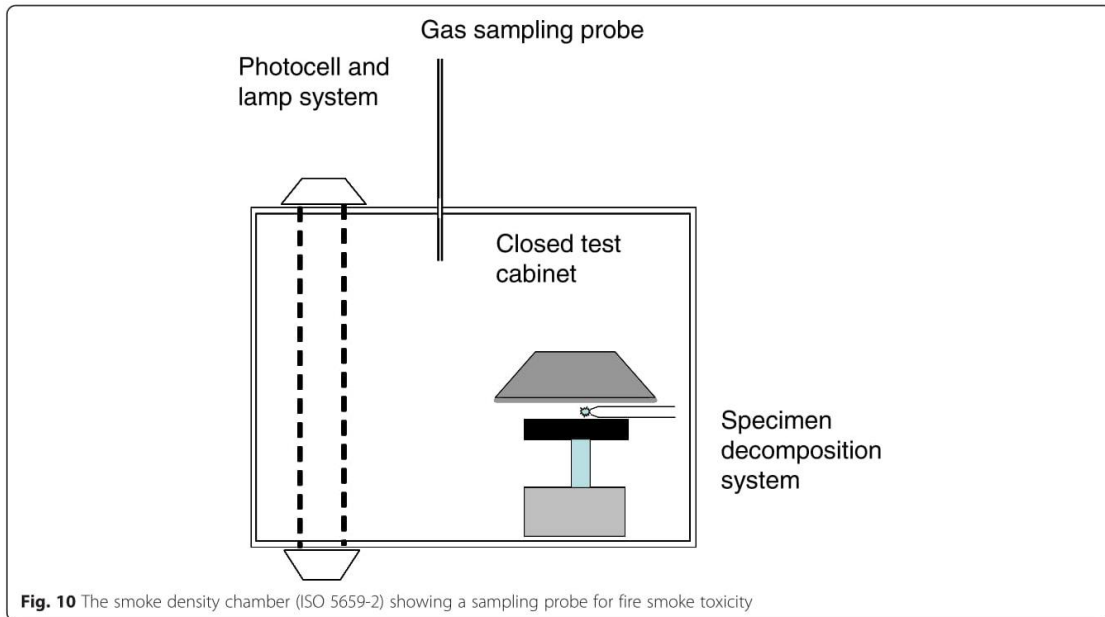
The most widely used fire-test apparatus, stipulated in smoke regulations in most countries of the developed world, is the smoke density chamber as described in ISO 5659–2 2012, and shown schematically in Fig. 10. Its widespread availability has encouraged its adaptation to toxic gas generation and assessment. The standard specifies four test conditions, but fails to link them to particular fire scenarios. The conditions specified are: 25 kW m^{-2} without piloted ignition; 25 kW m^{-2} with piloted ignition; 50 kW m^{-2} without piloted ignition;

and 50 kW m^{-2} with piloted ignition. The sample is a $75 \times 75 \text{ mm}$ square solid sheet and the standard for smoke measurement states that the results are only valid at the thickness tested (typically 1–4 mm). For a fixed chamber volume (0.51 m^3), assuming complete combustion, the sample thickness will dictate the ventilation condition, thus a thin sample will burn under well-ventilated conditions with minimum toxic products, while a thicker sample might be expected to produce a high yield of CO and other products of incomplete combustion. The protocol has been modified as a toxicity test by the mass transport industries, in the aircraft (EN 2826 2011), maritime (Fire Test Procedure Code 2010), and railway tests (CEN/TS 45545–2 2009). Some of these methods attempt to address the transition through the fire stages by monitoring the formation of toxic gases as a function of time, as the oxygen concentration falls, and the fire condition changes from well-ventilated to under-ventilated. However, unlike a real fire, the heat flux remains constant, and so when the oxygen concentration falls, the flame may be extinguished.

The transport industries have adopted the smoke density chamber (SDC) ISO 5659–2 (2012) and ASTM E662, for quantification of toxic product yields (Fire Test Procedure Code 2010; CEN/TS 45545–2 2009) using simple pass/fail chemical detection (e.g. Draeger tubes), conventional or Fourier transform infrared spectroscopy (FTIR) gas analysis, despite significant problems of reproducibility. It has been suggested that the reproducibility problems arise from the single point measurement (the tip of the probe may be in the centre of the plume, below it, or if mixing is more efficient, the upper layer may be recirculated through the flame), or the timing of the effluent sampling may cause instabilities (for example an initial proposal to sample after 8 min was replaced by a proposal to sample when the smoke density reached its maximum). The revised protocol is based on continuous sampling of the fire effluent.

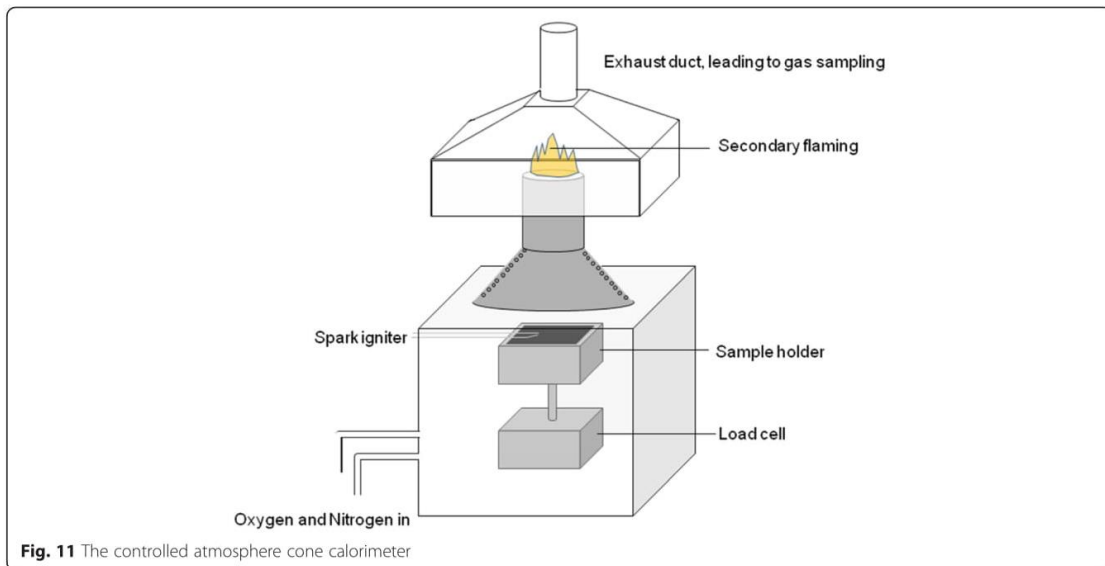
The controlled atmosphere cone calorimeter (CACC)

The cone calorimeter (ISO 5660–1 2002) is probably the most widely used apparatus for measurement of flammability properties such as ignitability and heat release rate (Schartel & Hull 2007). It can be used for testing samples $100 \times 100 \text{ mm}$ and up to 50 mm thick, in both the horizontal and vertical orientation. The open cone calorimeter replicates the early well-ventilated stage of flaming where a fire would be too small to produce enough toxicants to cause harm except in very small enclosures. However, a non-standard modification of the apparatus has been described, enclosing the fire model in a controlled ventilation chamber, in an attempt to replicate oxygen-depleted conditions. In this modification, the controlled atmosphere cone calorimeter (CACC)



(Babrauskas et al. 1992), shown in Fig. 11, a conical heater used as a fire model is enclosed in a heat resistant glass chamber (400 mm high with 300 × 300 mm base) so that the air flow around the specimen may be controlled by diluting the oxygen content with nitrogen. In some cases the effluent continues to burn as it emerges from the chamber, (secondary flaming in Fig. 11) ultimately giving well-ventilated flaming. In others, under

reduced oxygen concentrations, the fuel lifts from the surface, but ignition does not occur (Christy et al. 1995). Hietaniemi et al. (1999) used the controlled atmosphere cone calorimeter, but argues correctly, in the authors' opinion, that an instantaneous "effective" global equivalence ratio ϕ_{eff} should be used, rather than an averaged local equivalence ratio, based on the oxygen supply to the chamber, because, in some experiments, substantial secondary



flaming occurred outside the test chamber, such that the amount of oxygen available to combustion exceeded the amount that was fed to the enclosed chamber.

The steady state tube furnace (SSTF)

The steady state tube furnace (ISO/TS 19700 2013), shown in Fig. 12, feeds the sample (typically around 25 g of pellets or granules) into its hot zone at a fixed rate, under a controlled air supply, inside a horizontal silica tube of diameter 48 mm, allowing adequate mixing of fuel and oxidant. It forces combustion by driving the sample into a furnace of increasing heat flux at a fixed rate, so that, by running several tests with the same material with different ventilation conditions, each fire stage can be replicated by steady state burning. The products generated in the flame zone then pass through the heated furnace tube, maintaining a high temperature, as in the upper layer of a compartment fire. The toxic product yields may be quantified from the gas concentrations and mass feed rate during the steady state burn period. It has been designed to generate data for input to fire hazard assessments, using the methodology in ISO 13344 (1996) and ISO 13571 (2012), particularly in relation to the ISO fire stages. The sample is spread evenly in a silica boat over a length of 800 mm and fed into a tube furnace at a typical rate of 1 g min^{-1} with flowing air at a rate of $2\text{--}10 \text{ L min}^{-1}$. Secondary air is added in a mixing chamber to give a total gas flow of 50 L min^{-1} .

Relationship to full-scale fires

The yields of CO and HCN from five bench-scale methods have been compared to large-scale data under a range of flaming fire conditions (Stec & Hull 2014). Toxic product yield data from the smoke density chamber (ISO 5659-2 2012), the controlled atmosphere cone calorimeter (based on ISO 5660-1 2002), the fire propagation apparatus (FPA) (ASTM E 2058), the French railway test (NFX) (NF X 70-100 2006), and the steady state tube furnace (SSTF) (ISO/TS 19700 2013) were

compared to published large-scale enclosure fire data (from a standard ISO 9705 room) for two polymers, polypropylene (PP) and polyamide 6.6 (PA 6.6). The results from the SSTF and FPA show the best agreement with those from the full and 1/3 scale ISO room for both materials under a range of fire conditions. The CACC and SDC show reasonable agreement for well-ventilated burning, but fail to replicate the more hazardous under-ventilated fire conditions. The NFX generates data intermediate between the well-ventilated and under-ventilated fire conditions.

Toxic products formed during flaming combustion of polyurethane foams

In the UK, the rapid rise in fire deaths, in particular those from smoke toxicity, between the late 1950s and the early 1980s has been attributed to the rapid growth in low cost polyurethane foam furniture, with superior comfort and lower cost than the natural fillings that preceded it. The higher flammability of these new furniture products took people by surprise, and has been blamed for an increased number of serious fires and a tripling of fire deaths over 20 years (Fig. 13) (UK Fire Statistics 2013).

Over this period there was a corresponding shift from the main cause of death in fires being attributed to "burns" to being attributed to "inhalation of smoke and toxic gases". Further to this, a similar pattern began to emerge in the injuries of fire victims (Fig. 14) (UK Fire Statistics 2013).

The yields of some of the most toxic gases from unwanted fires (such as CO, HCN and some organic irritants) have been demonstrated to be directly related to the combustion conditions (Purser 2002). In the case of flaming combustion, one of the most important factors relating to the toxic product yield is the fuel/air ratio which, as defined earlier, can be expressed as an equivalence ratio (ϕ). As the availability of oxygen becomes lower in proportion to the amount of fuel, the yields of certain toxic gases will increase. In

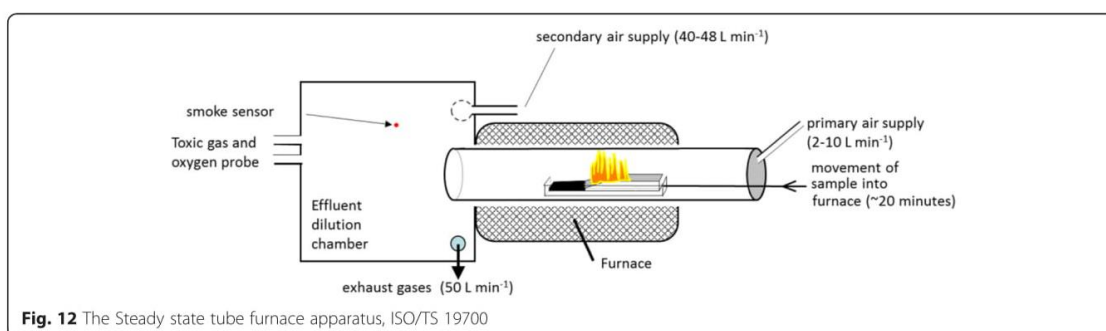


Fig. 12 The Steady state tube furnace apparatus, ISO/TS 19700

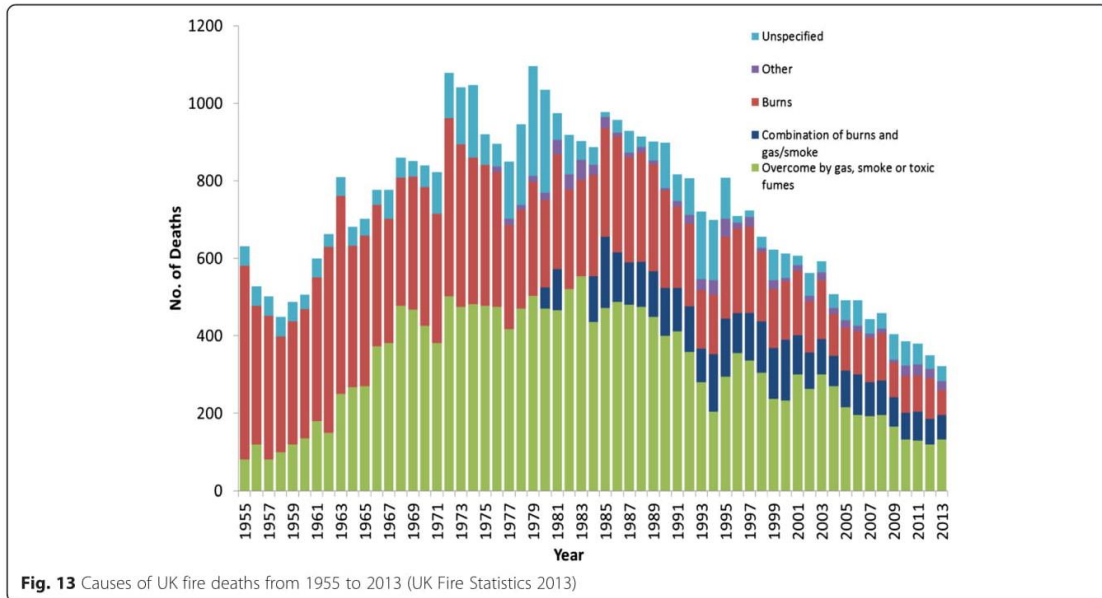


Fig. 13 Causes of UK fire deaths from 1955 to 2013 (UK Fire Statistics 2013)

ventilation controlled fires (such as those occurring in a room, building or other enclosure), the yields of these gases from the flaming combustion of polyurethane foams generally follow the same trend. As a result of this, studies that use ventilation controlled conditions, such as those using the steady state tube furnace (ISO/TS 19700 2013), are more likely to give a realistic representation of these reduced oxygen environment fire conditions.

Stec and Hull (2011) assessed the fire toxicity of building insulation materials using a steady state tube furnace as described in ISO/TS 19700 (2013). The samples tested included both commercial rigid polyurethane foam and polyisocyanurate foam. Under well-ventilated flaming ($\phi < 0.8$), the yields of CO_2 and NO_2 were at their highest, while the yields of CO and HCN were at their lowest. However, as the fire condition became under-ventilated ($\phi > 1.5$), the yields of both CO and HCN

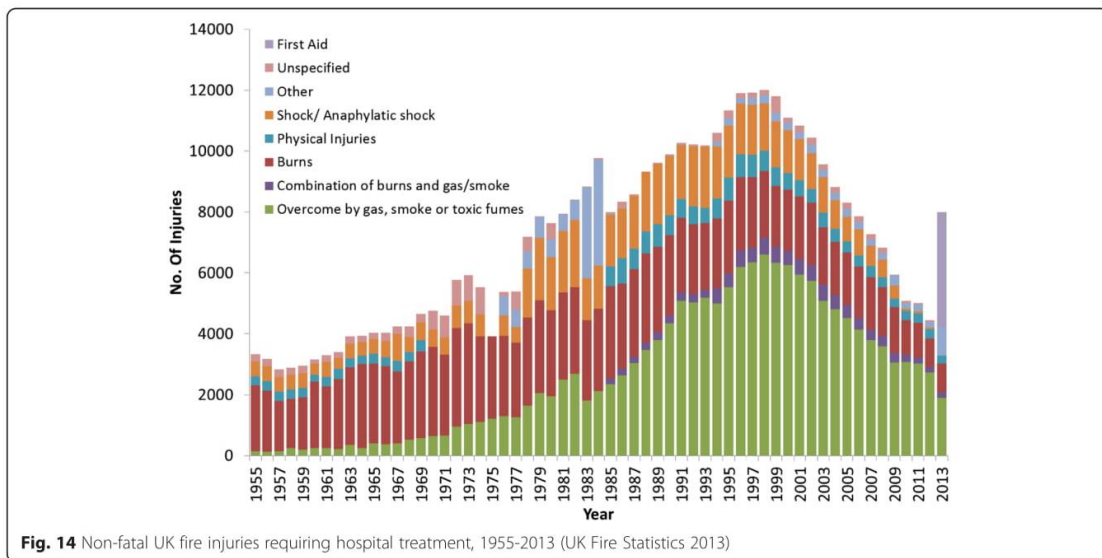


Fig. 14 Non-fatal UK fire injuries requiring hospital treatment, 1955-2013 (UK Fire Statistics 2013)

Table 5 Toxic product yields the flaming combustion of a rigid polyurethane foam and polyisocyanurate foam (Stec & Hull 2011)

Material	Furnace temperature (°C)	ϕ	CO Yield/mg g ⁻¹	HCN Yield/mg g ⁻¹
Rigid Polyurethane Foam	650	0.69	60	6
	650	1.24	220	9
	825	2.00	240	12
Polyisocyanurate Foam	650	0.75	80	7
	650	1.34	220	10
	825	1.97	225	17

increased for both rigid polyurethane and the polyisocyanurate, while the yields of CO₂ and NO₂ decreased. The yields of CO and HCN at varying ϕ and temperature are presented in Table 5. For both materials there is a clear increase in yield from the well-ventilated to under-ventilated conditions. The rigid polyurethane foam produced slightly more CO than the polyisocyanurate at $\phi \sim 2.0$ (240 mg g⁻¹ vs 225 mg g⁻¹). The polyisocyanurate, on the other hand, produced slightly more HCN than the rigid foam (17 mg g⁻¹ vs 12 mg g⁻¹). Additionally, the amount of CO generated for both materials began to taper off at ϕ 1.2-2.0 as the available oxygen becomes so low that the generation of CO becomes limited, while the yield of HCN continues to increase with equivalence ratio and temperature. The authors noted that the yields of CO during the well-ventilated testing were higher than expected for both materials, and attributed this to the possible presence of gas phase free radical quenchers, such as halogens or phosphorous containing flame retardants, which would reduce the conversion of CO to CO₂ (Schnipper & Smith-Hansen 1995).

In another investigation, using a steady state tube furnace, Blomqvist et al. (2007) assessed the toxic product yields of a flexible polyurethane foam that was designed for use in hospital mattresses. The test conditions were designed so that the fire conditions met the ISO 19706 (2007) fire type 2 (well-ventilated flaming fire $\phi < 0.75$) and fire type 3b (post-flashover fire in large or open compartments $\phi \sim 2.0$). The yields of toxic products followed the expected trend of being higher in the under-ventilated conditions. The average well-ventilated yield of HCN was found to be 4 mg g⁻¹, while it was 9 mg g⁻¹ for under-ventilated conditions. The peak HCN value reached was 10 mg per g⁻¹ in the under-ventilated tests. The yield of CO had a wide range during the under-ventilated tests due to inconsistent flaming of the sample with yields from 100–250 mg g⁻¹. Additionally, NO was detected during the well-ventilated tests and NH₃ during the under-ventilated tests. This agrees with the fact that oxidation of NH₃ and HCN to NO (and NO₂, although it was not analysed

in these experiments) would occur more readily during well-ventilated burning. The authors noted no significant difference in the range of yields of isocyanates detected in either well- or under-ventilated conditions with a range of 1.0-1.6 mg g⁻¹.

Very few authors have assessed the yields of isocyanates produced during the flaming combustion of polyurethane foams and as such there is a limited amount of data available. Investigations by Hertzberg et al. (2003) used a cone calorimeter to assess the yields of amines, aminoisocyanates and isocyanates from the flaming combustion of a flexible polyurethane foam. The average combined yield of isocyanates recovered was 0.869 mg g⁻¹ and the average yield of amines and aminoisocyanates was 0.321 mg g⁻¹. These yields are comparable to that of the results reported by Blomqvist et al. (2007). Additionally, the authors reported a yield of 13–15 mg g⁻¹ of CO, 1.4–1.5 mg g⁻¹ of HCN, and 10–12 mg g⁻¹ of NO. The authors noted that the yields of the toxicants produced an atmosphere in the tests which fell well below their Immediately Dangerous to Life and Health (IDLH) values. However, the lower yields can be attributed to the fact that the cone calorimeter is a well-ventilated scenario, estimated as $\phi \sim 0.7$ (Schartel & Hull 2007). Taking this into consideration, the reported yields of isocyanates, aminoisocyanates and amines are still relevant, as the results of Blomqvist et al. (2007) suggests that their yields are not heavily dependent on the ventilation conditions and that the yields would likely only increase by a small amount during under-ventilated flaming.

While the link between CO yield and equivalence ratio is well established, the yield of HCN in ventilation limited conditions shows more complicated behaviour for polyurethanes. While it is evident that the HCN yield increases as a fire becomes more under-ventilated, the link between the nitrogen content of the fuel and the yield of HCN is less clear. In a series of investigations, Purser and Purser (2008a) examined the yields of HCN from a range of materials and the conversion of fuel nitrogen to HCN. A "combustion modified high resilience" flexible polyurethane foam (CMHR-PUF) and a polyisocyanurate (PIR) foam were analysed a steady state tube furnace apparatus. Tests were carried out on the CMHR-PUF at 650 °C and 850 °C and at 700 °C for the PIR in order to achieve steady flaming conditions. Both of the materials showed a clear relationship with the HCN yield increasing with ϕ . At 650 °C, the yield of HCN from the CMHR-PUF increased up to $\phi \sim 2.0$ where it reached a peak of 14 mg of HCN per gram of polymer burned. However, when $\phi > 2.0$ the yield of HCN decreased, falling to 10 mg g⁻¹ at $\phi \sim 2.75$. At 850 °C the yield of HCN was higher with 16 mg g⁻¹ at $\phi \sim 2.0$. The PIR foam produced similar HCN yields to the CMHR-PUF until ϕ 1.5, after which it increased more

rapidly to give a yield of 20 mg g⁻¹ at $\phi \sim 1.75$. This value decreased to 18 mg g⁻¹ at $\phi \sim 2.0$.

Elemental analysis of the polymers showed that the CMHR-FPUR contained 8.22 % nitrogen by weight and the PIR contained 6.15 % nitrogen by weight. Based on this data, the HCN recovery fraction was calculated for both materials. The PIR at $\phi 1.75$ resulted in 15 % of the fuel nitrogen being recovered as HCN. At $\phi \sim 2.0$ the CMHR-FPUR resulted in 8 % and 11 % nitrogen recovered as HCN for 650 °C and 850 °C respectively. The authors acknowledged that the lower nitrogen recovery fraction for the flexible foam could be due to fuel nitrogen being lost as isocyanates, which are known to escape into the effluent plume, while for rigid foams they are more likely to be trapped in the burning solid (Woolley & Fardell 1977). For the range of materials investigated, the authors also noted that those containing fire retardants (including the CMHR-PUF and PIR) resulted in a higher recovery fraction of fuel N as HCN. Similarly to the trend reported by Stec and Hull (2011) in well-ventilated conditions, this can be attributed to gas phase free radical quenching in the material by the chlorine present in both the CMHR-PUF and PIR (2.53 % and 3.56 % chlorine by weight, respectively).

Alongside the experiments performed in the steady state tube furnace, the PIR was also investigated in a half scale ISO 9705 room-corridor test and in a full size ISO 9705 (1993) room. During these tests, the PIR was set up as wall panels covered on two faces with aluminium foil. The cribs used in the ISO 9705 tests were constructed from PIR "sticks" which burned rapidly, albeit with minimal damage to the room. The full size ISO 9705 test resulted in well-ventilated flaming ($\phi 0.26-0.5$) due to the relatively large volume of air and relatively small sample size. The full-scale test showed good accordance with the SSTF data considering the inherent unreliability of large-scale testing. The half-scale ISO 9705 experiments showed a wider range of ventilation conditions up to $\phi \sim 2.0$. However there was significant scattering of the results with both high and low outliers (26 mg g⁻¹ at $\phi 1.22$ and 9 mg g⁻¹ at $\phi 1.95$). Taking into consideration the issues with repeatability of large-scale testing, the authors asserted that the similar trend in HCN yields supported the good relationship between the tube-furnace and large-scale results.

The increased yield of HCN for the CMHR-FPUR between 650 °C and 850 °C is likely due to the increased fragmentation of nitrogenous organic compounds in the flame, similar to the behaviour during non-flaming combustion in air reported by Woolley et al. (1972). Michal (1982) reported a similar trend at a fixed air flow rate. A sample of rigid polyurethane foam was heated in a static tube furnace with an air flow of 50 ml min⁻¹ at a range of temperatures from 600 to 1200 °C and the yield of HCN was quantified.

The results showed a HCN yield of 15.8 mg g⁻¹ at 600 °C. The yield was much lower at 800 °C with 7.4 mg g⁻¹ but at 1000 °C and 1200 °C the yield increased significantly to 33.9 mg g⁻¹ and 48.1 mg g⁻¹ respectively. The specific mass of the polyurethane sample was not provided by the author and the ventilation conditions were not clear as a result of this. The significant increased yields at 1000 °C and 1200 °C could also be attributed to pyrolysis of the nitrogenous combustion products into HCN due to the low air flow rate.

In many studies (such as those by Stec and Hull (2011), Purser and Purser (2008a) and Blomqvist et al. (2007)), the sample is raised to a fixed furnace temperature, which is further increased in the gas phase during flaming combustion. This will result in a HCN yield related that specific furnace temperature. However, during the combustion of polyurethane foams, the HCN yield is notably higher when the fire progresses from smouldering to flaming combustion. This was observed by Levin et al. (1985) when a flexible polyurethane foam was first heated at a temperature below its auto-ignition temperature, followed by flaming combustion of the remaining char and residue at a higher temperature. The authors intended to compare the HCN yields for the non-flaming and flaming combustion of the foam in a smoke chamber apparatus (as described in Levin et al. 1982) to that of a large scale test room. The test room was 2.4 × 3.0 × 3.0 m with a door (dimensions not specified) and a 1 to 2 kg slab of foam in the centre of the room. Smouldering was forced by an electrically heated resistance wire embedded in the sample and a load cell measured the mass of the sample throughout the experiment. In the smoke chamber, the highest reported yield during flaming combustion was 1.02 mg g⁻¹. In the large scale test room, the sample smouldered for 1.5 to 2 h, resulting in a HCN yield of 1.03 mg g⁻¹. Once the material ignited, the yield of HCN increased to 3.8 mg g⁻¹. While the smoke chamber experiment is known to give low HCN yields, and both scenarios are well-ventilated, the yield of HCN was almost 4 times as high during flaming combustion if the sample was allowed to smoulder first.

This prompted the authors to perform further studies in order to understand why allowing the foam to smoulder increased the yield of HCN during flaming combustion. Using a cup furnace with a 200 L sampling chamber (identical in design to the one used in the smoke chamber experiments), a 3.88 g sample of foam was heated to just below its ignition temperature (370 °C) which yielded <1 mg g⁻¹ HCN. In the chamber, 0.23 g of black char and 0.04 g of yellow oil were recovered. When the black char was burned at 600 °C, it yielded 14.95 mg of HCN (65 mg per gram of char) and the yellow oil yielded 21 mg per gram of oil. Elemental analysis of the polymer

and the char showed that 80 % of the nitrogen in the polymer was lost when heated at 370 °C, but only 0.6 % was recovered as HCN when burned at 600 °C. However, while the char produced when the polymer was heated at 370 °C contained only 20 % of the total nitrogen from the polymer, 40 % of that (8 % of the total nitrogen in the polymer) was recovered as HCN when the char was burned at 600 °C. This suggests that the nitrogen in the char will more readily form HCN, even when the flaming is well-ventilated. The amount of nitrogen recovered from the char (8 %) at 600 °C is of a similar order to the results reported by Purser and Purser (2008a) in the steady state tube furnace suggesting that the amount of nitrogen in the polyurethane foam converted into HCN when the material is allowed to smoulder first before flaming is similar to that of steady under-ventilated flaming. In a report from the same laboratory, Braun et al. (1990) also reported increased HCN yields when the sample was allowed to smoulder before flaming in similar apparatus as above. In a real fire, involving cycles of growth and decay of flaming combustion, the resulting yields of HCN from the combustion of polyurethane foams are likely to be higher than predicted in some bench-scale methods as a result of this two-step decomposition mechanism.

The widespread use of flexible polyurethane foams in furniture and other upholstery, where they are usually covered in some kind of fabric has prompted some authors to investigate the effects of covering the foam on the yield of toxic products. Levin et al. (1986) investigated the toxicity of flexible polyurethane foam and a polyester fabric both separately and together. Using a smoke chamber set up for animal exposure experiments (as described in Levin et al. 1982), the authors exposed male Fisher 344 rats in a 200 L exposure chamber to the fire effluent from the flaming and non-flaming combustion of both materials. The reported yields were extremely low for both CO and HCN, as the NBS smoke chamber apparatus is a well-ventilated fire scenario reported to give low HCN yields (Table 6). Flaming combustion of the polyurethane foam did not cause any animal deaths, however the non-flaming combustion

resulted in deaths post-exposure. The authors noted that in both the flaming and non-flaming combustion of the polyurethane foam, the concentrations of toxicants did not reach high enough concentrations to predict deaths. The polyester fabric produced 92–93 mg g⁻¹ of CO when burned with very little difference in the flaming or non-flaming conditions. This was enough to cause deaths both during and post-exposure. When tested with the polyester covering the polyurethane, the yield of HCN during flaming combustion was higher than that of just the polyurethane foam on its own. However, the yield of CO was lower in both the non-flaming and flaming combustion. The overall toxicity of the combined materials was higher, and the average concentrations of the gases throughout the tests were consistently higher than that of the individual materials in both flaming and non-flaming conditions. The authors noted that the total concentrations of CO and HCN during flaming combustion were greater than the sum of those from the individual materials. It is difficult to draw more general conclusion from this work because the fuel-to-air ratio was not quantified, and the degree of mixing of fresh air and fire effluent, in the exposure chamber, is unknown. However, it does suggest that yield of toxic products is effected by covering the foam with another material during flaming combustion.

Similarly, Busker et al. (1999) tested both rigid and flexible polyurethane foams using a bespoke smoke chamber apparatus to assess the toxicity of the flaming combustion products of the materials to rats. The samples were heated at 800 °C in a static tube furnace, with the effluent being cooled to <50 °C before entering an exposure unit. The rigid polyurethane foam yielded ~55 mg g⁻¹ CO and ~0.5 mg g⁻¹ of HCN. The flexible foam produced ~175 mg g⁻¹ of CO and 5 mg g⁻¹ of HCN. The authors also noted that the presence of aldehydes was detected during the flaming combustion of the flexible foam, albeit in extremely low yields. Based on the temperature of the test, the yields of HCN are extremely low when compared with the CO yields. The authors did not

Table 6 Concentrations of CO and HCN from flexible polyurethane foam, polyester fabric and polyester fabric on polyurethane foam (Levin et al. 1986)

Flaming/non-flaming and temperature	Material	CO		HCN	
		Concentration/ppm	Yield/mg g ⁻¹	Concentration/ppm	Yield/mg g ⁻¹
Non-flaming 374–377 °C	Polyurethane Foam	740	22.8	9	0.3
	Polyester Fabric	2910	93	-	-
	Polyester Fabric on Polyurethane Foam	1390	33.28	5	0.12
Flaming 523–527 °C	Polyurethane Foam	840	26.0	27	1.515
	Polyester Fabric	2990	92.2	-	-
	Polyester Fabric on Polyurethane Foam	3070	75.72	63	1.87

specify which analytical methods were used in the quantification of the fire gases, only that they were sampled via a sampling bag.

Several authors have investigated the relationship between bench-scale test data and large-scale test data using polyurethane foams. Babrauskas et al. (1991a) compared a number of test methods. The authors tested a rigid polyurethane foam using a NBS cup furnace (as described in Levin et al. 1982), a developmental method (SwRI/NIST method) which used a radiant heater on the sample which lead into a 200 L exposure chamber, a cone calorimeter (ISO 5660 2002), a furniture calorimeter (as described in Babrauskas et al. 1982), and a three-compartment large scale test. The three-compartment test consisted of a 2.4 × 3.7 × 2.4 m burn room, a 2.4 × 4.6 × 2.4 m corridor and a 2.4 × 3.7 × 2.4 m target room where samples would be taken. The three compartments were connected by doors and the target room contained an open vent. Although the authors intended for the bench scale test methods and the large scale test to represent post-flashover room fires, the tests resulted in CO and HCN yields that suggested the combustion conditions were not under-ventilated (Table 7). The test method that produced toxic product yields associated with under-ventilated flaming was the NBS cup furnace toxicity method, which yielded 180–210 mg g⁻¹ of CO and 16–20 mg g⁻¹. This is unusual as this test method is usually well-ventilated and the results are not similar to reports of other authors (such as Levin et al. 1985 and Levin et al. 1986).

A more recent assessment by Marsh and Gann (2013) tested a flexible polyurethane foam with a cotton polyester cover in a range of test methods including the radiant heat apparatus (NFPA 269 2012), the ISO 5659–2 (2012) smoke density chamber, a controlled atmosphere cone calorimeter (ASTM E 1354) and the steady state tube furnace (ISO/TS 19700 2013). The authors presented a large set of data for all of the test methods, including a range of test conditions, air flow rates, oxygen concentration, and mass loadings. The reported yields for the tests performed can be found in Table 8. The radiant heat apparatus, smoke chamber and controlled atmosphere cone calorimeter produced much lower CO yields than would be expected for under-ventilated flaming. The steady state tube furnace produced a CO yield that was closer to what would be expected for under-

ventilated conditions. The authors made this assertion based on the yield of average CO from post-flashover fires being 200 ± 9 mg g⁻¹. HCN analysis was performed using infrared (IR) spectroscopy using a short path-length gas cell, which is a questionable method for the quantification of HCN due to its poor IR absorption, high potential for interferences and a poor limit of detection. This resulted in the reported HCN yields for the under-ventilated conditions being lower than expected in all of the tests. Taking this into consideration, the steady state tube furnace and the controlled atmosphere cone calorimeter both produced the highest yields of HCN in under-ventilated conditions.

The authors acknowledged that further investigation of the steady state tube furnace was warranted as in some of the testing they suspected an instrumental error, since they were unable to account for roughly two-thirds of the total carbon from the sample and detected unusually low levels of CO₂ during the under-ventilated tests. While there were some problems, the data does show that the yields of toxicants from the polyurethane foam were generally most representative of post-flashover conditions in the test methods that were designed for ventilation controlled conditions, such as the steady state tube furnace and the controlled atmosphere cone calorimeter.

As polyurethane foams have very low thermal inertia, application of heat or a small flame can be enough to ignite them. In order to reduce the ignitability, and to a less extent the surface spread of flame and peak heat release rate, fire retardants are commonly added to commercial polyurethane foams in order to meet specific regulatory demands. A comprehensive review of fire retardants and their use in polyurethane foams was published by Singh and Jain (2009). The review refers to a publication by Babrauskas et al. (1991b) wherein polyurethane containing a phosphate fire retardant caused immediate death of all of the animals. Early work by Voorhees (1975) identified what they described as 'extreme toxicity' of the combustion products of a phosphate fire retarded polyurethane foam. Voorhees suggested that the compound was a bicyclic phosphate compound and noted grand mal seizures followed by death in rats with a loading as low as 4 % by weight of the fire retardant. Analysis of the compound, trimethylol propane phosphate (TMPP), by Kimmerle (1976) found it to have a

Table 7 Comparison of yields of CO and HCN for a series of tests (Babrauskas et al. 1991a)

Test method	Test conditions	CO Yield/mg g ⁻¹	HCN Yield/mg g ⁻¹
NBS Cup Furnace Method	550 °C	180–210	16–20
SwRI/NIST Method	50 kW m ⁻²	80–120	1.9–4.4
Cone Calorimeter Method	Range for 35–75 kW m ⁻²	42–80	4–5
Furniture Calorimeter	330 × 330 × 254 mm crib, 1.0 kg	80	N/a
Three-compartment Room Test	See description in text	100–140	5–11

Table 8 Yields of CO and HCN from a range of test methods (Marsh & Gann 2013)

Test type	Test variables			CO Yield/mg g ⁻¹	HCN Yield/mg g ⁻¹	
Radiant Furnace	Initial Oxygen %					
				28	<3.0	
Smoke Density Chamber	Irradiance/kW m ⁻²		Pilot			
			Unpiloted	19	3.4	
			Piloted	66	1.0	
			Piloted	43	6	
Steady State Tube Furnace	Temperature					
				26	<3.0	
Controlled Atmosphere Cone Calorimeter	Irradiance/kW m ⁻²		Air Flow/L s ⁻¹	Initial Oxygen %		
	50		25	21	27	3.7
				18	35	7.7
				16	44	12.5
	50	12.5		21	24	3.6
				16	35	9.6
				14	33	3.9
	25	25		21	24	-
18				29	-	
16				29	-	

high acute toxicity when tested on rats. The formation of the toxicant in question was the result of an unusual reaction of the polyol in the foam, trimethylol propane, with the phosphate fire retardant in the gas phase.

Paabo and Levin (1987) reviewed the literature of the toxic product generated by the combustion of rigid polyurethane foams. The review suggested that the addition of fire retardants did not appear increase the overall combustion toxicity of polyurethane foams. However, this did not take into consideration the incapacitating effects of the release of irritant gases. A more recent review, by Levchik and Weil (2004), assessed the decomposition, combustion and fire-retardancy of polyurethanes. The author acknowledged that there is a range of contradictory results available in the literature regarding their fire toxicity. It is likely that the fire toxicity of fire retarded polyurethane materials is largely dependent on the specific fire retardant present. For example, Levin and coworkers reported that melamine-treated flexible polyurethane foam generated 6 times more HCN than an equal amount of non-melamine treated foam. However, the presence of Cu₂O reduced the HCN generated by the flexible polyurethane foam by 70-90 % at low temperatures. The authors associated this with the effects of the Cu₂O catalytically oxidising the HCN into N₂, CO₂, H₂O and a small amount of nitrogen oxides.

Since then, Blais and Carpenter (2015) investigated a flexible polyurethane foam with and without a chloro phosphate (tris-dichloro-propyl phosphate TDCPP) fire retardant using a smoke box (ISO 5659-2 2012) to assess the toxicity. The authors asserted that fire retarding flexible polyurethane foam did not increase its acute or chronic toxicity when compared to non-fire retarded flexible foam. They also asserted that the toxicity of the fire retarded foam was less than or equal to wood on a mass/mass basis and that wood contributes significantly more to residential fires in terms of fire smoke toxicity. However, due to the poor reproducibility of smoke chamber experiments, the tendency for it to give very low HCN yields, and the fact that the experiment is well-ventilated, the reported toxicity is likely much lower than in a real fire situation. In a letter to the editor of the journal, Barbrauskas et al. (2015) questioned their methodology and noted that the authors did not address the release of HCl and its contribution to the acute fire toxicity of the fire retarded foam.

Historically, material-LC₅₀ data has been reported directly based on animal lethality testing, however due to the declining use of animal testing in fire toxicity assessment, calculations based on standard lethality data (such as ISO 13344 1996) are more commonly used. As the toxic product yields of polyurethane foams are directly related to the ventilation conditions, so is the materials

Table 9 Fire Toxicity of polyurethane foam and polyisocyanurate foam in a range of conditions, represented as a material-LC₅₀ (Stec & Hull 2011)

Material	Fire conditions	ϕ	Material-LC ₅₀ /g m ⁻³
Polyurethane Foam	Smouldering	-	337.2
	Well-ventilated	0.69	15.7
	Under-ventilated	1.24	10.3
	Under-ventilated	2.00	11.4
Polyisocyanurate Foam	Smouldering	-	498.4
	Well-ventilated	0.75	16.5
	Under-ventilated	1.34	10.7
	Under-ventilated	1.97	8.3

LC₅₀ value. Stec and Hull (2011) presented material-LC₅₀ data for rigid polyurethane foam and polyisocyanurate foam, calculated using rat lethality data from ISO 13344 (1996). A summary of these results can be found in Table 9. The overall toxicity of the polyisocyanurate foam shows a clear increase as the fire became more under-ventilated, while the rigid polyurethane foam showed a slight decrease at ϕ 1.24–2.00. This slight decrease is probably within the limits of experimental error, as it does not follow the general trend shown by most materials. Using the methodology in ISO 13344, the authors also calculated the fractional effective dose (FED) of the individual toxicants sampled. The FED is expressed as the sum of contributions to toxicity from individual species and normalised to 1 g of fuel in 200 L fire effluent, as used in BS 6853 (1999). The calculations showed that, for both the rigid polyurethane and the polyisocyanurate, hydrogen cyanide is the major toxicant in smouldering, well-ventilated and under-ventilated flaming. The authors acknowledged that they did not include isocyanates in their calculations.

Neviaser and Gann (2004) compiled the toxic potency data for a range of materials including a number of fire retarded and non-fire retarded polyurethane foams. The authors compiled toxicological data from a range of primary online databases and also requests were made to collect unpublished data that were not publically available. From this, the library of data was sorted into categories of combustion/pyrolysis conditions, material/product, type of test animal and toxicological endpoint. The authors noted that a large number of the data available relating to the test conditions were vague or completely undefined. In particular, reports that used non-standard tube furnace apparatus lacked sufficient information about the conditions of the experiment and as such were not included. The data was presented as material-LC₅₀ values for 30 min exposures with 14-day post-exposure of test animals and can be found in Tables 10, 11 and 12.

Table 10 LC₅₀ values for well-ventilated flaming combustion (Neviaser & Gann 2004)

Material	Reference	Material-LC ₅₀ (30 min + 14 day post)/g m ⁻³
Flexible Polyurethane Foam		
NFR FPU #12	Levin <i>et al</i> 1983a	40.0
FR FPU #11	Levin <i>et al</i> 1983a	40.0
No details provided	Babrauskas <i>et al</i> 1991b	52.0
Melamine type foam	Babrauskas <i>et al</i> 1991b	12.5
Melamine type foam with vinyl fabric	Babrauskas <i>et al</i> 1991b	26.0
FR FPU #14	Levin <i>et al</i> 1983a	27.8
FR foam- 22.3 kg m ⁻³	Braun <i>et al</i> 1990	26.0
FR GM-23	Farrar <i>et al</i> 1979	34.5
FR GM-27	Farrar <i>et al</i> 1979	33.1
NFR FPU #13	Levin <i>et al</i> 1986	40.0
NFR foam 22.3 kg/m ⁻³	Braun <i>et al</i> 1990	40.0
NFR GM-21	Levin <i>et al</i> 1983b	38.0
NFR GM-21	Levin <i>et al</i> 1983b	49.5
NFR GM-21	Levin <i>et al</i> 1983b	40.0
NFR GM-21	Farrar <i>et al</i> 1979	43.2
NFR GM-25	Farrar <i>et al</i> 1979	37.5
NFR Foam	Farrar & Galster 1980	43.2
NFR Upholstered Chairs with FPU, cover fabric and steel frame. Foam density: 25 kg m ⁻³	Barbrauskas <i>et al.</i> 1988	35.0
Rigid Polyurethane Foam		
NFR Foam, 25 mm thick, 96 kg m ⁻³	Babrauskas <i>et al</i> 1991a	11.0
FR GM-31	Farrar <i>et al</i> 1979	14.2
No details provided	Babrauskas <i>et al</i> 1991b	22.0
NFR GM-30	Levin <i>et al</i> 1983b	38.4
NFR GM-30	Levin <i>et al</i> 1983b	13.3
NFR GM-30	Levin <i>et al</i> 1983b	11.3
NFR isocyanurate, GM-41	Farrar <i>et al</i> 1979	11.4
NFR isocyanurate, GM-43	Farrar <i>et al</i> 1979	5.8
NFR GM-29	Farrar <i>et al</i> 1979	11.2
NFR GM-35	Farrar <i>et al</i> 1979	12.1
NFR GM-37	Farrar <i>et al</i> 1979	10.9
NFR GM-39, sprayed	Farrar <i>et al</i> 1979	16.6

During flaming combustion, many fire retarded flexible polyurethane foams showed similar or slightly higher toxic potency than the non-fire retarded foams in both well-ventilated and under-ventilated conditions. While limited data were available regarding the flaming combustion of rigid polyurethane foams, the results were of a similar scale to those presented by Stec and Hull (2011). While the data presented is a useful compilation of toxic potency data from the available literature before 2004, the report does not take into consideration the

Table 11 LC₅₀ values for under-ventilated flaming combustion (Neviasser & Gann 2004)

Material	Reference	Material-LC ₅₀ (30 min + 14 day post)/ g m ⁻³
Flexible polyurethane foam		
No details provided	Babrauskas et al. 1991b	18.0
FR upholstered chairs with FPUR padding, cover fabric and a steel frame	Barbrauskas et al. 1988	23.0
Melamine type foam	Babrauskas et al. 1991b	8.0
Melamine type foam with vinyl fabric	Babrauskas et al. 1991b	15.0
Melamine type foam with vinyl fabric	Babrauskas et al. 1991b	15.0
Rigid polyurethane foam		
No details provided	Babrauskas et al. 1991b	14.0

conclusions of individual authors, the exact specifics of the test condition, and the validity of the results. The data also does not specify the fire retardants used. Overall, the report provides access to a large pool of data organised into a material-LC₅₀ and also helps demonstrate that the large majority of data available is for well-ventilated tests.

Conclusions

The non-flaming decomposition of polyurethanes in air or nitrogen can be summarised effectively using a generalised mechanism based on the available literature (Fig. 9). The mechanisms of decomposition are well understood and the decomposition products of both rigid and flexible polyurethane foams are very similar at high temperatures. At lower temperatures, decomposition differs, depending on the composition and physical properties of the polymer, although clear trends can be identified. A detailed understanding of the thermal decomposition chemistry of polyurethane foams is necessary in order to relate the toxicants generated during both flaming and non-flaming combustion of the polymer to its structure.

CO and HCN are the main asphyxiants produced during the combustion of polyurethanes and there have been a large number of studies published regarding their yields. Isocyanates should be considered when assessing the fire toxicity of polyurethane foams, due to their acute irritating effects and chronic effects associated with exposure. However, there is very little literature available regarding the yields of isocyanates produced by the combustion of polyurethane foams.

Table 12 LC₅₀ values for oxidative pyrolysis (Neviasser & Gann 2004)

Material	Reference	Material-LC ₅₀ (30 min + 14 day post)/ g m ⁻³
Flexible polyurethane foam		
NFR FPU #12	Levin et al 1983a	37.8
NFR FPU #13	Levin et al 1986	37.0
NFR Foam: 22.3 kg m ⁻³	Braun et al 1990	33.0
NFR GM-21	Levin et al 1983b	27.8
NFR GM-21	Levin et al 1983b	40.0
NFR GM-21	Levin et al 1983b	26.6
FR FPU #11	Levin et al 1983a	17.2
FR FPU #14	Levin et al 1983a	40.0
FR Foam: 22.3 kg m ⁻³	Braun et al 1990	23.0
FR GM-23	Farrar et al 1979	12.6
FR GM-27	Farrar et al 1979	30.5
NFR GM-21	Farrar et al 1979	13.4
NFR GM-25	Farrar et al 1979	36.9
NFR Foam	Farrar & Galster 1980	14.3
NFR GM-21: 2 PCF	Anderson et al 1983	34.7
Rigid polyurethane foam		
NFR GM-30	Levin et al 1983b	34.0
NFR GM-30	Levin et al 1983b	39.6
NFR GM-30	Levin et al 1983b	35.1
FR GM-31	Farrar et al 1979	40.0
NFR Isocyanurate; GM-41	Farrar et al 1979	8.0
NFR isocyanurate; GM-43	Farrar et al 1979	5.0
NFR GM-29	Farrar et al 1979	40.0
NFR GM-35	Farrar et al 1979	36.7
NFR GM-37	Farrar et al 1979	36.7
NFR GM-39; sprayed	Farrar et al 1979	10.9

During flaming combustion of polyurethane foams, the yield of toxicants can be directly related to the fuel/air ratio, expressed as an equivalence ratio (ϕ). This results in relatively high yields of CO and HCN during under-ventilated flaming and relatively low yields during well-ventilated flaming. Test methods, such as the steady state tube furnace (ISO/TS 19700) and the controlled atmosphere cone calorimeter (ASTM E 1354), facilitate ventilated controlled conditions which give yields of CO and HCN comparable to those observed in under-ventilated post-flashover compartment fires. The average CO yield expected from under-ventilated flaming is ~200 mg g⁻¹ for polyurethane materials.

HCN, in particular, contributes significantly to the overall fire toxicity of polyurethane foams. Around 10–15 % of the nitrogen in the polymer can be converted

into HCN with some being released in isocyanates, aminoisocyanates and amines in the fire effluent. Additionally, HCN yields in both flaming and non-flaming conditions increases with temperature. This can be explained by the fragmentation of nitrogen containing organics in the flame and in the effluent, as suggested by studies of the inert-atmosphere decomposition of polyurethane materials. HCN yields reported in under-ventilated conditions vary depending on the composition of the material; with flexible foams producing less than rigid foams and polyisocyanurates producing the most overall.

The overall toxicity of polyurethane materials followed a similar trend to their HCN yields; with flexible foams generally being the least toxic, rigid foams being slightly more toxic and polyisocyanurate foams being the most toxic.

There is some contradiction the literature as to the effect fire retardants have on the overall toxicity of polyurethane foams. A large majority of the literature indicates that the addition of fire retardants does not increase toxicity of polyurethane foams. This is due to the large range of available fire retardants found in polyurethane foams, which suggests that the toxicity will likely follow the general trends in the literature for all materials regarding fire retardants. Fire retardants, such as gas-phase free radical quenchers, have been reported to increase the yields of CO in well-ventilated conditions by preventing the oxidation of CO to CO₂. Other fire retardants such as melamine are reported to significantly increase the HCN yield of polyurethane foams. The presence of Cu₂O drastically decreased the yield of HCN in polyurethane foams at lower temperatures, but had little effect at high temperatures.

As the global usage of polyurethane foams is expected to continue to increase yearly, it is important that the fire community have a clear understanding of the fire toxicity of polyurethane foams and the reasons why they produce significant amounts of toxic gases during combustion. Since HCN is a major contributor to the fire toxicity of polyurethane foams, the mechanisms by which they decompose are vital in understanding why they produce large-quantities of HCN during under-ventilated burning.

Abbreviations

2,4-TDI: 2,4-Toluene diisocyanate; 2,6-TDI: 2,6-Toluene diisocyanate; ASET: available safe escape time; CACC: controlled atmosphere cone calorimeter; CMHR-PUF: combustion modified high resilience polyurethane foam; COHb: carboxyhaemoglobin; DAT: diaminotoluene; FED: fractional effective dose; FPA: fire propagation apparatus; HDI: hexamethylene diisocyanate; IPDI: isophorone diisocyanate; MDI: methylene diphenyl diisocyanate; NDI: 1,5-naphthalene diisocyanate; PAHs: polycyclic aromatic hydrocarbons; PIR: polyisocyanurate; PPM: parts per million; RSET: required safe escape time; SDC: smoke density chamber; TGA: thermogravimetric analysis; TMPP: trimethylol propane phosphate.

Competing interests

The authors declare that they have no competing interests.

Authors' contributions

STM wrote the manuscript and produced all of the images used in figures. TRH wrote the fire toxicity section of the manuscript. Both authors read and approved the manuscript.

Acknowledgements

The authors would like to thank Dr. Linda Bengtstrom for her contribution regarding the toxicity of isocyanates.

Funding

STM would like to acknowledge the University of Central Lancashire for provision of a studentship.

Received: 3 February 2016 Accepted: 31 March 2016

Published online: 21 April 2016

References

- Alarie Y (2002) Toxicity of Fire Smoke. *Critical Reviews in Toxicology* 32(4):259
- Allan D, Daly J, Liggat JJ (2013) Thermal volatilisation analysis of TDI-based flexible polyurethane foam. *Polymer Degradation and Stability* 98:535–541
- Anderson RA, Watson AA, Harland WA (1981) Fire Deaths in the Glasgow Area: I General Considerations and Pathology. *Med Sci Law* 21:60
- Anderson RC, Croce PA, Feeley FG, Sakura JD (1983) Study to assess the feasibility of incorporating combustion toxicity requirements into building materials and furnishing codes of New York State: Final report, vol I, II, III, Arthur D. Little, Inc. Report, Reference 88712, May 1983.
- Andersson B, Markert F, Holmstedt G (2005) Combustion products generated by hetero-organic fuels on four different fire test scales. *Fire Safety Journal* 40:439–465
- Aneja A (2002) Chapter 2, Structure–property Relationships of Flexible Polyurethane Foams, PhD. thesis, Virginia Tech, p6-40
- ASTM E 1354 Standard Test Method for Heat and Visible Smoke Release Rates for Materials and Products Using an Oxygen Consumption Calorimeter
- ASTM E 662 Standard Test Method for Specific Optical Density of Smoke Generated by Solid Materials
- Avar G, Meier WU, Casselmann H, Achten D (2012) *Polymer Science: A Comprehensive Reference*, Polymer Science: A Comprehensive Reference, 10, p411–441.
- Babrauskas V, Lawson JR, Walton WD, Twilley WH (1982) Upholstered Furniture Heat Release Rates Measured with a Furniture Calorimeter. NBSIR 82–2604. National Bureau of Standards, Washington D.C.
- Babrauskas V, Harris RH, Braun E, Levin BC, Paabo M, Gann RG (1991a) The role of bench-scale test data in assessing real-scale fire toxicity. Technical Note 1284, National Bureau of Standards and Technology, Gaithersburg MD
- Babrauskas V, Levin BC, Gann R, Paabo M, Harris RH, Peacock RD, Yusa S (1991b) Toxic potency measurement for fire hazard analysis, special publication 827, National Institute of Standards and Technology. Gaithersburg, MD
- Babrauskas V, Twilley WH, Janssens M, Yusa S (1992) Cone calorimeter for controlled-atmosphere studies. *Fire and Materials* 16:p37–43
- Barbrauskas V, Harris RH, Gann RG, Levin BC, Lee BT, Peakcock RD, Paabo M, Twilley W, Yoklavich MF, Clark HM (1988) Fire hazard comparison of fire-retarded and non-fire-retarded products, Special Publication 749. National Bureau of Standards, Gaithersburg MD
- Barbrauskas V, Singla V, Lucas D, Rich D (2015) Letter to the Editor- Questions about the conclusions in Blais and Carpenter 2013. *Fire Technology* 51:p213–217
- Blais M, Carpenter K (2015) Flexible Polyurethane Foams: A comparative measurement of toxic vapors and other toxic emissions in controlled combustion environments of foams with and without fire retardants. *Fire Technology* 51:p3–18
- Blomqvist P, Lonnermark A (2001) Characterization of the combustion products in large-scale fire tests: comparison of three experimental configurations. *Fire and Materials* 25:p71–81
- Blomqvist P, Hertzberg T, Tuovinen H, Arrhenius K, Rosell L (2007) Detailed determination of smoke gas contents using a small-scale controlled equivalence ratio tube furnace method. *Fire and Materials* 31:p495–521
- Bott B, Firth JG, Jones TA (1969) Evolution of toxic gases from heated plastics. *Brit Polym J* 1:p203–204
- Braun E, Gann RG, Levin BC, Paabo M (1990) Combustion product toxic potency measurements: comparison of a small scale test and “real-world” fires. *Journal of Fire Sciences* 8:p63–79

- BS 6853 (1999) Code of practise for fire precautions in the design and construction of passenger carrying trains
- Busker RW, Hammer AH, Kuijpers WC, Poot CAJ, Bergers WWA, Bruijnzeel, PLB (1999) Toxicity testing of combustion products of polyurethane and polyvinylchloride. TNO Report. PML 1998-A97. TNO Prins Maurits Laboratory, The Netherlands. p 1-30.
- CEN/TS 45545-2 (2009) Railway applications - Fire protection on railway vehicles – Part 2: Requirements for fire behaviour of materials and components
- Chambers J, Jiricny J, Reese CB (1981) The Thermal Decomposition of Polyurethanes and Polyisocyanurates. *Fire and Materials* 5(4):p133–141
- Christy M, Petrella R, Penkala J (1995) Controlled-atmosphere cone calorimeter. *Fire and Polymers II: Materials and Tests for Hazard Prevention* 599:p498–517
- Chun BH, Li X, Im EJ, Lee KH, Kim SH (2007) Comparison of Pyrolysis Kinetics between Rigid and Flexible Polyurethanes. *J Ind Eng Chem* 13(7):p1188–1194
- EN 2826. (2011) Aerospace series - Burning behaviour of non-metallic materials under the influence of radiating heat and flames - Determination of gas components in the smoke; ABD 0031 Fire-Smoke-Toxicity (FST) Test Specification (Airbus Industries); Boeing BSS 7239, Test method for toxic gas generation by materials on combustion.
- Farrar DG, Galster WA (1980) Biological end-points for the assessment of the toxicity of products of combustion of material. *Journal of Fire and Materials* 4:p50–58
- Farrar DG, Hartzell GE, Blank TL, Galster WA (1979) Development of a protocol for the assessment of the toxicity of combustion products resulting from the burning of cellular plastics, University of Utah Report, UTEC 79/130; RP-75-2-1 Renewal, RP-77-U-5. City, Salt Lake
- UK Fire Statistics 2013 (and preceding years) – United Kingdom
- Fire Test Procedure Code (2010) Maritime Safety Committee, (MSC 87/26/Add.3) Annex 34, Part 2 Smoke and Toxicity Test. International Maritime Organisation, London
- Garrido MA, Font R (2015) Pyrolysis and combustion study of flexible polyurethane foam. *Journal of Analytical and Applied pyrolysis* 113:p202–215
- Gharehbagh A, Ahmadi Z (2012) Chapter 6: Polyurethane Flexible Foam Fire Behaviour, *Polyurethane*. In: Fahima Z, Eram S (eds), InTech. p 102-120. ISBN 978-953-51-0726-2
- Gottuk DT, Lattimer BY (2002) SFPE Handbook of Fire Protection Engineering, 3rd ed. (P.J. DiNenno et al., eds). National Fire Protection Association, Quincy, MA, pp 54–82
- Guo X, Wang L, Zhanga L, Lia S, Hao J (2014) Nitrogenous emissions from the catalytic pyrolysis of waste rigid polyurethane foam. *Journal of Analytical and Applied pyrolysis* 108:p143–150
- Hartzell G (1993) Overview of Combustion Toxicology. *Toxicology* 115:7
- Henneken H, Vogel M, Karst U (2007) Determination of airborne isocyanates. *Anal Bioanal Chem* 387:p219–236
- Herrington R, Hock K (1998) Flexible Polyurethane Foams, 2nd edn. Chem Co., Dow
- Hertzberg T, Blomqvist P, Dalene M, Skarping G (2003) Particles and Isocyanates from Fires. SP Swedish National Testing and Research Institute, Borås
- Hietaniemi J, Kallonen R, Mikkola E (1999) Burning characteristics of selected substances: Production of heat, smoke and chemical species. *Fire and Materials* 23:p171–185
- Hull TR, Paul KT (2007) Bench-scale assessment of combustion toxicity-A critical analysis of current protocols. *Fire Safety Journal* 42:p340–365
- ISO 12136 (2011) Reaction to fire tests – Measurement of material properties using a fire propagation apparatus
- ISO 13344 (1996) Estimation of lethal toxic potency of fire effluents
- ISO 13571 (2012) Life-threatening components of fire-Guidelines for the estimation of time available for escape using fire data
- ISO/TS 19700 (2013) Controlled equivalence ratio method for the determination of hazardous components of fire effluents – the steady state tube furnace.
- ISO 19706 (2011) Guidelines for assessing the fire threat to people.
- ISO 5659-2 (2012) Plastics - Smoke generation - Part 2: Determination of optical density by a single-chamber test
- ISO 5660-1 (2002) Fire tests – Reaction to fire – Part 1: Rate of heat release from building products (cone calorimeter method)
- ISO 9705 (1993) Fire tests – Full-scale room tests for surface products
- Kaplan HL (1987b) Effects of irritant gases on avoidance/escape performance and respiratory response of the baboon. *Toxicology* 47:165–170
- Kaplan HL, Grand AF, Hartzell GE (1984a) Toxicity and the smoke problem. *Fire Safety Journal* 7:p11
- Kavanagh BP, Pearl RG (1995) Inhaled nitric oxide in anesthesia and critical care medicine. *Int Anesthesiol Clin* 33:181
- Kimmerle G (1976) Toxicity of Combustion Products with Particular Reference to Polyurethane. *Ann occup Hyg* 19:269–273
- Levchik SV, Weil ED (2004) Thermal Decomposition, combustion and fire-retardancy of polyurethanes - a review of the recent literature. *Polymer International* 53:p1585–1610
- Levin BC, Fowell AJ, Birky MM, Paabo M, Stolte A, Malek D (1982) Further development of a test method for the assessment of the acute inhalation toxicity of combustion products. NBSIR 82–2532. National Bureau of Standards, Washington D.C.
- Levin BC, Paabo M, Fultz ML, Bailey C, Yin W, Harris SE (1983a) Acute inhalation toxicological evaluation of combustion products from fire-retarded and non-fire retarded flexible polyurethane foam and polyester. NBSIR 83–2719. National Bureau of Standards, Gaithersburg, MD
- Levin BC, Paabo M, Birky MM (1983b) Interlaboratory evaluation of the 1980 version of the national bureau of standards test method for assessing the acute inhalation toxicity of combustion products, NBSIR 83–2678, National Bureau of Standards, Gaithersburg, MD
- Levin BC, Paabo M, Fultz ML, Bailey CS (1985) Generation of Hydrogen Cyanide from Flexible Polyurethane Foam Decomposed under Different Combustion Conditions. *Fire and Materials* 9:p125–134
- Levin BC, Paabo M, Bailey CS, Harris SE (1986) Toxicity of the combustion products from a flexible polyurethane foam and a polyester fabric evaluated separately and together by the NBS Toxicity Test Method. *Fire Safety Science - Proceedings of the First International Symposium*, p1111-1122
- Markets and Markets report (2011) Methylene Diphenyl Diisocyanate (MDI), Toluene Diisocyanate (TDI) and Polyurethane Market (2011 – 2016); Markets and Markets CH 1596, July 2011
- Marsh ND, Gann RG (2013) Smoke Component Yields from Bench-Scale Fire Tests: 4. Comparison with Room Fire Results, NIST Technical Note 1763, National Institute of Standards and Technology, Gaithersburg, MD
- Michal J (1982) Determination of Hydrogen Cyanide in Thermal Degradation Products of Polymeric Materials. *Fire and Materials* 6:p13–15
- Neviaser JL, Gann RG (2004) Evaluation of Toxic Potency values for Smoke from Products and Materials. *Fire Technology* 40:p117–199
- NFPA 269 (2012) Standard test method for developing toxic potency data for use in fire hazard modelling
- NFX 70 100-1:2006 Fire Tests - Analysis Of Gaseous Effluents - Part 1: Methods For Analysing Gases Stemming From Thermal Degradation
- NIOSH (1989) A summary of health hazard evaluations: Isocyanates, 1989 to 2002
- Paabo M, Levin BC (1987) A review of the literature on the gaseous products and toxicity generated from the pyrolysis and combustion of rigid polyurethane foams. *Fire and Materials* 11:p1–29
- Paul KT, Hull TR, Lebek K, Stec AA (2008) Fire smoke toxicity: The effect of nitrogen oxides. *Fire Safety Journal* 43:243–251
- Piirilä PL, Meuronen A, Majuri ML, Luukkonen R, Mäntylä T, Wolff HJ (2008) Inflammation and functional outcome in diisocyanate-induced asthma after cessation of exposure. *Allergy* 63:p583–591
- Pitts WM (1995) The global equivalence ratio concept and the formation mechanisms of carbon monoxide in enclosure fires. *Prog Energy Combust Sci* 21:197–237
- Purser DA (2002) Toxicity Assessment of Combustion Products, The SFPE Handbook of Fire Protection Engineering 3rd Edition, Edited by DiNenno, P.J. National Fire Protection Association, Quincy, pp 2–83
- Purser DA (2007) The application of exposure concentration and dose to evaluation of effects of irritants as components of fire hazard. *Interflam Conference Proceedings*. Interscience Publications, London
- Purser DA (2008b) Chapter 2: SFPE Handbook of Fire Protection Engineering (Ed. P.J. DiNenno) Fourth Edition. National Fire Protection Association, Quincy MA, USA, pp 2–96
- Purser DA, Purser JA (2008a) HCN yields and fate of fuel nitrogen for materials under different combustion conditions in the ISO 19700 tube furnace. *Fire Safety Science - Proceedings of the ninth international symposium*. p 1117–1128. International Association for Fire Safety Science
- Ravey M, Pearce EM (1997) Flexible Polyurethane foam. I. Thermal Decomposition of Polyether-based, Water-blown Commercial type of Flexible Polyurethane Foam. *Journal of Applied Polymer Science* 63:p47–74
- Rein G, Lautenberger C, Fernandez-Pell AC (2006) Application of Genetic Algorithms and Thermogravimetry to Determine the Kinetics of Polyurethane Foam in Smoldering Combustion. *Combustion and Flame* 146(1–2):p95–108
- Rogaume T, Bustamante-Valencia L, Guillaume E, Richard F, Luche J, Rein G, Torero JL (2011) Development of the Thermal Decomposition Mechanism of

- Polyether Polyurethane Foam Using Both Condensed and Gas-Phase Release Data. *Combustion Science and Technology* 183(7):p627–644
- Saunders JH (1959) the Reactions of Isocyanates and Isocyanate Derivatives at Elevated Temperatures. *Rubber Chemistry and Technology* 32(2):p337–345
- Schartel B, Hull TR (2007) Development of fire-retarded materials - Interpretation of cone calorimeter data. *Fire and Materials* 31:p327–354
- Schnipper L, Smith-Hansen ES (1995) Reduced combustion efficiency of chlorinated compounds, resulting in higher yields of carbon monoxide. *Fire and Materials* 19:p61–64
- Shufen L, Zhi J, Kaijun Y, Shuqin Y, Chow WK (2006) Studies on the Thermal Behavior of Polyurethanes. *Polymer-Plastics Technology and Engineering* 45:p95–108
- Singh H, Jain AK (2009) Ignition, Combustion, Toxicity, and Fire Retardancy of Polyurethane Foams: A Comprehensive Review. *Journal of Applied Polymer Science* 111:p1115–1143
- Stec AA, Hull TR (2011) Assessment of the fire toxicity of building insulation materials. *Energy and Buildings* 43:p498–506
- Stec AA, Hull TR (2014) Fire Toxicity Assessment: Comparison of Asphyxiant Yields from Laboratory and Large Scale Flaming Fires. *Fire Safety Science* 11:p404–418
- Stec AA, Hull TR, Lebek K (2008) Characterisation of the steady state tube furnace (ISO TS 19700) for fire toxicity assessment. *Polymer Degradation and Stability* 93:p2058–2065
- Tewarson A (2002) SFPE Handbook of Fire Protection Engineering, 3rd ed. P.J. DiNenno et al. eds. National Fire Protection Association, 82, p 161
- Vilar WD (2002) Chemistry and Technology of Polyurethanes - Chapter 1. Vilar Consultoria Técnica Ltda, Rio de Janeiro
- Voorhees J (1975) Extreme Toxicity from Combustion Products of Fire-Retarded Polyurethane Foam. *Science* 187:p742–744
- Wisniewski AV, Lemus R, Karol MH, Redlich CA (1999) Isocyanate-conjugated human lung epithelial cell proteins: A link between exposure and asthma? *J Allergy Clin Immunol* 104:p341–347
- Woolley WD, Fardell PJ (1977) The prediction of combustion products. *Fire Res* 1:p11–21
- Woolley WD, Fardell PJ, Buckland IG (1975) The Thermal Decomposition Products of Rigid Polyurethane. Foams Under Laboratory Conditions, *Fire Research Note*, No 1039.
- Woolley WD, Wadley AI, Field P (1972) Studies of the thermal decomposition of flexible polyurethane foams in air. *Fire Research Notes* 951:p1–17

Flame Retardants in UK Furniture Increase Smoke Toxicity More than they Reduce Fire Growth Rate

Published in Chemosphere in 2017. Full Citation: McKenna ST et al (2018) Flame retardants in UK furniture increase smoke toxicity more than they reduce fire growth rate, Chemosphere, 196, p429-439

Flame retardants in UK furniture increase smoke toxicity more than they reduce fire growth rate

Sean McKenna¹, Robert Birtles^{1,2}, Kathryn Dickens¹, Richard Walker^{1,3}, Michael Spearpoint^{4,5}, Anna A Stec¹ and T Richard Hull^{1*}.

1. Centre for Fire and Hazard Science, University of Central Lancashire, Preston, PR1 2HE, UK
2. Greater Manchester Fire and Rescue Service, Manchester, M4 5HU, UK
3. West Midlands Fire Service Headquarters, 99 Vauxhall Road, Birmingham B7 4HW, UK
4. Department of Civil and Natural Resources Engineering, University of Canterbury, Christchurch 8140, New Zealand
5. Olsson Fire and Risk, Manchester, M4 6WX, UK

*Corresponding author: trhull@uclan.ac.uk

Abstract

This paper uses fire statistics to show the importance of fire toxicity on fire deaths and injuries, and the importance of upholstered furniture and bedding on fatalities from unwanted fires. The aim was to compare the fire hazards (fire growth and smoke toxicity) using different upholstery materials. Four compositions of sofa-bed were compared: three meeting UK Furniture Flammability Regulations (FFR), and one using materials without flame retardants intended for the mainland European market. Two of the UK sofa-beds relied on chemical flame retardants to meet the FFR, the third used natural materials and a technical weave in order to pass the test. Each composition was tested in the bench-scale cone calorimeter (ISO 5660) and burnt as a whole sofa-bed in a sofa configuration in a 3.4×2.25×2.4m³ test room. All of the sofas were ignited with a No. 7 wood crib; the temperatures and yields of toxic products are reported. The sofa-beds containing flame retardants burnt somewhat more slowly than the non-flame retarded EU sofa-bed, but in doing so produced significantly greater quantities of the main fire toxicants, carbon monoxide and hydrogen cyanide. Assessment of the effluents' potential to incapacitate and kill is provided showing the two UK flame retardant sofa-beds to be the most dangerous, followed by the sofa-bed made with European materials. The UK sofa-bed made only from natural materials (Cottonsafe®) burnt very slowly and produced very low concentrations of toxic gases. Including fire toxicity in the FFR would reduce the chemical flame retardants and improve fire safety.

Introduction

Fire statistics

Fire deaths in the UK showed a dramatic increase from 1955 until the mid-1980s (Figure 1)¹. It has been generally accepted that the extra deaths resulted from the increased flammability and smoke toxicity of synthetic polymers, which became widely available in the 1970s and 1980s, particularly in domestic furnishings. The greatest change over this period was the replacement of natural materials, such as horsehair and cotton, with flexible polyurethane foam (PUF) as fillings in upholstered furniture. This change resulted in: increased ignitability and fire growth (PUF is a better insulator than cotton or horsehair, so a smaller heat source will cause ignition and the fire will grow quickly because less heat is lost); more dense smoke impeding escape (from the aromatic structures in PUF); and greater smoke toxicity (the burning PUF produces large quantities of the two asphyxiants, carbon monoxide (CO) and hydrogen cyanide (HCN))^{2,3}. In the UK, the Furniture and Furnishings (Fire) (Safety) Regulations were introduced in 1988 requiring all domestic upholstered furniture to meet requirements for lower flammability, specified in BS 5852⁴ (as modified by the Schedules to the Regulations), and making it illegal to sell non-compliant furniture, new or second-hand. The fabric covering domestic upholstered furniture must pass the cigarette and match ignition tests. Foam and composite fillings must also be resistant to ignition from the “No. 5 wood crib” specified in BS 5852 (as modified).

The UK is currently consulting on a revision to the furniture flammability regulations, for a number of reasons, which include:

- The current test methods have been in place for nearly 30 years, during which time manufacturing materials and processes have radically changed. Furniture manufacturers have optimised their fabrics and fillings to pass the test, with less regard as to how the finished furniture may behave when on fire. For example, modern furniture often incorporates a non-woven polyester “comfort layer” between the fabric and foam, but this makes the fabric more vulnerable to ignition in the actual furniture than in the test.
- The test protocol requires fabrics to be tested on non-compliant foam without flame retardants, as found in furniture before the Regulations were implemented. Components identified in the 1980s need to be tested, but modern furniture may also contain a polyester comfort layer (as above), along with flammable materials such as cardboard, elastic, hessian, thermoplastics etc., which are not included in the current test, but contribute to the burning behaviour of the furniture.

Both the existing and proposed requirements can be met by using less flammable materials, or by the incorporation of flame retardants. Flame retardants offered the most cost effective solution, and allowed manufacturers more flexibility in choice of materials and design. In a report commissioned by the flame retardant industry⁵, and a subsequent report for the UK government⁶, it was argued that “*the introduction of fire-safe furniture [in the UK] from 1988 onwards is estimated to have resulted in at least 50% of the estimated 2002 savings in injuries and domestic fire deaths*”, the other 50% being attributed to low cost smoke detectors. Factors such as changes in cigarette smoking habits, the change from exposed flame heating sources and a general improvement in standard of living were not considered⁷.

New Zealand is a country comparable to the UK in many ways, but where there is no requirement for domestic furniture to be below particular flammability limits. New Zealand's fire death rate shown alongside the UK's in Figure 1⁸. It is evident that despite the greater statistical fluctuations from New Zealand's smaller population, the decrease in fire death rate is comparable to that in the UK. A detailed study produced for the European Commission⁹ on the risks and benefits of adding fire retardants to furniture, analysed the fire fatality data from individual European countries with different levels of flammability regulation. While the study acknowledged the difficulty in comparing statistics from different countries, it concluded that *"in some instances, drops in the number of fire deaths coincide with the introduction of non-flammability requirements for domestic consumer products. In other instances, however, there is no change in the on-going trend of fire deaths. This suggests that these numbers do not reflect the stringency of non-flammability requirements, respectively that non-flammability requirements do not visibly decrease the number of fire deaths."*

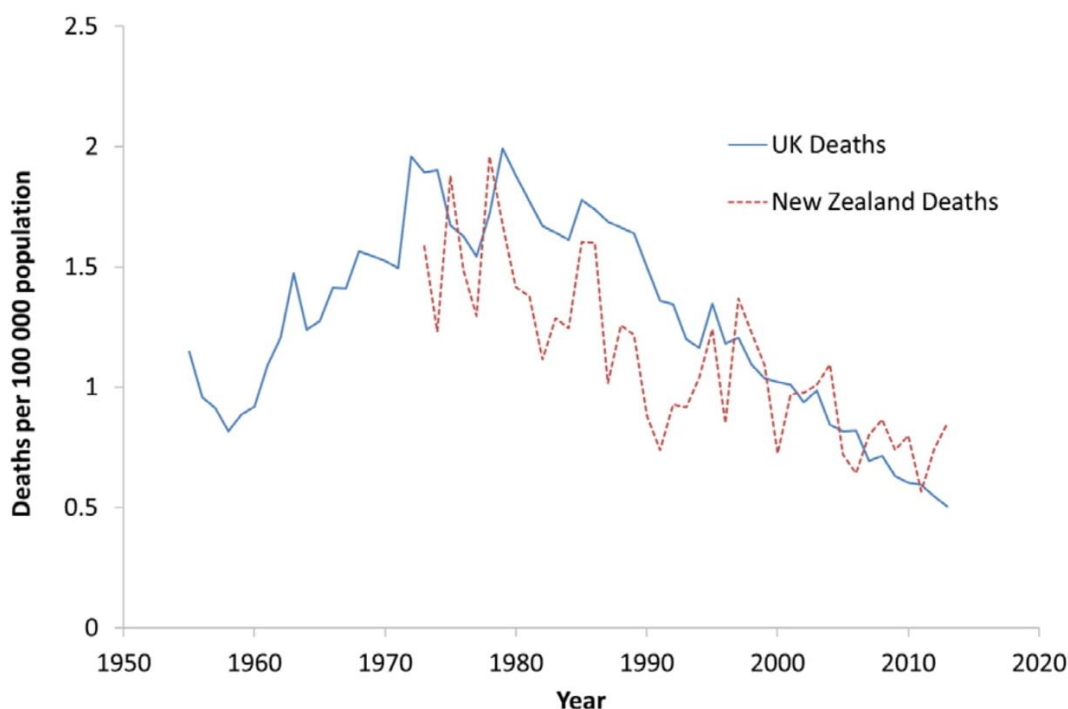


Figure 1 Fire deaths per 100 000 population in UK¹ (with furniture flammability regulations) and in New Zealand⁸ (where there are no domestic furniture flammability regulations).

Further analysis of the UK fire statistics for the period 2009-2014 shows that 77 % of fire fatalities occur in dwellings¹⁰. These have been broken down by location within the dwelling in Table 1. Although only 12.6 % of fires occur in bedrooms, living rooms and dining rooms, these account for 71.2 % of the fatalities, with a much higher fatality rate. Since most upholstered furniture is located in these rooms, this underlines its importance in fire fatalities (although in fatal fires, which are usually fully developed, reliable identification of the first item ignited is often impossible). The time series data from 1955 to 2013 (Figure 2 and Figure 3) show an increasing proportion of fire deaths resulting from inhalation of toxic smoke^{1,2}. Indeed, since 1998 the majority of fire deaths, and since 1991, the majority of fire injuries have resulted from the inhalation of toxic smoke. Explaining these increases is one of the goals of the current study.

Table 1 Proportion of dwelling fires, fire fatalities and fatality rate for UK fires from 2009-2014¹

Location within dwelling	No. of fires %	Fatalities %	Fatality rate per 1000 fire
Kitchen	42.7	18.0	1.9
Bed/living/dining room	12.6	71.2	25.2
Other	44.7	10.8	1.1

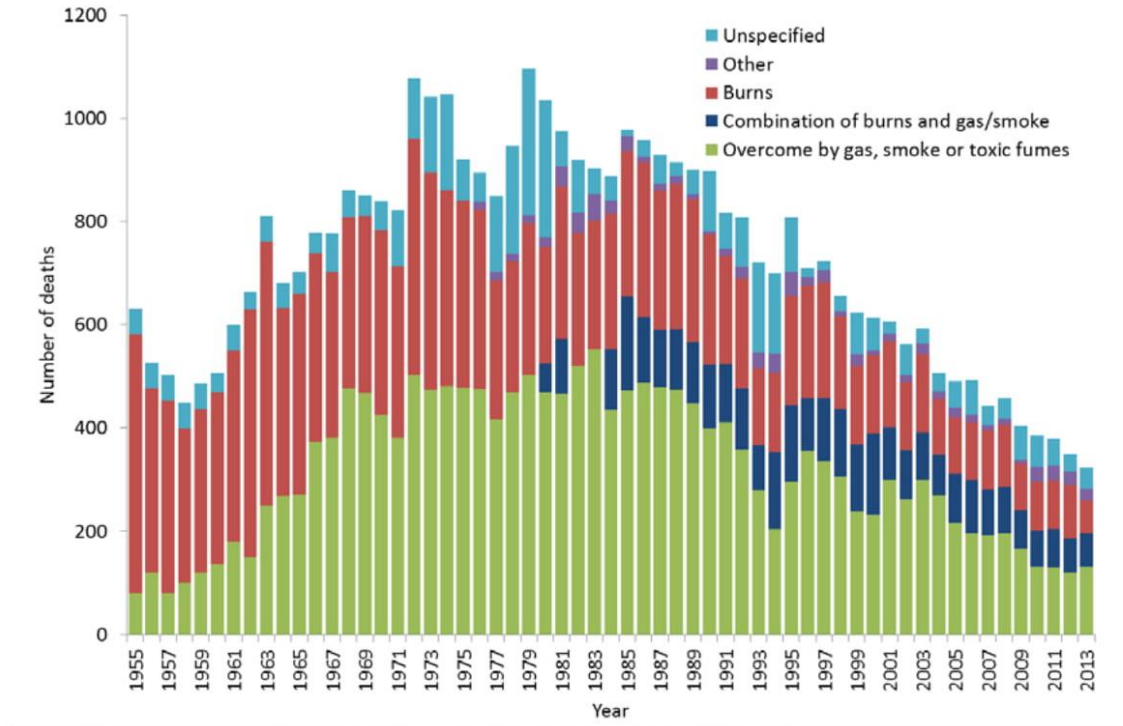


Figure 2 Causes of UK fire deaths from 1955 to 2013 (data taken from refs 1 and 2).

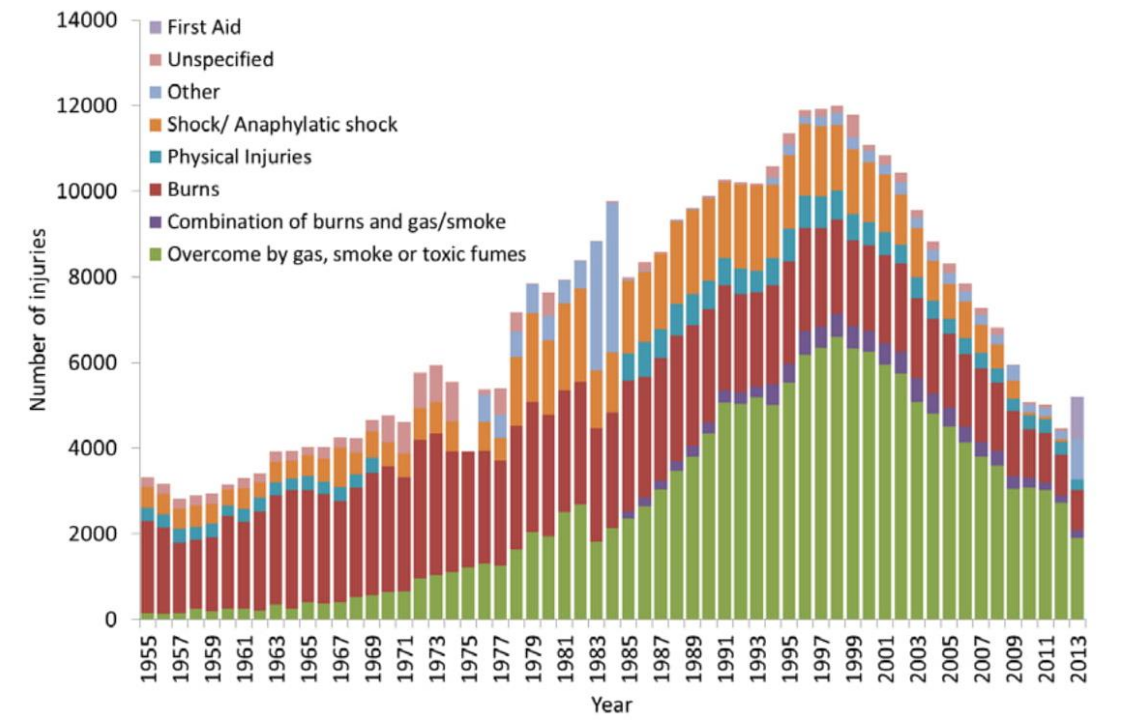


Figure 3 Nature of UK fire injuries from 1955 to 2013 (data taken from refs 1 and 2).

Despite being recognised as a major cause of death, and a major cause of injury, there has never been a requirement to assess the toxicity of burning furniture in the UK, outside the mass transport industries. It has been argued that while escape is possible from a house or apartment, it is unreasonable to expect escape from a burning train, ship or aeroplane. This clearly has implications for those unable to escape: for example through disability, or living in high-rise apartments. It has also been argued that if ignition could be prevented, that would avoid the more costly process of quantifying fire toxicity. The fact that upholstered furniture fires still cause most UK fire deaths shows that the furniture flammability regulations are not effective in eliminating these deaths^{1, 10, 2}.

A large number of studies^{11, 12, 13, 14, 15, 16, 17} have pointed to the toxic and ecotoxic effects of flame retardants, which have been reviewed elsewhere¹⁸. Moreover, the UK has been shown to have the highest levels of flame retardants in household dust, presumably originating from the treatments applied to upholstered furniture^{19, 20}. This paper contributes to the assessment of the benefits and risks of flame retardant usage by including the effects of flame retardants on the smoke toxicity so that a scientifically derived balance can be achieved.

Toxic Potency of Fire Effluent

When the higher fire toxicity of synthetic polymers, and the upholstered furniture made from them, first became apparent in the 1970s, this was investigated by exposing laboratory animals to fire effluents. This led to detailed correlations relating the toxicant concentrations to lethality or incapacitation, generally using additive models to predict the effect of multiple toxicants on animal subjects, which could then be extrapolated to humans^{21, 22}.

Death or incapacitation may be predicted by quantifying the fire effluents using chemical analysis in different fire conditions. Lethality may be predicted using equations, based on rat lethality data, from ISO 13344²³. Incapacitation (the inability to effect one's own escape) may be predicted using methodology and consensus estimate data in ISO 13571²⁴.

The effect of a fire effluent can be expressed as a Fractional Effective Dose (FED), based on its chemical composition. An FED equal to one indicates that the effluent will be effective in causing incapacitation or death to 50% of the exposed population. For incapacitation, ISO 13571 considers the four major hazards which may prevent escape (asphyxiant gases, irritant gases, heat and visible smoke obscuration). It includes a separate calculation for prediction of incapacitation by each of the four hazards for humans exposed to fire effluents. Equation 12 allows estimation of when the asphyxiants CO and HCN will cause incapacitation.

$$FED = \sum_{t_1}^{t_2} \frac{[CO]}{35000} \Delta t + \sum_{t_1}^{t_2} \frac{[HCN]^{2.36}}{1.2 \times 10^6} \Delta t$$

Gas concentrations in [] are expressed in $\mu\text{L L}^{-1}$ or ppm; time, t, is in min.

Equation 1²⁴

For lethality, this can be calculated using Equation 21 for a 30 minute exposure, using the ratio of each toxicant concentration to its lethal concentration (LC_{50}). Since carbon dioxide (CO_2) increases the respiration rate, Equation 1 uses a multiplication factor for CO_2 -driven hyperventilation, V_{CO_2} , to

increase the FED contribution from all the toxic species, and incorporates an acidosis factor, A, to account for toxicity of CO₂ in its own right²³.

$$FED = \left\{ \frac{[CO]}{LC_{50,CO}} + \frac{[HCN]}{LC_{50,HCN}} + \frac{[HCl]}{LC_{50,HCl}} + \frac{[NO_2]}{LC_{50,NO_2}} + \dots + organics \right\} \times V_{CO_2} + A + \frac{21 - [O_2]}{21 - 5.4}$$

$$V_{CO_2} = 1 + \frac{\exp(0.14[CO_2]) - 1}{2}$$

A is an acidosis factor equal to $[CO_2] \times 0.05$.

Gas concentrations are expressed in vol%, or the same units as the corresponding LC₅₀ value.

Equation 2²³

Influence of flame retardants on fire toxicity

Gas phase flame retardants, such as those based on organohalogen or organophosphorus compounds, interfere with the free radical reactions responsible for flaming combustion²⁵. This results in incomplete oxidation of vapour phase fuel molecules, leading to higher yields of all products of incomplete combustion²⁶. These are all more toxic than the cleaner products of complete combustion (carbon dioxide and water), and include carbon monoxide, hydrogen cyanide, hydrocarbons, oxygenated organics (including organo-irritants, such as acrolein and formaldehyde) and larger cyclic molecules such as polycyclic aromatic hydrocarbons and soot particulates. Fire toxicity increases as combustion becomes more incomplete, which can arise from chemical quenching (for example by gas phase flame retardants), insufficient heat (for example during smouldering), or when the fire becomes ventilation controlled, and there is insufficient oxygen for complete combustion²⁷. Recently it has been shown that the phosphorus flame retardants which act predominantly in the gas phase have a smaller influence on increasing the CO and HCN yields than the corresponding brominated flame retardants²⁸.

Influence of fire conditions on toxic product yields.

Burning behaviour and toxic product yield depend most strongly on a few of factors. Material composition, temperature and oxygen concentration are normally the most important^{29, 30}. As fires grow, they become ventilation controlled, and fires in buildings rapidly change from well-ventilated to under-ventilated. Data from large scale fires^{31,32} in enclosures show much higher levels of both asphyxiant gases CO and HCN under conditions of developed flaming than those from small, well-ventilated tests, such as the cone calorimeter³³ (ISO 5660). For a particular material, under different fire conditions, the HCN yield has been shown to rise proportionately with the CO yield^{34, 35, 36}.

Background to the current study

The current study uses a simple sofa-bed (a double mattress which folds to make a sofa) on a steel test frame, instead of the normal wooden frame to investigate the fire toxicity of different fabric-filling combinations. Four mattress formulations have been tested in duplicate, using commercially available fabrics and fillings: UK sourced fire retardant fabric, non-woven polyester comfort layer and combustion-modified foam (UKFR); a fire retardant fabric meeting UK furniture flammability regulations sourced in China (ChFR) on the same comfort layer and foam as with the UKFR sample; fabric and foam for the mainland European market (where there are no furniture flammability regulations) (EUMat); and a technically woven cover fabric, including cotton and wool with wool,

cotton and polyester fillings, specially designed to meet the UK furniture flammability regulations without the use of chemical flame retardants (sold under the trade name Cottonsafe®)(FRfreeCS).

The flammability of the fabric-filling combinations were tested in the laboratory using a cone calorimeter, and using large-scale burns, in a modified steel shipping container with restricted ventilation, to represent a normal UK living room. The burning behaviour and toxic gas concentration were used to quantify the fire hazards of each sofa-bed.

Three effects of flame retardants on fire safety can be identified: changing the ignitability; changing the rate of fire growth; and changing the toxicity of the smoke. This study does not address the first effect, because successful ignition suppression by flame retardants is rarely reported, and large dwelling fires frequently involve upholstered furniture, whether or not it was the first item ignited. Without ignition suppression data, it is very difficult to make an objective statement about the benefits of flame retardants. The study specifically compares the fire growth rate and fire smoke toxicity of the four furniture-fabric constructions outlined.

Experimental

Materials

Two mattresses of each of the specifications shown in Table 2 were made especially for the tests by Cottonsafe® Natural Mattress, Devon, UK, together with a single steel frame. Each mattress had dimensions 1.9 m × 1.5 m × 0.15 m. Figure 4 shows the mattress in the sofa configuration as used in these tests. The same materials were used to prepare filling/fabric test samples for the bench-scale cone calorimetry tests.



Figure 4 Folded mattress as sofa, shown on normal wooden frame³⁷.

Table 2 Mattress compositions and identification

Sample ID	Construction
UKFR	Combustion modified flexible polyurethane foam; polyester comfort layer; fire retardant fabric cover (sourced from the UK).
ChFR	Combustion modified flexible polyurethane foam; polyester comfort layer; fire retardant fabric cover (sourced from China).
EUMat	Flexible polyurethane foam; polyester comfort layer; untreated fabric cover (sourced from Europe).
FRfreeCS	Polycotton pad surrounded by woollen comfort layer; technically woven cotton and wool cover. No chemical fire retardant treatments (made in the UK).

Analysis for Flame Retardants

No detailed information on the fabric formulation was provided by the suppliers, so the fabric samples were sent for independent analysis at the specialist facility at Duke University, NC, US. They positively identified decabromodiphenyl ether (BDE-209) and decabromodiphenyl ethane (DBDPE) in the UKFR fabric. This was surprising, because BDE-209 has been listed by the Stockholm convention, and although its “sunset date” in Europe is March 2018, it is thought to have been largely withdrawn from the market. The ChFR fabric was found to contain *tris*-(chloropropyl) phosphate (TCIPP), and decabromodiphenyl ethane (DBDPE).

Individual materials were also subject to in-house elemental analysis using CHNS (Thermo Scientific Flash 2000 Organic Elemental Analyser), SEM-EDAX (FEI Quanta 200), and X-Ray fluorescence (Bruker Trace IV-SD handheld XRF) at both 25 keV and 40 keV. Foam/filling samples containing heteroelements were subject to solvent extraction in hexane (4 h) followed by direct injection mass spectrometry (MS) (Finnigan LCQ Advantage Max) and pyrolysis GC-MS (CDS analytical pyroprobe 5000 series connected to a Trace GC ultra DSQ II) to identify flame retardants.

Cone Calorimetry

The cone calorimeter, described in ISO 5660³³, is a standard method for burning small samples under a constant heat flux, with ignition piloted by an electronic spark, under well-ventilated conditions. The bench-scale composite test samples were prepared to quantify their ignition and burning behaviour. The test pieces consisted of the bulk pad (~ 90 mm × 90 mm × 15 mm thick), comfort layer (~ 90 mm × 90 mm × 7 mm thick) and fabric cover layer wrapped around the sample (~ 300 mm × 300 mm). The samples were stapled to create a pillow-like sample with a total thickness of ~25mm. Aluminium foil was wrapped around the sides and underneath the sample to prevent fuel loss as molten drips. The composite test samples were tested in a Govmark cone calorimeter at 35 kW m⁻² incident heat flux with upper sample retaining frame, in accordance with ISO 5660, running each sample in triplicate.

In addition to the standard protocol, gas analysis was undertaken to quantify the yield of HCN from each sample during the cone calorimeter test, collecting effluent in metered bubblers for subsequent analysis, carried out in duplicate. In both cone calorimetry and large scale tests the HCN was quantified using the Chloramine T method described in ISO 19701³⁸.

Large Scale Tests

The sofa-beds were burnt in a 3.4 m × 2.25 m × 2.4 m test room made by modifying a steel shipping container, located outside (Figure 5). An outlet vent (1 040 mm × 200 mm) was cut into one of the steel walls 600 mm from the top of the container. The entrance was closed with a plasterboard wall supported by timber framing, containing a ventilation inlet (323 mm × 323 mm) located 300 mm above floor level, on the opposite side of the container to the outlet vent. The outlet was twice the area of the inlet so that only cool air flowed into the container through the inlet, and only hot effluent left through the outlet. A door was also built into this wall to allow test mattresses to be changed and samples ignited. The floor was wooden, and the sofa-bed was placed on a sheet of plasterboard.

A thermocouple tree with four K-type thermocouples was placed inside the test room. The thermocouples were situated 0.5 m above floor level (at a similar height to the crib on the test sample), at 1.1 m, and at 1.6 m and 2.0 m (just below and above the outlet vent). This allowed for a

temperature profile to be measured inside the container. Two additional thermocouples were placed at the outlet vent to measure the temperature of the smoke plume.

In order to ensure that each mattress ignited first time, a larger, No. 7 crib, containing 125 g of Scots Pine (*Pinus Silvestris*), arranged as an open frame to give adequate ventilation, was employed to ensure sustained ignition, since three of the four compositions were supplied as having already resisted ignition using the No. 5 wooden crib (containing 17 g wood). A small piece of lint provided the initial ignition point at the base of the structure. The crib was located centrally on the sofa, at the back of the seat, next to the back rest.

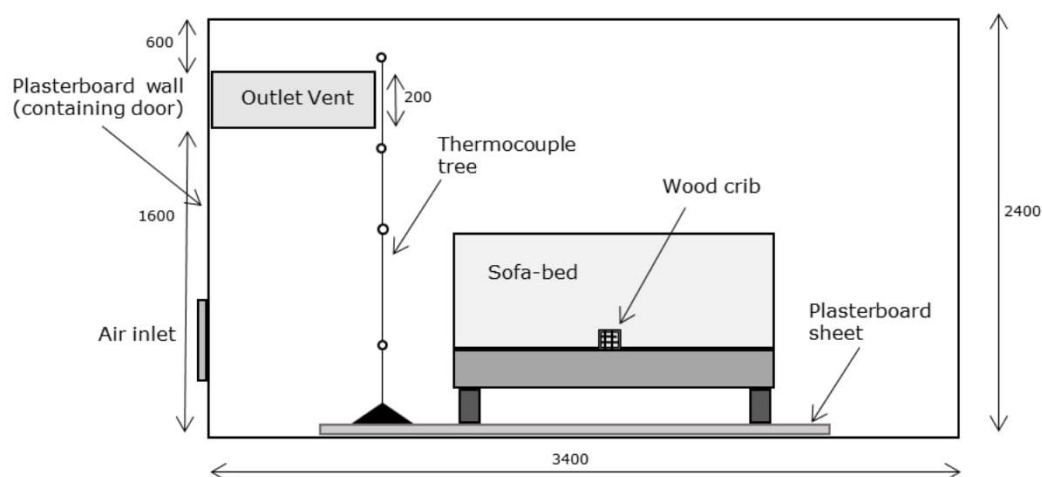


Figure 5 Side view of the test room showing sofa bed, thermocouple tree, and location of inlet and outlet vents (all dimensions in mm)

Gas sampling

Field sampling kits had been built in-house for continuous monitoring of CO, carbon dioxide (CO₂) and oxygen (O₂), and for quantifying HCN by bubbling metered volumes of fire effluent through aqueous sodium hydroxide solution (0.1 mol dm⁻³)³⁹. Up to seven dreschel bottles could be switched into the sampling line sequentially, to quantify seven temporal variations in HCN concentration.

Experimental protocol

Gas sampling was switched on and allowed to stabilise. The crib was ignited, the time noted, and the door in the plasterboard wall closed. Ignition was observed through a small viewing port in the plasterboard wall. The tests were allowed to continue until extinction, with the exception of the FRfreeCS mattress, which was extinguished after an hour to fit within the testing schedule.

Results

Characterisation of Materials

The elemental analysis of the materials using CHNS, X-Ray Fluorescence (XRF), and SEM-EDAX is summarised in Table 3.

Table 3 CHNS, XRF and SEM EDAX analysis of fabric, foam and filling.

Component	C %	H %	N %	S %	Oxygen and other elements %	Elements detected by EDAX/XRF
UKFR Fabric	38.07	5.40	0.00	0	56.53	O, Cl, Br
UK/Ch Foam	52.53	7.27	12.88	0	27.32	O, P, Cl
UK/Ch/EU Polyester	61.09	4.26	0.13	0	34.51	O
ChFR Fabric	52.86	4.18	0.00	0	42.96	O, Cl, Br, Sb
EUMat Fabric	41.71	6.28	0.04	0	51.97	O
EUMat Foam	57.23	5.87	5.51	0	31.39	O
FRfreeCS Fabric	41.31	6.14	0.07	0	52.48	O
FRfreeCS wool	44.44	6.93	13.71	2.27	32.64	O, S
FRfreeCS Polycotton	52.25	5.10	0.00	0	42.66	O

The elemental analysis showed the presence of phosphorus and chlorine in the foam, and in the UK and China-sourced fabrics. Solvent extraction, followed by direct injection mass spectrometry indicated the presence of tris(1-chloro-2-propyl) phosphate (TCPP m.w 327.56, detected m/z 327.0). Further analysis using pyrolysis-GCMS detected TCPP (68.4%) and two isomers, bis(1-chloro-2-propyl)-2-chloropropyl phosphate (26.3%) and bis(2-chloropropyl)-1-chloro-2-propyl phosphate (5.3%). This ratio of TCPP isomers is similar to the commonly sold compositions Fyrol PCF[®] and Antiblaze 80[®], supporting the conclusion that the flame retardant in the combustion modified polyurethane foam is TCIPP. The ChFR fabric also contained antimony (presumably as Sb₂O₃), which would function as a synergist with the brominated flame retardant. Thus gas phase flame inhibitors were present in both the foam and the fabric of both the UKFR and ChFR mattresses. No evidence of flame retardants was found in the EUMat fabric or foam.

Cone Calorimetry

All four samples ignited within the first 20 s of exposure to the cone heater and continued to burn for similar times (~400 s), except the UKFR sample, which extinguished much earlier (~100 s). A summary of cone calorimetry results is presented in Table 4 and the heat release rate (HRR) curves are presented in Figure 6.

Table 4 Summary data from cone calorimetry on furniture composites at 35 kW m⁻² incident heat flux (HRR is heat release rate, and PHRR is peak heat release rate).

Material	Sample mass /g	Mass loss %	Mass loss rate /g m ⁻² s ⁻¹	Time to ignition /s	Total heat release /MJ m ⁻²	Peak HRR /kW m ⁻²	Time to PHRR /s	CO Yield g/g	HCN Yield mg/g
UKFR	38.3	25.3	6.3 ± 0.05	7.6 ± 1.9	4.7 ± 0.15	112.1 ± 36	24.5 ± 13	0.062 ± 0.002	0.42 ± 0.17
ChFR	39.8	70.6	8.9 ± 0.3	12.0 ± 3.1	38.4 ± 4.8	164.5 ± 16.7	39.0 ± 2.8	0.160 ± 0.009	0.97 ± 0.24
EUMat	34.5	73.3	5.3 ± 0.3	5.2 ± 1.1	45.2 ± 1.4	212.9 ± 18.4	47.0 ± 2.8	0.008 ± 0.001	0.31 ± 0.001
FRfreeCS	37.0	69.3	3.6 ± 0.6	6.8 ± 0.6	40.9 ± 2.0	185.7 ± 4.8	25.5 ± 0.6	0.015 ± 0.003	0.09 ± 0.02

The UKFR composite ignited around the same time as the samples without flame retardants but had the lowest total heat release of the four samples due to rapid self-extinguishment. The low mass loss shows that most of the polyurethane foam, which made up the bulk of the sample, did not burn under these conditions. It is therefore appropriate that the yields of the two asphyxiants CO and HCN are presented on a mass-loss basis. The ChFR sample produced the highest yield of CO, followed by the UKFR sample, showing the effect of gas-phase free radical quenchers (like TCIPP, DBDPE and BDE-209) that inhibit the conversion of CO to CO₂ by reducing the concentration of the OH· radical²⁸. The HCN yields, which generally increase in proportion to CO yields³⁴, show the same effect of being enhanced by the presence of a gas-phase flame retardant⁴⁰, but are relatively low, as would be expected from a well-ventilated test.

The ChFR sample suppressed ignition for longer than the other materials, but had a high mass loss and peak HRR (PHRR). The EUMat and FRfreeCS samples showed similar total heat release and mass loss to the ChFR sample, with slightly higher PHRR.

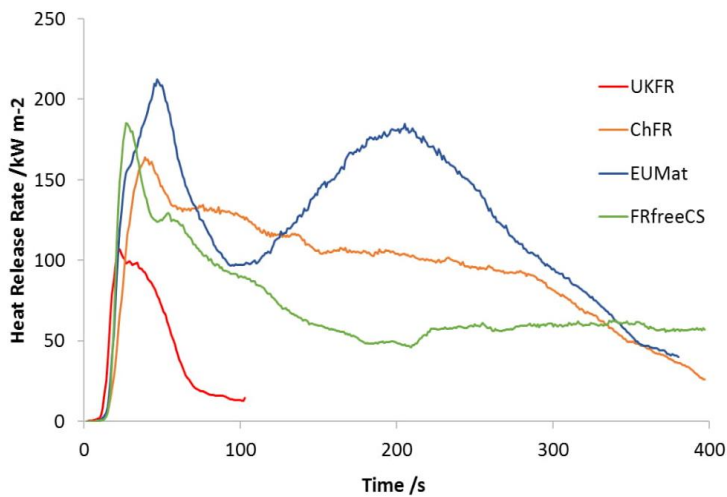


Figure 6 Representative heat release rate curves measured in cone calorimeter at 35 kW m⁻².

Large Scale Tests

Ignition, temperature and mass loss data

Sustained ignition was observed in all eight tests on the four compositions following application of an ignited No.7 wood crib. Table 5 shows the mass of each mattress before and after the test, the time for the mattress to ignite, and the maximum temperature recorded by the thermocouples in the test room. The mass after the test for FRfreeCS could not be determined as each mattress had been extinguished with copious quantities of water.

Table 5 Mass loss, temperature and time data from the large-scale tests.

Sample	Mass /kg	Mass after test /kg	Ignition time /s	Maximum temperature /°C	Time of maximum temp /s
UKFR1	12.3	2.4	297	286	635
UKFR2	12.0	2.0	131	365	586
ChFR1	12.6	2.1	525	287	704
ChFR2	12.6	4.5	297	285	767
EUMat1	11.2	0.4	128	600	516
EUMat2	11.1	0.323	212	542	736
FRfreeCS1	21.1	-	228	220	4070
FRfreeCS2	21.6	-	143	171	3553

Figure 7 shows the temperature recorded on the highest thermocouple (2.0 m) for each test. Reasonable reproducibility was obtained for each pair of apparently identical mattresses, despite the different weather conditions and wind directions on the day of each test. The UKFR1 and ChFR1 tests were the only two tests performed on the first day, in significantly windier and wetter conditions; visual observation showed the wind moving the crib flame away from the back of the sofa in the first two tests; they showed longer ignition delay times than the subsequent tests, where calmer, more stable weather conditions prevailed, until the end of the test programme. The EUMat sofa-beds ignited most quickly and reached the highest temperatures, followed by the UKFR then the ChFR sofas.

The FRfreeCS sofas ignited but flaming ceased after ~30s, which was followed by smouldering combustion, until they re-ignited at 1200 s in test 1 and 1730 s in test 2. After an hour the

temperature in the container was much lower than any of the other tests, when flames were extinguished. Visual observations showed that the majority of the sample had not burned, suggesting that the sofa burning could have continued slowly for some time.

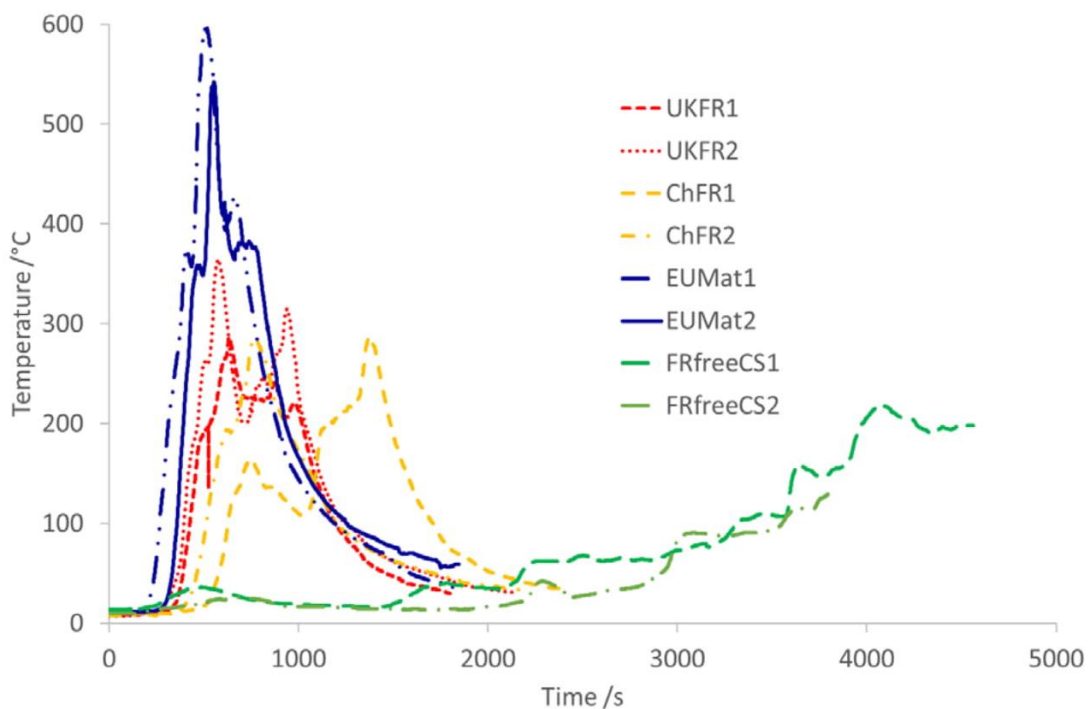


Figure 7 Temperatures at 2 m thermocouple during large scale tests.

Gas measurements

CO, CO₂ and O₂ concentrations were continuously monitored for each experiment, and HCN was sampled in bubblers from the outlet vent, using portable gas analysers. Unfortunately, the analysers malfunctioned for the first two tests, UKFR 1 and ChFR 1, so no replicate data are available for these mattresses.

Figure 8 shows the CO concentrations for each mattress, with the greatest peak in the EUMat1 test, followed by the UKFR2 and EUMat2 tests. ChFR2 showed a later peak of lower intensity, while the FRfreeCS showed very low levels of CO throughout the burn.

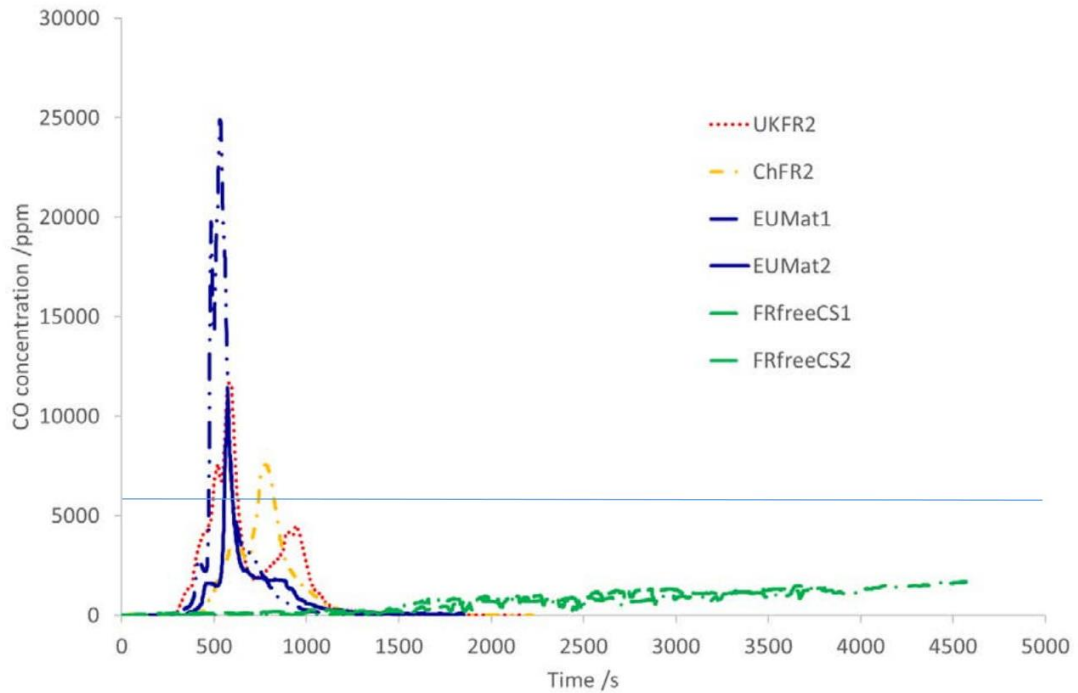


Figure 8 Carbon monoxide concentration (showing LC_{50} for 30 minutes exposure at 5700 ppm from ISO 13344²³).

The HCN concentrations, sampled at the outlet, were calculated from the measured concentrations collected in the bubblers for fixed time intervals (typically 3 to 5 min). In order to better represent the temporal variation, the HCN/CO ratio was determined from the measured values for each mattress, and the CO concentrations multiplied by this ratio to obtain the curves shown in Figure 9, following the methodology described elsewhere³⁵. These show the highest peak HCN concentration, of around 800 ppm, for EUMat1 and UKFR2 tests, followed ChFR2. The HCN peak for EUMat2 is very much smaller. The length of the burn for the FRfreeCS meant that bubbler samples were somewhat unevenly spaced, placing greater reliance on extrapolation of CO data. The lack of HCN after 2 500 s is consistent with the cover fabric containing wool (and therefore being a source of HCN), while the cotton filling does not produce HCN.

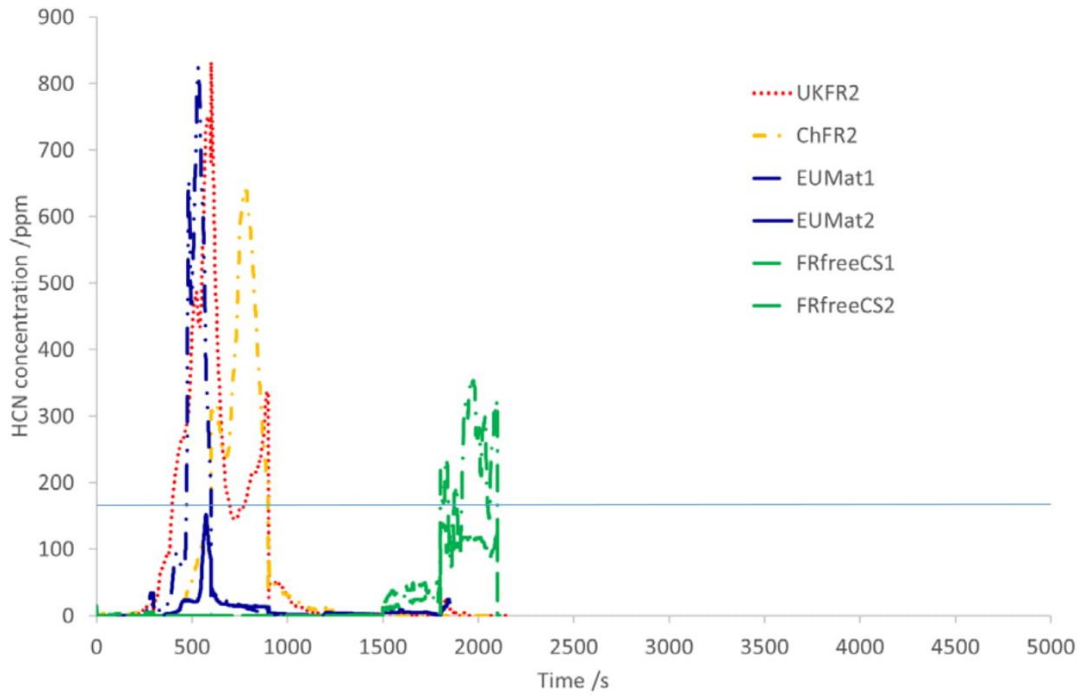


Figure 9 Hydrogen cyanide concentrations calculated from bubbler concentrations, and the relationship with CO concentration (showing LC_{50} for 30 minutes exposure at 165 ppm from ISO 13344²³).

In order to relate gas concentrations to total yields of each toxicant, it is necessary to know the effluent flow leaving the test room. This was not measured directly in the tests, but calculated from the temperature profile and vent openings as described in the literature⁴¹. The heat from the fire causes the effluent to expand, making it less dense, which drives it through the outlet, causing fresh air to be drawn through the inlet. Such buoyant flows can be estimated from the temperature and vent sizes. The calculation is based on the assumption that the gas is split into two uniform layers – an upper hot layer, and a cooler lower layer with densities ρ_h and ρ_c respectively.

The densities were calculated from the gas laws, assuming a molecular weight of both fresh air and smoke laden air of 28.95 g mol^{-1} . This is reasonable, given the abundance of nitrogen in both air and effluent, and the replacement of O_2 with CO , CO_2 , water etc. The effluent velocity v_{eff} was estimated from

$$v_{eff} = \sqrt{2g \frac{(\rho_c - \rho_h)}{\rho_h} y}$$

Equation 3

where g is the acceleration due to gravity and y is the height of the vent above the cool-hot layer boundary from which the mass flow and volume flow of effluent were determined as a function of time for each test. This is based on the detailed guidance in ref. 41.

Yields summary

The yield data in Table 6 show the evolution of the two main asphyxiants, CO and HCN for the different furniture compositions. CO is present in the effluents from nearly all unwanted fires, whereas HCN is only detected where the fuel contains a significant amount of nitrogen.

With respect to the scale-up of yield data between the cone calorimeter (Table 4) and the large scale test (Table 6), UKFR and EUMat, CO and HCN yields are an order of magnitude greater in the sofa burn than in the cone calorimeter, showing the cone calorimeter does not replicate the behaviour of large scale under-ventilated fires. For the ChFR materials, the yields are similar in both scales, demonstrating that the cone calorimeter does replicate the effect of gas phase inhibition on the CO yield. For the FRfreeCS, superficially, there appears good agreement, but the burning behaviour was so different (flaming in cone calorimeter, mostly smouldering in the large-scale) such comparisons are unjustified.

Mass loss yields of CO and HCN presented in Table 6 are comparable and relate to other reports, such as CO and HCN yields from a burning polyurethane foam-fabric sofa of 0.015 and 0.004 kg/kg pre-flashover, and 0.04 and 0.015 post-flashover, respectively⁴².

Table 6 Calculated total volumes and mass-loss yields of carbon monoxide and hydrogen cyanide (ND non-detected; limit of detection for HCN 0.0005 kg/kg)

Sample	CO Total Volume /m ³	HCN Total Volume /m ³	CO Mass loss yield kg/kg	HCN Mass loss yield kg/kg	Volume of incapacitating effluent /m ³
UKFR2	1.366	0.082	0.171	0.010	105 after 1000 s
ChFR2	0.922	0.064	0.142	0.009	79 after 1000 s
EUMat1	1.354	0.037	0.157	0.004	94 after 1000 s
EUMat2	0.647	0.007	0.075	0.001	57 after 1000 s
FRfreeCS1	1.027	0.007	0.063	ND	40 after 4000 s
FRfreeCS2	0.542	ND	0.032	ND	25 after 3800 s

Estimates of incapacitation

In addition to CO and HCN being responsible for almost all smoke inhalation deaths, at lower doses exposure to either or both of these gases results in incapacitation. Equation 1 has been used to estimate the effect of a fire effluent on exposed occupants.

A single UKFR sofa-bed, burning in a room (with the same ventilation as the shipping container, such as a partly open door), will produce an effluent capable of causing incapacitation (unconsciousness) when dispersed across a volume of 105 m³ (the size of a small house or apartment), 1000 s from ignition of the sofa-bed. Other burning mattress compositions will produce the incapacitating volumes shown in Table 6, assuming the effluent fills the volume uniformly.

This shows that the burning UKFR sofa-bed has the greatest capacity for incapacitation. This is based on the data from a single burn, and both the ChFR and EUMat sofa-beds also produce large volumes of incapacitating effluent, so this statement is not entirely conclusive. This arises from the effect of flame retardants increasing the yield the two most toxic products of incomplete combustion, CO and HCN. Despite a higher overall temperature and greater burning rate, the smoke from the ChFR has a similar potential for incapacitation as the non-flame retardant EUMat sofa-bed. The burning FRfreeCS has the least potential for incapacitation, and this occurs much later, 4000 s after ignition, rather than just 1000 s.

The contributions of CO and HCN towards incapacitation, calculated from Equation 1 are shown in Figure 10, assuming the effluent is dispersed within a volume of 100 m³. An FED equal to one would be expected to cause incapacitation to 50% of the exposed population. The non-linearity of FED to HCN (as $FED \propto [HCN]^{2.36}$) in , and the arbitrary use of a 100 m³ volume makes the UKFR mattress disproportionately worse than the ChFR or EUMat1 sofa-beds , where Table 6 shows that the differences in HCN yields are not so large.

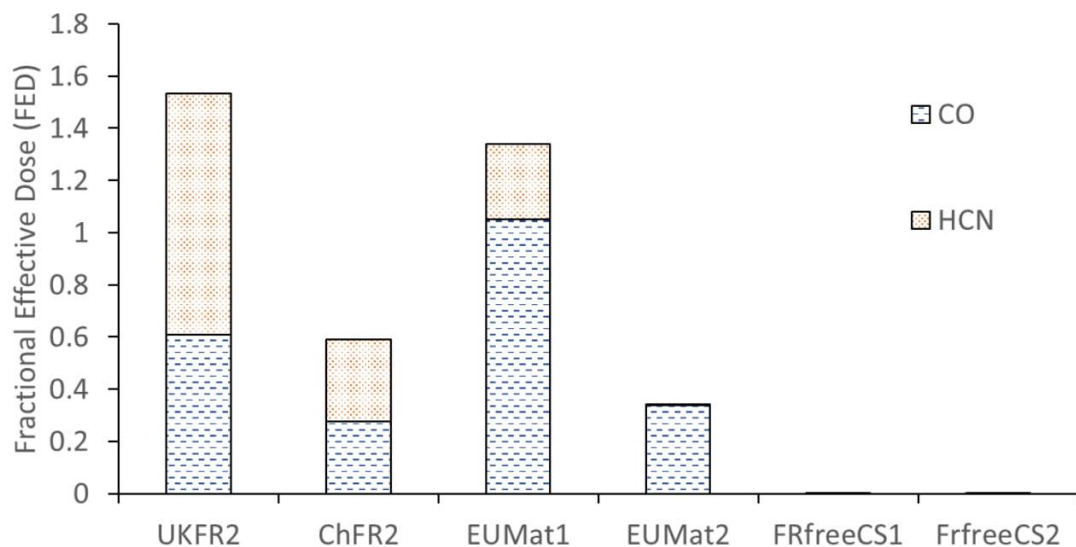


Figure 10 Fractional Effective Dose for incapacitation at 1000 s, assuming a total volume of 500 m³.

Estimates of lethality

HCN deprives the body of oxygen, and so stimulates respiration, increasing the uptake of toxicants, causing rapid unconsciousness⁴³. At this point respiration falls back to normal levels, but since the unconscious victim can no longer escape they are likely to continue to inhale CO and HCN until death. Figure 11 shows the fractional effective dose for lethality for 30 min exposure to the effluent produced from burning each sofa-bed, when uniformly dispersed in a volume of 500 m³. The 30 min exposure presupposes the victims were unable to escape. In the case of the FRfreeCS mattress, this period of 30 min would not start until around 1 h after ignition. The greater contribution of HCN to

the toxicity is evident for the two compositions containing flame retardants, although all three foams (UKFR, ChFR and EUMat) are likely to contain similar amounts of nitrogen.

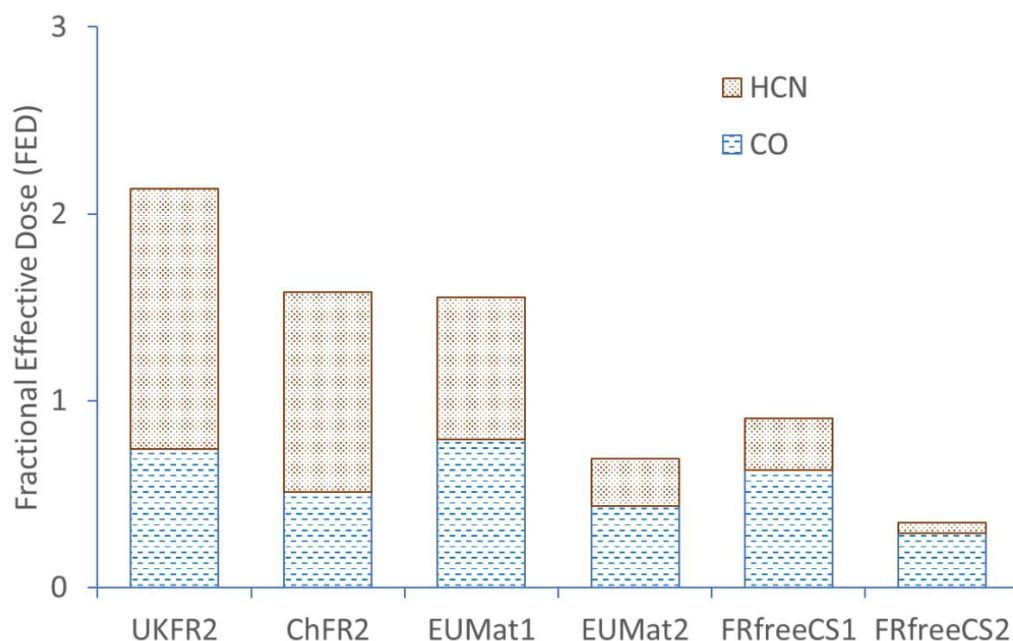


Figure 11 Fractional Effective Dose for lethality, assuming a 500 m³ volume and 30 min exposure

Conclusions

The fire statistics in the introductory section shows that the claims made by flame retardant manufacturers, and repeated by the UK government, quantifying the effects of the furniture flammability regulations in reducing fire deaths are questionable. The time series data shows that smoke toxicity causes the majority of deaths and the majority of injuries from unwanted fires, and that these majorities were increasing. The fire death rate underlined the importance of upholstered furniture and bedding in fire fatalities, despite being a small proportion of the number of fires.

The aim of this study was to quantify the volume and toxicity of the effluents produce from burning sofas with different compositions, and particularly to see the effect of flame retardants on the fire growth rate and toxic product yields, since both these parameters would influence the hazard to life from fire. This aim has been partially met, and certainly highlights the need for further work in this important area. The study was based on four representative furniture formulations. It shows a significant hazard associated with the increased fire toxicity, resulting from incorporating flame retardants into furniture. Unfortunately, the data from the first two tests was not recorded, increasing the uncertainty of the results being representative of a more generalised trend. Clearly, further tests need to be carried out on a wider representative range of furniture in order to establish whether these observations can be generalised across the range of furniture products.

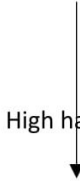
Despite the variation inherent in the fire tests, clear differences were observed in burning behaviour and toxic product yield of different compositions. However, for three of the four formulations, in the large scale test, there was very little difference in the time to ignition or fire growth rate, despite

two of the three containing flame retardants. From the data in Figure 7 showing the peak temperature of the EUMat sofas was greater than any others, suggesting a larger peak of burning intensity. It is apparent that flame retardants affect both flammability and toxicity, although the differences are not consistent between scales.

Table 7 summarises a qualitative rank order of each sofa-bed composition from the bench and large scale tests, from low to high hazard. It is important to note that the bench-scale data refer to well-ventilated burning, while the large-scale data represent under-ventilated burning. The yields of CO and HCN presented in Table 4 and Table 6 are greater by factors of around 5 and 10 respectively, for the large-scale fires, particularly for the EUMat and FRfreeCS sofas, which did not contain gas phase flame retardants. From Table 7, it is clear that the best performance has been achieved on a large-scale for the FRfreeCS mattress without any flame retardants. In upholstered furniture, flame retardants increase the toxicity of the smoke. The overall effect of the flame retardants (as seen in the large-scale tests) is to increase the fire hazard relative to the non-flame retarded EUMat. Based on the compositions used in this study, it is evident that meeting the UK furniture flammability regulations without the use of chemical flame retardants provides the lowest fire hazard, or the greatest level of fire safety.

Table 7 Fire performance of different compositions at different scales of test.

Bench Scale		Large Scale		
Flammability	Toxicity	Flammability	Toxicity	
UKFR	FRfreeCS	FRfreeCS	FRfreeCS	Low hazard
ChFR	EUMat	ChFR	EUMat	
FRfreeCS	UKFR	UKFR	ChFR	High hazard
EUMat	ChFR	EUMat	UKFR	



This work has shown that one of the most essential components of the fire hazard assessment from upholstered furniture and bedding has been disregarded in the furniture flammability regulations. It has been shown that fire toxicity is the main cause of death and injury in fires, and that upholstery and bedding fires cause a disproportionate number of fatalities, yet there is no requirement to assess the toxicity of burning domestic furniture. This has led to an over-reliance on chemical additives (flame retardants) to meet the UK's furniture flammability regulations. While we are unlikely to ever have robust data showing how effective flame retardants are in suppressing ignition, it is evident that once ignition occurs, the presence of flame retardants has little effect on the fire growth rate, but does have an adverse effect on the smoke toxicity.

However, further work is needed to ensure the results are representative of the situation across the UK. It is important to note that currently only samples of new furniture are tested and required to meet the furniture flammability regulations. All the sociological indicators show that fire deaths

predominate in the poorest sections of society, where sofas are likely to be 10 or more years old. Reports in the literature show that the UK has the highest levels of flame retardants in household dust in the world⁴⁴ which are probably released from upholstered furniture and bedding during its lifetime, negating any potential fire safety benefit from the furniture flammability regulations, while causing problems of endocrine disruption (such as developmental disorders, difficulty in becoming pregnant, and obesity) from inhalation or ingestion of the contaminated dust.

Acknowledgements

One of us (RB) would like to thank Greater Manchester Fire and Rescue Service for provision of a studentship. One of us (RGW) would like to thank West Midlands Fire Service for provision of a studentship. We would all like to thank Mark Downen of Cottonsafe Natural Mattress for provision of samples, help and advice, and Lancashire Fire and Rescue Service for provision of test facilities at their Washington Hall training centre.

- 1 Fire statistics monitor: April 2015–March 2016, UK Government, Home Office, <https://www.gov.uk/government/statistics/fire-statistics-monitor-april-2015-to-march-2016> and preceding editions.
- 2 Woolley, W.D., Raftery, M.M., Smoke and toxicity hazards of plastics in fires, (1975) *Journal of Hazardous Materials*, 1 (3), pp. 215-222.
- 3 Alarie, Y., Toxicity of fire smoke, (2002) *Critical Reviews in Toxicology*, 32 (4), pp. 259-289.
- 4 BS 5852:2006 Methods of test for assessment of the ignitability of upholstered seating by smouldering and flaming ignition sources.
- 5 A Emsley, L Lim, G Stevens, P Williams, International Fire Statistics and the Potential Benefits of Fire Counter-Measures, for European Flame Retardant Association (EFRA) PRC/92/2005/EFRA, May 2005
- 6 A statistical report to investigate the effectiveness of the Furniture and Furnishings (Fire) (Safety) Regulations, 1988, Greenstreet Berman Ltd, for the UK's Department for Business, Innovation and Skills, December 2009
- 7 Hull, T.R., Law, R.J., Bergman, Å., Environmental Drivers for Replacement of Halogenated Flame Retardants, (2014) *Polymer Green Flame Retardants*, pp. 119-179.
- 8 Prior to 1994: http://www.stats.govt.nz/browse_for_stats/snapshots-of-nz/digital-yearbook-collection.aspx. 1994-2000: <http://www.civil.canterbury.ac.nz/fire/pdfreports/CWong.pdf>. 2000 onwards <http://www.fire.org.nz/About-Us/Facts-and-Figures/Pages/Statistics-Data-Fields.html>
- 9 Arcadis EBRC, Report for European Commission (DG Health and Consumers) - Evaluation of data on flame retardants in consumer products – Final report 17.020200/09/549040, Brussels, 2011. http://ec.europa.eu/consumers/safety/news/flame_retardant_substances_study_en.pdf
- 10 Walker R G, PhD Thesis, University of Central Lancashire, UK, 2017.
- 11 De Wit, C.A., An overview of brominated flame retardants in the environment, (2002) *Chemosphere*, 46 (5), pp. 583-624.
- 12 Hites, R.A., Polybrominated Diphenyl Ethers in the Environment and in People: A Meta-Analysis of Concentrations, (2004) *Environmental Science and Technology*, 38 (4), pp. 945-956.
- 13 Darnerud, P.O., Eriksen, G.S., Jóhannesson, T., Larsen, P.B., Viluksela, M., Polybrominated diphenyl ethers: Occurrence, dietary exposure, and toxicology, (2001) *Environmental Health Perspectives*, 109 (SUPPL. 1), pp. 49-68.
- 14 Darnerud, P.O. Toxic effects of brominated flame retardants in man and in wildlife, (2003) *Environment International*, 29 (6), pp. 841-853.
- 15 Law, R.J., Allchin, C.R., de Boer, J., Covaci, A., Herzke, D., Lepom, P., Morris, S., Tronczynski, J., de Wit, C.A. Levels and trends of brominated flame retardants in the European environment, (2006) *Chemosphere*, 64 (2), pp. 187-208.

-
- 16 Covaci, A., Harrad, S., Abdallah, M.A.-E., Ali, N., Law, R.J., Herzke, D., de Wit, C.A. Novel brominated flame retardants: A review of their analysis, environmental fate and behaviour, (2011) *Environment International*, 37 (2), pp. 532-556.
 - 17 van der Veen, I., de Boer, J. Phosphorus flame retardants: Properties, production, environmental occurrence, toxicity and analysis, (2012) *Chemosphere*, 88 (10), pp. 1119-1153.
 - 18 Shaw S D, Blum A, Weber R, Kannan K, Rich D, Lucas D, Koshland C P, Dobraca D, Hanson S, Birnbaum L S. Halogenated flame retardants: Do the fire safety benefits justify the risks? *Rev Environ Health* 2010;25:261-305.
 - 19 Brommer, S., Harrad, S., Sources and human exposure implications of concentrations of organophosphate flame retardants in dust from UK cars, classrooms, living rooms, and offices, (2015) *Environment International*, 83, pp. 202-207.
 - 20 Stubbings, W.A., Drage, D.S., Harrad, S., Chlorinated organophosphate and “legacy” brominated flame retardants in UK waste soft furnishings: A preliminary study, (2016) *Emerging Contaminants*, 2 (4), pp. 185-190.
 - 21 Babrauskas, V., Levin, B.C., Gann, R.G., Paabo, M., Harris Jr., R.H., Peacock, R.D., Yusa, S., Toxic potency measurement for fire hazard analysis, (1992) *Fire Technology*, 28 (2), pp. 163-167.
 - 22 Purser, D.A., The evolution of toxic effluents in fires and the assessment of toxic hazard, (1992) *Toxicology Letters*, 64-65 (C), pp. 247-255.
 - 23 ISO 13344:2015, Estimation of the lethal toxic potency of fire effluents.
 - 24 ISO 13571:2012, Life threat from fires – Guidance on the estimation of time available for escape using fire data.
 - 25 Hull, T.R., Stec, A.A., Paul, K.T., Hydrogen chloride in fires, (2008) *Fire Safety Science*, pp. 665-676.
 - 26 Kaczorek, K., Stec, A.A., Hull, T.R., Carbon monoxide generation in fires: Effect of temperature on halogenated and aromatic fuels, (2011) *Fire Safety Science*, pp. 253-263.
 - 27 Hull, T.R., Stec, A.A., Lebek, K., and Price, D., (2007) Factors Affecting the Combustion toxicity of Polymeric Materials, *Polymer Degradation and Stability*, 92:2239-2246.
 - 28 Molyneux, S., Hull, T.R., Stec, A.A. (2014) The Effect of Gas Phase Flame Retardants on Fire Effluent Toxicity, *Polymer Degradation and Stability* 106:36-46.
 - 29 Stec, A.A., Hull, T.R., Lebek, K., Purser, J.A., Purser, D.A., The effect of temperature and ventilation condition on the toxic product yields from burning polymers, (2008) *Fire and Materials*, 32 (1), pp. 49-60.
 - 30 Stec, A.A., Hull, T.R., Torero, J.L., Carvel, R., Rein, G., Bourbigot, S., Samym, F., Camino, G., Fina, A., Nazare, S., Delichatsios, M., Effects of fire retardants and nanofillers on the fire toxicity, (2009) *ACS Symposium Series*, 1013, pp. 342-366.
 - 31 Blomqvist, P., and Lonnermark, A., *Fire and Materials*. 25, 71-81, (2001).
 - 32 Andersson B., Markert F., and Holmstedt G., *Fire Safety Journal*, 40, 439-465, (2005).
 - 33 ISO 5660-1:2015 Reaction-to-fire tests — Heat release, smoke production and mass loss rate — Part 1: Heat release rate (cone calorimeter method) and smoke production rate (dynamic measurement)
 - 34 Molyneux, S.A., Stec, A.A., Hull, T.R., The correlation between carbon monoxide and hydrogen cyanide in fire effluents of flame retarded polymers, (2014) *Fire Safety Science*, 11, pp. 389-403.
 - 35 Wang, Z., Jia, F., Galea, E.R., A generalized relationship between the normalized yields of carbon monoxide and hydrogen cyanide, (2011) *Fire and Materials*, 35 (8), pp. 577-591.
 - 36 Purser, D., Purser, J., HCN yields and fate of fuel nitrogen for materials under different combustion conditions in the ISO 19700 tube furnace and large-scale fires, (2008) *Fire Safety Science*, pp. 1117-1128.
 - 37 <https://cottonsafenaturalmattress.co.uk/natural-mattresses/bond-3-seater-futon-sofa-bed/> accessed 3rd Dec 2017.
 - 38 ISO 19701:2013 Methods for sampling and analysis of fire effluents, ISO, Geneva.

-
- 39 Stec, A.A., Molyneux, S., Crewe, R.J., Sampling and Analysis of Toxic Gases from Large-Scale Fire Experiments, submitted to Fire Safety Journal, 2017.
 - 40 Schnipper, A., Smith-Hansen, L., Thomsen, E.S., Reduced combustion efficiency of chlorinated compounds, resulting in higher yields of carbon monoxide, (1995) Fire and Materials, 19 (2), pp. 61-64.
 - 41 Tanaka, T. Vent flows, (2016) SFPE Handbook of Fire Protection Engineering, Fifth Edition, pp. 455-485.
 - 42 Gann, R. G., Averill, J. D., Johnsson, E. L., Nyden, M. R., Peacock, R. D., Fire effluent component yields from room-scale fire tests, Fire and Materials, 34, 285-314, 2010.
 - 43 Stec A and Hull R (editors), Fire Toxicity, Woodhead/Elsevier, Cambridge, UK, 2010
 - 44 Kuang, J., Ma, Y., Harrad, S., Concentrations of "legacy" and novel brominated flame retardants in matched samples of UK kitchen and living room/bedroom dust, (2016) Chemosphere, 149, 224-230.

Fire Behaviour of Modern Façade Materials – Understanding the Grenfell Tower Fire
Submitted to Journal of Hazardous Materials and accepted in December 2018. Article is in
press at the time of writing. <https://doi.org/10.1016/j.jhazmat.2018.12.077>

Fire behaviour of modern façade materials – understanding the Grenfell Tower fire

Sean T. McKenna, Nicola Jones, Gabrielle Peck, Kathryn Dickens, Weronika Pawelec, Stefano Oradei, Stephen Harris, Anna A Stec and T Richard Hull*
Centre for Fire and Hazard Sciences,
University of Central Lancashire, PR1 2HE, UK

* Corresponding author: trhull@uclan.ac.uk; Telephone +44 1772 893543; Fax +44 1772 894981.

Abstract

The 2017 Grenfell Tower fire spread rapidly around the combustible façade system on the outside of the building, killing 72 people. We used a range of micro- and bench-scale methods to understand the fire behaviour of different types of façade product, including those used on the Tower, in order to explain the speed, ferocity and lethality of the fire. Compared to the least flammable panels, polyethylene-aluminium composites showed 55x greater peak heat release rates (pHRR) and 70x greater total heat release (THR), while widely-used high-pressure laminate panels showed 25x greater pHRR and 115x greater THR. Compared to the least combustible insulation products, polyisocyanurate foam showed 16x greater pHRR and 35x greater THR, while phenolic foam showed 9x greater pHRR and 48x greater THR. A few burning drips of polyethylene from the panelling are enough to ignite the foam insulation, providing a novel explanation for rapid flame-spread within the facade. Smoke from polyisocyanurates was 15x, and phenolics 5x more toxic than from mineral wool insulation. 1kg of burning polyisocyanurate insulation is sufficient to fill a 50m³ room with an incapacitating and ultimately lethal effluent. Simple, additive models are proposed, which provide the same rank order as BS8414 large-scale regulatory tests.

1 Introduction

In 2006, restrictions on the use of combustible materials on the outside of tall buildings in the UK were relaxed, while targets for energy efficiency were raised. In 2016, the Grenfell Tower was refurbished with an insulated rainscreen façade system consisting of combustible polyisocyanurate (PIR) foam insulation and aluminium-polyethylene composite material, separated by a ventilated cavity (Figure 1) covering the exterior of the building. On 14th June 2017, a fire, reported to have started in a fridge-freezer in a fourth floor apartment, broke out to ignite the recently installed façade system, after which it spread very rapidly around the outside of the building, and into almost all the other apartments, ultimately killing 72 occupants. The different components of the façade system were certified to have passed regulatory tests for fire safety, although it is arguable whether the refurbished façade system was actually compliant. The background to the fire and the regulatory regime for fire safety of tall buildings is detailed in the supplementary material (SM).

In addition to rapid fire spread around the Tower, large volumes of smoke were produced. Smoke inhalation is known to be the largest cause of death and the largest cause of injury from fire in the UK and US [1, 2]. In most cases the smoke from the burning façade appears to have entered the building before the contents of each apartment ignited, so the smoke toxicity of the façade is an important factor in the tragedy. On exposure to smoke, the victim becomes incapacitated (unconscious), and unless they are rescued, death is likely to follow. Incapacitation and lethality may

be estimated for 50% of an exposed population in terms of a fractional effective dose (FED), following ISO 13571 [3] (incapacitation) or ISO 13344 [4] (lethality). When the FED equals 1, the equations predict that half of the exposed population would be incapacitated or killed. Fire safety engineers may use a precautionary factor of 10 (i.e. $FED < 0.1$) to ensure the life safety of occupants in the event of fire.

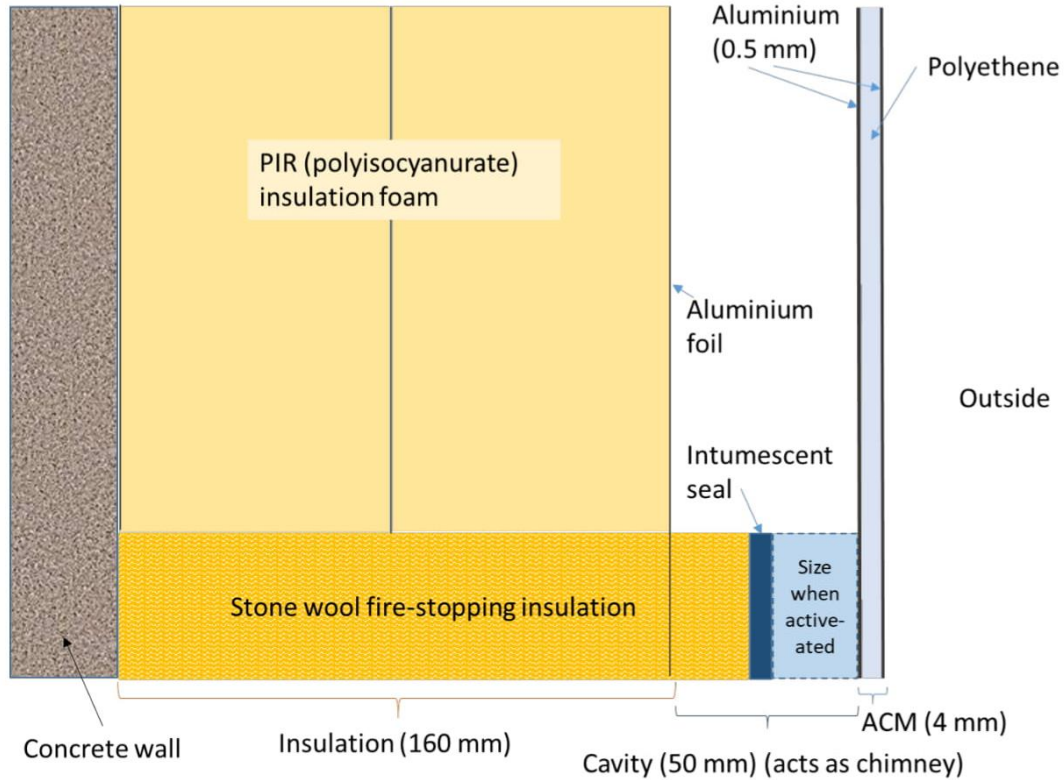


Figure 1 Façade system in the Grenfell Tower

Fire toxicity is a function of both material and fire condition. It has been shown that the yield of major asphyxiants hydrogen cyanide (HCN) and carbon monoxide (CO) increases by a factor of 5 to 20 as the fire grows from well-ventilated to under-ventilated [5]. The steady state tube furnace (ISO TS 19700) [6] has been specifically designed to replicate the smoke toxicity of individual fire stages [7]. The ventilation condition of burning polyethylene (PE), pouring out of the aluminium composite material (ACM) screens is uncertain, while the insulation foams behind the ACM will have undergone the more toxic under-ventilated burning. Woolley and Raftery reported the increasing danger of smoke toxicity over 40 years ago [8], specifically highlighting the release of HCN from rigid and flexible urethane foams. It has been shown that when PIR foam burns it generates HCN and CO in dangerous quantities [9]. Investigation reports have shown that almost all of the Grenfell Tower occupants who died in the building collapsed because the fumes prevented escape [10]. Several survivors were treated for cyanide poisoning, and many victims had collapsed on the stairs.

The refurbishment of tall concrete buildings often involves covering the exterior with a rainscreen facade system, consisting of an outer-screen, a cavity and an inner layer of insulation. The outer-screen may be aluminium composite material (ACM), high-pressure laminate (HPL), or mineral fibre board. ACM consists of two thin sheets of aluminium (~ 0.5 mm) sandwiching a layer of polymer (usually PE), PE filled with metal hydroxide fire retardant (FR), or predominantly non-combustible

(NC), as inorganic composite or metallic filling. FR panels contain around 65% aluminium hydroxide or magnesium hydroxide, having a fire retarding effect through endothermic dehydration and the subsequent release of water, to suppress flaming [11].

At the time of the fire, two phenolic foams (PF) and one PIR foam were certified to be compliant with the UK building regulations for tall building exteriors. The certificates for the PIR foam and one phenolic foam have subsequently been withdrawn by their manufacturers. In this study, various outer-screens, and the certified insulation foams, were tested alongside other phenolic and PIR foams and two non-combustible insulation boards, of glass wool (GW) and stone wool (SW).

The aim of this paper was to assess the fire safety of combinations of typical rainscreen façade products using micro-scale decomposition and bench-scale fire behaviour and toxic product evolution. The results are related to the large-scale government tests [12], following the Grenfell fire, on 8 m rainscreen façade systems.

2 Experimental

Commercial products designed for use in façade systems and the subject of this study are shown in Table 1 and Table 2. They were analysed to determine their composition, thermal decomposition and fire behaviour. ACM_PE1, PF2 and PIR2 are reported to have been used extensively on the Grenfell Tower refurbishment. Other products have been selected to illustrate the range of different fire performance from different materials. The PIR2 product is unusual in that it has thin layers of glass wool sandwiched between thick (~25 mm) layers of PIR foam.

Table 1 Panel Materials

Code	Filling	Density (kg m ⁻³)	Thickness (mm)
ACM_PE1	PE	1400 (950*)	4
ACM_PE2	PE	1375 (925*)	4
ACM_FR1	PE with FR	1900 (1625*)	4
ACM_FR2	PE with FR	1900 (1650*)	4
ACM_FR3	PE with FR	1900 (1600*)	4
ACM_NC1	Mineral filled	1900 (1625*)	4
ACM_NC2	Corrugated aluminium	1100	4
HPL_PF	High pressure laminate (phenol formaldehyde)	1350	10
HPL_FR	High pressure laminate (phenol formaldehyde FR)	1350	8
MWB_1	Mineral wool board	1200	8
MWB_2	Mineral wool board	1250	9

*Measured density of filler material excluding aluminium

Table 2 Insulation Materials

Code	Description	Density (kg m ⁻³)
PF1	Phenolic foam	42.8
PF2	Phenolic foam	41.8
PF3	Phenolic foam	45.0
PIR1	PIR foam	32.4
PIR2	PIR foam	35.0
PIR3	PIR foam	35.0
SW	Stone wool	37.0 (78.0)*
GW	Glass Wool	36.0

*Value reported is of lower density (insulating) layer, value in brackets is density of higher density external facing layer.

For the ACM products, the aluminium sheets were removed in order to investigate the composition and micro-scale thermal decomposition of the filling material.

Elemental Analysis: Outer-screen products, fillings for ACM products, and insulation boards were subject to elemental analysis using CHNS (Thermo Scientific Flash 2000 Organic Elemental Analyser), SEM-EDAX (FEI Quanta 200), and X-Ray fluorescence (Bruker Trace IV-SD handheld XRF) at 25 keV.

Polymer Characterisation: The polymeric filling of the ACM_PE, ACM_FR and ACM_NC samples were characterised by diamond-attenuated total reflectance-FTIR spectrophotometry using a Nicolet IS 5 FTIR.

Thermal Analysis: Samples of around 10 mg were subjected to thermogravimetric analysis (TGA) in air and nitrogen in a Stanton Redcroft STA 780, and differential scanning calorimetry (DSC) in a TA Instruments 2920, all at a heating rate of 10 °C min⁻¹.

Bomb Calorimetry: The gross heat of combustion was measured in an oxygen bomb calorimeter (Parr 6200) according to ISO 1716:2002, running 2 replicate tests for each sample.

Microscale Combustion Calorimetry: Samples of around 2 to 3 mg were decomposed under pyrolysis and oxidative conditions (Method A and B in ASTM D7309 respectively) [13].

Cone Calorimetry: All samples were tested at an applied heat flux of 50 kW m⁻², following ISO 5660 [14]. In order to investigate the burning behaviour of panel materials covered on both sides with 0.5 mm aluminium sheet, a novel methodology was devised, allowing the combustible contents to be ignited, while still testing a section of the whole panel. Outer-screen products of 70 x 70 mm², were placed centrally with the painted side uppermost in the 100 x 100 mm² sample holder. However, the results have been re-scaled so they are presented in kW m⁻². ACM products were tested complete with the aluminium sheets. The insulation materials were tested as blocks of 20 x 100 x 100 mm³ cut from the larger boards, without the external aluminium foil facing. All samples were tested without the upper retaining frame. Where foam samples showed significant distortion, they were held in place using a wire grill specified in ISO 5660.

Smoke Toxicity: The smoke toxicity of the insulation materials was determined using the steady state tube furnace (SSTF), following ISO TS 19700 [6] under the three flaming fire conditions described in ISO 19706 [7]: well-ventilated (stage 2); small under-ventilated (3a); and large under-ventilated (3b).

3 Results

3.1 Microscale Decomposition

In the immediate aftermath of the Grenfell Tower fire, the UK government were advised to commission a series of initial screening tests on the combustibility of ACM filling samples taken from high-rise buildings [15] using bomb calorimetry. A summary of the findings from this screening is presented in the discussion. The heats of combustion of all products were measured using bomb calorimetry and microscale combustion calorimetry (MCC). The thermal decomposition in air and nitrogen was investigated for all ACM filling materials, outer-screen and insulation products. The data and commentary appears in SM.

3.1.1 Bomb Calorimetry and Microscale Combustion Calorimetry (Method B)

Table 3 shows the heat of combustion of each façade product or its filling (for ACM) determined by bomb calorimetry and MCC method B. The results show good agreement with the UK government data [12] and reasonable agreement between the bomb calorimeter and MCC method B, for the panel materials, discussed further in SM. The results show the very large contribution to heat release during combustion (measured by either method) from PE filled ACM and the significant reduction of adding 60% or more filler. The results also show the significant heat release of the plastic foam insulation per unit mass. The data are used to estimate the relative contributions to façade fires.

Table 3 Heat release of façade materials by bomb calorimetry and microscale combustion calorimetry (Method B)

Sample	Heat of Combustion: Bomb calorimetry /kJ g ⁻¹	Heat of Combustion: Microscale combustion calorimetry /kJ g ⁻¹
ACM_PE1	46.2	43.6
ACM_PE2	46.5	43.0
ACM_FR1	13.8	12.4
ACM_FR2	14.2	11.8
ACM_FR3	13.9	12.8
ACM_NC1	3.4	2.2
ACM_NC2	*	5.2
HPL_PF	21.3	19.3
HPL_FR	19.8	18.2
MWB_1	4.2	3.8
MWB_2	2.8	3.3
PF1	27.2	18.2
PF2	26.3	17.7
PF3	27.2	16.4
PIR1	28.1	21.9
PIR2	31.4	18.3
PIR3	29.8	23.7
SW	**	1.56
GW	2.43	1.95

* Corrugated aluminium could not be tested by bomb calorimetry as the metal oxidised too vigorously.

** A positive value of the heat of combustion could not be obtained from the stone wool sample, suggesting a very low binder content.

3.1.2 Microscale Combustion Calorimetry (Method A)

The rate of heat release following anaerobic pyrolysis of the panel fillings is shown in Figure 2, with a peak of heat release under pyrolysis conditions for all ACM filler materials just below 500°C. Method A is considered to be more representative of fire behaviour [16], as there is no oxygen between the flame and the fuel. The large and sharp peak of the PE filling is very significant, both to this work, and the Grenfell Tower fire. The total heat release is the area under each curve, and the peak is the pyrolysis temperature. For ACM, it shows the contribution different filler loadings make to the heat release rate, and that the peak decomposition temperature of the polymeric fuel is always close to 500 °C, except for the HPL products (HPL_PF, 350 °C and HPL_FR, 290 °C).

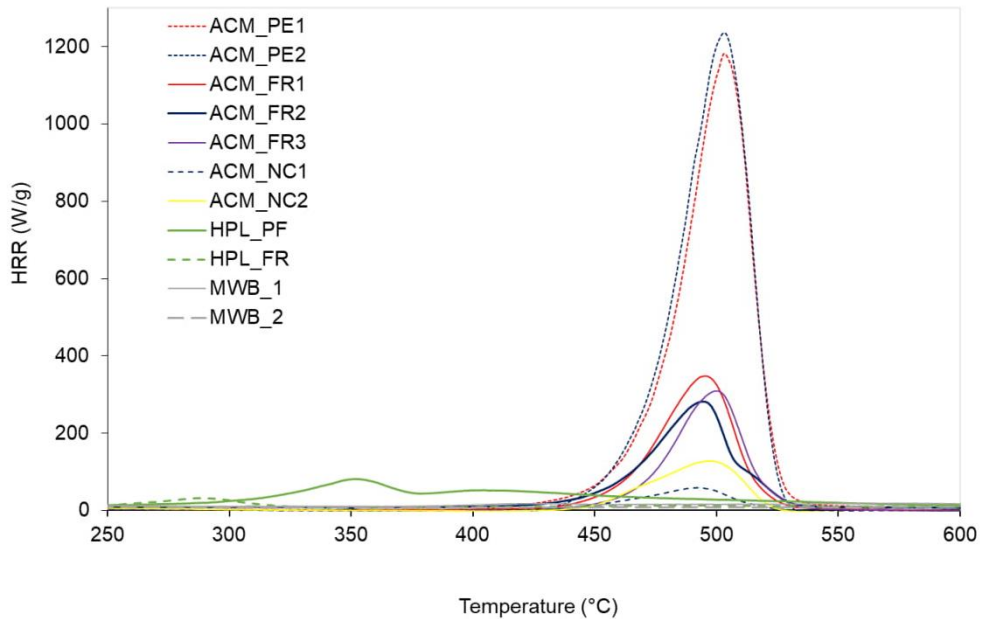


Figure 2 Heat release of panel filling material by MCC Method A

Figure 3 shows very different rate of heat release data for the insulation, with much more gradual heat release occurring over the full temperature range (70 to 700 °C), compared to the outer-screen materials, and distinct peaks at 300 to 400 °C for PIR foams and at 500 °C for phenolic foams. The steady low heat release from the binders of the stone and glass wool show clear differences between these products and the foams.

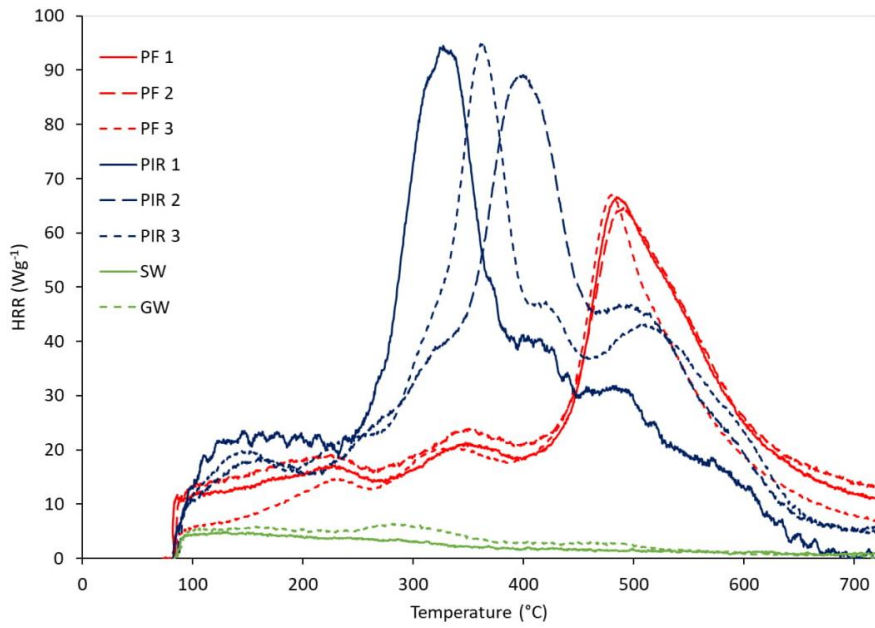


Figure 3 Heat release of insulation materials by MCC Method A (note the use of different scales to Figure 2).

3.2 Bench-Scale burning behaviour

3.2.1 Panel Products

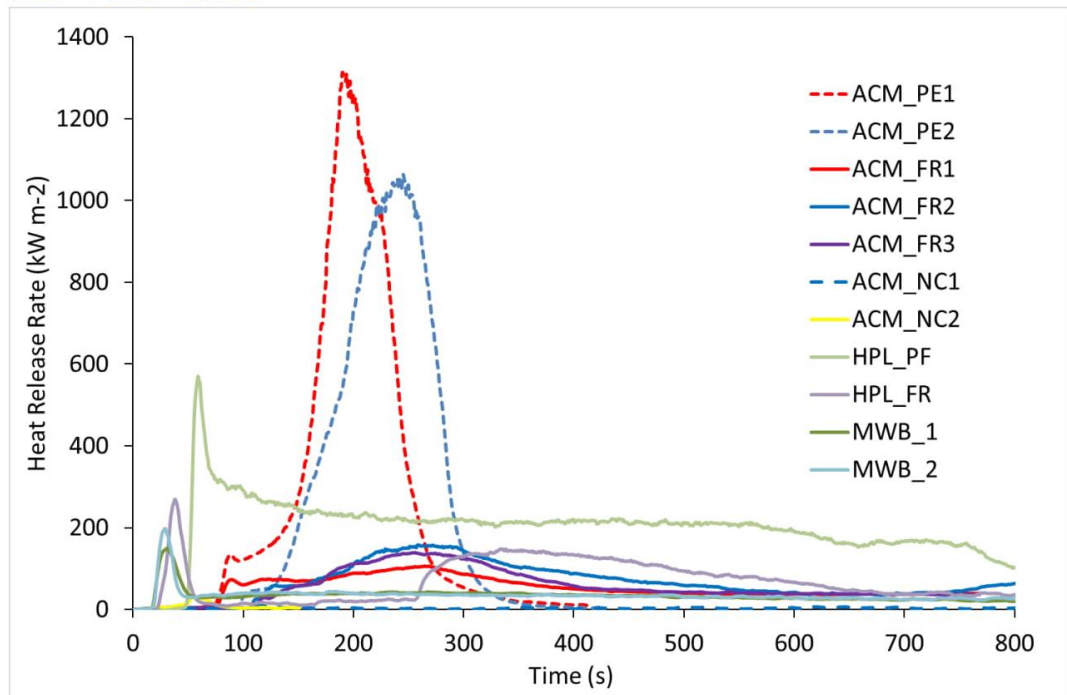


Figure 4 HRR of 70 x 70 mm² panels in the cone calorimeter at 50 kW m⁻².

The novel methodology for testing sections of panel proved effective in assessing their contribution to the façade's flammability. The heat release rate (HRR) in cone calorimetry (Figure 4) shows notable differences in combustibility of the different panels. All of the panel materials ignited in the cone calorimeter, although this only appeared to involve the paint finish for ACM_NC1 and NC2 and MWB_1 and MWB_2. High, sharp peaks of heat release rate were observed for ACM_PE1 and ACM_PE2, reaching a maximum of 1300 and 1050 kW m⁻² at 190 and 250 s respectively. Moreover, ACM_PE1 and ACM_FR1, both from the same manufacturer, showed a notably earlier time to ignition than their competitor panels. Given this similarity of the TGA curves for these fillings, this suggests a thicker or more easily ignited paint layer, or a difference in absorptivity of radiant heat after the paint layers were burnt off. Almost no residue remained between the aluminium plates after the test for PE1 and PE2. The ACM_FRs underwent sustained flaming, but with a significantly lower HRR. It is clear that the combination of the protective aluminium sheets, and the metal hydroxide fire retardant at around 65% loading effectively reduces the flammability under these conditions. The Al(OH)₃ of ACM_FR2 is notably less effective than the Mg(OH)₂ of ACM_FR1 and ACM_FR3 at similar loadings.

3.2.2 Insulation

All the insulation foams show very rapid ignition and early peak HRR. However, the highest peaks are an order of magnitude less than those of the ACM_PE. Figure 5 shows clear differences between the burning behaviour of PIR and phenolic foams. The PIRs show a higher initial peak HRR and lower steady burning rate, after formation of a protective char layer; the phenolic foams show a lower initial peak HRR but a higher steady burning rate. PIR2 was cut just below the glass wool layer; PIR2* was cut just above the glass wool layer to investigate its effect on the burning behaviour. This shows a slightly lower first peak HRR, but surprisingly, an enhanced second peak, at around 60 s. A summary table of the parameters measured by cone calorimetry and a commentary on the data is provided in SM. A cone calorimetric study [17] of three commercial PIR and one phenolic foam showed similar results to those above, but highlighted the importance of the protective char layer on the burning behaviour.

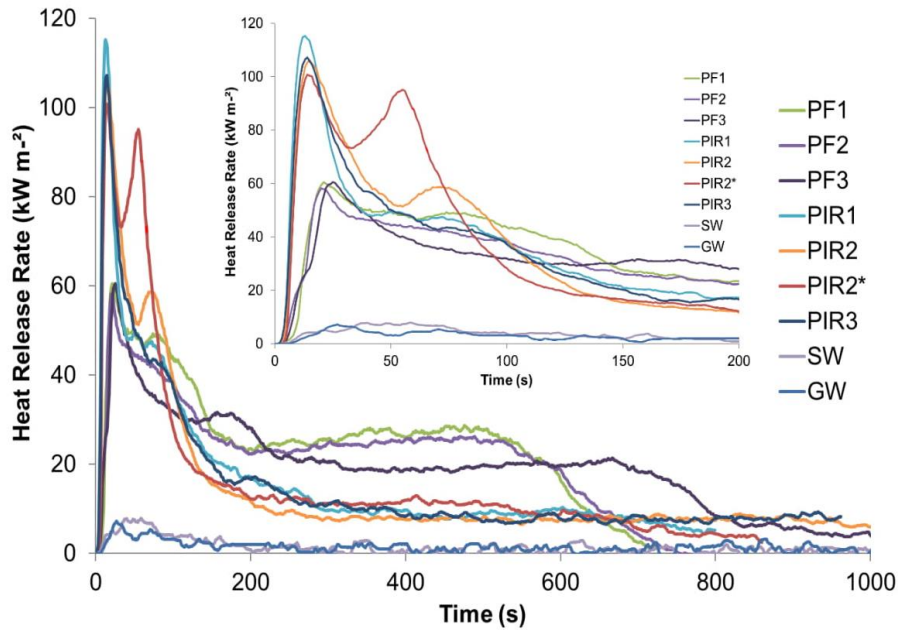


Figure 5 HRR of insulation materials in the cone calorimeter at 50 kW m^{-2} . Inset shows early detail.

The effect of ACM PIR combination

A qualitative experiment demonstrated the effect of combining ACM with PIR in a façade. A piece of ACM_PE ($70 \times 70 \text{ mm}^2$) was suspended 50 mm above a block of PIR ($100 \times 100 \times 75 \text{ mm}^3$). Both products were mounted with their faces vertical. The ACM was heated with a small Bunsen flame until drips of the molten PE ignited. These fell onto the PIR and caused almost immediate ignition of the foam. The combination of the burning foam and the dripping PE rapidly led to self-sustaining combustion of the combination. This is illustrated in Figure 6.

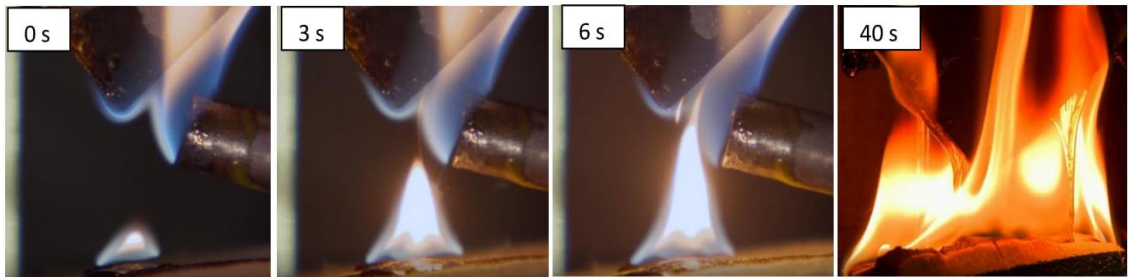


Figure 6 Ignition of PIR by burning drips from ACM_PE showing time after first flaming drip.

3.3 Bench-Scale Smoke Toxicity

The SSTF yields are shown in Table 4. Each insulation product was burnt under three fire conditions, representing well-ventilated (ISO fire stage 2), small under-ventilated (3a) and large under-ventilated (3b). Only insulation products were investigated. The smoke toxicity of ACM fillings, and the yield data for insulation is discussed further in SM.

The HCN yields for phenolic foam are low, corresponding to their low nitrogen content, but increase with under-ventilation. The HCN yields for the PIR are significantly larger and increase by a factor of 2 to 4 in the transition from well-ventilated to under-ventilated.

The mineral wool insulation did not ignite, so its non-flaming combustion cannot be compared directly to the flaming combustion of the foams. However, they were tested under the three conditions used here for the combustible materials for completeness. The yields are all very low, as may be expected, and correspond to a small amount of binder, as seen in TGA and MCC etc. An attempt [18] to use the controlled atmosphere cone calorimeter [19] to assess the fire behaviour of PIR foam in under-ventilated conditions produced mixed results. As expected, the mass-loss fell with decreasing oxygen concentration, but surprisingly, the CO and HCN yields also fell, while the hydrocarbon yields increased, showing that flaming combustion was not the predominant gas phase process.

Table 4 SSTF yield data 1

Sample	ISO Fire Stage	Mass loss %	CO ₂ Yield g/g	CO Yield g/g	HCN Yield g/g	HCl	NO	NO ₂	H ₃ PO ₄
PF1	2	97.5	2.509 ± 0.049	0.023 ± 0.007	<0.001	0.001 ± 0.0001	<0.001	<0.001	<0.001
	3a	72.7	0.495 ± 0.016	0.320 ± 0.003	0.001 ± <0.0001	0.002 ± 0.0001	<0.001	<0.001	<0.001
	3b	72.3	0.630 ± 0.029	0.280 ± 0.033	0.001 ± 0.0001	0.007 ± 0.0006	<0.001	<0.001	0.002 ± 0.0002
PF2	2	98.1	2.094 ± 0.351	0.031 ± 0.007	<0.001	0.005 ± 0.0007	<0.001	<0.001	<0.001
	3a	75.7	0.511 ± 0.019	0.282 ± 0.011	0.002 ± 0.0001	0.001 ± 0.0001	<0.001	<0.001	<0.001
	3b	73.7	0.638 ± 0.058	0.229 ± 0.028	0.005 ± 0.0008	0.004 ± 0.0006	<0.001	<0.001	0.002 ± 0.0003
PF3	2	95.7	2.529 ± 0.099	0.028 ± 0.022	<0.001	<0.001	<0.001	<0.001	<0.001
	3a	66.1	0.473 ± 0.072	0.317 ± 0.006	0.003 ± 0.0002	0.001 ± 0.0001	<0.001	<0.001	0.003 ± 0.0002
	3b	63.6	0.562 ± 0.187	0.223 ± 0.014	0.003 ± 0.0003	0.001 ± 0.0001	<0.001	<0.001	0.001 ± 0.0001
PIR1	2	95.3	2.077 ± 0.045	0.106 ± 0.028	0.006 ± 0.0003	0.008 ± 0.0004	<0.001	<0.001	<0.001
	3a	76.6	0.610 ± 0.040	0.217 ± 0.070	0.011 ± 0.0009	0.005 ± 0.0004	0.001 ± 0.0001	<0.001	<0.001
	3b	78.9	0.554 ± 0.025	0.416 ± 0.048	0.015 ± 0.0008	0.003 ± 0.0002	0.002 ± 0.0001	<0.001	0.001 ± 0.0001
PIR2	2	92.0	2.376 ± 0.080	0.014 ± 0.007	0.004 ± 0.0001	0.013 ± 0.0004	<0.001	<0.001	<0.001
	3a	75.9	0.447 ± 0.013	0.340 ± 0.031	0.017 ± 0.0010	0.006 ± 0.0003	0.003 ± 0.0002	<0.001	<0.001
	3b	74.4	0.520 ± 0.061	0.341 ± 0.085	0.014 ± 0.0032	0.007 ± 0.0016	0.001 ± 0.0002	<0.001	<0.001
PIR3	2	94.4	2.375 ± 0.024	0.037 ± 0.014	0.004 ± 0.0002	0.019 ± 0.0011	<0.001	<0.001	0.002 ± 0.0001
	3a	77.4	0.511 ± 0.054	0.331 ± 0.049	0.014 ± 0.0006	0.006 ± 0.0003	0.002 ± 0.0001	<0.001	0.001 ± 0.0001
	3b	78.9	0.652 ± 0.056	0.249 ± 0.025	0.014 ± 0.0004	0.004 ± 0.0001	<0.001	<0.001	<0.001
SW*	2 – NF	1.77	0.027 ± 0.007	0.010 ± 0.002	<0.001	<0.001	<0.001	<0.001	<0.001
	3a – NF	1.67	0.020 ± 0.006	0.009 ± 0.001	<0.001	<0.001	<0.001	<0.001	<0.001
	3b – NF	1.64	0.051 ± 0.011	<0.001	<0.001	<0.001	<0.001	<0.001	<0.001
GW*	2 – NF	6.21	0.093 ± 0.018	0.018 ± 0.003	<0.001	<0.001	<0.001	<0.001	<0.001
	3a – NF	8.63	0.144 ± 0.015	0.011 ± 0.001	<0.001	<0.001	<0.001	<0.001	<0.001
	3b – NF	12.7	0.189 ± 0.024	<0.001	<0.001	<0.001	<0.001	<0.001	<0.001

* Also tested at 900°C but did not ignite; NF = not flaming

4 Discussion

Table 5 summarises the conclusions from the compositional analysis of the outer-screen products and fillings, based on manufacturer's information, analytical data and the reasoning presented in SM. The information is necessary in order to interpret their fire behaviour.

Table 5 Conclusions of screen product composition investigation

Code	Filling/Composition
ACM_PE1	LDPE (100%)
ACM_PE2	LDPE (100%)
ACM_FR1	LDPE with 65-70% Mg(OH) ₂
ACM_FR2	LDPE with 64-69% Al(OH) ₃
ACM_FR3	LDPE with 65-71% Mg(OH) ₂
ACM_NC1	LDPE (5%), Al(OH) ₃ (15%), Mg(OH) ₂ (33%), CaCO ₃ (45%)
ACM_NC2	Aluminium (86%), epoxy resin (14%)
HPL_PF	Wood fibre bound with phenol-formaldehyde resin
HPL_FR	Fire retarded version of HPL_PF
MWB_1	Mineral fibre and organic binder (16%)
MWB_2	Mineral fibre and organic binder (9%)

The insulation materials are adequately described by the manufacturer's generic descriptions in Table 2.

The thermal decomposition data (from TGA) presented in SM, show good agreement with the micro-scale combustion data from MCC and bomb calorimetry. For the fillings, heat releases around 45, 13 and 3 kJ g⁻¹ and mass losses of 95, 50 and 15% at 700 °C in nitrogen or air were found for the PE, FR and NC fillings respectively. The disproportionately higher mass losses for the FR materials correspond to the presence of aluminium and magnesium hydroxides which dehydrate on heating. For the insulation materials, the heat release in the bomb calorimeter is greater, mainly due to the more severe oxidation conditions than in the MCC. However, significantly less heat is released by the glass or stone wool samples than the combustible foams.

4.1 Calculation of energy release.

The heat release on complete combustion of the façade system has been estimated from its chemical composition and literature values, and from the measured values reported above. The façade system on the Grenfell Tower consisted of 3 mm PE sandwiched between two 0.5 mm sheets of aluminium on the outer face, with 160 mm of PIR insulation on the external face of the concrete. Using literature values for the density and heat of combustion of PE, PIR and aluminium respectively of 0.95 g cm⁻³ and 43 kJ g⁻¹; 0.0332 g cm⁻³ and 25 kJ g⁻¹; and 2.7 g cm⁻³ and 31 kJ g⁻¹, the heat release per unit area of façade on complete combustion of the PE is 123 MJ m⁻², for PIR it is 132 MJ m⁻², and for aluminium it is 84 MJ m⁻². Thus, on complete combustion, each square metre of the façade system can contribute 255 MJ (excluding aluminium) to 339 MJ (including aluminium) to the fire. Photographs of the burning Tower show falling sheets of aluminium and the debris at the foot of the Tower is littered with pieces of aluminium sheet [10], so it seems reasonable to conclude that the aluminium did not make a significant contribution to the heat release *in situ*.

In order to understand the burning behaviour of different combinations of building products, estimates of peak and total heat release have been made from small-scale tests. Table 6 shows the contribution to the heat release from each component of the façade system, as measured in the current work, using data on physical properties from Table 1 and 2, MCC,

Table 3, and cone calorimetry, Table S2, employing the approach described above. All insulation was calculated as 100 mm thick corresponding to the government tests [12].

Table 6 Potential heat release from each component of the façade system

Sample	Cone calorimeter data		MCC data
	Peak HRR /kW m ⁻²	Total heat release /MJ m ⁻²	Total heat release /MJ m ⁻²
ACM_PE1	1364	105.4	124
ACM_PE2	1123	106.6	119
ACM_FR1	123	59.6	60
ACM_FR2	195	70.9	58
ACM_FR3	144	65.07	61
ACM_NC1	13.8	2.57	11
ACM_NC2	30.2	0.87	17
HPL_PF	530	172.71	260
HPL_FR	263	67.49	196
MWB_1	150	37.03	36
MWB_2	194	27.75	38
PF1	63.7	18.71	78
PF2	62.0	17.56	74
PF3	64.8	19.67	74
PIR1	116	13.33	71
PIR2	106	15.6	64
PIR3	107	14.5	83
SW	5.6	0.06	9
GW	8.7	0.67	7

4.1.1 Correlation of micro- and bench-scale results to DCLG tests

In order to link the government test results [12] to the fire behaviour observed in this study, the potential contribution to flame spread has been estimated, based on the data measured here. Two methodological approaches were used. The first calculated the total energy release from the heat of

combustion data, per m² of façade, from MCC method B data, and cone calorimetry. The second used the sum of the pHRR from the products, in kW m⁻² from cone calorimetry, since the pHRR drives fire growth [20]. Table 7 shows the potential heat release by each component of the façade system used in the government BS8414-1 tests. A critique of the BS 8414 standard, the BR 135 criteria, and the DCLG tests has been reported elsewhere [21].

Table 7 Predicted behaviour of combinations of façade components, and comparison with government test results [12], in order of fire performance

Test number	Products in test	UK government test result (BS8414-1)	Σ(Heat of combustion per unit area) MCC method B / kW m ⁻²	Σ(Heat of combustion per unit area) cone calorimeter / kW m ⁻²	Σ(Peak Heat Release Rate) cone calorimeter / kW m ⁻²
1	ACM PE + PIR	Test stopped (9 min)	188	121	1471
2	ACM PE + SW	Test stopped (7 min)	134	105	1370
3	ACM FR + PIR	Test stopped (25 min)	125	75	230
7	ACM FR + PF	Test stopped (28 min)	134	77	185
4	ACM FR + SW	Test passed	70	60	129
5	ACM NC + PIR	Test passed	75	18	120
6	ACM NC + SW	Test passed	20	3	19

This very crude assessment is based on the large contribution to the peak of heat release from the PE flowing out of the ACM and the smaller contribution to peak heat release rate from the burning insulation material. The ACM_FR + PF of test 7 performed better than the ACM_FR and PIR of test 3 inasmuch as the thermocouples recorded a 600 °C rise for 30 seconds at 1530 s, rather than 1220 s, although the test criteria [22] only consider temperatures exceeding 600 °C for the first 15 min (900 s) of the test.

In the aftermath of the Grenfell Tower fire, the test results for three other cladding systems meeting the test criteria were made publicly available: two use stone wool, one with ACM_FR, the other with ACM_NC, for which our simple method predicts a pass. Another system used ACM_FR with PF insulation, similar to that which failed in the government tests due to “flame spread above the test apparatus”. This system has the lowest total peak HRR from cone calorimetry (212 kW m⁻²) of those failing the government test. Thus, the use of total peak HRR from cone calorimetry or MCC appears to be as good a predictor of behaviour in rainscreen façade systems as the BS 8414-1 test. The cost of these tests is around 0.01 of the large-scale tests.

No BS 8414-1 test reports appear to have been made publically available for HPL screened systems, although they are widely used in rainscreen systems on multi-storey residential buildings. Using the data reported here, and the thresholds for passing the DCLG test, the performance in the large-scale test of HPL_PF, HPL_FR and MWB1 and 2 outer-screens and different insulation products is predicted in Table 8. The intermediate values in Table 7 for heat of combustion in MCC, 100 kW m⁻², cone calorimeter, 68 kW m⁻², and peak HRR, 157 kW m⁻² have been used as pass/fail criteria.

It is apparent that none of the HPL_PF or HPL_FR screened systems would be expected to pass using any of the three criteria, while consistent predictions were not found from any of the MWB

combinations, except MWB1 with SW. Since the peak HRRs for MWB screens result from burning paint, they are probably unrepresentative of the large-scale test performance.

Thus, the differences in fire behaviour between the combustible materials and non-combustible materials are so great that they can easily be quantified using tests costing hundreds of pounds or less, rather than the tens of thousands of pounds required to run a single BS 8414-1 test. In addition, the robustness of the bench-scale material tests prevents misleading test results from being reported, based on optimising the design of the façade system to pass the test, irrespective of how representative it is of actual building façades. It is important to note that the design and construction of the façade for the test is normally the responsibility of the product manufacturer, not the test laboratory. The Forum of Fire Testing Laboratories [23] proposed the use of microscale decomposition and numerical models to replace large-scale fire tests, and thus eliminate these sorts of problems, over a decade ago.

Table 8 Predicted behaviour of combinations of façade with HPL panels

Products in test	Σ (Heat of combustion per unit area) MCC method B / kW m ⁻²	Pass/Fail (Pass < 100)	Σ (Heat of combustion per unit area) cone calorimeter / kW m ⁻²	Pass/Fail (Pass < 68)	Σ (Peak Heat Release Rate) cone calorimeter / kW m ⁻²	Pass/Fail (Pass < 157)
HPL_PF + PIR	324	✗	188	✗	636	✗
HPL_PF + SW	270	✗	173	✗	535	✗
HPL_PF + PF	334	✗	190	✗	592	✗
HPL_FR + PIR	261	✗	83	✗	370	✗
HPL_FR + SW	206	✗	68	✗	269	✗
HPL_FR + PF	270	✗	85	✗	325	✗
MWB1 + PIR	101	✗	53	✓	256	✗
MWB1 + SW	46	✓	37	✓	155	✓
MWB1 + PF	110	✗	55	✓	212	✗
MWB2 + PIR	102	✗	43	✓	300	✗
MWB2 + SW	47	✓	28	✓	199	✗
MWB2 + PF	112	✗	45	✓	256	✗

In a study sponsored by the insulation manufacturer, Kingspan, Guillaume [24] argues that only the fire performance of the whole façade need be considered, not the individual components. The tests used a 2.4 m ACM rainscreen façade (following ISO 13785-1), fitted with cavity barriers, using a fire source of 100 kW and a 2 mm aluminium protective L-profile, and only the ACM made a significant contribution to the burning behaviour. However, the test claims to be a 1/30th-scale BS8414-1, while the fire source is only 1/30th of BS8414-1, which does not test the façade system adequately.

4.2 Smoke Toxicity

As discussed in SM, the fire condition and hence the toxicity of burning ACM fillings on the side of a building is too difficult to predict from bench-scale experiments. The burning of the PIR and phenolic foam behind the ACM on Grenfell Tower would almost certainly have been under-ventilated (uv) between fire stages 3a and 3b. Figure 7 shows the relative contribution to incapacitation of HCN and CO from burning 1 kg of insulation material after 5 min exposure under the stated fire condition with the effluent dispersed over a volume of 50 m³ (a large room or small apartment) based on ISO 13571. Burning this amount of phenolic foam in uv conditions is predicted to cause incapacitation to somewhat less than 50% of the exposed population, as the FED is less than one. However, burning this amount of any of the three PIR foams used in this study would exceed the threshold for incapacitation by a factor of between 2 and 4 in uv conditions. The higher toxicity of PIR results from the presence of nitrogen in the polymer, which forms HCN on burning, particularly in uv conditions. Once incapacitation has occurred (in this case HCN causes loss of consciousness), the victim can no longer effect of their own escape, and unless rescued, will continue to uptake CO and HCN until breathing ceases.

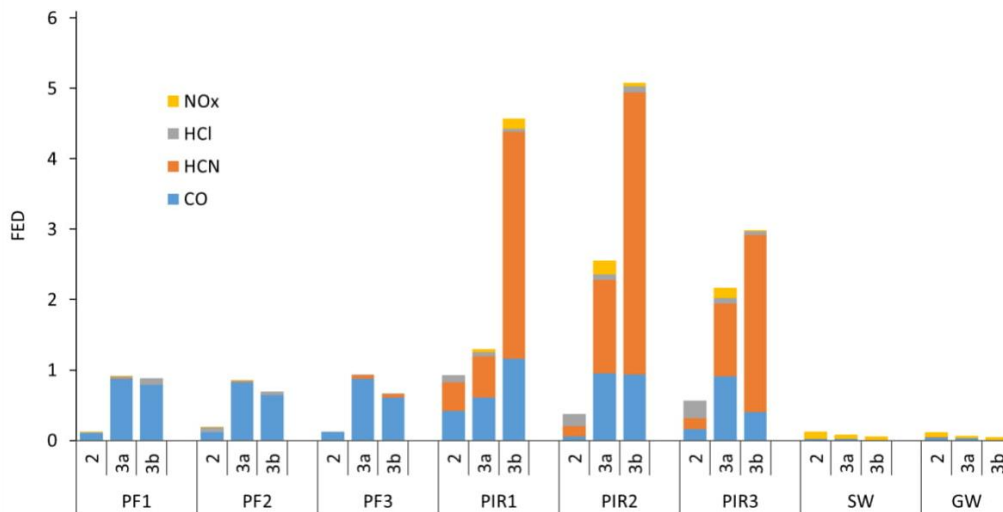


Figure 7 FED for incapacitation following 5 minutes exposure from burning 1 kg with the effluent dispersed in a volume of 50 m³.

Figure 8 shows the prediction of lethality from the same effluents. This shows a similar trend to that of incapacitation in Figure 7, but the relative contribution of HCN to CO is reduced. However, HCN still makes a significant contribution to the toxicity of the effluents from all the foams, far exceeding the toxicity from CO for under-ventilated burning of the PIR foams. The FED for lethality is calculated from ISO 13344, based on a 30 min exposure time. The low levels of binder in SW and GW generate correspondingly low levels of asphyxiants, and low toxicity. Coupled with their inability to propagate combustion, this shows why they are a safe alternative to combustible insulation. The material-IC₅₀ and material-LC₅₀ values discussed in SM and shown in Table S4 provide the most direct route to estimating a safe loading of insulation material.

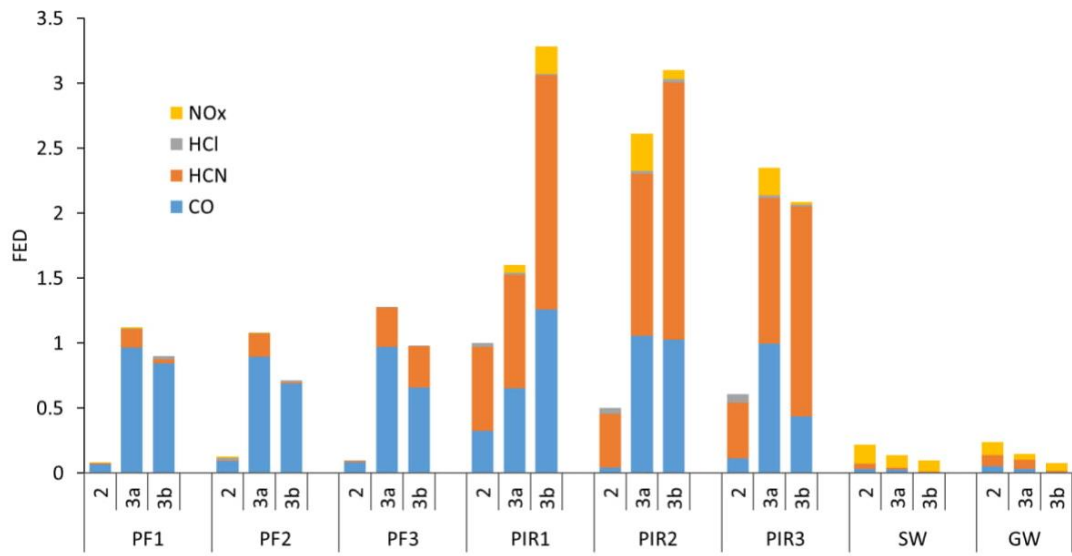


Figure 8 30 min lethal FED (ISO 13344) from burning 1 kg with the effluent dispersed in a volume of 50 m³.

4.3 The extent of the ACM problem

The government has established that there are 478 residential buildings over 18m with ACM cladding [15] in England. 150 are in private ownership and are believed to be non-compliant, but fuller data is unavailable. Figure 9 shows that for the remaining 328, 85% have ACM_PE combined with combustible foam (29%), mineral wool (34%) and unknown (23%). A minority (14%) have ACM_FR with different types of insulation, but none have ACM with a non-combustible core (ACM_NC).

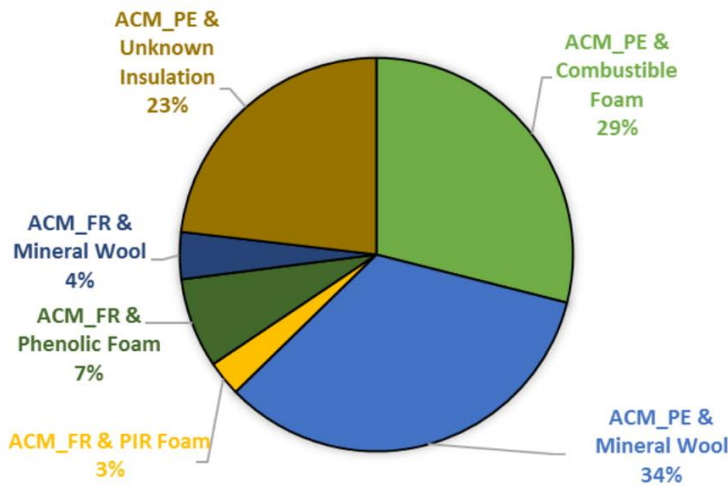


Figure 9 Tall buildings in England with ACM panels

Of the 328 buildings for which data is available, 316 do not comply with the UK Building Regulations. Of the non-compliant buildings, half are social housing (50%) with the remainder divided between student residences, and other public and private buildings, Figure 10.

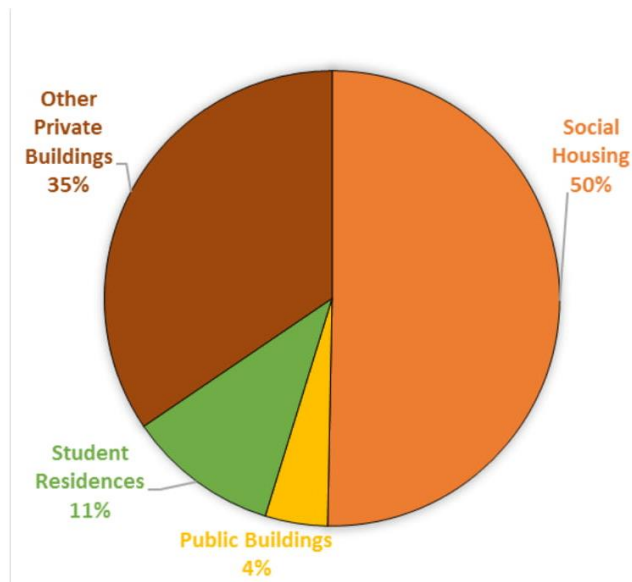


Figure 10 Use of tall buildings not meeting Building Regulations

A consultation document on the future of desktop studies (described in SM) showed that the government expected around 600 tall buildings per year to have combustible façades [25]. This includes buildings with rainscreen (or ventilated) façades clad with HPL etc., and External Thermal Insulation Composite Systems (ETICS) type façades, where a lightweight cement render covers the combustible insulation. Since combustible building exteriors have been permitted since 2006, if they became established building practice 10 years ago, this estimate suggests there could be as many as 6000 buildings over 18 m in England with combustible façades.

5 Conclusions

In the aftermath of the Grenfell Tower tragedy there are a number of unanswered questions. This study came about because of the lack of published information relating to the composition, decomposition and fire behaviour of available façade products, and the dependence on controversial large-scale tests. This paper provides that crucial information, and demonstrates its relationship to large-scale test performance. Moreover, the data show good consistency between scales and different decomposition conditions. It highlights large differences in fire behaviour between different products, both for outer-screens and insulation boards.

By comparing similar products of the same generic type (e.g. ACM_FR, or PIR) it shows that there is little difference in the decomposition and burning behaviour for that product type, and also in the case of the insulation materials, in the smoke toxicity.

The bench-scale burning behaviour shows the most dramatic differences between the ACM_PE and the ACM_FR and ACM_NC materials. This illustrates clearly how ACM_PE contributes to very rapid fire spread when used to clad the exterior of a building. It also identifies a potential problem with HPL_PF. The bench-scale burning behaviour of the PIR and PF shows the contrasting effect of the more resilient char on the PIR (higher initial peak followed by lower HRR) compared to the PF (lower peak HRR but a higher steady HRR). This difference is demonstrated by the TGA in air, where the mass loss rate of the PIR is initially higher, but around 450 °C the PF overtakes it. The lack of heat release from the stone and glass wool materials is expected, but is crucially important in understanding how to prevent further tragedies, demonstrating the existence of alternative non-combustible insulation materials.

In the under-ventilated conditions of flaming within the cavity, the smoke toxicity data show a factor of 3 increase for PIR, compared to PF. The non-combustible GW and SW products show smoke toxicity lower than the PIR by a factor of around 15. Again, these results have very clear implications for those selecting products to ensure the fire safety of occupants.

The simple additive models of total heat release and peak HRR underline the effects of large differences in fire behaviour, and allow elimination of the most dangerous combinations from façades. In contrast, the qualitative demonstration of PIR ignition by flaming drips of PE from ACM serves as a warning to treat systems as a whole, rather than the sum of their individual parts, since one component can interact synergistically or antagonistically with any other. The evidence presented in this paper challenges the statements such as “the test results with regard to heat release rates, smoke and toxic gas emissions show that the organic polyisocyanurate insulation and the mineral fibre insulation behave similarly during the fire” made by the combustible foam industry [26], that their insulation products do not constitute a safety hazard

If the data in this paper had been readily available, it may have contributed to the prohibition of combustible materials on the outside of tall buildings, as they are in most of Europe, and this tragedy could not have occurred. In the UK, the building fire regulations have just been modified to ban the use of combustible materials on the outside of tall buildings (November 2018) [27].

5.1 Acknowledgements

SO would like to thank the University of Bologna for funding a student exchange. No other external funding from any source was used to support this project.

-
- [1] UK Fire Statistics 2017 and preceding editions, Home Office, London, <https://www.gov.uk/government/collections/fire-statistics> (accessed 8/12/2018)
 - [2] Hall, J. R., *Fatal Effects of Fire*, National Fire Protection Association, Quincy, MA, (2011).
 - [3] ISO 13571:2012 Life-threatening components of fire - Guidelines for the estimation of time to compromised tenability in fires, ISO, Geneva.
 - [4] ISO 13344:2015, Estimation of the lethal toxic potency of fire effluents, ISO, Geneva.
 - [5] Hull, T.R., Stec, A.A., Lebek, K., Price, D., Factors affecting the combustion toxicity of polymeric materials, (2007), *Polym. Degrad. and Stab.*, 92 (12), pp. 2239-2246. <https://doi.org/10.1016/j.polymdegradstab.2007.03.032>
 - [6] ISO/TS 19700:2016 Controlled equivalence ratio method for the determination of hazardous components of fire effluents - Steady-state tube furnace, ISO, Geneva.
 - [7] ISO 19706:2011 Guidelines for assessing the fire threat to people, ISO, Geneva.
 - [8] Woolley, W.D., Raftery, M.M., Smoke and toxicity hazards of plastics in fires, (1975) *J. Hazard. Mater.*, 1 (3), pp. 215-222. [https://doi.org/10.1016/0304-3894\(75\)80014-8](https://doi.org/10.1016/0304-3894(75)80014-8)
 - [9] Anna A Stec and T Richard Hull, *Assessment of the fire toxicity of building insulation materials*, *Energy and Buildings*, 43, 498–506, (2011). <https://doi.org/10.1016/j.enbuild.2010.10.015>
 - [10] Dr Barbara Lane, Expert Witness Report, <https://www.grenfelltowerinquiry.org.uk/evidence/dr-barbara-lanes-expert-report> (accessed 25/06/2018).
 - [11] Hull, T.R., Witkowski, A., Hollingbery, L., Fire retardant action of mineral fillers, (2011) *Polym. Degrad. and Stab.*, 96 (8), pp. 1462-1469. <https://doi.org/10.1016/j.polymdegradstab.2011.05.006>
 - [12] DCLG fire test reports (2017): <https://www.gov.uk/government/news/latest-large-scale-government-fire-safety-test-result-published> (accessed 8/12/2018)
 - [13] ASTM D7309-13, Standard Test Method for Determining Flammability Characteristics of Plastics and Other Solid Materials Using Microscale Combustion Calorimetry, ASTM International, West Conshohocken, PA, 2013,
 - [14] ISO 5660-1:2015 Reaction-to-fire tests — Heat release, smoke production and mass loss rate — Part 1: Heat release rate (cone calorimeter method) and smoke production rate (dynamic measurement), ISO, Geneva.
 - [15] MHCLG Building Safety Programme: Monthly Data Release – August 2018, and preceding editions. <https://www.gov.uk/government/publications/building-safety-programme-monthly-data-release-august-2018> (accessed 8/12/2018)
 - [16] Schartel, B., Hull, T.R., Development of fire-retarded materials - Interpretation of cone calorimeter data, (2007) *Fire and Mater.*, 31 (5), pp. 327-354. <https://doi.org/10.1002/fam.949>

-
- [17] Hidalgo, J.P., Torero, J.L., Welch, S., Fire performance of charring closed-cell polymeric insulation materials: Polyisocyanurate and phenolic foam, (2018) *Fire and Mater.*, 42 (4), pp. 358-373. <https://doi.org/10.1002/fam.2501>
- [18] Marquis, D.M., Hermouet, F., Guillaume, É., Effects of reduced oxygen environment on the reaction to fire of a poly(urethane-isocyanurate) foam, (2017) *Fire and Mater.*, 41 (3), pp. 245-274. <https://doi.org/10.1002/fam.2378>
- [19] Babrauskas, V., Twilley, W.H., Janssens, M., Yusa, S., A cone calorimeter for controlled-atmosphere studies, (1992), *Fire and Mater.*, 16 (1), pp. 37-43., <https://doi.org/10.1002/fam.810160106>
- [20] Babrauskas, V., Peacock, R.D., Heat release rate: The single most important variable in fire hazard, (1992) *Fire Saf. J.*, 18 (3), pp. 255-272. [https://doi.org/10.1016/0379-7112\(92\)90019-9](https://doi.org/10.1016/0379-7112(92)90019-9)
- [21] Schulz, J., Kent, D., Crimi, A., Hull, T.R., A critical review of the UK's regulatory regime for combustible façades, Submitted to *Fire Technology*, August 2018.
- [22] Colwell, S. and Baker, T. (2013), BR 135: Fire Performance of external thermal insulation for walls of multistorey buildings, BRE Trust, Watford.
- [23] Bill Jr., R.G., Croce, P.A., The International FORUM of Fire Research Directors: A position paper on small-scale measurements for next generation standards, (2006) *Fire Saf. J.*, 41 (7), pp. 536-538. <https://doi.org/10.1016/j.firesaf.2006.05.005>
- [24] Guillaume, E., Fateh, T., Schillinger, R., Chiva, R., Ukleja, S., Study of fire behaviour of facade mock-ups equipped with aluminium composite material-based claddings, using intermediate-scale test method, (2018) *Fire and Mater.*, 42 (5), pp. 561-577. <https://doi.org/10.1002/fam.2635>
- [25] MHCLG Amendments to statutory guidance on assessments in lieu of test in Approved Document B (Fire Safety): A consultation paper <https://www.gov.uk/government/consultations/approved-document-b-fire-safety-amendments-to-statutory-guidance-on-assessments-in-lieu-of-tests> (accessed 8/12/2018)
- [26] Weghorst, R., Antonatus, E., Kahrman, S., Lukas, C., Bulk, J., An investigation into the relevance of the contribution to toxicity of different construction products in a furnished room fire, (2017) 15th International Conference and Exhibition on Fire and Materials 2017, 1, pp. 352-363.
- [27] Ministry of Housing, Communities & Local Government, UK, Guidance: Ban on combustible materials, November 2018 <https://www.gov.uk/guidance/ban-on-combustible-materials> (accessed 8/12/2018)

Supplementary Material to accompany

Fire behaviour of modern façade materials – understanding the Grenfell Tower fire

Sean T. McKenna, Nicola Jones, Gabrielle Peck, Kathryn Dickens, Weronika Pawelec, Stefano Oradei, Stephen Harris, Anna A Stec and T Richard Hull¹
Centre for Fire and Hazard Sciences,
University of Central Lancashire, PR1 2HE, UK

Introductory Section

The Background to the Fire

One year after the 1666 Great Fire of London, the London Building Act restricted the use of combustible materials, such as wood, on building exteriors. In the UK most buildings were constructed from non-combustible materials for the following 440 years. The 1960s brought a significant rise in the number of tall concrete buildings, alongside the replacement of wood with more combustible, synthetic polymers, derived from crude oil, as non-structural construction materials. In 2006, the restrictions on the use of combustible materials on the outside of tall buildings were relaxed, while demands for improved insulation to address climate change were increased. In the UK there have been no major revisions of the Building Regulations covering fire safety (Approved Document B (Fire Safety)(ADB))¹ since the 2000 edition, while there have been five editions of the equivalent document covering thermal insulation (Approved Document L: Conservation of Fuel and Power), with each edition specifying improved thermal performance. Modern materials offer architects a wider range of durable products, providing a rich variety of shapes and surface finishes with improved thermal performance, but unlike brick, stone or concrete, many are combustible. Changing methods of construction, increasingly using off-site pre-fabrication, and benefitting from the ease of manufacture of complex polymeric components, has also contributed to growth in combustible building exteriors. In 2014, the European building and construction sector consumed 9.6 million tonnes of plastics (20% of total European plastics consumption), making it the second largest plastic application after packaging².

The presence of combustible material on building envelopes is most critical to fire safety in the case of tall and multi-occupancy structures. Fire safety is usually ensured through compartmentation: the use of fire resistant walls, doors, ceilings and floors prevents fire spreading from one compartment to another inside the building. If there is inadequately protected combustible cladding on the external walls this undermines the compartmentation strategy by providing a conduit for fire spread to other compartments via the façade. When such external fire spread occurs, it particularly endangers the people who follow the UK fire service advice for occupants of tall buildings to “stay put” (wait to be rescued), as they advised during the fire at Grenfell Tower. This policy is only compatible with effective compartmentation.

The Grenfell Tower was completed in 1974, with concrete exterior walls. It is a 67 m structure with 25 storeys, of which the upper 22 were residential accommodation. In 2016, an £8.7 million refurbishment was completed, including £2.6 million for an insulated rainscreen façade system of

¹ trhull@uclan.ac.uk

combustible foam insulation and aluminium-polyethylene composite material (ACM_PE), separated by a cavity, covering the exterior of the building. On 14th June 2017, a fire, reported to have started in a fridge-freezer in a fourth floor apartment, broke out to ignite the recently installed façade system, after which it spread very rapidly up the outside of the building, and into almost all the other apartments. The interplay between the insulation, ACM_PE and the cavity, which acted as a chimney, is likely to have promoted such rapid flame spread. ADB states that all cavities must be fire stopped with cavity barriers every at each floor. For a vertically continuous façade this may be effected with a horizontal layer of non-combustible stone wool insulation, with an intumescent strip facing the air-gap, which, in the event of a fire, should swell and seal the gap. This is illustrated in Figure 1 of the main paper, where the dark blue strip should expand to the size of the light blue rectangle. To be effective at fire-stopping, these strips must be installed correctly. Photographs of the tower during renovation, and of the burnt tower indicate the presence of intumescent strips and the mineral wool layers, respectively. However, the rapid fire spread shows they were unsuccessful in stopping the flames. It may be that the temperature rise was too rapid for the strips to swell effectively. Ultimately, the intensity of the fire caused the polyethene, and then the aluminium, of the ACM to melt, drip and burn, leaving the cavity barrier without a surface to form a seal.

Approved Document B (Fire Safety)(ADB)¹ is the government’s guidance which shows how to meet the UK Building Regulations. Since 2005, for buildings over 18 m, ADB permits the use of combustible materials on the exterior of buildings, based on the results of “full scale test data”, and refers to the BRE UK’s document, BR 135³. ADB provides alternatives for meeting the regulations, which have been summarised by the Building Control Alliance Guidance Note 18⁴. This note lists four options for demonstrating compliance of a façade system for use on the outside of tall buildings: the materials should meet the criteria for non-combustibility; the façade system should have passed the large scale test, BS 8414⁵; a “desktop study report”, based on other test results indicates that if the façade system were tested in BS 8414, it would pass, since ADB specifies “full scale test *data*”; or a holistic fire safety engineering approach has been followed. Both the insulation foams reported to have been used on the Grenfell Tower, the polyisocyanurate (PIR) (Celotex RS 5000) and phenolic foam (Kingspan K15) are reported to have passed the BS 8414 test as part of a ventilated façade system. In the case of the PIR, a document on the manufacturer’s web site stated that the compliant configuration included protection by a 12 mm non-combustible fibre-cement board⁶ on the exterior face of the PIR foam but this certification was withdrawn early in 2018; the phenolic foam is reported to have passed with an air gap and fire retarded ACM (ACM_FR)⁷. The manufacturer of the polyethene cored ACM (Reynobond PE) stated that it, and the more fire-safe Reynobond FR, had both passed BS 476 part 6 and part 7 tests, and so achieved UK “Class O” fire ratings. It also achieved Euroclass B, but this fire performance classification was also withdrawn after the Grenfell fire. In the Class O tests, the aluminium sheet would have protected the combustible core from attack by flame, allowing the PE to drip away.

Opinions differ as to whether the combinations used on Grenfell Tower met the above guidance: a detailed report was published by the UK’s “Inside Housing” magazine⁸. In subsequent large-scale fire tests⁹, conducted for the UK government (Department of Communities and Local Government (DCLG)) at BRE, following BS 8414, it was shown that façade systems with combustible insulation and ACM_PE or ACM_FR did not pass the regulatory test, when insulated with PIR or phenolic foam, even when the intumescent strips functioned perfectly.

The Grenfell Tower fire was not an isolated incident. There have been several fires in tall buildings where the fire spread rapidly up the outside, but only involved ACM_PE, without combustible insulation. In the 2013 Grozny City Towers fire in Chechnya, the combustion of ACM_PE and stone

wool insulation led to a rapid flame spread, but the fire did not cause any deaths or spread into the building, which re-opened in 2015. The Address Downtown Hotel fire in Dubai, just before New Year 2016 also involved ACM_PE but no insulation: again the fire did not spread inside the building, and there were no deaths, although one guest had a heart attack during the evacuation. Thus, it seems likely that it was the combination of the ACM_PE, cavity and insulation that led to the Grenfell tragedy. This resulted in a more severe external fire, which then penetrated almost every apartment in the Tower.

Fire Toxicity

The biggest killer, and biggest cause of injury in fires is not heat, burns or structural collapse, but the toxicity of the fire effluent. This has been the case for several decades and has been reported regularly in summaries of the UK and US fire statistics^{10, 11}. In order to estimate the effects of the toxicant yields on an exposed human population it is necessary to use measured data and established models of toxicity. Incapacitation, or “the inability to effect one's own escape” is considered the critical point leading to fatality. Incapacitation resulting from inhalation of the two asphyxiant gases found in fire effluents hydrogen cyanide (HCN) and carbon monoxide (CO) may be predicted from equations presented in ISO 13571¹². Inhalation of HCN prevents the uptake of oxygen by the body's cells, by inhibiting the synthesis of ATP. This oxygen deprivation triggers hyperventilation in humans and primates, resulting in a factor of four increase in HCN uptake. This rapidly leads to collapse and loss of consciousness, whereupon the respiration rate returns to normal¹³. The prediction of incapacitation by HCN is therefore a power function (with the HCN concentration raised to the power 2.36, multiplied by each exposure duration at that concentration). HCN concentrations around 150 ppm lead to incapacitation within a few minutes. CO forms a stable carboxyhaemoglobin (COHb) complex, preventing oxygen transport by the blood. Over the short timescales of fire exposure its effect is linearly dose dependent (CO concentration multiplied by each exposure duration). ISO 13344¹⁴ uses rat lethality data to provide equations for prediction of the lethality of a fire effluent to humans, expressed in terms of the fractional effective dose (FED) based on an essentially additive model, which is augmented by a factor for carbon dioxide (CO₂) driven hyperventilation. The model assumes exposure for 30 min to fixed concentrations of toxicants.

It has been reported that there are large differences in the fire toxicity of different classes of insulation materials. It has been shown that when PIR foam burns it generates HCN and CO in dangerous quantities¹⁵ (1 kg of burning PIR foam insulation is enough to fill a 100 m³ apartment with a lethal toxic effluent). The relative contribution to the lethality of the HCN to CO in smoke from a developed PIR fire is around 3 to 1.

For most materials, the yields of the main asphyxiants, CO and HCN, and other products of incomplete combustion, increase with decreasing ventilation (or increasing equivalence ratio, ϕ). The equivalence ratio is the actual fuel-to-air ratio divided by the stoichiometric fuel-to-air ratio, so that fuel burning with $\phi = 2$ has half as much air as it needs for complete combustion to CO₂ and water.

Materials for rainscreen façade systems

A rainscreen façade system comprises a thin outer panel (also known as a “rainscreen”), a ventilated cavity, to prevent moisture accumulation, and an inner layer to provide thermal insulation. The outer panel can be metal (e.g. zinc, steel or aluminium), but the higher heat capacity of the metal encourages condensation, leading to unsightly mineral deposits, so lower thermal capacity alternatives are often preferred. These include aluminium composite material (ACM), high-pressure laminate (HPL), and mineral fibre boards.

Results Section

Elemental Analysis

The elemental analysis of the materials using CHNS, X-Ray Fluorescence (XRF), and SEM-EDAX is summarised in Table S1. For the ACM_PE1 and ACM_PE2 panel fillings the H : C atomic ratios (2.35 and 2.34 respectively) are consistent with polyethene (CH₂). For the ACM_FR1, FR2 and FR3 fillings, higher H : C atomic ratios (3.15, 3.58, and 2.88 respectively) are consistent with mineral filled PE containing magnesium hydroxide or aluminium hydroxide at loadings around 57, 69 and 66% respectively. Nitrogen and sulphur may have been present in a surfactant used to increase the compatibility of the polymer to the hydroxide. The H : C atomic ratios of the phenolic foams (1.08, 1.10 and 1.19) are consistent with its molecular formulation, the two samples containing 2% nitrogen probably contain urea, used as a comonomer to increase the cross-linking. The sulphur in PF may be present because *p*-toluene sulphonic acid is used to catalyse polymerisation of phenolic resins, or from thiols added to increase cross-linking. Approximate empirical formula can be calculated: for phenolic foam (C₁₀H₁₁O₃N_{0.3}S_{0.2}); and PIR (C₁₀H₁₀O₃N); assuming all the “remaining %” is oxygen. The presence of PE in the ACM_PE samples was confirmed as low density polyethene (LDPE) by diamond-ATR-FTIR spectra, shown in Figure S1.

Table S1 CHNS, XRF and SEM EDAX analysis of panel, ACM panel filling and insulation.

Sample	C %	H %	N %	S %	Remaining %	Elements detected by EDAX/XRF
ACM_PE1	84.4	16.5	0.0	0.0	0.0	None Detected
ACM_PE2	82.9	16.2	0.0	0.1	0.7	None Detected
ACM_FR1	33.8	8.9	0.3	0.0	57.0	O, Mg
ACM_FR2	23.9	7.1	0.0	0.0	68.9	O, Al
ACM_FR3	27.2	6.5	0.0	0.0	66.3	O, Mg, Al, Si, Ca
ACM_NC1	14.7	1.7	3.8	0.0	79.8	O, Na, Mg, Al, Si, Fe
ACM_NC2	68.3	12.8	0.0	0.0	18.9	Al
HPL_PF	50.3	7.3	0.1	0.0	42.36	O
HPL_FR	44.2	6.4	0.4	0.0	49.1	O, P
MWB_1	12.8	0.9	0.2	0.0	86.1	O, Ti, Na, Mg, Al, Si, Fe
MWB_2	1.4	0.2	0.1	0.0	98.25	O, Na, Mg, Al, Si, Ca, Fe
PF1	61.6	5.6	2.0	7.0	23.8	O, S, P, Cl
PF2	60.8	5.6	2.0	7.1	24.5	O, S, Cl
PF3	61.2	6.1	0.1	3.9	28.7	O, S, P, Cl
PIR1	64.9	5.2	6.9	0.1	22.9	O, P, Cl
PIR2	65.1	5.7	7.9	0.0	21.3	O, P, Cl
PIR3	65.1	5.8	7.7	0.0	21.4	O, P, Cl
SW	2.50	0.3	0.1	0.0	97.1	O, Mg, Al, Si, Ca
GW	1.8	0.2	0.4	0	97.6	Na, Si, Ca, O

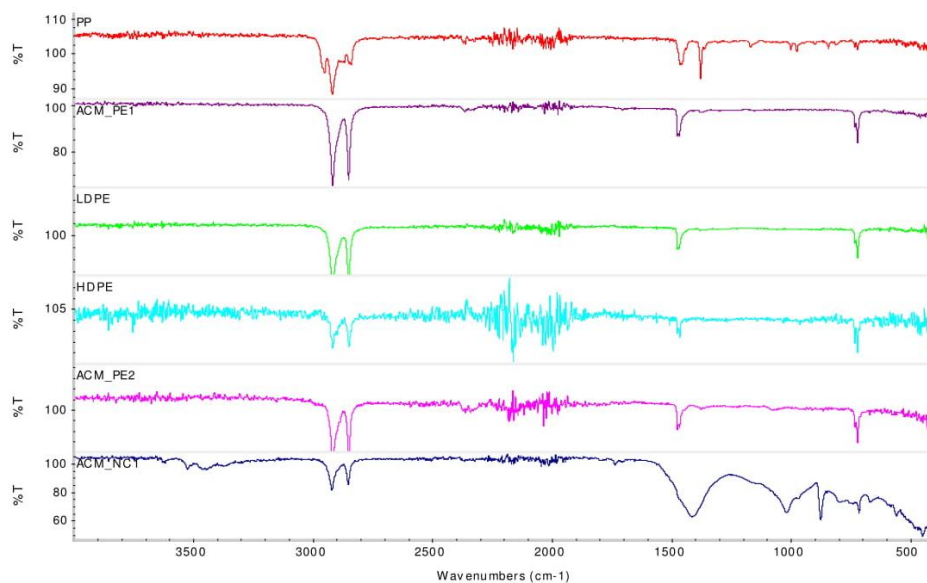


Figure S1. FTIR for ACM_PE1 and ACM_PE2 and ACM_NC1, filling, correlating with LDPE (reference spectra for polypropylene (PP) and high density polyethylene (HDPE) are also shown).

Bomb Calorimetry and Microscale Combustion Calorimetry

The consistently lower values from MCC compared to the bomb calorimeter arise because the MCC disregards the latent heat of condensation of water produced during combustion (the lower value is sometimes referred to as the “net” or “sensible” heat of combustion). For the insulation materials, the lower values in MCC method B also result from the higher degree of oxidation in bomb calorimeter conditions (partial pressure of oxygen, $p_{O_2} = 25$ bar), compared to the MCC (heated to 700 °C in 20% O_2 or $p_{O_2} = 0.2$ bar).

Thermal Analysis

Outer-Screen Products and ACM fillings

TGA in nitrogen is accepted as the best model for thermal decomposition under a flame, as the oxygen concentration is typically less than 1%¹⁶. The TGA in nitrogen for the outer-screen products and ACM fillings (Figure S2) shows a single rapid decomposition step for ACM_PE1 and PE2 confirming that they are predominantly PE. For ACM_FR2 a significant mass loss around 300 °C indicates the presence of around 64% $Al(OH)_3$. ACM_FR1 and FR3 show a mass loss around 360 °C of a little less than 20%, which would correspond to a 65% loading of $Mg(OH)_2$. The residues of FR1, 2 and 3 at 700 °C are 48, 45 and 49% respectively, corresponding to filler loadings of 70, 69 and 71%. The discrepancy between these two estimates arises because the first assumes all water is lost at 300 to 360 °C, while the second assumes no polymeric residue remains at 700 °C. The ACM_NC1 loses around 5% mass below 300 °C, 10% around 450 °C and a further 5% above 650 °C, while the ACM_NC2 loses 14% mass quite sharply around 460 °C, as the glue around the corrugated aluminium is pyrolysed. The MWB1 loses 5% mass between 500 and 700 °C. The TGAs of the two HPL products show very early onsets of decomposition (below 100 °C) and significant mass losses around 300 °C. The HPL_FR shows an earlier onset than HPL_PF, but lower overall mass loss, suggesting a greater degree of cross-linking and char formation.

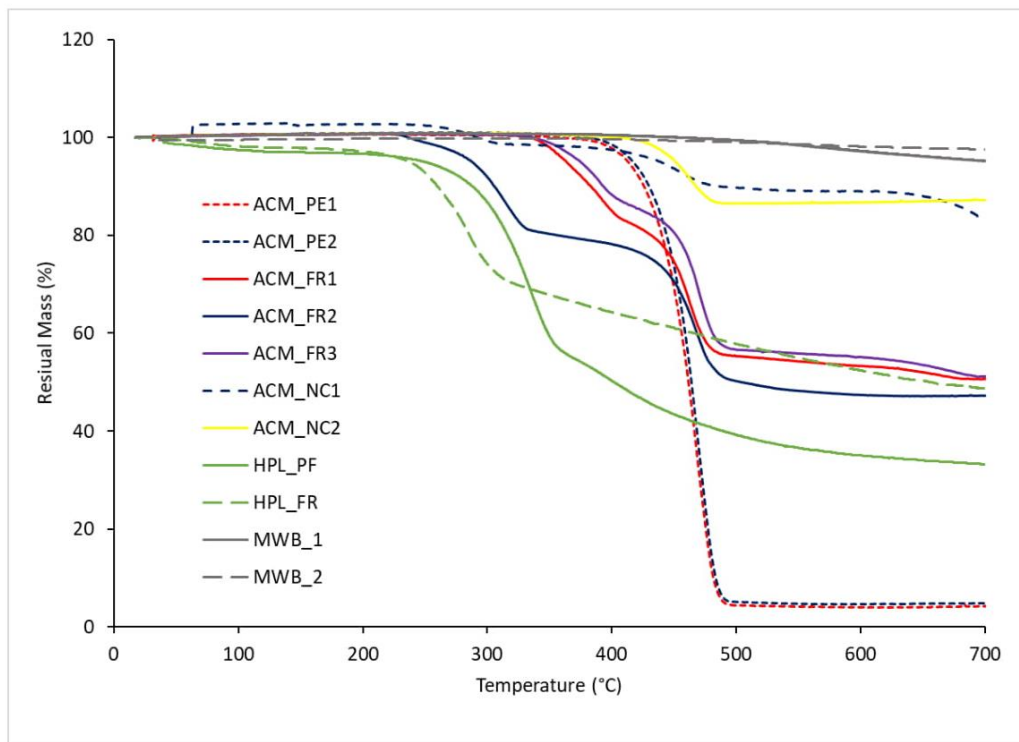


Figure S2 TGA of panel fillings in nitrogen

The differential scanning calorimetry (DSC) traces for ACM fillings and MWB1 in nitrogen were recorded predominantly to identify the materials present in the ACM fillings (FR etc.). Figure S3 shows a strong endothermic peak at 295°C for ACM_NC1 and at 320°C for ACM_FR2; there are similar strong peaks at 390°C for ACM_FR1 and for ACM_FR3. These correspond to the decomposition temperatures of $\text{Al}(\text{OH})_3$ and $\text{Mg}(\text{OH})_2$ respectively. The decomposition temperatures are higher when compounded into a polymer. ACM_NC2 shows a very sharp endothermic peak at 660°C corresponding to the melting of aluminium metal.

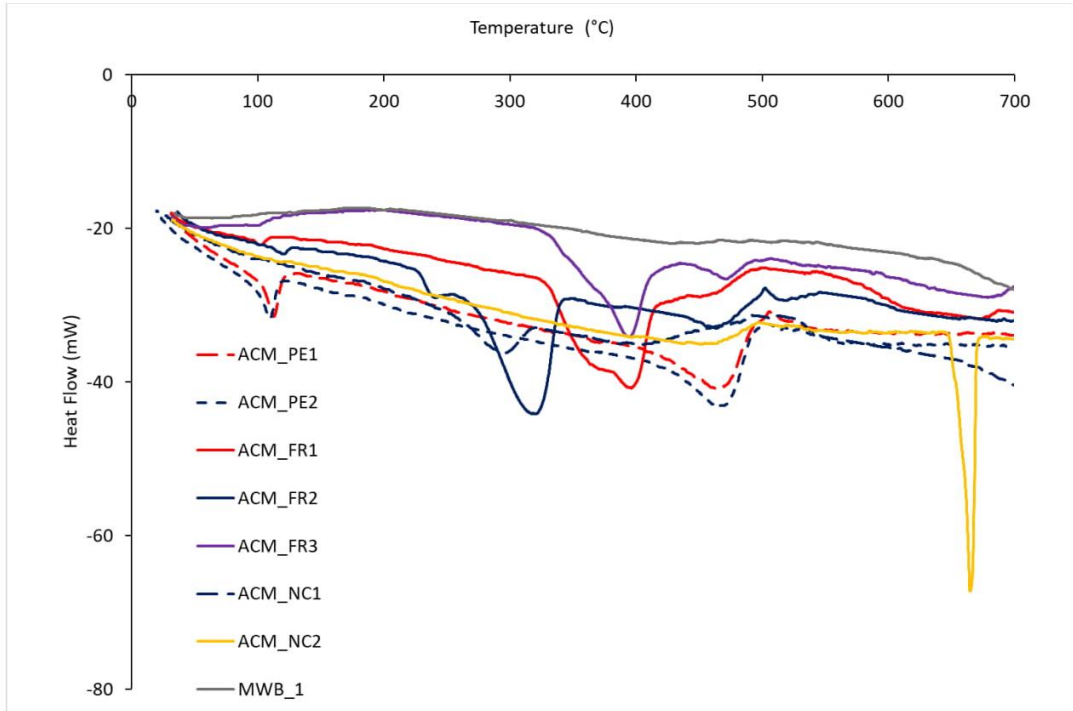


Figure S3 DSC curves of panel fillings in nitrogen

Figure S4 shows the TGA of outer-screen products and ACM fillings in air. This shows earlier onset and completion of decomposition for all organic components – the PE in ACM_PE1 and PE2, the PE component of ACM_FR1, FR2 and FR3, and ACM_NC1. The glue in ACM_NC2 decomposes slowly from 250 to 410 °C then rapidly at 420 °C, leaving the residual corrugated aluminium filling. The binder in MWB_1 and 2 decompose more quickly, from 350 to 520 °C in air, leaving residues of 84 and 91% respectively. HPL products show similar behaviour in air as in nitrogen, but the decomposition is more extensive showing around 10 and 15% residue at 700 °C for HPL_PF and HPL_FR respectively.

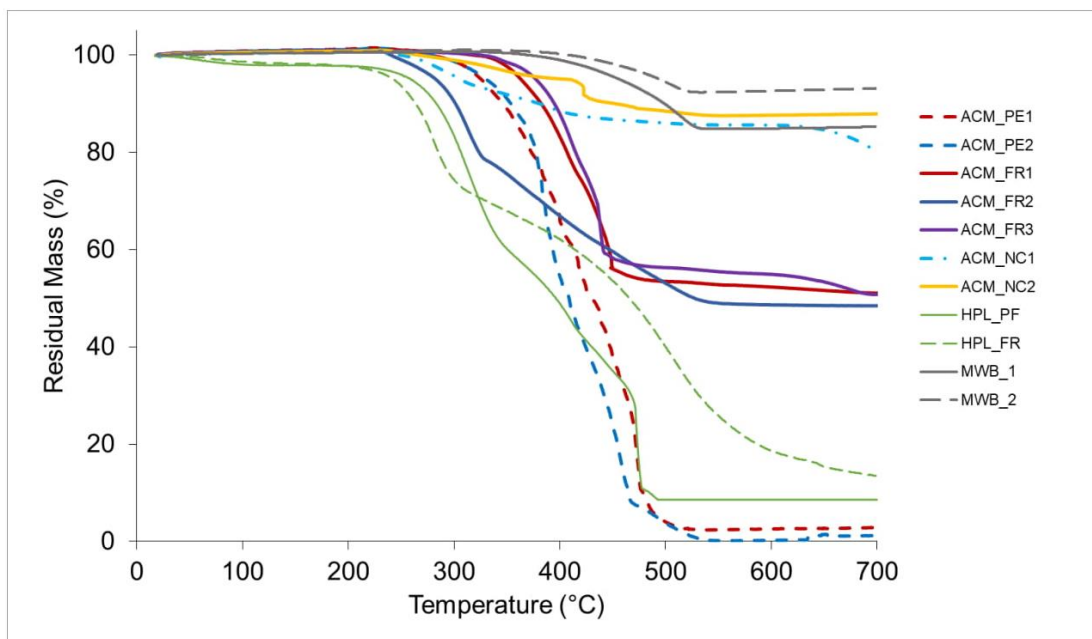


Figure S4 TGA of panel fillings in air.

Insulation Products

The TGA in nitrogen for insulation materials (Figure S5) shows broad similarities between the three phenolic foams, with progressive decomposition from around 50 °C, yielding a residue at 700 °C around 40 to 50% in nitrogen. All PIRs undergo slow decomposition from around 100 to 300 °C, then PIR1 shows noticeably different decomposition to PIR2 and PIR3 in nitrogen, with a rapid mass loss from 300 to 340 °C, followed by a slow mass loss up to 650 °C. PIR2 and PIR3 show more progressive mass loss from 300 to 600 °C, with residues around 20 to 30%. SW shows 2% mass loss and GW 5% up to 700 °C.

The TGA in air for insulation materials (Figure S6) shows similar decomposition behaviour, but with earlier onset temperatures, and greater mass losses, as may be expected.

The phenolic foams show sharper decomposition from 350 to 480 °C with residue at 700 °C, 7 to 12% in air for PF1 and PF2 respectively under these oxidising conditions. The PIRs show multi-stage decomposition, presumably corresponding to the energy required to cleave the different bonds present in the polymer, leaving residues at 700 °C between 0 to 5%.

SW shows a greater mass loss in air than nitrogen, coinciding with the mass loss of GW at 700 °C. This indicates a similar binder content of both fibre insulation products.

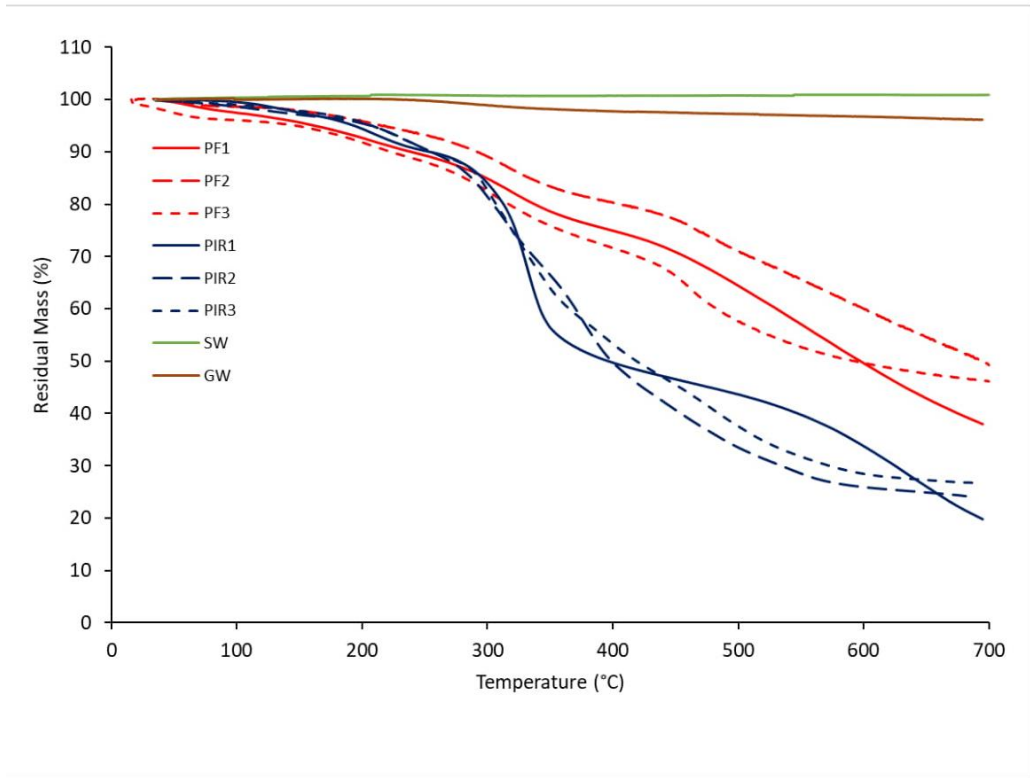


Figure S5 TGA in nitrogen for insulation materials

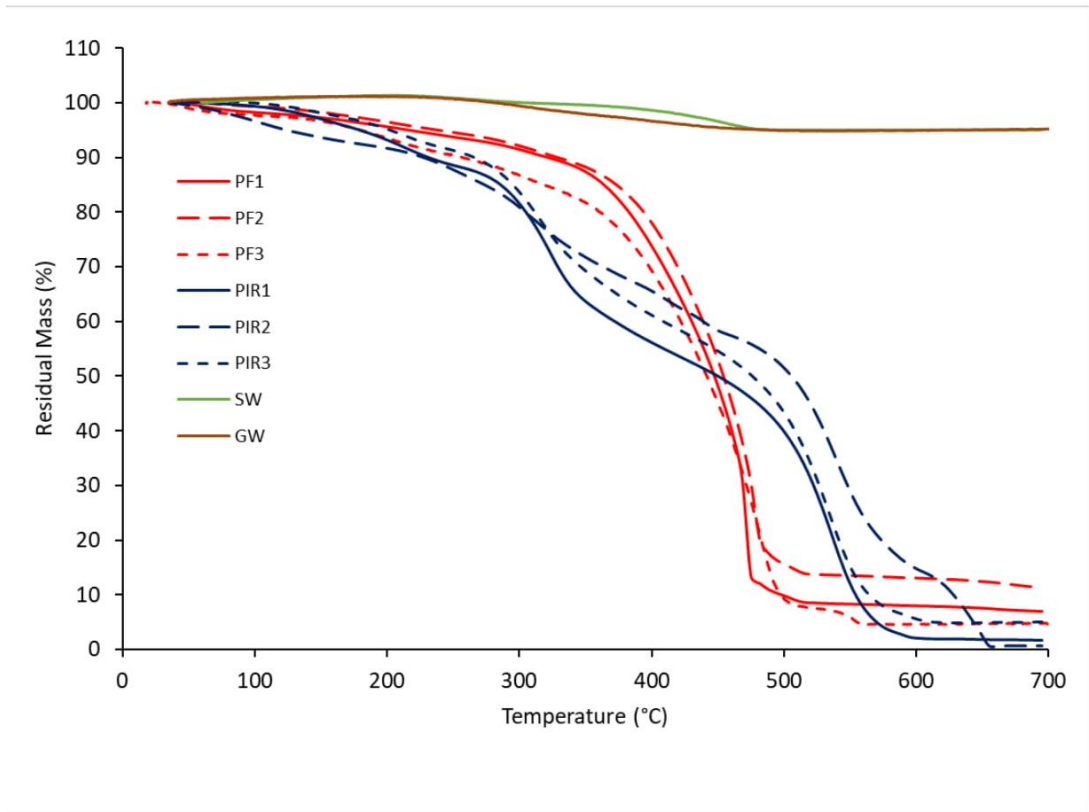


Figure S6 TGA in air for insulation materials.

Cone Calorimetry

Table S2 summarises the major flammability parameters from cone calorimetry for the panel and insulation materials. ACM_PE1 and ACM_PE2 show relatively long times to ignition, which is initially that of the paint layer, but very large peak HRRs. During the long pre-ignition time, the PE will have begun to melt and decompose, contributing to the high peak HRR. The heats of combustion are comparable to the lower values from the MCC (Table 3, main paper). The mass losses show that approximately half the mass of ACM_PE is aluminium metal. In contrast ACM_FR1, 2 and 3 show similar times to ignition, but an order of magnitude lower peak HRR. This shows the disproportionate benefit of filling two-thirds of the composite with metal hydroxide – in addition to endothermic decomposition and water release, the physical interference with the flow of molten PE by the residual metal oxide is clearly effective in limiting its contribution to fire growth.

Table S2 Summary of cone calorimeter output data

Sample	Time to ignition [s]	Av. dev	Peak HRR [kW m ⁻²]	Av. dev	Time to pHRR [s]	Av. dev	Total Heat Release [MJ m ⁻²]	Av. dev	Effective Heat of combustion [MJ kg ⁻¹]	Av. dev	Mass loss [%]	Av. dev
ACM_PE1	75.1	3.4	1364	76.9	192	2.87	105.4	0.74	41.0	0.01	48.9	0.97
ACM_PE2	94.6	2.4	1123	25.6	242	7.41	106.6	0.45	41.8	0.17	50.8	0.11
ACM_FR1	74.8	2.6	123	18.3	242	28.6	59.6	3.85	25.1	1.59	32.9	0.03
ACM_FR2	123	0	157	0.6	299	41	52	0.08	23	2	38	2.6
ACM_FR3	112	8	145	29	244	12	50	14	24	4	29	3
ACM_NC1	-	-	13.8	1.6	110	1.70	2.57	1.60	6.21	1.08	8.29	0.65
ACM_NC2	52.3	7.8	30.2	5.5	54.0	0.82	0.87	0.66	9.07	2.46	3.37	0.40
HPL_PF	43.8	3.5	529.7	41.7	57.7	2.87	173	2.85	18.0	0.99	90.5	3.14
HPL_FR	29.4	13.5	263.1	37.8	44.0	9.90	67.5	4.28	11.2	1.81	68.5	5.02
MWB_1	15.2	0.9	149.7	10.3	29.0	1.41	37.0	1.53	18.3	1.50	19.2	2.44
MWB_2	14.5	2.9	193.8	3.0	26.7	1.25	27.8	3.51	29.5	4.07	8.04	0.11
PF1	8.56	2.7	63.7	5.5	20.0	2.83	18.7	0.69	23.7	0.66	100	0.12
PF2	7.81	3.7	62	3.0	18.0	3.56	17.6	0.7	20.2	0.77	98.4	0.54
PF3	8.83	5.2	64.8	3.0	20.7	4.78	19.7	0.98	20.6	0.54	97.1	0.80
PIR1	1.06	0.05	115.9	3.5	12.0	0.82	13.3	0.39	19.2	1.24	91.0	4.42
PIR2	1.60	0.06	106.4	2.6	14.3	0.47	15.6	0.57	21.6	1.29	94.7	1.34
PIR2*	1.21	0.1	101.1	4.6	13.3	0.47	14.3	1.06	20.1	1.25	96.9	0.97
PIR3	1.48	0.3	107.3	2.8	13.0	0	14.5	0.83	20.0	1.62	94.8	2.29
SW	-	-	5.6	1.1	25.0	2.16	0.06	0.09	22.7	10.1	4.16	0.79
GW	-	-	8.7	0.8	36.5	3.5	0.67	0.067	25.6	3.78	7.71	2.55

* This sample was cut just above the glass wool layer

From the formulations (around one third PE), the THR of the ACM_FR seem surprisingly large. The ACM_PE samples produced more CO than ACM_FR by a factor of around 20. This indicates more efficient combustion of the ACM FR materials, probably resulting from catalytic char oxidation by the residual Al₂O₃ and MgO.

Debris from the Grenfell Tower fire show fragments of aluminium sheet which had clearly been detached by melting, indicating that the 50 kW m⁻² fire condition was less severe than in the tower fire itself.

The effective heats of combustion (EHC) in cone calorimetry are reported on a mass-loss basis (the heat release is divided by the mass-loss, which excludes the metal oxide residue) whereas in MCC or bomb calorimetry, they are reported on a mass-charge basis.

The HPL_PF shows the greatest fire growth rate (FIGRA: the line from origin to the first, highest peak of any of the outer-screen materials), and a steady heat release rate, around 250 kW m⁻². However, it is important to recognise that these products were tested as used, and are thicker than the ACM. HPL_PF was 10 mm whereas the ACMs were all 4 mm, with only 3 mm of “fuel”, hence the disproportionately greater THR for a lower EHC. After initial ignition of the paint layer, the HPL_FR shows effective suppression of burning for the first 250 s, then contributes a steady heat release rate around 100 kW m⁻². The THR and EHC are lower than for HPL_PF, and 30% of the mass remains.

The ACM_NC and MWB screens show initial peaks of HRR corresponding to ignition of paint. The NC screens show very low THR of 1 to 3 MJ m⁻² while the thicker MWB panels show a higher THR of 28 to 37 MJ m⁻².

The plastic foam insulation materials show much shorter times to ignition, around 8 s for PF and 1 s for PIR, but (partly because of the lack of pre-ignition heating) much lower peak HRRs (around 62 kW m⁻² and 110 kW m⁻² respectively) than the ACM_PE panels.

Both the SW and GW show very low levels of heat release, corresponding to the small amount of binder present, which slowly pyrolyses at a heat flux of 50 kW m⁻², giving a 5% mass loss, but an EHC of around 30 MJ kg⁻¹ when reported on a mass-loss basis, typical of a polymeric binder.

It should be noted that oxygen depletion calorimetry (ODC) used in the cone calorimeter and the MCC excludes endothermic decomposition of mineral fillers from the heat release, although their effects are evident in the increased time to ignition and lower peak heat release rates. For a compound of PE and ATH in a 1 : 2 ratio, as in ACM_FR2, the overestimation of the heat release is 16%¹⁷. In the experiments reported from cone calorimetry, the physical inhibition of flowing of molten PE by Al₂O₃ and MgO probably had a greater effect in reducing the heat release than the error arising from ODC.

Smoke toxicity

The steady state tube furnace (ISO TS 19700)¹⁸ has been specifically designed to replicate individual fire stages¹⁹. ISO TS 19700 provides guidance for meeting these fire conditions. In this study, the target conditions were $\phi = 0.5$ to 0.7 for well-ventilated, and $\phi = 1.4$ to 2.2 for both small and large under-ventilated flaming, using furnace temperatures of 650 and 825 °C, respectively. The mass loss decreases by around 25% with the transition from well- to under-ventilated, also changing the equivalence ratio, making precise target conditions harder to meet. Table S3 shows the actual condition and the relationship to the ISO fire stage.

The fire toxicity of polyolefins has been reported²⁰, and also shown to be dependent on the ventilation condition (as the oxygen availability falls, so the CO yield rises). The CO yield varies from

around 0.01 g(CO) per g(polymer) in well-ventilated flaming to 0.2 or 0.3 g g⁻¹ in under-ventilated conditions¹⁹. The presence of metal hydroxide fire retardant fillers has been shown to have a negligible effect on the CO yield per g of polymer in polyolefins²¹. It is reasonable to assume that the fire toxicity of the panel materials will be a simple function of their PE content and their burning conditions, with CO as the major toxicant. Their enclosure between aluminium sheets and the melt-dripping fire behaviour on the side of a burning building make it a difficult to assign a fire condition or replicate their burning on a bench-scale.

Table S3 SSTF fire condition, equivalence ratio, mass loss and ISO fire stage.

Sample	Furnace Temperature /°C	Equivalence ratio, ϕ	Mass loss %	ISO Fire stage
PF1	650	0.69 ± 0.02	97.46	2
	650	1.53 ± 0.03	72.68	3a
	825	1.73 ± 0.14	72.34	3b
PF2	650	0.63 ± 0.09	98.1	2
	650	1.66 ± 0.06	75.73	3a
	825	1.60 ± 0.24	73.73	3b
PF3	650	0.61 ± 0.09	95.68	2
	650	1.63 ± 0.10	66.14	3a
	825	1.40 ± 0.14	63.59	3b
PIR1	650	0.63 ± 0.03	95.32	2
	650	1.69 ± 0.14	76.57	3a
	825	2.13 ± 0.12	78.91	3b
PIR2	650	0.70 ± 0.02	92.02	2
	650	1.82 ± 0.11	75.86	3a
	825	1.94 ± 0.44	74.42	3b
PIR3	650	0.70 ± 0.04	94.35	2
	650	1.73 ± 0.08	77.35	3a
	825	1.98 ± 0.06	78.89	3b
SW*	650 – NF	N/A	1.77	2 – NF
	650 – NF	N/A	1.67	3a – NF
	825 – NF	N/A	1.64	3b – NF
GW*	650 – NF	N/A	6.21	2 – NF
	650 – NF	N/A	8.63	3a – NF
	825 – NF	N/A	12.69	3b – NF

Both mineral wool insulation products were tested in the furnace at 900 °C in well-ventilated conditions as stated in ISO TS 19700, but neither ignited. They were also tested under the three conditions used here for the combustible materials for completeness, although, as there was no flaming no equivalence ratio can be assigned to their burning condition, and the toxicity cannot be compared directly to the flaming combustion of the foams. In general, flaming combustion accelerates the decomposition processes, resulting in a reduction in smoke toxicity compared to non-flaming decomposition.

Based on the % C in Table S1, the theoretical maximum CO₂ yield is around 2.3 g/g for PF and PIR foams. The yields for well-ventilated conditions agree reasonably well, showing self-consistency within the data. The difference in CO and HCN yields in different ventilation conditions emphasizes the importance of fire condition in fire toxicity assessment. For the phenolic foam, the CO yield

shows a factor of 10 increase when the fire grows from well-ventilated to under-ventilated. For the PIRs the factor varies with the foam, ranging from 4 to 20.

The lower CO₂ yield, and higher CO and HCN yields for PIR1 than for the other PIRs, in well-ventilated conditions, suggest more efficient gas phase inhibition leading to more products of incomplete combustion.

The hydrogen chloride (HCl) yields are higher for the PIR foams, consistent with the use of chlorinated organophosphate ester flame retardants in the formulations. Moreover, they are highest in well-ventilated conditions. HCl is known to adhere to smoke particles; the higher smoke particulate yields from under-ventilated flaming may have trapped the HCl and deposited it before analysis. The nitric oxide, nitrogen dioxide and phosphoric acid yields are very low.

Discussion Section

BRE/DCLG BS 8414 tests

After the Grenfell Tower fire, the government-appointed Expert Advisory Panel recommended DCLG to commission BRE to conduct large scale tests on a series of seven façade systems, using ACM with PE, FR and NC filling, and PIR, phenolic and SW insulation. The large scale test followed BS 8414-1⁵, designed to represent “a fully-developed (post-flashover) fire in a room, venting through an opening such as a window aperture that exposes the cladding to the effects of external flames”. The test apparatus is shown in Figure 7. An internal L-shaped masonry corner of 1 m x 2 m and at least 8 m tall is covered with the façade system. At the bottom of the 2 m face, a large opening is filled with an approximately 400 kg wooden crib, designed to output 4 500 MJ over 30 min, with a peak output of 3 ± 0.5 MW. The crib should burn for 30 min, be extinguished, but the test facade allowed to continue burning for a further 30 min. For buildings taller than 18 m, the performance criteria set out in BR 135³ require the test to be completed without flame spread above the façade, and the temperature 5 m above the combustion chamber not to rise more than 600 °C in the first 15 min. The only guidance provided in BS 8414-1 on construction of the façade system is “The test specimen shall include all relevant components assembled and installed in accordance with the manufacturer's instructions.” In practice, the test laboratories deem it to be the manufacturer’s responsibility to install the test specimen. In the case of the DCLG tests, the task was conducted by a cladding installation company. Although not specified in BS 8414-1 or the manufacturer’s instructions, in these tests, a 5 mm thick aluminium “window pod” surrounded the wooden crib, protruding 30 mm out of the face of the façade. Insulation panels 100 mm thick were fixed to the walls, then ACM attached, forming a 50 mm cavity. A set of 3 vertical and 4 horizontal fire-stopping barriers were installed: above the wooden crib opening; 2.4 m, 4.7 m and 6.3 m above the opening. Each barrier was 75 mm thick, and protruded 25 mm from the face of the insulation, and was faced with an intumescent strip between the stone wool and ACM (similar to the layout shown in Figure 1 (main paper)).

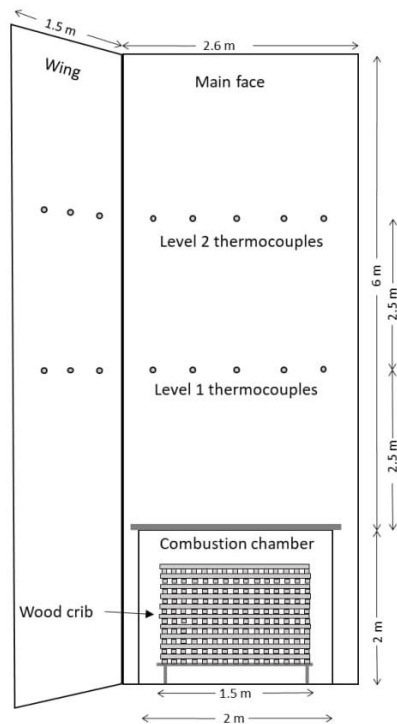


Figure 7 The BS 8414 test rig.

In the first two tests, where PE filled ACM was tested with PIR and stone wool insulation, the intumescent cavity barriers were reported to have sealed the gaps effectively, but the heat from the wooden crib caused enough PE to melt and drip from the ACM that flaming was observed above the façade in both tests, which were halted after 7 to 9 minutes before the insulation had started to burn. In the third test, on the fire retarded ACM, with PIR insulation, the test continued long enough to involve the PIR insulation, but was stopped after 25 min. In the fourth test, the combination of fire retarded ACM and stone wool insulation met the BR 135 criteria. In the fifth and six tests, mineral filled ACM was tested with PIR foam and stone wool insulation, and both systems passed. After it became apparent that phenolic foam had also been installed on Grenfell Tower, the seventh test was arranged with fire retarded ACM and phenolic foam insulation, which also failed.

Smoke Toxicity

Direct estimation of safe loading of materials (material-IC₅₀ and material-LC₅₀)

The material-IC₅₀ and material-LC₅₀ values shown in Table S4 provide the most direct route to estimating a safe loading of insulation material. The material-IC₅₀ and LC₅₀ are the masses of material required to produce an incapacitating and lethal concentration of effluent per unit volume, respectively. They are therefore inversely proportional to toxicity. The 5 min material-IC₅₀ and 30 min material-LC₅₀ values are broadly similar for each product. Thus, unless an occupant can be safely evacuated from the effluent within 5 min, incapacitation is likely to be followed by death. For example 500 g of PIR 1, burning in large under ventilated conditions (3b) would fill 100 m³ with an effluent lethal to 50% of the exposed population.

Table S4 Material-IC₅₀ and material-LC₅₀ values¹⁴ for each insulation material and fire condition

Sample	ISO Fire Stage	Material-IC ₅₀ /g m ⁻³ (5 min exposure)	Material-LC ₅₀ /g m ⁻³ (30 min exposure)
PF1	2	62.32	45.57
	3a	21.64	14.01
	3b	22.39	17.01
PF2	2	56.93	43.94
	3a	23.11	14.55
	3b	27.39	20.99
PF3	2	57.9	43.02
	3a	21.22	12.47
	3b	27.5	15.98
PIR1	2	20.73	13.29
	3a	17.15	9.98
	3b	8.84	5.00
PIR2	2	31.9	21.04
	3a	11.3	6.28
	3b	8.85	5.30
PIR3	2	27.19	18.52
	3a	12.42	6.95
	3b	12.93	7.75
SW*	2 – NF	150.32	74.19
	3a – NF	226.22	117.39
	3b – NF	326.56	163.96
GW*	2 – NF	133.34	66.69
	3a – NF	190.8	100.03
	3b – NF	362.16	171.36

References

- 1 *Approved Document B: Fire Safety – Volume 2: Buildings other than dwellinghouses*, (2006, including 2010 and 2013 amendments), Building Regulations, HM Government, London.
[https://www.planningportal.co.uk/info/200135/approved_documents/63/part b - fire safety/2](https://www.planningportal.co.uk/info/200135/approved_documents/63/part_b_-_fire_safety/2) (accessed 7/12/2018)
- 2 *Plastics – The Facts 2017*, Plastics Europe, Brussels.
[https://www.plasticseurope.org/application/files/1715/2111/1527/Plastics the facts 2017 FINAL for website.pdf](https://www.plasticseurope.org/application/files/1715/2111/1527/Plastics_the_facts_2017_FINAL_for_website.pdf) (accessed 7/12/2018)
- 3 Colwell, S., and Baker, T., *Fire Performance of external thermal insulation for walls of multistorey buildings*, 3rd Edition, BRE Trust, Watford, 2013.
- 4 *BCA Technical Guidance Note 18, Use of Combustible Cladding Materials on Residential Buildings*, Building Control Alliance, London, June 2014.
<http://buildingcontrolalliance.org/wp-content/uploads/2018/10/BCA-GN-18-Use-of-combustible-cladding-materials-Rev-1-Jun-15-MHCLG-Circular.pdf> (accessed 7/12/2018)
- 5 *BS 8414-1:2015+A1:2017 Fire performance of external cladding systems. Test method for non-loadbearing external cladding systems applied to the masonry face of a building*, BSI, London.
- 6 Celotex Ltd - Celotex RS5000 Insulation Board (Rain screen application). Certificate No. EW491,
https://www.labss.org/sites/default/files/ew491_celotex_ltd_0.pdf (accessed 19/07/2017)

-
- 7 BRE Global - BR 135 classified external cladding systems <https://www.bre.co.uk/regulatory-testing> (accessed 7/12/2018)
 - 8 Apps, P., Barnes, S., Barratt, L., The Paper Trail: the Failure of Building Regulations, Inside Housing, March 2018 <https://www.insidehousing.co.uk/news/news/the-paper-trail-the-failure-of-building-regulations-55445> (accessed 7/12/2018)
 - 9 Independent report - Fire test report: DCLG BS 8414 test no.1 <https://www.gov.uk/government/publications/fire-test-report-dclg-bs-8414-test-no1> (accessed 7/12/2018)
 - 10 UK Fire Statistics 2017 and preceding editions, Home Office, London, <https://www.gov.uk/government/collections/fire-statistics> (accessed 7/12/2018)
 - 11 Hall, J. R., Fatal Effects of Fire, National Fire Protection Association, Quincy, MA, (2011).
 - 12 ISO 13571:2012 Life-threatening components of fire - Guidelines for the estimation of time to compromised tenability in fires, ISO, Geneva.
 - 13 Purser, D.A., Chapter 3, Asphyxiant components of fire effluents, (2010) in Fire Toxicity, edited by A Stec and R Hull, Woodhead/Elsevier pp. 118-198. <https://doi.org/10.1533/9781845698072.2.51>
 - 14 ISO 13344:2015, Estimation of the lethal toxic potency of fire effluents, ISO, Geneva.
 - 15 Anna A Stec and T Richard Hull, *Assessment of the fire toxicity of building insulation materials*, Energy and Buildings, 43, 498–506, (2011). <https://doi.org/10.1016/j.enbuild.2010.10.015>
 - 16 Schartel, B., Hull, T.R., Development of fire-retarded materials - Interpretation of cone calorimeter data, (2007) Fire and Materials, 31 (5), pp. 327-354.
 - 17 Hewitt F, Hull TR. Mineral Filler Fire Retardants, in Palsule S, editor. *Polymers and Polymeric Composites: A Reference Series*. Berlin, Heidelberg, Springer Berlin Heidelberg, 2016, pp 1-26 https://doi.org/10.1007/978-3-319-28117-9_2
 - 18 ISO/TS 19700:2016 Controlled equivalence ratio method for the determination of hazardous components of fire effluents - Steady-state tube furnace, ISO, Geneva.
 - 19 ISO 19706:2011 Guidelines for assessing the fire threat to people, ISO, Geneva.
 - 20 Hull, T.R., Stec, A.A., Lebek, K., Price, D., Factors affecting the combustion toxicity of polymeric materials, (2007), Polymer Degradation and Stability, 92 (12), pp. 2239-2246. <https://doi.org/10.1016/j.polymdegradstab.2007.03.032>
 - 21 Hull, T.R., Quinn, R.E., Areri, I.G., Purser, D.A., Combustion toxicity of fire retarded EVA, (2002) Polymer Degradation and Stability, 77 (2), pp. 235-242. [https://doi.org/10.1016/S0141-3910\(02\)00039-3](https://doi.org/10.1016/S0141-3910(02)00039-3)